Broadband Access Networks Using Hybrid Radio/Fiber Systems

A THESIS FOR THE DEGREE OF DOCTOR OF PHILOSOPHY

Presented to

Dublin City University (DCU)

by

Aleksandra M Kaszubowska

B Eng, SMIEEE

School of Electronic Engineering

Dublin City University

Research Supervisor

Dr Liam Barry

May 2004

Approval

Name	Aleksandra M Kaszubowska
Degree	Doctor of Philosophy
Title of Thesis	Broadband Access Networks Using Hybrid Radio/Fiber Systems
Examining Committee	Dr Jennifer McManis (Dublin City University) Chair
	_____
	Prof Richard Penty (University of Cambridge) External Examiner
	_____
	Dr Philip Perry (Dublin City University) Internal Examiner
	_____
	Dr Liam Barry (Dublin City University) Supervisor
Date Approved	_____

Declaration

I hereby certify that this material, which I now submit for assessment on the programme of study leading to the award of Doctor of Philosophy is entirely my own work and has not been taken from the work of others save and to the extent that such work has been cited and acknowledged within the text on my work

ID No _____

Signed _____

Date _____

Dedication

To Mama, Mano, Karolina and Julia

Acknowledgement

First and foremost I would like to thank my supervisor Dr Liam Barry for his guidance, support and understanding, without which completion of this work would not have been possible One could not wish for a better supervisor

I would like to express my deepest gratitude to my parents, especially to my mother for all the love and support she has given me and for all the sacrifices she has made for me I would also like to thank my big sister Karolina for being such a good friend I truly appreciate all that you have done for me

No words can express my gratitude to my beloved Mano, whose love, help and support kept me going even in the most difficult moments Without him I would not had been able to finish this work

I owe a special thank you to Amma and Appa, who did not hesitate to travel thousands of kilometres to be with me and help me finish my thesis

I would be failing in my duty if I did not acknowledge all the help I received from my lecturer, Dr Jan Lamperski His support and advice helped though my period of study and it is his effort that mainly contributed to my coming over to Ireland

I owe a lot to the technicians in the Electronic Engineering department especially to Robert Clare

Furthermore I would like to thank my lab mates Paul Maguire, Brendan Kennedy, Damien O'Rourke, Antonia Dantcha and Aisling Clarke A special word of thanks goes to Frank Smyth for his help with the simulation

Finally to my friends for their help and support Sanda and Radu, Gabriel and Cristina, Valentin, Arul and Ram Unfortunately it is impossible to list everyone who played a role in bringing my work to completion Nevertheless they will always be in my thoughts

Abstract

Developing broadband access networks is one of the most urgent needs in the telecommunications world The wireless systems provide an efficient solution to address the requirements for last mile connectivity of data, Internet and voice services Radio systems using millimetre-wave frequencies can supply home users with capacities in the order of 50-200 Mbit/s Such bit rates allow the transmission of broadband applications including digital TV, video-on-demand etc In order to provide the massive capacities that are required for the distribution of such broadband data between Central Station and Base Stations, optical fiber can be employed The enormous transmission bandwidth and low loss of the fiber ensure that high capacity microwave signals can be encoded on an optical carrier and successfully transmitted from a Central to Base Station

The goal of this project was to develop and test a radio over fiber communication system This involved investigating the generation of microwave optical signals for transmission in optical fiber, followed by an examination of the effect of fiber propagation on the microwave optical signals

Table of Contents

Approval ____ *ii*

Declaration ____ *iii*

Dedication ____ *iv*

Acknowledgement ____ *v*

Abstract ____ *vi*

Table of Contents ____ *vii*

List of Figures ____ *xi*

1 Introduction ____ *1*

1 1 Introduction to radio/fiber systems ____ **1**

1 2 Basics of the cellular systems ____ **3**

1 2 1 Fundamentals of the cellular communication ____ 3

1 2 2 Characteristic of the radio channel ____ 5

1 2 3 Antennas characteristics ____ 6

1 2 4 Link analysis ____ 7

1 3 Fiber - optic systems ____ **9**

1 3 1 Light sources for optical telecommunication ____ 9

1 3 2 Optical fiber ____ 14

1 3 3 Optical detectors ____ 17

1 3 4 System design ____ 18

References ____ **20**

2 Radio/Fiber Systems – Overview ____ *22*

2 1 Applications of radio/fiber systems ____ **22**

2 2 Architecture of Radio/Fiber system ____ **24**

2 3 Component design issues for radio/fiber systems ____ **25**

2 3 1 Electrical domain 26

2 3 2 Optical domain 26

2 4 Transmission of RF signals 28

2 4 1 Radio transmission 28

2 4 2 Transmission over fiber 30

2 5 Protocols for future radio/fiber systems 32

References 35

3 Generation of Millimeter-Wave Signals 40

3 1 Direct modulation of a laser 40

3 1 1 External light injection 43

3 1 2 External light injection – simulation 45

3 1 3 External light injection - experiments 48

3 1 4 Resonant modulation 52

3 2 External Modulation 53

3 2 1 Simulation of 2f and 4f generation 56

3 3 Heterodyning 58

3 3 1 Heterodyning - simulation 62

3 4 Optical frequency conversion 66

3 5 Remote upconversion using heterojunction bipolar phototransistor 66

3 6 Comparison of different methods 67

References 69

4 Radio/Fiber System Based on Externally Injected Laser Transmitter 74

4 1 Single Channel System 74

4 2 Two channel system 79

4 2 1 Data transmission 79

4 2 2 Two-tone test 82

4 3 Chromatic Dispersion in Millimetre-wave Transmission Systems **84**

4 3 1 Effect of the chromatic dispersion on the millimeter-wave transmission 84

4 3 2 Overcoming the chromatic dispersion – SSB Modulation 86

4 3 3 Experimental investigation of dispersion 87

References **91**

5 Multichannel System *93*

5 1 Multiplexing techniques used in multichannel systems **93**

5 1 1 Subcarrier Multiplexing 93

5 1 2 Orthogonal Frequency Division Multiplexing 97

5 2 Distortions associated with multicarrier transmission **98**

5 2 1 Sources of distortion 98

5 2 2 Methods of combating distortion in multichannel systems 99

5 3 Multichannel system – experiments **100**

5 3 1 Five-channel system based on direct modulation 100

5 3 2 Five-channel system based on external modulator 110

5 4 WDM/SCM transmission system **113**

5 4 1 Wavelength interleaving 118

References **122**

6 Modelling of a Radio/Fiber System *126*

6 1 SCM System based on a directly modulated laser **126**

6 1 1 Improvement of performance – Free running versus externally injected laser 127

6 2 Multichannel transmission over the fiber **143**

6 2 1 SCM transmission over the fiber 145

6 2 2 WDM/SCM transmission over the fiber 153

References 162

Conclusions *164*

Appendix A *I*

Rate Equations – Steady State Solution I

Dynamic solutions III

Appendix B *XIII*

Appendix C *XVI*

Steady state solution to rate equations XVI

SCM system XX

Random Bit Allocator XXVI

Bit Allocator XXVII

Data_Ode45 m XXVIII

Appendix D *XXIX*

List of Figures

Figure 1-1 Radio/fiber system - basic configuration 2

Figure 1-2 Variation of field strength as a function of distance from the transmitter [7] 6

Figure 1-3 Atmosphere attenuation profile [10] 8

Figure 1-4 Optical communications system 9

Figure 1-5 Power-current relationship for a laser diode 10

Figure 1-6 Digital modulation of a laser diode 11

Figure 1-7 Analogue modulation of a laser diode 11

Figure 1-8 Frequency response of a laser 12

Figure 1-9 Spectrum of a FP laser (a) CW (b) under direct modulation 13

Figure 1-10 Step index fiber (a) refractive index profile (b) end view, (c) cross-section side view 14

Figure 1-11 Attenuation profile for a silica glass fiber [19] 15

Figure 1-12 Total dispersion for conventional fiber [19] 16

Figure 2-1 Spectrum allocation for broadband wireless systems 22

Figure 2-2 Star - ring architecture 24

Figure 2-3 Star-tree topology 25

Figure 2-4 Received RF power vs fiber length for transmission of 16 GHz signal 31

Figure 3-1 Simulation model - external injection 45

Figure 3-2 Frequency response of the free running laser (squares), laser under the external injection (circles) 46

Figure 3-3 Optical spectrum (a) under external injection, (b) free running 46

Figure 3-4 RF spectrum of the signal from self-pulsating laser 47

Figure 3-5 21 GHz detected waveform from self-pulsating laser 47

Figure 3-6 Self-pulsating frequency vs injected optical power 48

Figure 3-7 External light injection - experimental set-up 49

Figure 3-8 Enhancement of the modulation bandwidth of the laser diode achieved by external light injection (a) free running, with injection level set to (b) 4 dBm, (c) 5 dBm, (d) 6 dBm 49

Figure 3-9 Optical spectrum of the self-pulsating laser 50

Figure 3-10 Temporal output of the laser under external injection 51

Figure 3-11 Electrical spectrum of the self-pulsating laser 51

Figure 3-12 Self-pulsating frequency as a function of injected optical power 52

Figure 3-13 MZM transfer function 53

Figure 3-14 Analog modulation using MZM 55

Figure 3-15 2f generation using MZM 55

Figure 3-16 Simulation model - 2f and 4f generation 56

Figure 3-17 Optical spectrum (a) 2f generation, (b) 4f generation 57

Figure 3-18 Electrical spectrum - 2f generation 57

Figure 3-19 Electrical spectrum - 4f generation 58

Figure 3-20 Generated sine wave (a) 2f, (b) 4f 58

Figure 3-21 Heterodyning using two lasers - simulation model 62

Figure 3-22 Combined optical spectrum - uncorrelated lasers 63

Figure 3-23 Electrical spectrum - lasers linewidth 40 MHz 64

Figure 3-24 Heterodyning using bimodal laser - simulation model 64

Figure 3-25 Optical spectrum of injection-locked lasers 65

Figure 3-26 Electrical spectrum of the generated RF carrier 65

Figure 4-1 Experimental set-up for radio/fiber system using directly modulated laser with external injection 74

Figure 4-2 Electrical spectrum of the data signal from the pattern generator 75

Figure 4-3 Electrical spectrum of the data signal mixed with signal from Local Oscillator 75

Figure 4-4 Output power vs bias current for laser used in experiments 76

Figure 4-5 Modulating response of the laser (a) free running, (b) under external injection 76

Figure 4-6 Optical spectrums of the laser (a) in free running conditions, (b) under external injection 77

Figure 4-7 Received eye diagrams of 155 Mbit/s signal from the optically fed microwave system using (a) free running laser, (b) laser with the external injection level of 5 dBm 78

Figure 4-8 BER against received optical power of 155 Mbit/s signal from the optically fed microwave system using a) free running laser b) laser with an external injection level of 5 dBm 79

Figure 4-9 Two channel system - experimental set-up 80

Figure 4-10 RF spectrum of the modulation signal 80

Figure 4-11 Spectra of the detected signal (a) without injection (b) with injection 81

Figure 4-12 Received eye diagrams (a) laser with external injection, (b) free running laser 81

Figure 4-13 BER vs received optical power with and without injection (circles - 18 6 GHz, squares - 19 GHz) 82

Figure 4-14 Two-tone measurement - laser with external injection 83

Figure 4-15 Two-tone measurement - free running laser 83

Figure 4-16 Theoretical plot of RF power as a function of fiber length 86

Figure 4-17 Transmission of DSB and SSB signals over the fiber -experimental set-up 87

Figure 4-18 Optical spectrum of the DSB signal 88

Figure 4-19 Optical spectrum of the SSB signal 88

Figure 4-20 Frequency response of the filter 89

Figure 4-21 Signal amplitude as a function of fiber length for DSB (diamonds) and SSB (circles) signal 90

Figure 5-1 4 QAM amplitude-phase plane 94

Figure 5-2 SCM - basic configuration 95

Figure 5-3 Employment of SSB modulation increases spectral efficiency of the system [18] 96

Figure 5-4 Optical spectral efficiency of SCM system in comparison to TDM system 97

Figure 5-5 Experimental set-up of a five-channel system based on an externally injected laser 101

Figure 5-6 BER as a function of received optical power for different channel spacing 102

Figure 5-7 Eye diagrams for IMD's at (a) 50 MHz, (b) 150 MHz – received optical power –18 dBm 103

Figure 5-8 Influence of IMD s on system performance 103

Figure 5-9 Electrical spectrum of SCM signal - laser with external injection - equal channel spacing 104

Figure 5-10 Five-channel system based on free running laser 104

Figure 5-11 Eye diagrams for IMD's at (a) 50 MHz (b) 150 MHz- received optical power – 11 dBm 105

Figure 5-12 Influence of IMD_3 – free running laser modulated at relaxation frequency 106

Figure 5-13 Eye diagrams for IMD's @ (a) 50 MHz, (b) 150 MHz - laser modulated @ 6 GHz - received optical power –9 dBm 106

Figure 5-14 I MD_3 influence - laser modulated at 6 GHz 107

Figure 5-15 Frequency response of the NTT Electronics laser 108

Figure 5-16 Influence of IMD's for laser modulated at relaxation frequency 108

Figure 5-17 Influence of IMD3 on system performance - laser modulated @ 6 GHz 109

Figure 5-18 RF spectrum of the detected signal- modulating frequency close to relaxation oscillation 109

Figure 5-19 RF spectrum of the detected signal - laser modulated at the flat part of the frequency response 110

Figure 5-20 Five channel system based on external modulator - experimental set-up 111

Figure 5-21 Transfer characteristic of the external modulator 111

Figure 5-22 Electrical spectrum of SCM signal 112

Figure 5-23 Influence of IMD_3 - system based on external modulator 113

Figure 5-24 WDM/SCM experimental set-up 114

Figure 5-25 Bragg grating profiles (a) reflection, (b) transmission 115

Figure 5-26 Optical spectrum of the WDM/SCM signal 115

Figure 5-27 Demultiplexed central WDM channel 116

Figure 5-28 Received eye diagrams of 155 Mbit/s data signal (a) back-to-back set-up and (b) after demultiplexing of WDM signal for central optical channel 116

Figure 5-29 BER vs received optical power for central optical channel demultiplexed from WDM system (squares), central optical channel back-to-back case (circles) 117

Figure 5-30 Received eye diagrams of 155 Mbit/s data signal after propagation of WDM/SCM signal through 12 km of standard fiber with Bragg filter positioned to (a) select single side band optical signal, (b) select double side band optical signal 118

Figure 5-31 Different schemes of WDM channel allocation 119

Figure 5-32 BER vs channel spacing 120

Figure 5-33 Optical spectrum of the demultiplexed signal (channel spacing = 0 24 nm) 121

Figure 6-1 Laser P/I curve 129

Figure 6-2 Frequency response of (a) free running laser, (b) laser under external injection 129

Figure 6-3 Electrical spectrum of the modulating signal - single channel system 130

Figure 6-4 Electrical spectrum of the detected signal - free running laser 131

Figure 6-5 Electrical spectrum of the detected signal - laser with external injection 131

Figure 6-6 Eye diagram - free running laser 132

Figure 6-7 Eye diagram - externally injected laser 132

Figure 6-8 BER vs received optical power free running laser (squares), externally injected laser (diamonds) 133

Figure 6-9 Electrical spectrum of the modulating SCM signal 134

Figure 6-10 Electrical spectrum of the detected signal - free running laser 135

Figure 6-11 Eye diagram - free running laser 135

Figure 6-12 Electrical spectrum of the detected signal – laser under external injection 136

Figure 6-13 Eye diagram - laser under external injection 137

Figure 6-14 BER vs received optical power for the central SCM channel free running laser (diamonds), laser under external injection (triangles) 137

Figure 6-15 Electrical spectrum of detected signal with even channel spacing (central channel switched off) 139

Figure 6-16 Electrical spectrum of detected signal with uneven channel spacing (central channel switched off) 139

Figure 6-17 Influence of IMD_3 on system performance - free running laser 140

Figure 6-18 Influence of IMD_3 on system performance - externally injected laser 140

Figure 6-19 Electrical spectrum of laser modulated at relaxation frequency - even channels spacing 141

Figure 6-20 Electrical spectrum of laser modulated at relaxation frequency - uneven channels spacing 141

Figure 6-21 Influence of IMD_3 on system performance for free running laser modulated at relaxation frequency 142

Figure 6-22 Laser module parameters 145

Figure 6-23 Frequency response of laser used in the simulation 146

Figure 6-24 Simulation model 146

Figure 6-25 SCM module 147

Figure 6-26 Parameters of the pin module used 147

Figure 6-27 Parameters of the fiber module used 148

Figure 6-28 Optical spectrum of the SCM signal 149

Figure 6-29 The output of the fiber after optical filtering 150

Figure 6-30 RF spectrum of the detected signal 150

Figure 6-31 Influence of IMD's for laser modulated at relaxation frequency 151

Figure 6-32 BER vs input optical power for 20 km fiber link 152

Figure 6-33 Eye diagram of the central SCM channel for 7 dBm optical power level 152

Figure 6-34 Eye diagram of the central SCM channel for 16 dBm optical power level 153

Figure 6-35 WDM/SCM system - simulation model 154

Figure 6-36 Optical spectrum of WDM/SCM signal 154

Figure 6-37 Optical spectrum of the demultiplexed central WDM channel for 25 GHz channel spacing 155

Figure 6-38 Detected RF spectrum of the central WDM channel (25 GHz channel spacing) 156

Figure 6-39 BER vs WDM channel spacing for first channel (diamonds), central channel (squares) and fifth channel (triangles) 156

Figure 6-40 Optical filter response 157

Figure 6-41 Optical spectrum of the demultiplexed central WDM channel (44 GHz channel spacing) 158

Figure 6-42 Detected RF spectrum of the central WDM channel (44 GHz channel spacing) 158

Figure 6-43 BER vs fiber input power for central WDM channels for 50 GHz channel spacing 159

Figure 6-44 Eye diagram of the central WDM central SCM channel after propagation over 20 km of fiber (fiber input power 7 dBm) 160

Figure 6-45 Eye diagram of the central WDM central SCM channel after propagation over 20 km of fiber (fiber input power 15 dBm) 160

1 Introduction

1 1 Introduction to radio/fiber systems

The ever growing demand for high bandwidth, allowing broadband applications to be delivered to end-users, forces the system operators to seek new ways to increase the bandwidth and capacity of telecommunication systems It is expected that radio over fiber may be a solution to many problems associated with bandwidth issues Combining optical and radio techniques makes use of both their merits fiber provides a high capacity medium with electromagnetic interference immunity and low attenuation, while radio solves the problem of "the last mile" enabling broadband data to be delivered to the end-users in a quick and cheap manner It can also serve mobile users The architecture of the radio part of the system is likely to be realised in a similar way that is used in mobile systems This means that the terrain over which the system operates is going to be divided into a number of cells Such an organisation ensures the best usage of the available spectrum The radio/fiber systems are likely to use frequencies ranging from around 2 5 GHz up to 200 GHz Frequencies from 18 GHz and above are especially attractive for high capacity networks due to the large bandwidth available for data transfer Furthermore the high oxygen absorption in this range of frequencies gives a large frequency reuse factor, thereby implying a small cell size Subsequently a large number of Remote Antenna Units (RAU) is required to transmit the signals to users in each cell Therefore the deployment of microwave wireless networks would strongly depend on the cost and complexity of the RAU

Future millimetre wave access networks are likely to employ an architecture in which signals are generated at a central location and then distributed to remote RAU using optical fibre, before being transmitted over small areas using millimetre wave antennas Optical feeding of RAU in such systems is an attractive approach, because it enables a large number of RAU's to share the transmitting and processing equipment remotely located from the customer serving area Such architecture should prove to be extremely attractive and cost effective for the provision of future broadband services to a large density of customers

The radio/fiber system consists of the Control Station (CS), RAU and the user terminal The CS is responsible for generating optical signals transmitted through the fiber to the RAU, and also for the interaction between the users of the system with other networks The responsibility for opto-electronic conversion of the signal received from the CS and its transmission through air to the user is handled by RAU The end terminal consists of an RF receiver and a transmitter [1] The schematic of a basic configuration of the radio/fiber system is shown in the *Figure 1-1*

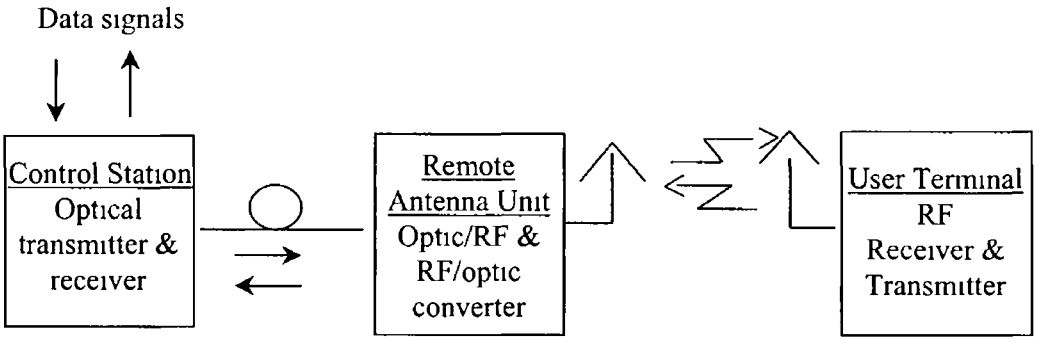

Figure 1-1 *Radio/fiber system - basic configuration*

The advantages of such a realization of the system are

- Simplicity – there is no need for RF frequency conversion or receiver hardware at the Remote Antenna Unit Therefore the RAU is simple, of small size, light weight and low power consumption,
- Increased flexibility - dynamic RF carrier allocation can be implemented from CS,
- Stability of the radio carrier frequency – signals are generated in CS - away from severe climate variations,
- Repairs and services upgrades at a centralized location are most convenient and cost effective

The disadvantage of centralized infrastructure is that the signal travels in analogue form in the fiber Since the detection of the transmitted data is not performed until the RF signal is received at the user end, the noise and nonlinearity generated by the optical transmitter and receiver will combine with interference and multipath effects from the wireless environment to degrade the system quality of the service [2]

The architecture described above can find its applications in broadband communications systems such as

- Satellite communications – earth stations can be situated away from the control area, in order to improve the visibility or reduce interference with terrestrial systems, and fed using optical fiber,
- Multipoint Video Distribution System (MVDS) – transmit-only service which can deliver many TV channels to areas the size of a small town,
- Vehicle communications and control – transmission of low rate signals along major roads,
- Wireless LANs – allowing a broadband connection to the Internet over the air

1 2 Basics of the cellular systems

Wireless communication systems have become an indispensable part of our life The popularity of the mobile telephone, which allows only voice and low data rates transmission, has now surpassed even the most optimistic anticipations In the near future, services such as video on demand, interactive multimedia and high speed Internet will make mobile telephony even more desirable Continuous development of the technology brings the date of introduction of these new systems nearer and nearer

1 2 1 Fundamentals of the cellular communication

1 2 1 1 Organisation of the cellular system

The typical cellular system consists of a Central Station (CS), which controls a set of Base Stations (BS) and is responsible for exchanging the data between a cellular system and the other systems e g Public Switched Telephone Network (PSTN) The terrain over which the cellular system works is divided into cells, each one being served by one BS The BS is responsible for communication with the Mobile Station (MS) The cellular system also includes registers, which store information about all subscribers of the system as well as the guest users This information is used to find a MS in the system, identify it, encode and decode data exchanged between the MS and BS [3, 4]

The cellular concept was the breakthrough in solving the problem of spectrum congestion and user capacity Because of the small area of the cell, the transmitting antenna can operate at a much lower power then in other radio systems This makes

the usage of the spectrum much more efficient Each BS is assigned a portion of the total number of channels available to the entire system and nearby stations are allocated different groups of channels The same frequency can be reused many times, in cells physically separated since the co-channel interference from cells transmitting on the same frequency are considerably low As the demand for services increases the number of BS may be increased (along with reduction in the transmitting power) thereby providing additional radio capacity with no additional increase in radio spectrum The other method of enhancing the capacity of the system is cell splitting This is used to handle the additional traffic within particular existing cell and involves changing the boundary of the cells, height and the power of the BS [5]

1 2 1 2 Sources of the interference in cellular systems

The frequency reuse implies that in the system there is more than one BS transmitting data using the same frequency Cells using the same set of channels are called co-channel cells and signals generated by them are the source of co-channel interference The Signal to Interference Ratio (SIR) in case of co-channel interference, for the system where the size of the cells is approximately the same, does not depend on the power of the transmitter and becomes a function of the radius of the cell (R) and the distance to the centre of the nearest co-channel cell (D) The ratio D/R is called the co-channel reuse ratio (Q) Small values of Q provide larger capacity since the cluster size is small, whereas large values of Q improve the transmission quality due to smaller level of co-channel interferences Thus the trade off must be made between these two objectives in cellular design [4, 6]

Another source of interferences are signals transmitted using adjacent frequencies to the desired channel This is called the adjacent channel interference This problem is especially important in case of the near-far effect, when two stations transmitting on adjacent channels are different distances from the BS In this case the BS may have a difficulty in receiving the signal transmitted by the weaker MS The adjacent channel interference may be limited by using narrowband filters in the BS and careful channel distribution, which means that the adjacent frequency will be assigned to the different BS [6, 7]

Reducing the interference in the cellular system is also achieved by constant power control, which assures that each MS transmits with the minimum power required for

maintaining good quality of the link This also helps to prolong the battery life, which is a vital matter for mobile equipment [8]

1 2 2 Characteristic of the radio channel

The organisation of the cellular system is determined in high degree by characteristics of the radio channel The radio channel is a very specific transmission medium In contrast to other transmission environments the signal from the transmitter can travel and reach the receiver after propagating along different paths This is known as multipath phenomena and is due to the fact that there is usually no "Line – Of – Sight" (LOS) between transmitter and receiver since the antenna of a mobile unit may lie below the surrounding buildings etc Radio waves undergo scattering and diffraction from the nearby obstacles, thereby making the energy reach the receiver via many paths and at varying times This results in a phase difference between particular components of the signal, which may interfere constructively and destructively with each other [4] Because the receiver antenna may be on the move, the surrounding constantly changes thereby changing the phase of particular signal components This means that the received signal at the particular moment in time can experience constructive interference and at the next moment face destructive interference This phenomenon is known as the signal fading In mobile radio communication we distinguish two different fading characteristics short-term fading and long-term fading [4, 9] The first one manifests itself as rapid fluctuations caused by the local multipath It is usually observed over a short distance of about half a wavelength The long-term fading is caused by the movement over distances large enough to produce gross variations in the overall path between BS and MS Therefore the mobile radio signal consists of a short-term fast-fading signal superimposed on a local mean value (see *Figure 1-2*) [10]

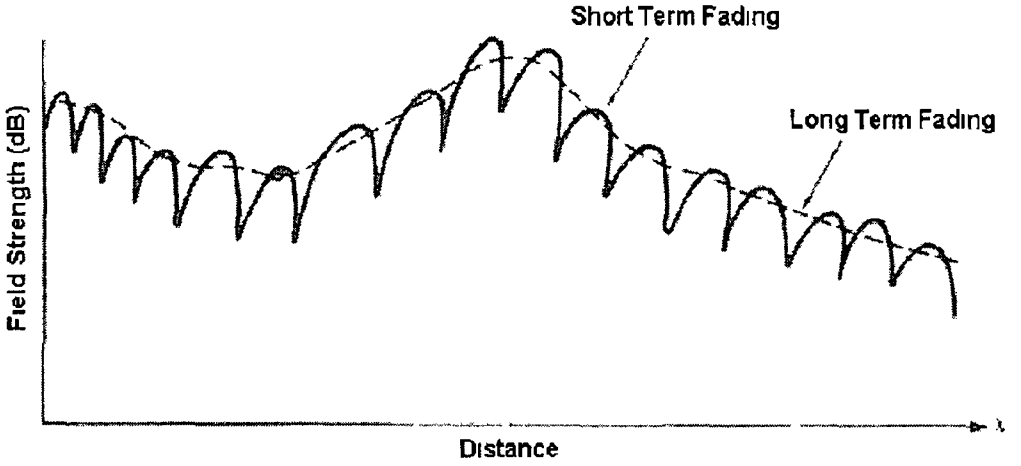

Figure 1-2 Variation of field strength as a function of distance from the transmitter [7]

The multipath phenomenon has one more contribution in the signal degradation it causes the Inter-Symbol Interference (ISI) Since the signal from each path arrives at a different time, the initial pulse is being spread in time The phenomenon known as a delay spread seriously limits the transmission bit rate [7, 11]

The other signal distortion in mobile communication is caused by the Doppler shift If the vehicle is moving at a speed v the received carrier is Doppler shifted by

$$f_d = \frac{v \cos\varphi}{\lambda}, \qquad \textbf{Equation 1-1}$$

where φ – path angle,

λ – carrier wavelength

The Doppler frequency is directly related to the phase change caused by the change in the path length The waves arriving at the receiver from head on to the MS experience a positive Doppler shift and waves arriving from behind the moving MS experience a negative Doppler shift [4, 5]

1 2 3 Antennas characteristics

The proper operation of the wireless system highly depends on the design and the deployment of antennas Since mobile systems are duplex systems, mobile and fixed antennas should have the same performance This is not always possible because the MS has a lower output power and is placed at a lower level above the ground than the BS

The most significant antenna parameter is its gain A high gain can be achieved by increasing the aperture area of the antenna Antenna gain is defined either with

respect to an isotropic antenna or with respect to the half-wave dipole An isotropic antenna is an idealized system that radiates equally in all direction The gain of the antenna in a particular direction is the ratio of the power density produced by it in that direction divided by the power density that would be radiated by an isotropic antenna with the same input power [4, 9]

For an isotropic antenna the power density is constant for all directions Real antennas have stronger power densities in some directions and weaker in other The ratio of the maximum power density of the antenna and the power density from an isotropic antenna defines the directivity of an antenna [6]

The shape of the antennas radiation pattern describes the directionality of the antenna The direction of the maximum power is called the primary beam, major lobe or the front lobe Lobes adjacent to the front lobe are called the side lobes and finally the lobe in the direction exactly opposite to the main lobe is called the back lobe The design goal is to create an antenna with power concentrated in the desired direction and with its side and back lobes as weak as possible The lobes other then the main lobe are a source of interferences between adjacent cells [11]

1 2 4 Link analysis

The power received by an antenna depends on the transmitted power P_T, distance between receiver and transmitter, gain of the receiving antenna and the topography of the terrain over which the signal is transmitted

If we denote the power at the receiver as P_R, then the received power can be calculated from

$$P_R = \left[\frac{\lambda}{4\pi\ r}\right]^2 P_T G_T G_R, \qquad \textbf{Equation 1-2}$$

where P_T – transmitted power,

G_T – gain of the transmitting antenna,

G_R – gain of the receiving antenna,

r – distance between transmitter and receiver

The formula above includes only the power loss from the spreading of the transmitted wave, but it does not take into account other losses such as absorption or scattering [4] The complete version of Equation 1-2 includes the factor L

representing these additional losses (*Figure 1-3*) In terms of decibels received power can be calculated from

$$P_R=20 \log \left[\frac{\lambda}{4\pi\ r}\right]+P_T+G_T+G_R-L, \qquad \textbf{Equation 1-3}$$

The term $20 \log \left[\frac{\lambda}{4\pi\ r}\right]$ refers to free-space loss (L_{los}) in dB and the product P_TG_T is called the Equivalent Isotropic Radiated Power (EIRP) [10]

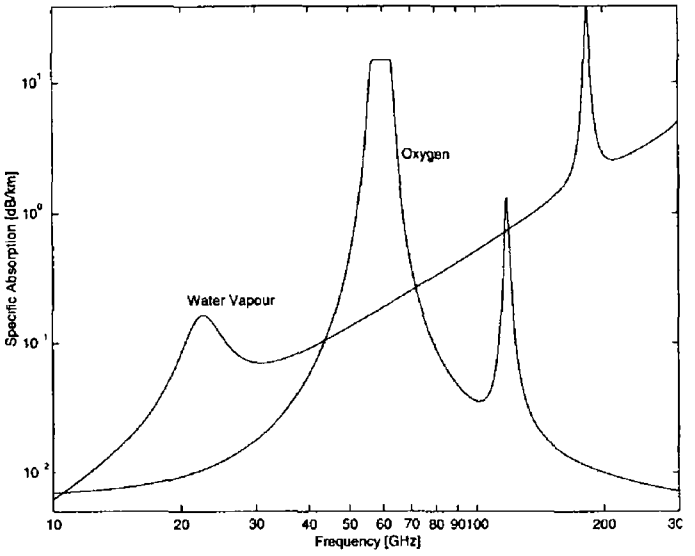

***Figure 1-3** Atmosphere attenuation profile [10]*

From Equation 1-3 one can see that the received power is inversely proportional to the carrier frequency and to the squared value of the transmitter – receiver distance The second statement is true only when there are no reflected waves In most cases this condition is not fulfilled The existence of many waves causes the signal to fade much faster than the formula indicates In fact considering only two beams of the signal one can find out that the received power drops not with r^2 but with r^4 For different environments the exponent changes from 2 to 5 [4]

In practise, due to a high complexity of the calculations, the Equation 1-3 is not used Instead there are few models for predicting the propagation loss in the system for example Okumura, Lee method or Hata formulas Although these are models based on the measurements made in Japanese cities, by using modification factors they can also be applied to other cities or even to the countryside [5, 6, 8]

1 3 Fiber - optic systems

Fiber systems have revolutionised the world of telecommunication The possibilities offered by them are much broader then those offered by the traditional systems built using copper wires The two most important advantages that result from using fiber are very low attenuation (around 0 2 dB/km) and enormous bandwidth These two advantages make optical fiber one of the most popular transmission mediums for all kind of services The simplest fiber system consists of a light source, fiber and a detector as shown in *Figure 1-4*

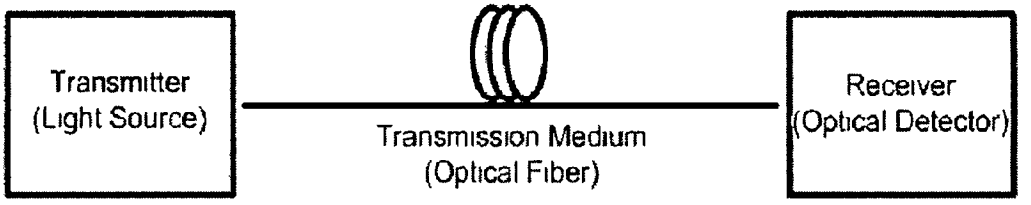

Figure 1-4 *Optical communications system*

1 3 1 Light sources for optical telecommunication

Light sources are used to convert the electrical signals into optical ones, which can then be sent through the fiber There are two basic types of light sources used in fiber telecommunications Light Emitting Diodes (LED) and laser diodes

A LED consists of a forward biased "pn" junction Light in a LED is generated by the process of spontaneous recombination of electron – hole pairs The spectrum line width of the light emitted by a LED is very wide Because of chromatic dispersion in the fiber, the wide spectrum of the generated light limits the possible applications of the LED The other drawbacks of the LED are generally low optical power coupled into a fiber (due to wide beam of LED) and relatively small modulation bandwidth (hundreds of MHz) [14] Nevertheless, LED's have also some advantages, which make them a useful source of light for such applications as transmission over short distances and applications requiring low data rates The above mentioned advantages are simple fabrication, low cost, reliability, low temperature dependence, simplicity of the drive circuit and linear relation between driving current and optical power [20]

Unlike LED's the laser light is generated by the process of stimulated emission i e the atom transition takes place as a result of interaction between an atom and the

photon, which has energy equal to the energy gap in the material The new photon generated in this way has the same characteristics as the photon, which interacted with the atom This means that their frequency, phase, polarization and direction are equal Light emitted by a laser is thus coherent, in contrast to light emitted by LED's [20, 12]

1 3 1 1 Characteristics of Laser Diodes

The static and dynamic characteristics of lasers have a vital influence on the performance of a communication system employing a laser transmitter They determine the usefulness of the source for various applications Some of the most important characteristics amongst them are the dependence of the laser output power on the bias current, the frequency response of the laser, the power vs wavelength dependence (optical spectrum of the laser) and the influence of direct modulation on the laser spectrum

Power/current relationship

The P/I curve of a typical laser is shown in the *Figure 1-5* From the plot it can be seen, that the output power of a laser increases slowly with the increase of the bias current till the current reaches a threshold value Beyond this point the optical power increases significantly even for a small increment in current The threshold current is usually in the range of about 15 to 40 mA The linearity of the laser P/I curve is especially important in applications such as direct modulation of the laser [12]

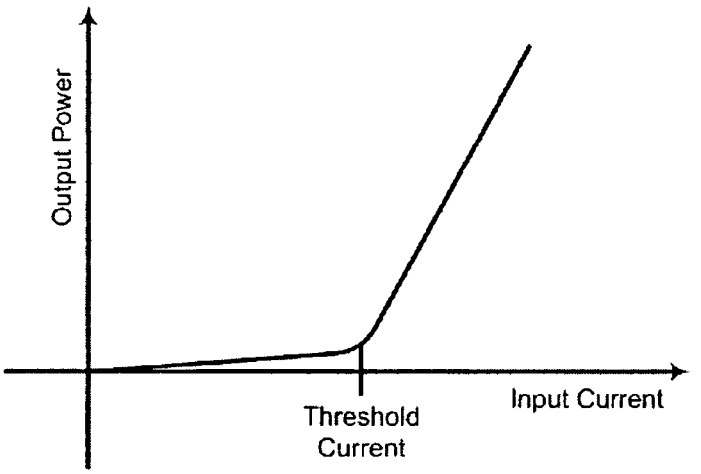

Figure 1-5 Power-current relationship for a laser diode

The digital modulation of a laser diode is illustrated in *Figure 1-6* A dc bias current is used in conjunction with the modulation signal, which places the current at

threshold when there is a logical zero Biasing above threshold results in a shorter rise time of the pulse and allows the laser to be modulated at a higher bit rate and with a smaller signal [14]

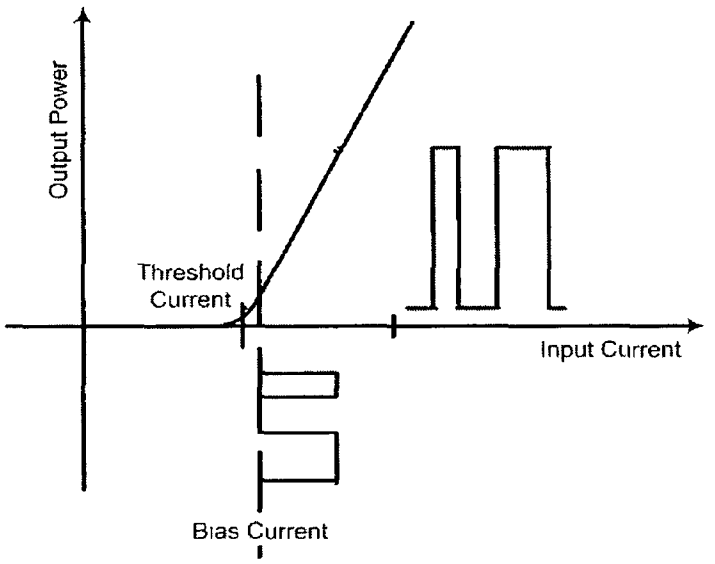

Figure 1-6 *Digital modulation of a laser diode*

For analogue modulation the dc bias has to be higher to ensure that the laser is operating in the linear region of the P/I curve throughout the whole period of the modulating signal (*Figure 1-7*) [2]

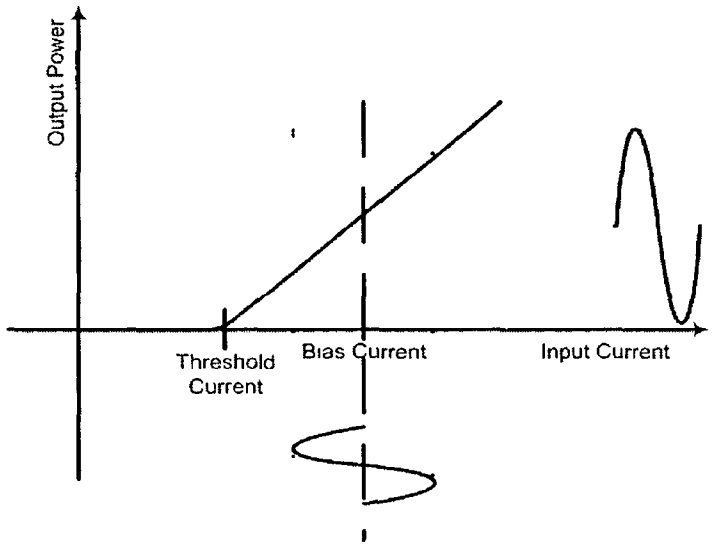

Figure 1-7 *Analogue modulation of a laser diode*

Modulation of a laser diode

A laser diode can be modulated directly by combining the modulating electrical signal with a bias current This leads to an intensity modulated output signal Typical modulation bandwidths of a laser vary from 2 - 5 GHz

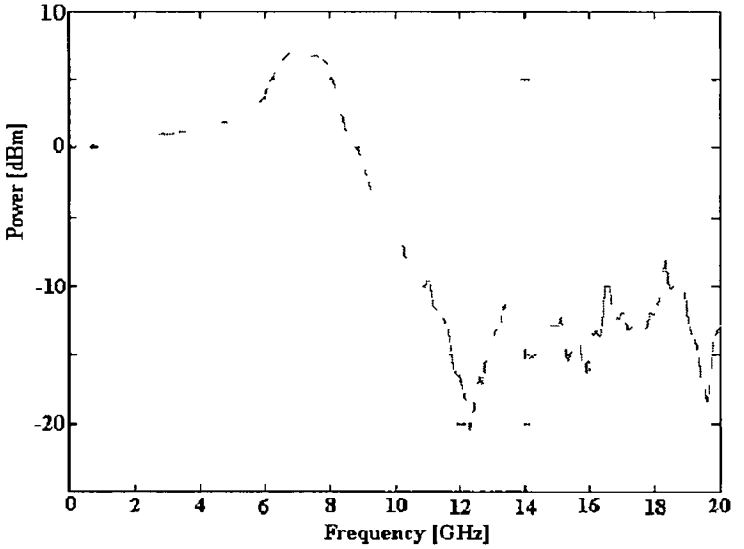

Figure 1-8 Frequency response of a laser

Figure 1-8 shows a response of a 1 55 μm Distributed Feedback Laser (DFB) biased at 35 mA It can be seen that the 3-dB bandwidth of this laser is 9 GHz It can also be seen that the output power of the laser increases at frequencies of 6 – 8 GHz This peak is present in laser responses and is due to the interactions between the photon density and the excess carrier density in the cavity The modulation bandwidth and the resonance frequency peak rise with the increase of the bias current The ultimate limitation for the modulation speed is set by the stimulated photon lifetime

Modulation of the laser drive current not only changes the output power of the laser, but also the emission frequency The carrier density in the cavity varies with changes in current and this in turn leads to a change in the refractive index n of the cavity Because the wavelength generated by the laser depends on the value of n the frequency emitted by the laser fluctuates with changes in injected current This phenomenon is known as chirp and causes spectral broadening [14] Chirp has negative influence on the transmission system performance because it increases the effect of dispersion on the signal propagating along the fiber The spectrum of a FP laser running CW and under direct modulation is shown in *Figure 1-9* We can see that the spectral width of each mode is broadened due to chirp

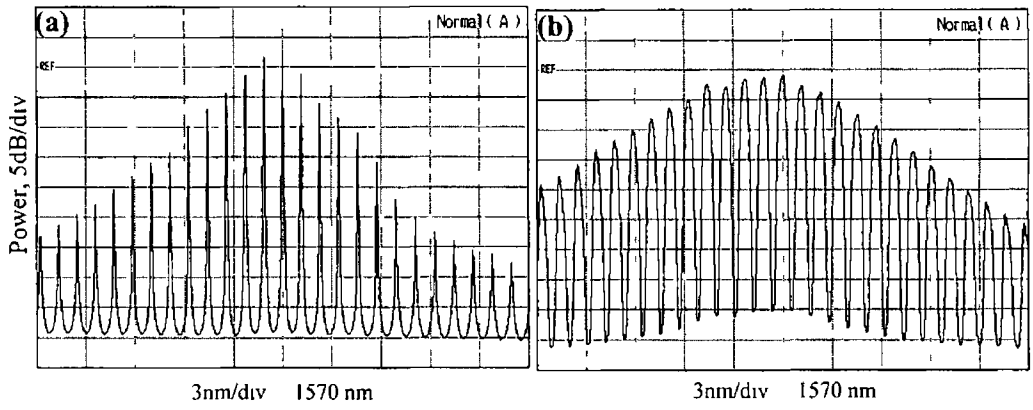

Figure 1-9 Spectrum of a FP laser (a) CW (b) under direct modulation

Laser output spectra

The spectrum of the laser diode depends on its structure The simplest laser consists of a p-n junction closed between two mirrors This structure is called a Fabry-Perot (FP) resonator In such a device the light travelling in the laser cavity is reflected from the mirror If for a particular wave, the round-trip time along the cavity equals an integral number of wavelength, the incident and reflected waves interfere constructively Otherwise the destructive interference takes place and the wave is attenuated [13] In effect the output of the laser consists only of wavelengths that fulfil the following condition

$$2\ D\ n = N\ \lambda, \qquad \textbf{Equation 1-4}$$

where D - distance between the mirrors,

n - refractive index of the laser material,

N - an integer

λ - wavelength [14]

Out of the infinite number of wavelengths that fulfil Equation 1-4, the laser emits only those, for which the gain (due to the resonance) exceeds the mirrors reflection loss and the attenuation of the laser cavity A typical spectrum of an FP laser is shown in *Figure 1-9* (a) The spacing between laser modes depends on the length of the laser cavity and typically is of the order of few nanometres [19] Signals generated by multimode lasers suffer from dispersion, while propagating along the fiber and they are not suitable for long haul communication This is due to their large spectral width In order to avoid signal degradation, while transmitting over long distances, single mode lasers such as Distributed Feed – Back (DFB) or Distributed Bragg Reflector (DBR) are used In these devices the Bragg grating is used to limit

the numbers of wavelengths generated by laser In the first case the grating is applied over the whole active region, while in DBR the grating replaces the mirror at the end of the cavity [19] Single mode lasers can be used in long haul communications, because signals generated by them are less prone to the fiber dispersion

1 3 2 Optical fiber

The typical medium used for the transmission of the optical signals generated by lasers and LED's is the optical fiber It is usually made of silica glass The light propagates through the core, which is the central part of the fiber Surrounding the core is a cladding Because the cladding has a lower refractive index than the core, light incident on the boundary between both of them is reflected back into the core (Total Internal Reflection)

One of the important fiber parameters is the core - cladding index difference defined as

$$\Delta = \frac{n_1 - n_2}{n_1}, \qquad \textbf{Equation 1-5}$$

where n_1, n_2 - refractive index of core and cladding respectively

The simplest type of fibre is known as a 'step-index' fibre (*Figure 1-10*), since there is a step in the value of the refractive index at the boundary between the core and the cladding

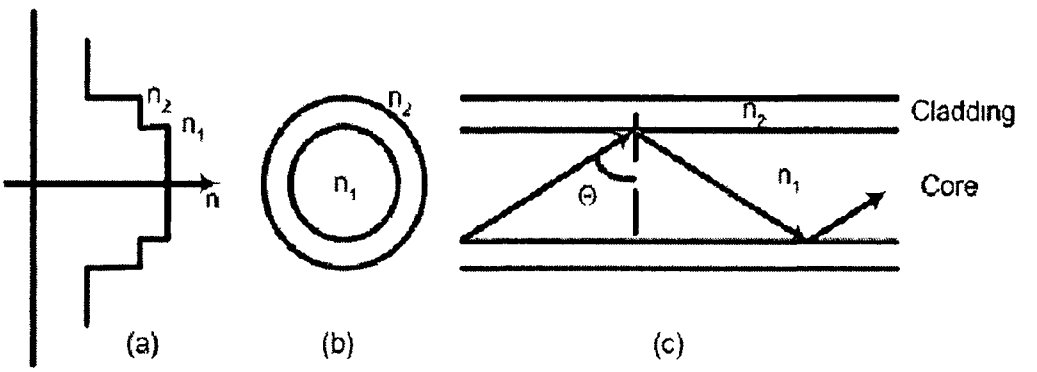

Figure 1-10 Step index fiber (a) refractive index profile (b) end view (c) cross-section side view

1 3 2 1 Fiber characteristics

The main fiber characteristics are attenuation, dispersion and fiber nonlinearity

Attenuation Since it determines the maximum transmission distance, attenuation is one of the most important parameters of the transmission medium Attenuation of presently produced fiber is equal 0 2 dB/km around the normally used transmission

window of 1550 nm, and is much lower than the attenuation of copper wires The main contributing factors of fiber attenuation are

Material absorption – the maximum absorption of the silica falls on the ultraviolet and on the far – infrared region The main impurity leading to absorption is the hydroxide (OH) ion, which has a fundamental vibratory absorption peak at about 2 73 μm Overtones of this peak give rise to the dominant peak near 1 37 μm (*Figure 1-11*)

Rayleigh scattering – is an intrinsic loss mechanism caused by the interaction of photons with the molecules of silica itself

Bending loss – loss introduced by physical stress on the fiber

The attenuation of a fiber determines the light wavelength used for transmission In the attenuation profile one can distinguish three regions with the minimum losses – so called transmission windows The most exploited is one with its centre wavelength of 1550 nm because of existence of optical amplifiers for this range of frequencies

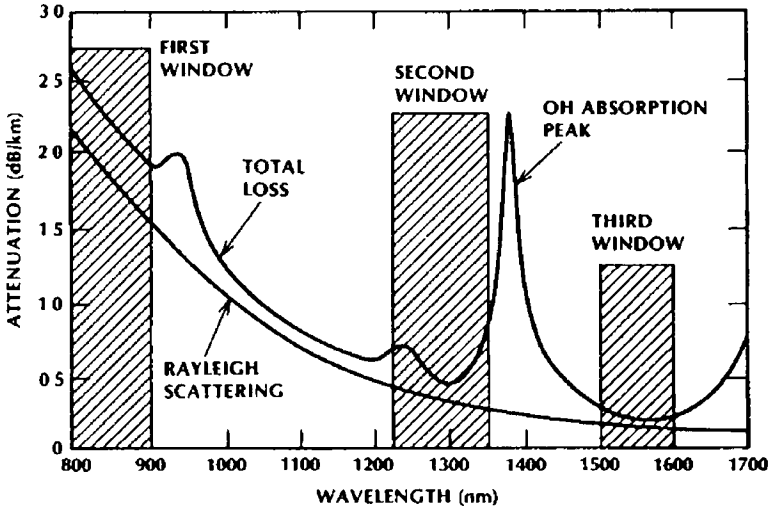

Figure 1-11 Attenuation profile for a silica glass fiber [19]

Dispersion This factor causes pulse broadening as a data signal propagates in the fiber, and limits the bandwidth – distance product of optical transmission systems Dispersion is not constant but depends on operating wavelength (*Figure 1-12*) There are two main types of dispersion in standard step index single mode fiber

Chromatic dispersion – is caused by the fact that the refractive index of the core is not constant but is a function of the wavelength Since the speed of the light in the fiber depends on the refractive index with the law

$$v_g = \frac{c}{n(\omega)}, \qquad \text{Equation 1-6}$$

(c – speed of light, n – refractive index, ω – frequency of the light), different frequencies travel in the fiber with different speed and again arrive the detector at different moments The broader the spectrum of the light, the stronger the effect of chromatic dispersion That is one of the most important reasons why we use lasers instead of LED and also why single mode lasers are preferable to multimode lasers for long haul systems

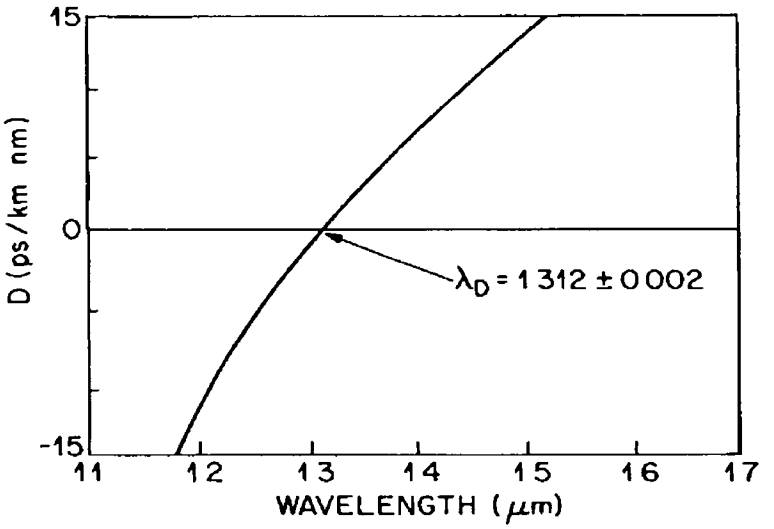

Figure 1-12 Total dispersion for conventional fiber [19]

Waveguide dispersion – this type of dispersion arises when the optical signal is not completely confined to the core Because the refractive index in the core is higher that in the cladding, shorter wavelengths, which are more confined to the core will travel slower that longer wavelengths The waveguide dispersion has a much smaller effect on the propagation of optical signals than chromatic dispersion but can be used for altering overall dispersion in the fiber

Nonlinearity For the high intensity of the light the refractive index of the fiber becomes non-linear and reveals a dependency on the intensity of the electromagnetic field The nonlinearity in the fiber manifests itself as two main effects self-phase modulation (SPM) and Cross-Phase Modulation (XPM) [15 - 17]

1 3 3 Optical detectors

The opto-electronic conversion, at the receiver in any optical communication system, is done by a photodetector This is a crucial component for an optical system, which to a large degree determines the overall system performance There are two basic types of photo detectors that can be used the pin photodiode and the Avalanche PhotoDiode (APD)

The pin photodiode is formed from a reversed bias pn junction where the n layer consists of two sub - layers, a lightly doped n layer and a highly doped n+ layer The n type material can be considered to be an intrinsic one and it makes the depletion region of the structure wider than in the case of a simple pn junction The light incident on the photodiode is absorbed and the electron - hole pair is generated A long depletion region increases the efficiency of the photodiode (more photons are absorbed in the depletion region), but at the same time decreases the bandwidth of the detector (carriers have to travel longer distances, before being collected at the photodiode terminals) thus slowing down device operation

The APD construction is more complicated in order to achieve an extremely high electrical field The APD consists of an absorption region where the primary carriers are generated and the gain region, where carriers are accelerated in order to achieve sufficient energy to excite new electron –hole pairs This process is known as an impact ionisation and it leads to an avalanche breakdown in ordinary reverse biased diodes APD requires very high reverse bias but in turn multiplication factors as great as 10^4 can be obtained

1 3 3 1 Parameters of the photodiodes

Quantum efficiency The quantum efficiency η is defined as the fraction of incident photons that are absorbed by the photodiode and generate electrons collected at the detectors terminals

$$\eta = \frac{r_e}{r_p}, \qquad \textbf{Equation 1-7}$$

where r_p - incident photon rate (photons per second),

r_e - corresponding electron rate (electron per second)

Responsivity It gives the transfer characteristic of the photodetector and is defined as

$$R = \frac{I_p}{P_o}\left[\frac{A}{W}\right], \qquad \textbf{Equation 1-8}$$

where: I_p - output photocurrent in amperes,

P_o – incident optical power in watts.

Bandwidth. The speed, at which a detector responds to changes in an optical input signal, is a vital parameter. Generally this value is expressed as the rise time or bandwidth of the detector. Rise time is the time the output signal takes to increase from 10% to 90% of the final level after the input is turned on instantaneously. The rise time factor can be connected to the 3 dB bandwidth of the detector by using the formula:

$$B = \frac{0.35}{\tau_r}, \qquad \textbf{Equation 1-9}$$

where: B - the bandwidth,

τ_r - the detectors rise time.

The detector bandwidth is very important for high-speed communications. In digital systems insufficient bandwidth can lead to pulse deformation and InterSymbol Interference (ISI), while in analog systems it will reduce the power of the signal [14].

Long wavelength cut off. Photodiodes will only detect photons with its energy being equal or greater than the energy gap of the material used to build the detector. Therefore for each photodetector there is a maximum wavelength, which can be detected. This cut off wavelength can be calculated from:

$$\lambda_c = \frac{\hbar c}{E_g}, \qquad \textbf{Equation 1-10}$$

where: $\hbar$ – Plank's constant, c – speed of light, E_g band - gap of the material [18, 19].

1.3.4 System design

The dominant criteria in designing an optical system are the desired transmission distance and the rate of information, which can be transmitted. Thus in order to design an optical communication system the power and the rise time budgets have to be considered.

1.3.4.1 Power budget

Correctly constructed power budget ensures that the signal after propagation over the entire system has enough power to achieve a desired Signal-to-Noise Ratio (SNR) or

Bit Error Rate (BER) at the receiver Power budget takes into account the transmitted power, receiver sensitivity (power required at the receiver to ensure "errorless" detection), amplification and total loss of the link It also includes a safety margin to allow system aging, fluctuations and repairs (extra splicing of broken fiber etc) In the simplest form the power budget is

$Power_{transmitter}$ – total loss + amplification = margin + receiver sensitivity [14, 19, 20]

1 3 4 2 Rise-time budget

A rise-time budget determines the total capacity of the system It takes into account the response times of all the system components The bandwidth of a system can be calculated from Equation 1-11 In the simplest case, the rise-time of a system is the cumulative rise-time of a transmitter, receiver and fiber and can be calculated from

$$t^2_{system} = \sqrt{t^2_{transmitter} + t^2_{receiver} + t^2_{fiber}}, \qquad \textbf{Equation 1-11}$$

The rise-time of a fiber depends on its dispersion properties and spectral width of the transmitter and is much lower for single mode fiber than for multimode fiber It also depends on the length of the fiber The longer the link, the slower the response [14, 19]

References

[1] R P Braun, "Fiber Radio Systems, Applications and Devices", ECOC'98 Tutorial

[2] B Wilson *et al* "Analogue Optical Fibre Communications", IEE, London 1995

[3] H Al-Raweshidy "Radio over Fiber Technologies for Mobile Communications Networks", Artech House, London 2002

[4] K Wesolowski "Mobile Communication Systems", John Wiley & Sons Ltd , 2002

[5] T S Rappaport, "Wireless Communications - principles and practice", Prentice Hall PTR, New Jersey 1996

[6] W C Y Lee "Mobile Cellular Telecommunications – analog and digital systems", McGraw-Hill, Inc , New York 1995

[7] W C Y Lee "Mobile Communications Design Fundamentals", John Wiley & Sons Inc New York 1993

[8] V K Garg *et al* "Wireless and Personal Communications Systems", Prentice Hall PTR, Upper Saddle River 1996

[9] K Siwiak "Radiowave Propagation and Antennas for Personal Communications", Artech House, London1995

[10] M P M Hall *et al* "Propagation of Radiowaves", The Institution of Electrical Engineers, London 1996

[11] P Bharita "Millimeter Wave Engineering and Applications", John Wiley & Sons, New York 1984

[12] G Keiser "Optical Fiber Communications", McGraw-Hill Higher Education, New York 2000

[13] A Yariv "Optical Electronics in Modern Communications", Oxford University Press, Oxford 1997

[14] J Hecht "Understanding Fiber Optics", Prentice-Hall International (UK) Ltd, 2002

[15] G P Agrawal "Nonlinear Fiber Optics", Academic Press, 1989

[16] H D Young "University Physics", Addison Wesley, 1992

[17] B Mukherjee "Optical Communications Systems", McGraw Hill, 1997

[18] J C Palais "Fiber Optic Communications", Prentice Hall, Upper Saddle River 1998

[19] J M Senior "Optical Fiber Communications – Principles and Practice", Prentice-Hall International (UK) Ltd, 1985

[20] A Rogers "Understanding Optical Fiber Communications", Artech House, Inc London, 2001

2 Radio/Fiber Systems – Overview

2 1 Applications of radio/fiber systems

As mentioned in the Introduction radio/fiber systems present many advantages over standard wired systems The bandwidth offered by them can be utilised to transmit many different signals and hence can be used for numerous applications

The radio spectrum has been divided by regulatory bodies into frequency bands devoted to different applications and systems The spectrum allocation is shown in *Figure 2-1*

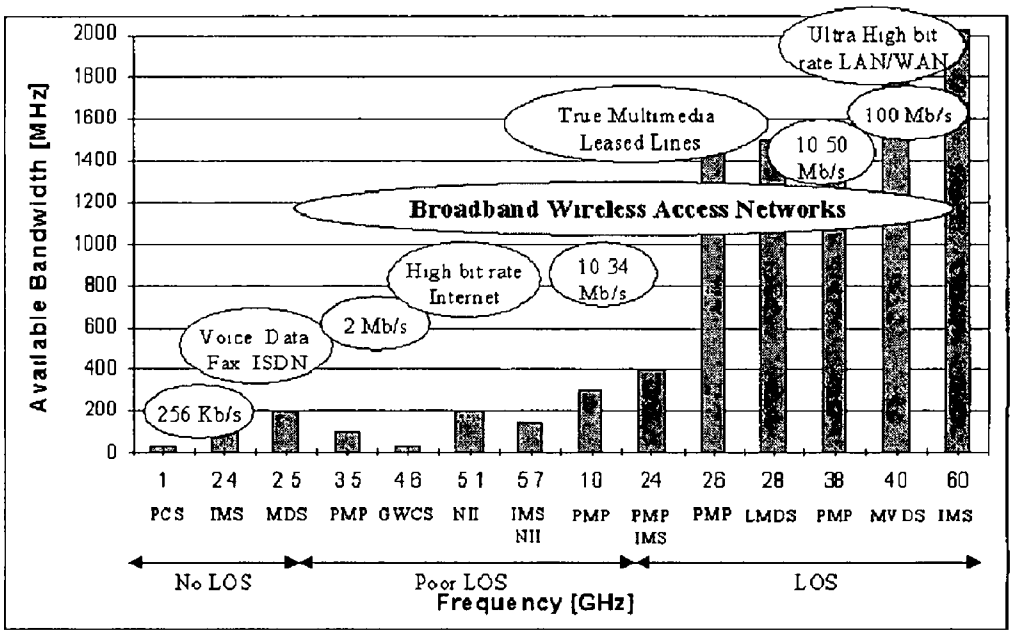

Figure 2-1 *Spectrum allocation for broadband wireless systems*

PCS- Personal Communications System

ISM- Industrial, Scientific and Medical

MDS- Multi-channel Distribution System

PMP-Point-Multi-Point

GWCS- General Wireless Communications Service

NII- National Information Infrastructure

LMDS- Local Multipoint Distribution System

MVDS- Microwave Video Distribution System

LOS- Line of Sight

As it can be seen from *Figure 2-1* radio/fiber system could be applied in systems using the frequencies from 2 5 to 60 GHz [1] With respect to the target users the systems are loosely divided into two groups

1 Point – to – multipoint communications (PMP) for low and medium subscriber densities (around 3 5 and 10 GHz)

2 PMP for high subscriber densities (24-26, 27-29 and above 40 GHz)

Many standards have been proposed for above-mentioned systems [2, 37]

1 IEEE 802 11 Standardisation Committee develops standards for the following frequency bands [3]

- 2 4 GHz – wireless-Local Area Network (W-LAN) supporting 11 Mb/s data rates with frequency hopping and direct spread spectrum techniques [4]
- 5 GHz – system using Orthogonal Frequency Division Multiplexing (OFDM) [5]
- 10 – 66 GHz – PMP system providing peak capacities up to 2 –155 Mb/s and supporting two modes of transmission continuous and burst transmission streams
- 2 –11 GHz PMP systems offering flexible connection for asymmetric traffic [6]

2 European Telecommunications Standards Institute/Broadband Radio Access Networks (ETSI/BRAN) develops new standards for networks providing transparent connectivity for licensed and license-exempt applications HIPERACCESS group focuses on systems using 40 GHz frequency band This system will use 25 MHz channels with a single carrier transmission for each BS [7, 8]

3 Local Multipoint Distribution System - technology used to deliver voice, data, Internet and video services with the use of 25 GHz and higher frequencies It offers data rates of 155 Mb/s It is a solution to local-access bottleneck [9]

4 Microwave Video Distribution Service (MVDS) – system design mainly to deliver digital video program It is being adapted for two-way connectivity [9]

5 Frequencies above 60 GHz can be also used for vehicle communications and control (Europe) Systems fulfilling this task will distribute a low data rate along major Europeans roads [6 -10]

2 2 Architecture of Radio/Fiber system

In hybrid radio/fiber systems the connection between the Central Office (CO) and Remote Antenna Unit (RAU) may be realised with the use of fiber Wavelength Division Multiplexing (WDM) may also be employed in above-mentioned systems, similar to other optical networks [11, 12] Utilisation of WDM allows many BS's to be fed by common fiber, reducing the cost of the system Many different topologies maybe employed for hybrid radio/fiber distribution systems The choice of architecture depends on numerous considerations such as crosstalk, efficient utilisation of fiber bandwidth etc

There are two main proposals for the architecture of a radio/fiber system employing WDM star - tree and star – ring topology A combination of all three (star- ring-tree) is also possible [13, 14]

In the star-ring configuration the CO is connected to many BSs BSs are divided into groups, each group being connected to one unidirectional fiber - ring Each ring uses the same set of wavelengths Each RAUis assigned one wavelength and uses it for the up- and the downlink A simplified schematic of the star-ring configuration is shown in *Figure 2-2*

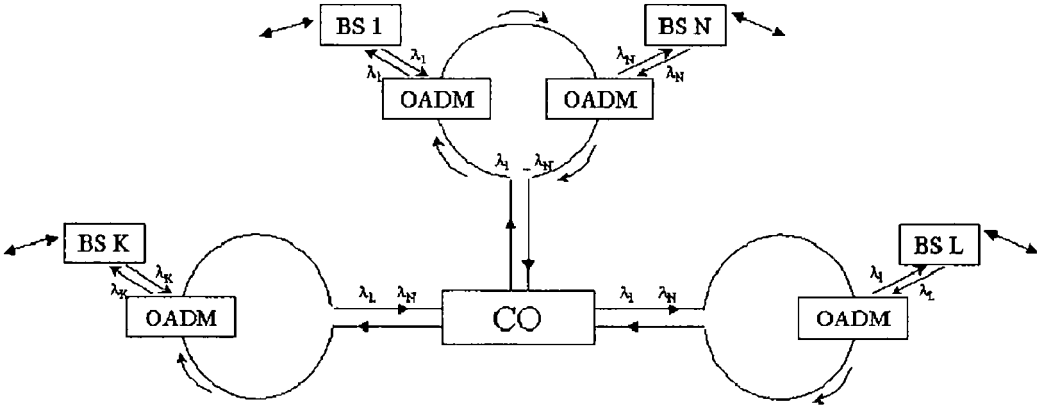

***Figure 2-2** Star - ring architecture*

In the star-tree topology, a bidirectional fiber link routes traffic to a single multiplexer/demultiplexer, which distributes different wavelengths to individual BSs [15] The up- and downlinks use different wavelengths unless two unidirectional fibers are installed (separate fiber for up- and downlink) The star-tree architecture is shown in *Figure 2-3*

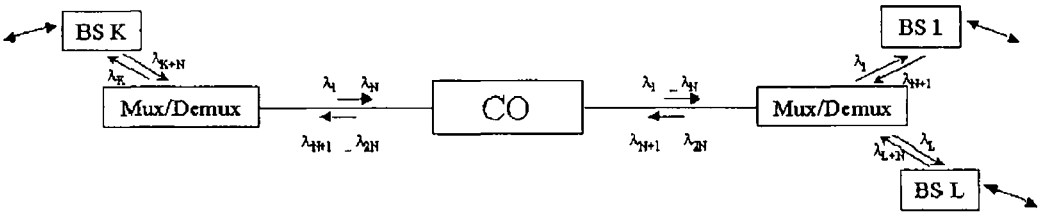

Figure 2-3 Star-tree topology

The topology chosen for a system will have an influence on system performance mainly due to the crosstalk In radio/fiber systems two reuse scenarios are used optical – the same wavelength can be used many times in separate rings (trees) and electrical - RF frequency can be reused in separate rings and trees, but also within the same ring (tree) for non-adjacent BS Because of components imperfections, signals transmitted in the network can leak and appear at ports that they are not supposed to These signals are the source of the crosstalk There are two types of crosstalk

1 in-band interfering signal is at the same wavelength as the required signal,
2 out-of-band interfering signal is at a different wavelength

The in-band crosstalk can be caused for example by imperfections in Optical Add Drop Multiplexers (OADM) In a ring configuration the signal on a certain wavelength, carrying the data from CO to BS, is dropped at an OADM This component will not remove the whole signal, thereby allowing some of it to leak through and continue propagating along the fiber If the same wavelength is used for communications for transmitting information from BS, the dropped signal will interfere with the added one The in-band crosstalk cannot be optically filtered It can be filtered electrically under the condition that the "add" and "drop" signals carry data on different RF frequency

Out-of-band crosstalk occurs for example in tree topology, when part of signal is reflected at the demultiplexer and travels back towards CO Out-of-band crosstalk can be filtered out optically [13]

2 3 Component design issues for radio/fiber systems

The realisation of a radio/fiber system presents a challenge in terms of both the required components and system design This is mainly due to the high frequencies that are used in radio/fiber networks The concerns that are raised could be categorised to be from two major areas within the radio/fibre networks

2 3 1 Electrical domain

On the electrical side we need high-speed electronics, such as signal generators, amplifiers, mixers etc , to drive the optical transmitters and process the signals Furthermore, the required microwave filters and antennas must also be capable of handling these high frequencies [9] There is a lot of research carried out in these areas and the main problem is associated with the design of components capable of delivering high powers at millimeter-wave frequencies This can be achieved by semiconductor components only in the lower millimeter-wave frequency range At higher frequencies electron tubes have to be used The travelling wave tube is the most common amongst them [16, 17] Similarly, in the case of filters for low power applications and frequencies not exceeding 10 GHz a novel technology known as the surface acoustic wave is becoming more and more popular However, for high powers and frequencies, waveguide and coaxial filters have to be used Also a lot of research has been undertaken in the field of antennas Even though the parabolic dish reflectors are still a popular solution, new configurations are also making considerable inroads (in many systems) This includes flat-plate, modular lensed antennas, active arrays and phased arrays [18 - 20] Fathy *et al* propose an innovative concept of a plasma-reconfigurable antenna, which can be modified dynamically to enable different functions The aperture of such an antenna can be specially tailored towards an application in order to increase its efficiency and signal processing speed The reconfigurable antenna enables frequency hopping, beam shaping and steering in a simple manner [21] Another type of reconfigurable antenna is the multibeam active phase array [22] The main advantage of using such antennas is their high reconfigurability, which means that almost any shape of coverage and any shape of low sidelobe area can be designed

Important issues in designing antennas for millimeter-wave systems are small size, low weight and high gain The latter criterion arises from the low output powers of opto/electronic converters, which in turn occurs as a direct consequence of the requirement for minimal power consumption of a RAU [10]

2 3 2 Optical domain

The optical domain also creates many obstacles that have to be overcome if radio/fiber systems are to be successfully employed The main challenge here is the

generation of high frequency signals in an optical manner The most commonly used method of electro/optic conversion involves direct modulation of the laser drive current This allows the generation of frequencies that typically do not exceed 10 – 15 GHz (due to the limited modulation bandwidth of a laser) The commercial realisation of very high-speed laser diodes still has a long way to go, even though there are reports involving the design of lasers that exhibit a 3 dB bandwidth of 40 GHz and output powers around 35 mW [23] Another technique associated with the generation of an optical RF signals entails external modulation In the optical domain, one of the most popular modulators is the Mach-Zehnder Interferometric modulator (MZI) However the Elector-Absorption (EA) modulators have recently attracted more and more interest because of their better linearity and easy integration with semiconductor lasers Even though external modulators with bandwidths of 70 GHz have been reported [24, 25], commercially available external modulators do not go beyond 40 GHz Therefore a lot of effort has been put into the search for alternate, cheap and reliable techniques of generating high frequency optical microwave signals A detailed description of the possible methods that could be used to achieve the fore-mentioned goal can be found in the next chapter

Increasing the performance of optical detectors is another challenge, faced within the optical domain, on the way to realising radio/fiber systems Nevertheless, researchers have demonstrated photodiodes with bandwidths of hundreds of gigahertz [26, 27] One of the up and coming architectures of photodiodes involves the use of side-illuminated structures, which in comparison to the common surface illuminated ones realise greater bandwidth and better efficiency As with the modulators, the possibility of integrating the photodetector with other optic and optoelectronic components is an important issue that offers high-speed operation, compactness and cost reduction It also enhances the coupling efficiency between the fiber and detector [28] Giraudet *et al* [29] have demonstrated the evanescently coupled waveguide-fed photodiode, which is a type of side-illuminated diode, with responsivity as high as 0 93 and 0 74 A/W for 60- and 100-GHz diodes respectively Another type of photodiode, which could find its application in future hybrid radio/fiber systems, is the Uni-Travelling-Carrier Photo-Diode (UTC-PD) In this type of structure the only active carriers travelling through the junction depletion region are electrons UTC-PD's provide large bandwidth and high-saturation output powers [30] Ito *et al* show an

UTC-PD with a bandwidth of 310 GHz and an output power 12 dBm at 60 GHz [31] Nevertheless, current commercial photodiodes with bandwidths up to 50 GHz are expensive and exhibit low efficiency [10] Another important factor, as mentioned before, is the power consumption of detectors This requirement for energy saving diodes has led to the creation of zero electrical power photodiodes, which do not require bias voltage to perform the O/E conversion [30, 32]

Apart from transmitters and receivers, one of the other important optical components of radio/fiber system employing WDM is the optical filter Typically demultiplexing of signals at the RAUwould require a flat transmission profile and a sharp roll-off Presently available Fibre Bragg Gratings (FBG) fulfil these requirements [33] However the cost of these FBG's has to be reduced

2 4 Transmission of RF signals

2 4 1 Radio transmission

Propagation of RF signals in the air strongly depends on the frequency of the signal Generally the links can be classified with respect to the path that the wave travels before arriving at the receiver Namely the three classes are non- Line-Of-Sight (LOS) links, poor LOS and LOS links as shown in *Figure 2-1* Low frequency signals do not need LOS since they can reach the receiver on being reflected by obstacles These frequencies undergo diffraction, which also allow them to overcome the shadowing effect caused by many disturbances on the way Unfortunately, in the case of short wavelengths the loss caused by diffraction is too high and hence the need for LOS transmission However these waves can still be reflected from buildings and other obstructions, which could result in multipath fading [34]

Another hindrance to the propagation of millimetre-waves is the attenuation caused by walls High frequency radio waves do not have the ability to penetrate buildings In order to ensure access to the network inside the buildings one has to install an indoor BS This obviously increases the cost of employing the system The need for mounting a RAUinside the building, forces the system designers to consider two different cases They are regarded separately as the indoor and outdoor propagation environments, since the propagation conditions for each of them are different

The main problem in designing the outdoor system using millimeter-wave carriers is the attenuation First of all the oxygen and water vapour attenuation line are situated in the millimeter-wave frequency band Thus, the attenuation is highest for frequencies around 60, 119 and 183 GHz, which correspond to the resonance of the oxygen molecule (first and second) and water vapour absorption respectively These attenuation peaks can be used advantageously in very high capacity communications systems, since high attenuation offers high separation between cells and allows the frequencies to be reused much more often than in other (e g GSM) systems [35]

Beside the molecular absorption, the influence of rain, snow or hail is much more severe on high frequency signals This makes the designing of millimeter-wave systems even more difficult, since the act of precipitation cannot be predicted In the system design process, rain statistics for the particular terrain are used to calculate the necessary power margins for required link availability [36]

The indoor transmission of millimeter-wave signals is free from fading due to rain and other weather conditions The main problem here is the multipath fading caused by the reflections from walls and other obstacles, and time variation of the channel due to constant movement, mainly of people, within the buildings Multipath propagation causes not only fading of the signal but also results in different travel times of the data transmitted The latter causes broadening of the data pulses as they travel in the channel Furthermore, if the delay of the signal from the reflected path is longer than the bit duration, multipath propagation causes Inter-Symbol Interference (ISI) The spread of power due to delay depends on the size of the room and its architecture It is important to note that even small rooms can have large delay spreads if their walls are highly reflective Reflected waves experience low attenuation and multiple reflections with significant delays will still have a strong effect on the overall delay spread [37] Delay spread limits the maximum bit rate at which the system can operate

Whether indoors or outdoors, the effects of multipath fading can be overcome by using the diversity techniques [34, 38] This is due to the fact that since the probability of simultaneous fading of signals transmitted either on different frequencies, different polarizations or from different places is very low There are many different diversity techniques

1 spatial diversity – signals are transmitted from two or more different antennas,
2 multicarrier transmission – data is sent using more than one frequency,

3 polarization diversity - transmitted signals have e g circular polarization instead of linear

Also wide band signals (e g spread spectrum) are more immune to fading then narrowband ones since multipath fading affects only a small portion of the signal bandwidth Different equalization methods could also be used to overcome the ill-effects of multipath fading, but they usually are complicated and require high processing powers [39]

2 4 2 Transmission over fiber

The most important of fiber parameters, while considering the transmission of optical millimeter-wave signals over the fiber, are attenuation and dispersion Attenuation causes a reduction in power of an analog signal propagating along the fiber in the same way as in digital systems On the other hand, the effect of dispersion is more complicated In digital systems dispersion causes a linear degradation of the transmitted signal due to pulse broadening Chromatic dispersion is caused by the fact that refractive index of the glass changes depending on the wavelength of the light Because the velocity of the light depends on the refractive index, different frequencies of the light travel in the fiber with different speeds The effect of chromatic dispersion becomes more important as the spectral width of the data signal increases

In analog millimetre-wave systems, dispersion causes the signal to degrade not linearly, but in a periodic manner In hybrid radio/fiber systems one wants to generate the radio carrier remotely in the CS, and then send it through the fiber to BS The radio frequency ranges between 18 – 200 GHz Intensity modulation of the light at the radio frequency produces two main components in the optical spectrum (Double Side Band modulation - DSB), each distant from the light carrier by the radio frequency The space between these side bands equals two times the RF frequency These components are affected by chromatic dispersion, which causes them to travel at different speeds in the fiber, which means that their relative phase also changes The higher the RF frequency, the faster the change in phase When the signal arrives at the receiver, both sidebands beat together producing the electrical RF output However, if the sidebands have opposite phases, they will interfere destructively and no RF signal will be obtained at the output of the receiver Fading is also a periodical occurrence because as the optical microwave signal continues to propagate the two side bands go

from being out of phase to being in phase and out of phase etc [40] The dependence of the electrical power of the received signal (16 GHz) on the transmission length is shown in *Figure 2-4* The first null in the received power appears at the length where the difference in travel times between side bands equals half of the carrier period The second and further nulls occur after double this length (difference in travel time equals full period of the RF signal) [41]

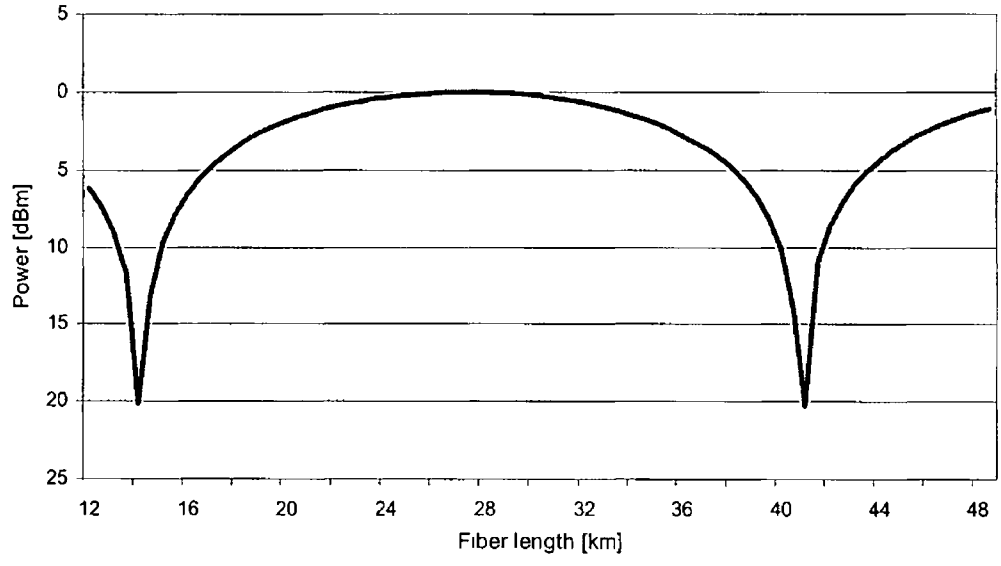

Figure 2-4 *Received RF power vs fiber length for transmission of 16 GHz signal*

DSB signals are thus unsuitable for transmission of RF signals due to dispersion Dispersion caused fading could be overcome by employing Single Side Band (SSB) modulation [42] The effect of dispersion on the propagation of RF signals along the fiber, and the methods of overcoming this problem will be discussed in more detail at a latter stage in this thesis

As mentioned before, future radio/fiber systems may employ WDM When the number of channels and power level of signals transmitted over the fiber increases, the effect of the fiber nonlinearity become more severe [43] Nonlinear effects such as Four Wave Mixing (FWM) or Cross Phase Modulation (XPM) can have a serious impact on system performance They can cause crosstalk not only between WDM channels but also between RF carriers carried by particular wavelength

Analog lightwave systems are more sensitive to noise and distortion than digital systems In order to overcome receiver and optical amplifier noise the average power in analog systems must be higher than for digital signals That is why, even though in

radio/fiber systems fiber link is not very long, fiber induced nonlinearity have a strong influence on system performance [44, 45]

While considering the transmission of RF signals in a radio/fiber system one has to separate the downlink case from the uplink case Signals travelling from the CO to RAU (downlink) experience distortions from fiber attenuation, nonlinearity and dispersion Because the RF signals are not processed in the BS, but sent straight to a user, any degradation of the signal caused by propagation over the fiber will add to those introduced by the radio link This puts huge constraints on signal quality and performance of system components [46] The uplink connection is even more challenging In this case the RAU receives signals from many users, each transmitting at a different frequency These signals are distorted by thermal noise of the RF receiver and by co-channel interference Adjacent channel interference from users transmitting on different frequencies is also present Adjacent channel interferences can be filtered out, while the mixing products of these signals, generated by nonlinearity of the system components, cannot It is important to note that the power level of the received signals would differ since the distance between users and the RAU can vary In the worst-case scenario, if the desired signal is weak or experiences fading, impact of intermodulation distortion can become severe [46] The wide variation in signals amplitudes in the uplink means that the impact of fiber nonlinearity will be much stronger for the uplink than the downlink case

2 5 Protocols for future radio/fiber systems

Performance of the radio/fiber system depends on characteristics of the radio channel such as multipath fading, weather, changing propagation conditions etc Furthermore, the quality of signal for each user in the network is different, depending on the users position as well as locations of other interfering users, traffic load and so on Proper design of the traffic management and connection control can improve the performance of the system In future radio/fiber systems the main challenge in choosing the network protocol arises from the requirement to support many different applications and types of traffic As regards applications there is a need for transmitting real-time data, by providing necessary bandwidth seamlessly across the network (wireless and wired) On the other hand dealing with different types of traffic brings about the problem of coping with symmetric and asymmetric traffic,

continuous and burst data etc In addition, protocol for a wireless system has to operate in situations, where users are moving, which changes the traffic pattern dynamically [39] Wireless links suffer from high BER due to fading The protocol used for radio/fiber systems will need an additional data link control sub-layer for error recovery Furthermore the finite frequency resources for radio transmission means that resource control will also be needed Finally mobility requires new functions to support hand-off, location management, MS authentication and registration and routing of mobile connections [47]

There are two main competitors for wireless broadband systems protocol Internet Protocol (IP) and Asynchronous Transfer Mode (ATM) IP has dominated the data world due to the growth in the Internet and hence it would be a natural choice for wireless Internet [48] Mobile users demand the possibility of receiving all the services available to fixed Internet users The current version of IP is not capable of coping efficiently with huge traffic variations and diversity of user devices while also taking care of the mobility issue Hence a lot of effort has been put into developing a new version of IP for mobile systems resulting in the so-called Mobile IP (MIP) [49, 50] Other problems associated with implementing IP in future radio/fiber systems lies in the fact that IP is a best effort delivery model and it does not allow different treatment of users This makes it unsuitable for many broadband, real-time applications [51] Adapting Internet to transmission of real-time traffic requires changing Transmission Control Protocol (TCP), which cannot guarantee a necessary quality of service (QoS) for such type of data This is a reason for developing Real-Time Transport Protocol (RTP), which is usually implemented on top of User Datagram Protocol (UDP) The next step towards ensuring the required QoS for real-time applications is the employment of Resource Reservation Protocol (RSVP) This is a control protocol, which allows the Internet real-time applications to reserve resources before they start transmitting data Nevertheless, RSVP is not designed for mobile communications This is why RSVP has to be adapted for usage in mobile system [52, 53]

Contrary to IP, ATM is known for its flexibility and resource management capabilities Because ATM cells are generated according to the need of the data source, this protocol can meet dynamic requirements of connections with variable data rates The main advantages of ATM are

- Flexible bandwidth allocation

- Efficient multiplexing burst as well as continuous data traffic
- Improved service reliability with packet-switching techniques
- Ease of interfacing with Broadband Integrated Services Digital Network (B-ISDN)

All these advantages make ATM the most suitable choice of protocol for radio/fiber systems [37, 54, 55] Consequently in 1996 the ATM Forum and ETSI started the work on the extension of the wired ATM to wireless ATM (WATM) [56]

References

[1] N B Pronis *et al* "Broadband Wireless System Overview", *IST Mobile Comms Summit*, Galway, Ireland 2000

[2] R B Marks *et al* "Wireless Internet", *IEEE Microwave Magazine*, vol 2, pp 47-56, 2001

[3] B Emmerson "Roaming for W-LAN Revenue", *International Telecomms*, vol 36, pp 34-38, 2002

[4] www standards ieee org/getieee802/download/802 11b-1999 pdf

[5] www standards ieee org/getieee802/download/802 11ba-2000 pdf

[6] A Dutta-Roy "Fixed Wireless Routes for Internet Access", *IEEE Spectrum*, pp 61-69, 1999

[7] ETSI, Broadband Radio Access Networks (BRAN), "HiperLAN Type 2, Data Link Control (DLC) Layer", *ETSI TS* 101 761-1, vol 2 1, Technical Specification

[8] http //portal etsi org/bran/Summary asp

[9] T Edwards "Gigahertz and Terahertz Technologies for Broadband Communications", Artech House Inc , London 2000

[10] B Wilson *et al* "Analogue Optical Fiber Communications", IEE, London 1995

[11] C A Brackett "Dense Wavelength Division Multiplexing Networks", *IEEE J of Selected Areas in Comms* , vol 8, pp 1323-1324, 1993

[12] S S Dixit *et al* "WDM Optical Networks A Reality Check", *IEEE Comms Magazine*, vol 38, pp 58-60, 2000

[13] D Castleford *et al* "Optical Crosstalk in Fiber/Radio WDM Networks", *IEEE Trans Microwave Theory Tech* , vol 49, pp 2030-2035, 2001

[14] C Lim *et al* "Capacity Analysis for WDM Fiber-Radio Backbones with Star-Tree and Ring Architecture Incorporating Wavelength Interleaving", *J Lightwave Technol* , vol 21, pp 3308-331, 2003

[15] G H Smith *et al* "A Millimeter-Wave Full-Duplex Fiber-Radio Star-Tree Architecture Incorporating WDM and SCM", *IEEE Photon Technol Lett*, vol 10, pp 1650-1652, 1998

[16] R K Parker *et al* "Vacuum Electronics", *IEEE Trans Microwave Theory Tech*, vol 50, pp 835-844, 2002

[17] J X Qiu *et al* "Travelling-Wave Tube Amplifier Performance Evaluation and Design Optimization for Applications in Digital Communications with Multilevel Modulations", *IEEE Trans Microwave Theory Tech* vol 51, pp 1911-1919, 2003

[18] C M Su *et al* "Narrow flat-plate antenna for 2 4 GHz WLAN Operation", *Electronics Lett* vol 39, pp 344-345, 2003

[19] W R Deal *et al* "A New Quasi-Yagi Antenna for Planar Active Antenna Arrays", *IEEE Trans Microwave Theory Tech*, vol 48, pp 910-918, 2000

[20] O Solgaard *et al* "Microoptical Phased Arrays for Spatial and Spectral Switching", *IEEE Comms Magazine*, pp 96-101, 2003

[21] A E Fathy *et al* "Silicon-Based Reconfigurable Antennas – concepts, Analysis, Implementation and Feasibility", *IEEE Trans Microwave Theory Tech*, vol 51, pp 1650-1661, 2003

[22] A Jacomb-Hood *et al* "Multibeam Active Phased Arrays for Communications Satellites", *IEEE Microwave Magazine*, vol 1, pp 40-47, 2000

[23] S Weisser *et al* "Damping-Limited Modulation Bandwidths up to 40 GHz in Undoped Short-Cavity $In_{0\,35}Ga_{0\,65}AS$-GaAs Multiple-Quantum-Well Lasers", *IEEE Photon Technol Lett*, vol 8, pp 608-610, 1996

[24] K Noguchi *et al* "Millimeter-Wave $TiLiNbO_3$ Optical Modulators", *J Lightwave Technol*, vol 16, pp 615-617, 1998

[25] W Bridges *et al* "Velocity-Matched Electro-Optic Modulator", *Proc SPIE*, vol 1371, pp 68-77, 1990

[26] Y Chen *et al* "375-GHz-Bandwidth Photoconductive Detector", *Applied Physics Lett*, vol 59, pp 1984-1986, 1991

[27] Y Chiu *et al* "High-Speed Low-Temperature-Grow GaAs p-i-n Travelling-Wave Photodetector", *IEEE Photon Technol Lett*, vol 10, pp 1012-1014, 1998

[28] L Giraudet *et al* "Optical Design of Evanescently Coupled, Waveguide-Fed Photodiodes for Ultrawide-Band Applications", *IEEE Photon Technol Lett*, vol 11, pp 111-113, 1999

[29] K Takahata *et al* "46 5-GHz-Bandwidth Monolithic Receiver OEIC Consisting of a Waveguide p-i-n Photodiode and a HEMT Distributed Amplifier", *IEEE Photon Technol Lett*, vol 10, pp 1150-1152, 1998

[30] H Ito *et al* "High-Power Photonic Microwave Generation at K- and Ka-Bands Using a Uni-Travelling-Carrier Photodiode", *J Lightwave Techonl*, vol 20, pp 1500-1505, 2002

[31] H Ito *et al* "InP/InGaAs Uni-Travelling-Carrier Photodiode with 310 GHz Bandwidth", *Electronics Lett*, vol 36, pp 1809-1810, 2000

[32] D Wake *et al* "Zero Bias Edge-Coupled InGaAs Photodiodes in Millimetre-Wave RoF Systems", *Electronics Lett*, vol 29, pp 1879-1880, 1993

[33] C Marra *et al* "Wavelength-Interleaved OADMs Incorporating Optimized Multiple Phase-Shifted FBGs for Fiber-Radio Systems", *J Lightwave Technol*, vol 21, pp 32-39, 2003

[34] K Wesolowski "Mobile Communication Systems", John Wiley & Sons Ltd, 2002

[35] P Bharita *et al* "Millimeter Wave Engineering and Applications", John Wiley & Sons, New York, 1984

[36] M P M Hall *et al* "Propagation of Radiowaves", IEE, London 1996

[37] R van Nee *et al* "OFDM for Wireless Multimedia Communications", Artech House Publisher, London 2000

[38] W C Y Lee "Mobile Communications Design Fundamentals", John Wiley & Sons Inc New York 1993

[39] B Bing "Broadband Wireless Access", Kluwer Academic Publishers, London 2000

[40] U Gliese *et al* "Chromatic Dispersion in Fiber-Optic Microwave and Millimeter-Wave Links", *IEEE Trans Microwave Theory Tech*, vol 44, pp 17161724, 1996

[41] J Park *et al* "Fiber Chromatic Dispersion Effects on Multichannel Digital Millimeter-Wave Transmission", *IEEE Photon Technol Lett* vol 8, pp 17161718, 1996

[42] G H Smith *et al* "Overcoming Chromatic-Dispersion Effect in Fiber-Wireless Systems Incorporating External Modulators", *IEEE Trans Microwave Theory Tech*, vol 45, pp 1410-1415, 1997

[43] G Keiser "Optical Fiber Communications", McGraw-Hill Higher Education, London, 2000

[44] M R Phillips *et al* "Crosstalk due to optical fiber nonlinearity in WDM CATV lightwave systems", *Optical Fiber Communication Conference*, vol 1, pp 21-26, 1999

[45] G K Gopalakrishnan *et al* "Experimental Study of Fiber Induced Distortion in Externally Modulated 1550 nm Analogue CATV Links", *Electronics Lett*, vol 32, pp 1309-1310, 1996

[46] J C Fan *et al* "Dynamic Range Requirements for Microcellular Personal Communication Systems Using Analog Fiber-Optic Link", *IEEE Trans Microwave Theory Tech*, vol 45, pp 1390-1397, 1997

[47] M Umehira *et al* "ATM Wireless Access for Mobile Multimedia Concept and Architecture", *IEEE Personal Communications*, pp 39-48, 1996

[48] *IEEE Wireless Communications*, Special Issue Mobile and Wireless Internet, vol 9, 2002

[49] A Grilo *et al* "Terminal Independent Mobility for IP (TIMIP)", *IEEE Comms Magazine*, vol 39, pp 34-41, 2001

[50] T T Kwon *et al* "Mobility Management for VoIP Service Mobile IP vs SIP", *IEEE Wireless Communications*, vol 9 pp 66-75, 2002

[51] A I Andritsou "Evolution in Broadband Wireless Access Networks", *39th European Telecommunications Congress*, Shannonside, Ireland 2000

[52] B Moon *et al* "RSVP Extension for Real-Time Services in Wireless Mobile Networks", *IEEE Comms Magazine,* vol 39, pp 52-59, 2001

[53] B Moon *et al* "Reliable RSVP Path Reservation for Multimedia Communications under an IP Micromobility Scenario", *IEEE Wireless Communications*, vol 9 pp 93-97, 2002

[54] E Ayanoglu *et al* "Wireless ATM limits, challenges, and proposals", *IEEE Personal Communications,* vol 3, pp 18-34, 1996

[55] B Walke *et al* "Wireless ATM air interface and network protocols of the mobile broadband system", *IEEE Personal Communications,* vol 3, pp 50-56, 1996

[56] Y Du *et al* "Wireless ATM LAN With and Without Infrastructure", *IEEE Comms Magazine*, pp 90-95, 1998

3 Generation of Millimeter-Wave Signals

Developing an optically fed microwave wireless network requires the amalgamation of many different technologies The main challenge on the transmission side is to generate the millimetre wave optical data signals, which would be suitable for subsequent transmission over optical fibre

There are many different techniques that could be used for the remote generation of millimetre wave signals The most important ones are listed below

1 direct modulation of a laser diode
2 external modulation
3 heterodyning
4 frequency conversion
5 remote upconversion using a phototransistor

The rest of this chapter consists of a detailed description of the above-listed techniques

3 1 Direct modulation of a laser

Direct modulation of laser is the simplest and the cheapest technique to generate the optical millimeter-wave signals This is achieved by applying the RF signal combined with the bias current to the laser transmitter The variation of the excitation current (i e number of electrons injected into the device) causes the variation in the number of photons generated and thus variation in the optical power generated by the laser The population of the electrons and photons in the cavity of a single mode laser and the phase of the generated light are described by the rate equations

$$\frac{dN(t)}{dt} = \frac{I(t)}{qV} - \frac{N(t)}{\tau_n} - g_0\left(N(t) - N_{om}\right)S(t), \qquad \textbf{Equation 3-1}$$

$$\frac{dS(t)}{dt} = \Gamma g_0\left(N(t) - N_{om}\right)S(t) - \frac{S(t)}{\tau_p} + \Gamma\beta\frac{N(t)}{\tau_n}, \qquad \textbf{Equation 3-2}$$

$$\frac{d\phi(t)}{dt} = \frac{\alpha}{2}\left(\Gamma g_0(N(t) - N_{om}) - \frac{1}{\tau_p}\right) - \omega, \qquad \textbf{Equation 3-3}$$

where N(t) – carrier number in the active volume,

I(t) – drive current,

q – electron charge,

V – volume of the active layer,

τ_n - carrier lifetime,

g_0 - gain coefficient,

N_{om} – carrier density at threshold,

S(t) - photon density,

Γ - optical confinement factor,

τ_p – photon lifetime,

β - spontaneous emission coefficient

$\varphi(t)$ – phase of the light,

α - linewidth enhancement factor,

ϖ - frequency of the laser

Equation 3-1, Equation 3-2 and Equation 3-3 describe the evolution of the carrier and photon densities and phase respectively These are simple single mode equations The first term on the R H S of the Equation 3-1 shows that the number of electrons in the conduction band and holes in the valence band increases with the drive current and is dependent on the ratio of the injected current and the volume of the active layer of the laser

The carrier number decreases due to spontaneous emission, which is inversely proportional to the carrier lifetime (second term), and due to stimulated emission, which takes place when the laser is biased above its threshold (third term) In this case the photons in the active region interact with electrons causing their transition from higher to lower energy bands and lasing occurs

The photon population is governed by Equation 3-2 The main contribution to the increase of the photon number is stimulated emission The photon number increases due to the spontaneous emission and decreases due to losses in the cavity such as absorption and resistive losses

The Equation 3-3 is important when one considers both the amplitude and phase modulation It also plays important role in determining the influence of the optical feedback and external injection The first term on the R H S of the equation is brought about due to the fact that the variation in carrier density changes the refractive index of the laser cavity This in turn changes the phase of the generated light The second term is the frequency of the generated light

The rate equations can be used to calculate the modulation response of a laser diode The driving current is assumed to consist of a DC value and an AC component

$$I(t) = I_0 + i_1 e^{j\varpi_m t}, \qquad \textbf{Equation 3-4}$$

and the small signal response p_1 and n_1 is defined by

$$S(t) = S_0 + s_1 e^{j\varpi_m t}, \qquad \textbf{Equation 3-5}$$

$$N(t) = N_0 + n_1 e^{j\varpi_m t}, \qquad \textbf{Equation 3-6}$$

where S_0 and N_0 are the steady state values of photon and carrier densities obtained by solving the rate equations with the L H S set to zero (as shown in Equation 3-7 and Equation 3-8) and ϖ_m is the modulating frequency [1]

$$0 = \frac{I_0}{qV} - \frac{N_0}{\tau} - g_0(N_0 - N_{om})S_0, \qquad \textbf{Equation 3-7}$$

$$0 = \Gamma g_0(N_0 - N_{om})S_0 - \frac{S_0}{\tau_p} - \Gamma\beta\frac{N_0}{\tau_n}, \qquad \textbf{Equation 3-8}$$

The full derivation of the formulas shown below is presented in Appendix A

The small signal response of a directly modulated laser is found by inserting Equation 3-4, Equation 3-5 and Equation 3-6 into Equation 3-1 and Equation 3-2 and performing the differentiation

$$-j\varpi n_1 = -\frac{i_1}{qV} + \left(\frac{1}{\tau_n} + g_0 S_0\right)n_1 + \frac{1}{\tau_p \Gamma}s_1, \qquad \textbf{Equation 3-9}$$

$$j\varpi s_1 = g_0 S_0 \Gamma n_1, \qquad \textbf{Equation 3-10}$$

Since the main interest focuses on the dependence of the photon density on the modulation frequency one can substitute n_1 calculated from Equation 3-9 into Equation 3-10 As a result one obtains a photon density – frequency relation

$$s_1(\varpi) = -\frac{\frac{i_1}{qV} g_0 S_0 \Gamma}{\varpi^2 - j\varpi\left(\frac{1}{\tau} + g_0 S_0\right) - \frac{g_0 S_0}{\tau_p}}, \qquad \textbf{Equation 3-11}$$

The typical frequency response of a laser is shown in *Figure 1-8* (Chapter 1) For low frequencies the response remains flat It increases rapidly for a particular frequency called the relaxation oscillation frequency - ω_r and drops sharply for ω

higher than ω_r The value of ω_r can be obtain by finding the minimum of the dominator in Equation 3 -11 (maximum value of p_1)

$$\varpi_r = \sqrt{\frac{g_0 S_0}{\tau_p} - \frac{1}{2}\left(\frac{1}{\tau_n} + g_0 S_0\right)^2}, \qquad \textbf{Equation 3-12}$$

The oscillation frequency can be, with good accuracy, treated as a measurement of the laser modulation bandwidth Typical modulation bandwidths of commercially available lasers diodes do not exceed 20 GHz A lot of effort has been put to enlarge the intrinsic modulation bandwidth, which includes sophisticated fabrication techniques and broadband matching techniques This however results in the increase of cost and complexity of these lasers

As it can see from Equation 3-12, the modulation bandwidth of a laser diode can be increased by reducing carrier and photon lifetime or by increasing bias current of the laser The initial condition could be achieved by altering the internal structure of the laser (e g varying cavity length), while the latter has to be kept within practical limits (maximum current rating of the device) Furthermore, operating the laser at a higher level than the optimum current could cause a faster ageing of the device

There are two other novel techniques namely external light injection [2, 3] and resonant modulation [4], which could be used to enhance the modulation bandwidth of a laser diode and are described in detail further on in this section

3 1 1 External light injection

Many recent experiments have shown that the modulation bandwidth can be increased significantly by employing external light injection The factor of improvement with the above-mentioned experiments could be as high as three [5 - 9] A typical set-up involves the usage of two lasers in a master-slave configuration The actual transmitter (laser under direct modulation) is the slave laser, while the master laser is a Continuous Wave (CW) source

The external light injection introduces a new term into laser rate equations, which is responsible for the increase in laser modulation bandwidth The equation describing the rate of change in photon population, after the external injection, can be expressed as

$$\frac{dS(t)}{dt} = \Gamma g_0 (N(t) - N_{om}) S(t) - \frac{S(t)}{\tau_p} + \Gamma\beta \frac{N(t)}{\tau_n} + 2K_c \sqrt{S_{inj} S(t)} Cos(\Delta\varphi)$$ **Equation 3-13**

The corresponding phase can be calculated form

$$\frac{d\phi(t)}{dt} = \frac{\alpha}{2}\left(\Gamma g_0 (N(t) - N_{om}) - \frac{1}{\tau_p}\right) - \Delta\omega - K_c \sqrt{\frac{S_{inj}}{S(t)}} Sin(\phi(t)),$$ **Equation 3-14**

where S_{inj} – injected power

$\varphi(t)$ - phase of the injected light,

K_c – coupling coefficient for the injected light into slave laser,

$\Delta\omega = \varpi - \omega_{inj}$ - detuning frequency between the slave and master laser

The equation for carrier population remains unchanged

Solving the equations in the same way as for the free running laser we obtain the following frequency response of the injected laser

$$s_1 = \frac{\frac{\iota_1 \Gamma g_0 S_0}{PqV}\left[1 - \frac{Y\alpha}{O}\right]}{j\varpi + \frac{X}{2S_0} + \frac{Y^2}{O} - \frac{S_0 Y\alpha g_0 s_1}{OP\tau_p} + \frac{Y\alpha g_0 X s_1}{OP} + \frac{S_0 g_0 s_1}{P\tau_p} - \frac{X s_1 g_0}{P}},$$ **Equation 3-15**

Where

$$X = 2K_c \sqrt{S_{inj} S_0} \cos(\phi_0),$$

$$Y = K_c \sqrt{\frac{S_{inj}}{S_0}} \sin(\varphi_0),$$

$$O = j\omega + \frac{X}{2S_0},$$

$$P = j\omega + \frac{1}{\tau_n} + g_0 S_0$$

We can see that by setting the injection level to zero we obtain the original response of a laser

Initially, simulations were carried out to examine the effects of external light injection Subsequent experiments where then performed to validate the simulation results obtained

3.1.2 External light injection – simulation

The external light injection was simulated using Virtual Photonics Inc (VPI). Transmission Maker. The simulation model is shown in *Figure 3-1*.

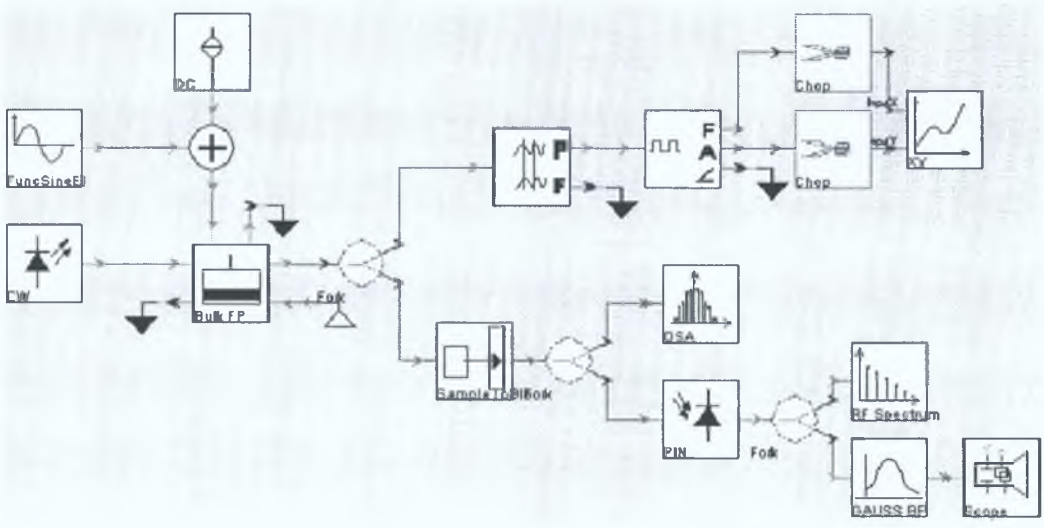

Figure 3-1: *Simulation model - external injection*

It consists of two lasers: a Fabry-Perot laser, which is the transmitter and the continuous wave (CW) source, from which light is injected into the FP laser. A DC bias of 90 mA, to which a sinusoidal modulation signal (amplitude 30 mA) is added, is applied to the transmitter. The frequency response is plotted by calculating the instantaneous power and frequency of an optical waveform, when the laser is directly modulated with a sine wave at frequencies ranging from 300 MHz to 26.6 GHz. The resulting frequency response of the laser in the free running case and under external injection (6 mW optical power at a detuned wavelength of 15 GHz from the slave laser) is shown in *Figure 3-2*. This result shows that by using external injection the modulation response can be significantly increased from 8 GHz in the free running case to 23 GHz under the injection.

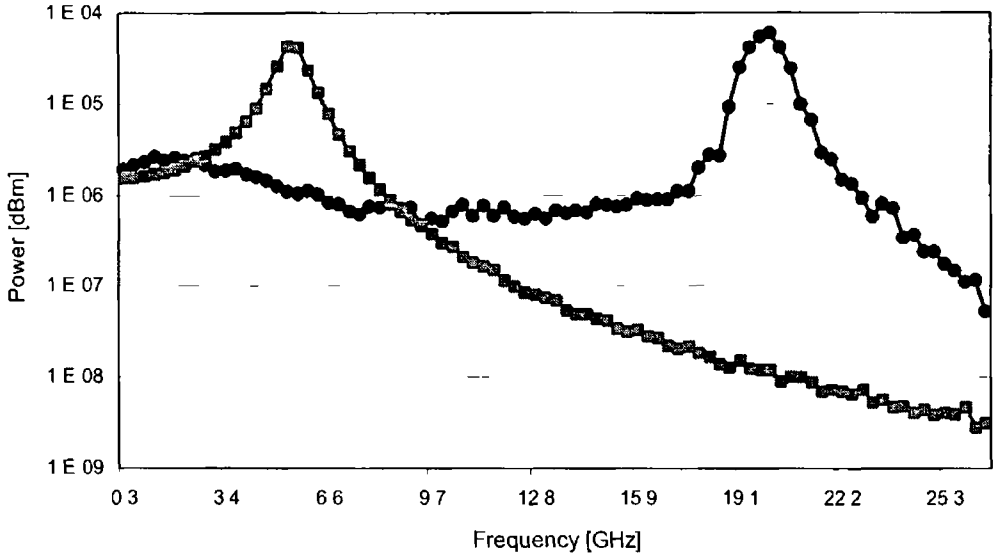

Figure 3-2 *Frequency response of the free running laser (squares) laser under the external injection (circles)*

Another interesting factor was observed when no modulation signal was applied to the externally injected laser The optical spectrum of the un-modulated laser output signal with and without injection is shown in *Figure 3-3* (a) and (b) respectively

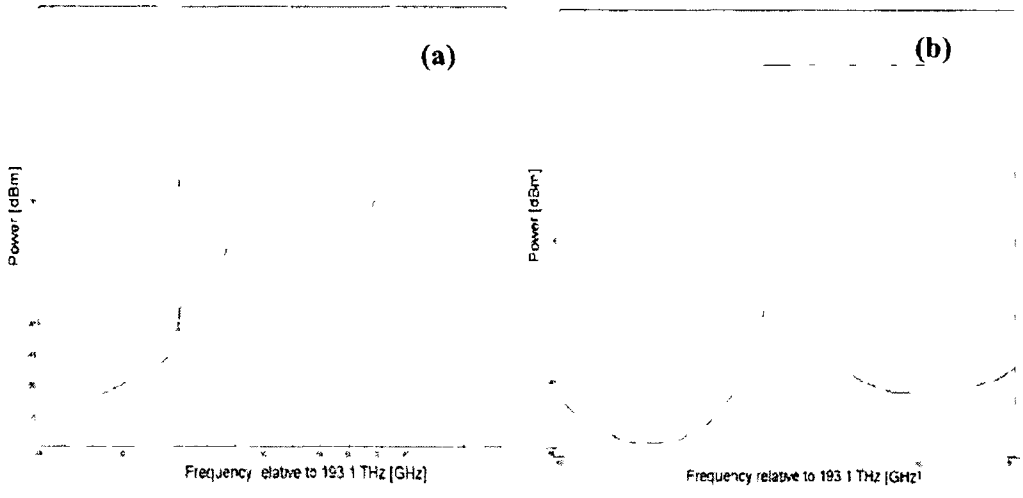

Figure 3-3 *Optical spectrum (a) under external injection (b) free running*

The detected optical signal was displayed using an RF spectrum analyser and an oscilloscope The electrical spectrum and the temporal signal are displayed in *Figure 3-4* and *Figure 3-5* respectively The temporal signal is passed through a filter (Gaussian pass-band) in order to see the actual oscillation at 21 GHz From the diagrams it can be seen that laser under external injection begins to self-pulsate [10, 11] Multiple side bands are clearly visible in the optical spectrum even though no modulating signal is applied to the transmitter The distance between the side bands

corresponds to the components present in the RF spectrum of the detected optical signal The laser oscillation can also be observed in the time domain in *Figure 3-5*

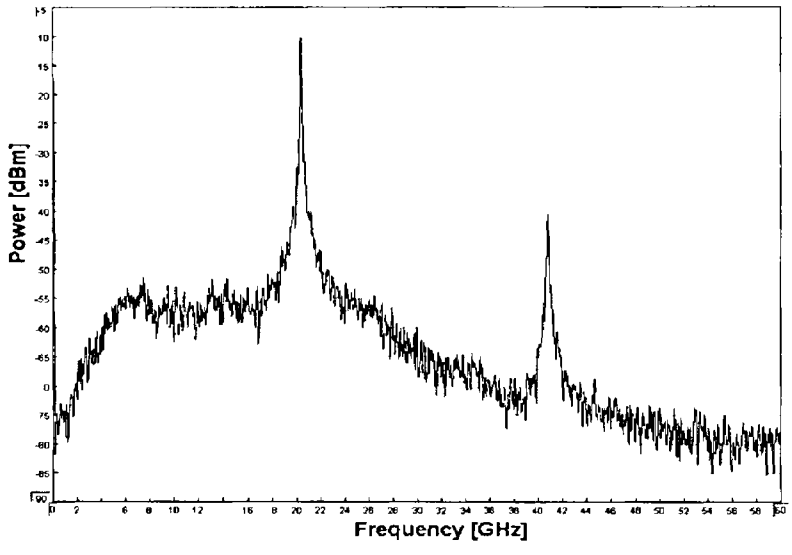

Figure 3-4 *RF spectrum of the signal from self-pulsating laser*

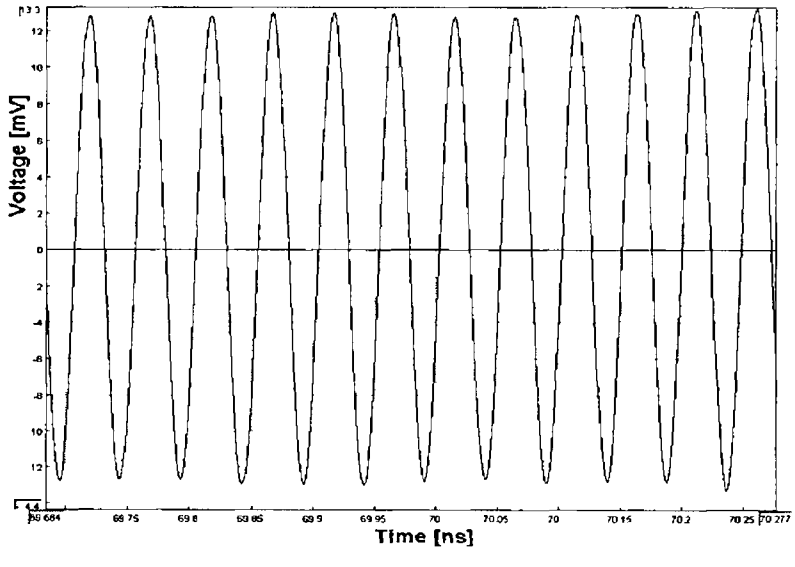

Figure 3-5 *21 GHz detected waveform from self-pulsating laser*

The frequency of the self-pulsation can be varied by changing the power injected to the laser *Figure 3-6* presents the dependence of the oscillation frequency as a function of injected power

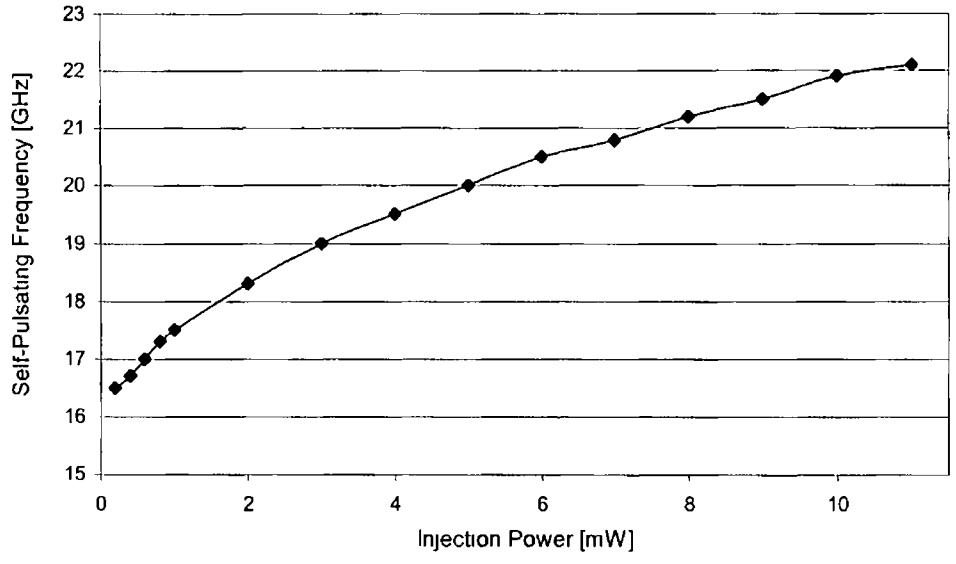

Figure 3-6 Self-pulsating frequency vs injected optical power

It can be seen that the frequency can be tuned between 16 5 to 22 GHz by increasing the optical power injected into the laser form 0 2 to 1 1 mW

The results obtained clearly show that the enhanced response at these frequencies is caused by the external injection inducing instability in the laser diode The instability in turn results in the output power from the laser undergoing strong oscillations due to beating between the optical field components in the laser cavity [12, 13]

3 1 3 External light injection - experiments

The experimental set-up used to investigate the effect of external light injection as well as to verify the simulation results is shown in *Figure 3-7* This configuration involves the use of a master laser (external cavity tunable laser), a slave 1 5 μm single mode laser diode, a detector (pin diode) and a network analyser (HP-8510C) The isolator used prevents any reflected light from coming back to the master laser Light from the master laser was coupled into the slave laser using a 3-dB coupler A Polarization Controller (PC) was used in order to optimise the coupling of the injected light into the laser cavity The total insertion loss introduced by the PC and the isolator was about 3 dB The modulation signal from the network analyser was combined with a bias current of 60 mA using a 40 GHz bias tee and then applied to the slave laser The modulated light emitted by the laser was detected using 50 GHz photodetector and the frequency response was measured using the network analyser

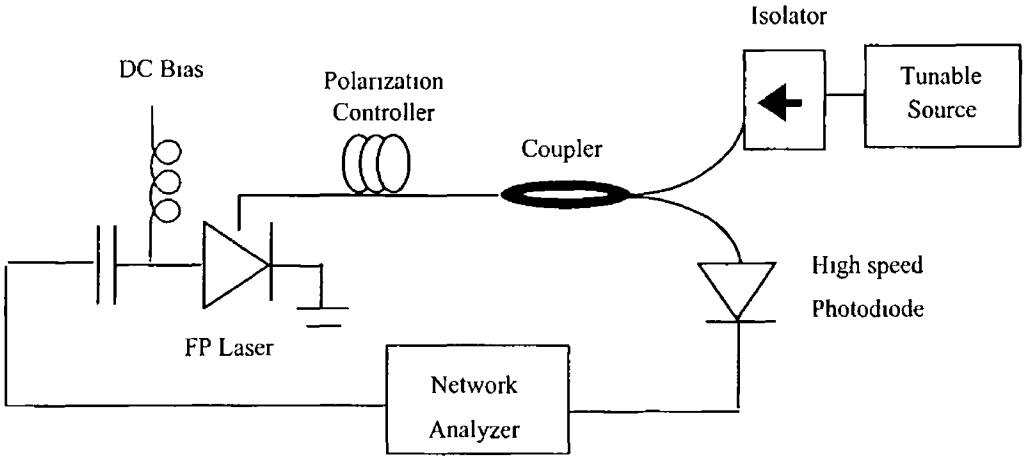

Figure 3-7 External light injection - experimental set-up

The frequency response of the laser obtained by using the network analyser is shown in the *Figure 3-8* The line denoted by (a) shows the free running case, where the inherent bandwidth of the laser was measured to be around 8 GHz The lines designated by (b) - (d) show the response, when strong external injection was applied to the laser The different cases correspond to different injection powers The best enhancement in modulation bandwidth (up to 21 GHz) of the slave laser was achieved, when the injected power was 6 dBm It is important to note that the injected powers mentioned are the powers at the output of the tunable laser The actual signal injected into laser cavity is much smaller due to losses introduced by isolator (around 2 dB), coupler (3 dB), polarisation controller (1 dB) and finally the coupling loss between fiber and laser (3 - 4 dB)

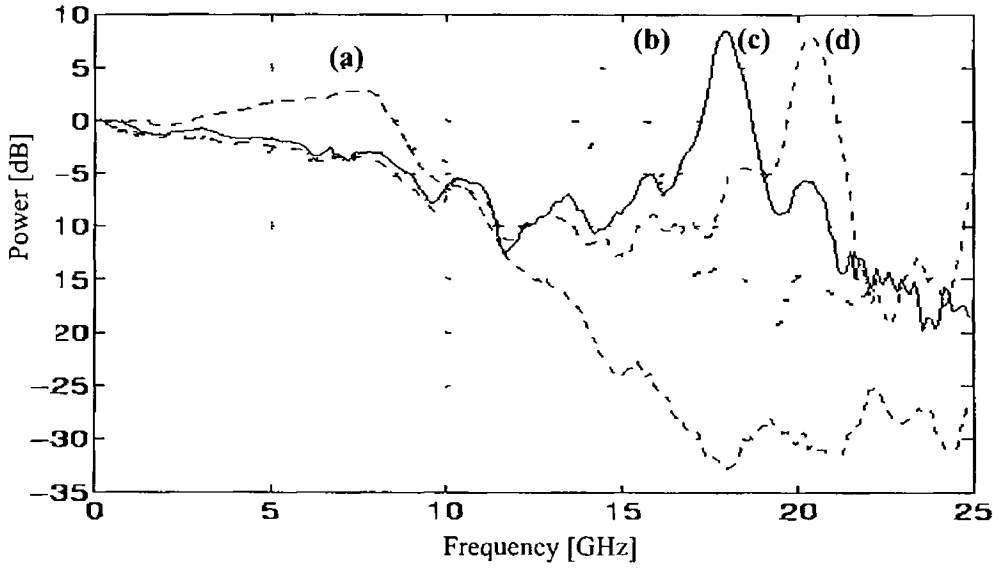

Figure 3-8 Enhancement of the modulation bandwidth of the laser diode achieved by external light injection (a) free running with injection level set to (b) 4 dBm (c) 5 dBm (d) 6 dBm

From the plot one can easily see that external light injection can not only significantly enhance the bandwidth of the laser but also increase the relative response of the laser at specific modulating frequencies

As in the case of the simulation, the enhanced response at these frequencies is caused by the external injection inducing the laser to self-pulsate *Figure 3-9* displays the optical spectrum from the laser when it is biased at 60 mA and the externally injected power from the external cavity laser is 3 5 mW One can clearly see the modulation on the spectrum at a frequency of around 20 GHz

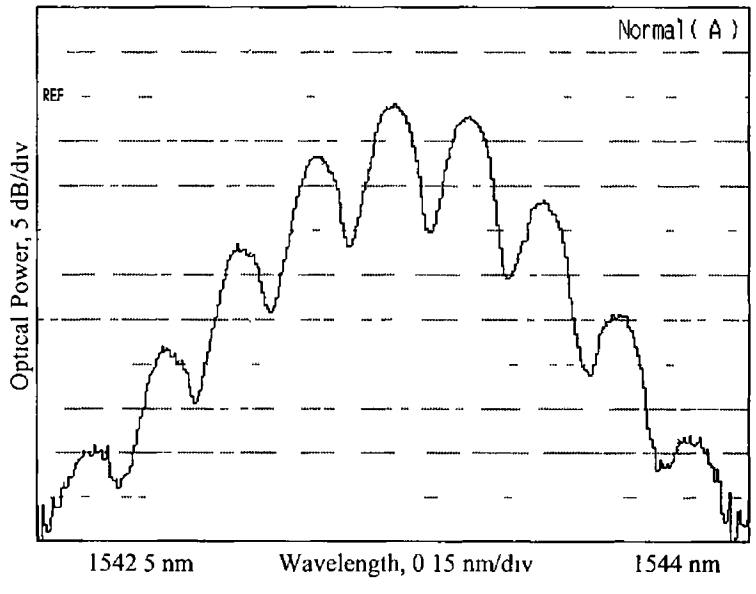

Figure 3-9 *Optical spectrum of the self-pulsating laser*

To further investigate the oscillation from the laser, the optical output from the laser under external injection was detected using a 50 GHz photodiode and displayed on a 50 GHz oscilloscope Triggering was achieved by splitting the electrical signal after the detector in two, and using one of the outputs as the trigger *Figure 3-10* shows the detected temporal optical output from the laser under external injection An oscillation at a frequency of around 20 GHz can clearly be seen Also noticeable is a significant level of noise and jitter on this signal This noise and jitter on the oscillation from the laser is also evident in the detected electrical spectrum (*Figure 3-11*) The broad linewidth is caused by the jitter between the DFB laser diode and the tunable cavity laser This is due to the instability of the wavelength generated by the DFB laser, which does not have any temperature control

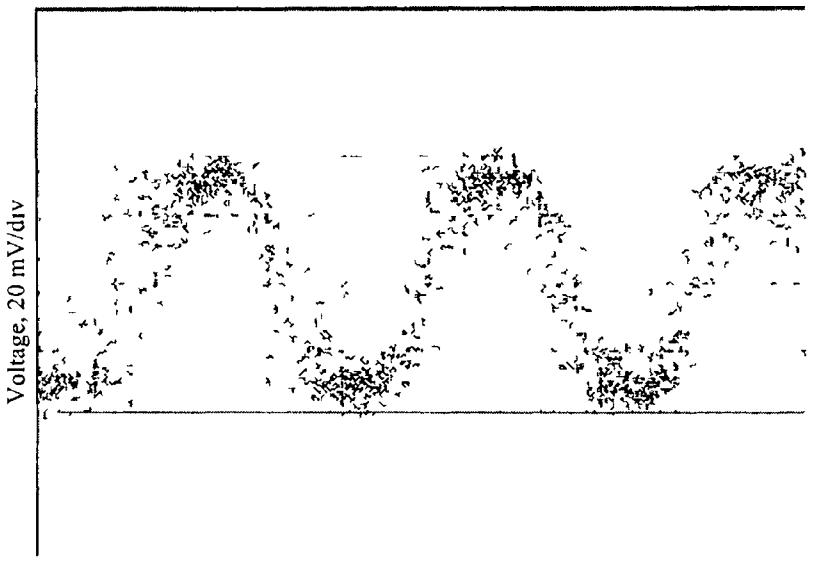

Figure 3-10 Temporal output of the laser under external injection

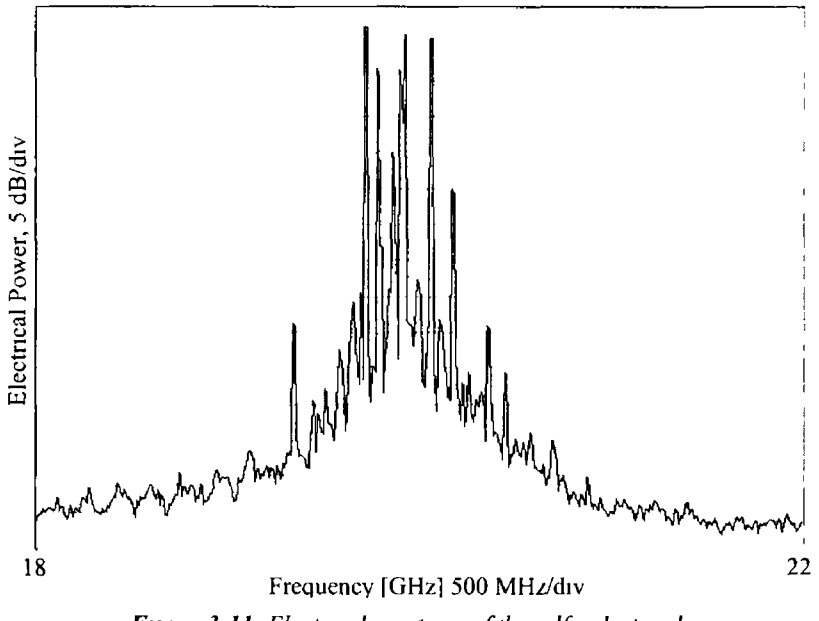

Figure 3-11 Electrical spectrum of the self-pulsating laser

It is important to note that by applying a modulating signal of a sufficient power level the self-pulsation frequency can be change to generate the desired signal It was measured that the minimum modulating power required to obtain a stable output signal was 5 dBm

As mentioned before, varying the injection level can also control the frequency of self-pulsation This phenomenon is illustrated in *Figure 3-12*, which shows the dependence of the generated signal as a function of the injected optical power

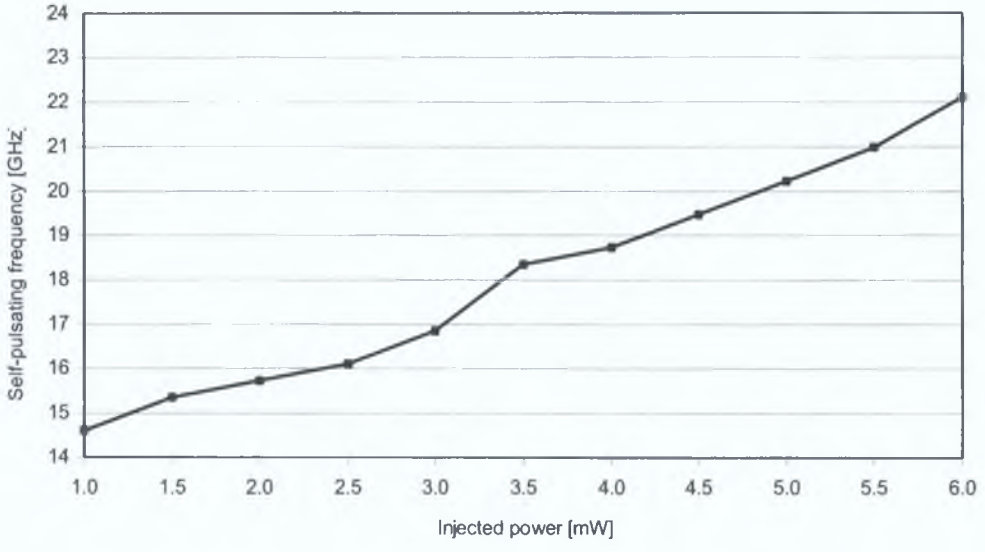

Figure 3-12: Self-pulsating frequency as a function of injected optical power

In addition, by measuring the peak-to-peak voltage of the oscillation on the oscilloscope, we were able to determine that the optical output from the laser was essentially 100% modulated (using the average power level falling on the detector and the responsivity of the detector) [14, 15].

The self-pulsation of the externally injected laser has two main implications. First, it is the reason for a huge increase in the laser resonance peak. On the other hand though, the range of frequencies, which are enhanced at any injection level is quite narrow, the bandwidth of the signals that could be generated using direct modulation of the externally injected laser would be limited.

It can be seen that the experimental results agree very well with the results obtained from the simulations.

3.1.4 Resonant modulation

Resonant modulation of a laser diode is a low-cost technique of generating high frequency narrow band (≤ 1 GHz) signals. This method is capable of generating frequencies approaching 100 GHz [4]. To achieve the resonantly enhanced operation a mirror is placed before the laser diode to form an external cavity. The length of the cavity is chosen such that its round trip time equals a multiple round trip time of the laser cavity. The optical feedback from the mirror causes the modulation response of the system to be enhanced at frequencies that correspond to the multiples of the cavity round trip. The laser's parasitic causes roll-off of the modulation response and

it ultimately limits the maximum modulation frequency [16] Resonant modulation can achieve modulation efficiencies that are higher than the low frequency response of a laser without an external cavity Georges *et al* [17] present a resonantly enhanced modulation of a laser with a modulation efficiency of 5 dB (in comparison to low frequency modulation) and a modulation bandwidth of 110 MHz and a carrier to noise ratio (CNR) that exceeds 90 dB (for 1 Hz bandwidth)

3 2 External Modulation

Another method for the generation of RF signals using intensity modulation of light is external modulation This makes a use of the fact that the refractive index of certain materials varies with applied electric field This phenomenon is known as the electro-optic effect [14] The most common and cheapest type of external modulators is the Mach-Zehnder Modulator (MZM) The MZM basically consists of two Y junctions The first one splits the incoming signal into two arms One of the arms (made of an electro-optic material e g lithium niobate) runs between two electrodes The modulating signal is then applied to the electrode, and it generates a changing electric field This field varies the phase of the light passing through the modulator arm The phase modulation is converted into intensity modulation after combining the light from both arms of the modulator using the second Y junction [18] The MZM exhibits a sinusoidal transfer function *Figure 3-13* shows a transfer function of EOspace MZM, which was used in the experiments described further on in Chapter 5

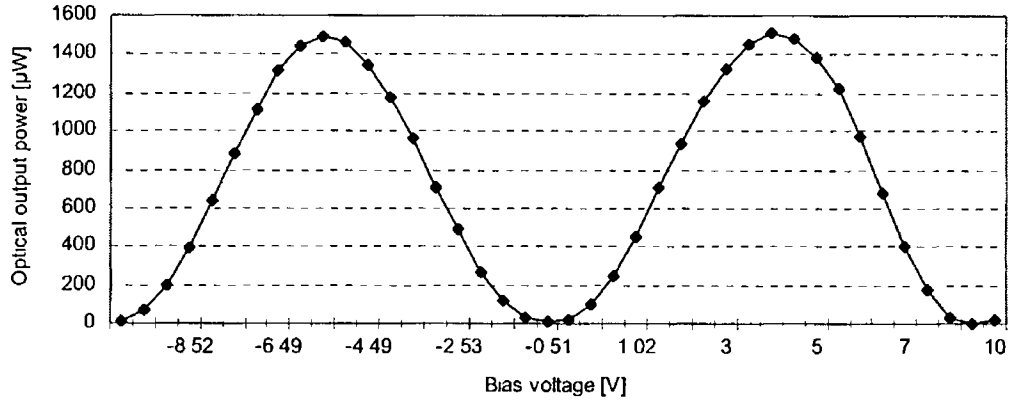

Figure 3-13 MZM transfer function

The output signal of the modulator can be described as

$$E_{out} = E_{in}(t)\cos\left(\frac{\pi}{2}\frac{V_{mod}(t)}{V_{\pi}}\right), \qquad \textbf{Equation 3-16}$$

Where $E_{in}(t)$ is the incident optical field applied to the modulator, $V_{mod}(t)$ is the modulating voltage and V_{π} is the modulating voltage required to change the phase of the light by 180° If we denote the modulating signal as

$$V_{mod} = V_{\pi}(1+\varepsilon) + \alpha V_{\pi}\cos(\omega t), \qquad \textbf{Equation 3-17}$$

where ε and α are normalised bias and drive levels respectively and ω is the modulating signal frequency, then the output field can be expressed as

$$E_{out} = \cos\left(\frac{\pi}{2}[(1+\varepsilon)+\alpha\cos(\omega t)]\right)\cos(\Omega t), \qquad \textbf{Equation 3-18}$$

where Ω is the angular frequency of the applied optical signal This expression can be expanded into a series of Bessel functions [19]

$$\begin{aligned} E_{out}(t) = {} & \frac{1}{2}J_0\left(\alpha\frac{\pi}{2}\right)\cos\left(\frac{\pi}{2}(1+\varepsilon)\right)\cos(\Omega t) \\ & -\frac{1}{2}J_1\left(\alpha\frac{\pi}{2}\right)\sin\left(\frac{\pi}{2}(1+\varepsilon)\right)\cos(\Omega t \pm \omega t) \\ & +\frac{1}{2}J_2\left(\alpha\frac{\pi}{2}\right)\cos\left(\frac{\pi}{2}(1+\varepsilon)\right)\cos(\Omega t \pm 2\omega t) \\ & -\frac{1}{2}J_3\left(\alpha\frac{\pi}{2}\right)\sin\left(\frac{\pi}{2}(1+\varepsilon)\right)\cos(\Omega t \pm 3\omega t) \end{aligned}, \qquad \textbf{Equation 3-19}$$

From Equation 3-19 one can see, that the generation of different frequency components is dependent on the bias Usually the bias voltage (normalised) is chosen between 0 and 1 and the dominant frequency component in the output signal is ωt For analog modulation the modulator is biased at 0 5, which ensures its most linear operation (*Figure 3-14*)

Commercially available external modulators are generally capable of generating RF signals up to 40 GHz Though, 60 GHz generation using Electro-Absorption Modulators (EAM) has been reported [20 - 22], these devices are still too expensive for commercial use

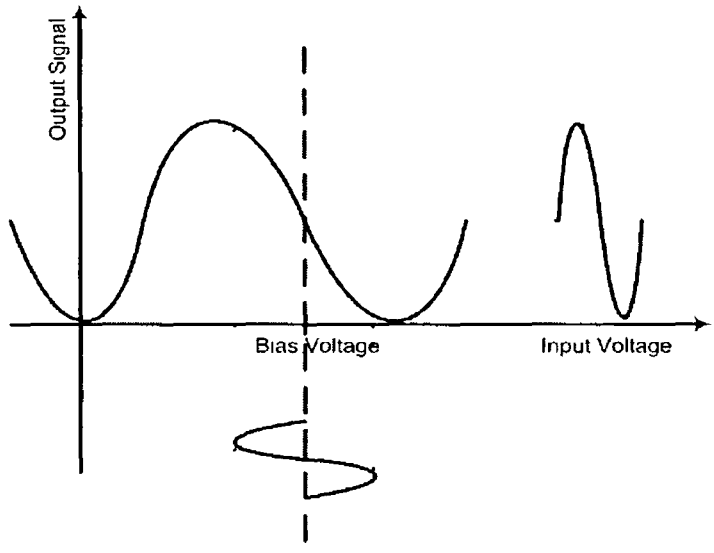

Figure 3-14 Analog modulation using MZM

In order to increase the frequency a novel technique has been proposed This technique makes use of the nonlinear transfer function of an MZM From Equation 3-19 one can see that by setting the bias voltage to 0, frequency multiplication could be achieved If $\varepsilon = 0$ the main component at Ω as well as all other even components are suppressed The optical spectrum consists of two main elements at $\Omega \pm \omega$, which when mixed in a pin diode will generate an electrical signal at a frequency of 2ω [23] This method is known as 2f generation and the basic operational principle associated with this method is shown in *Figure 3-15*

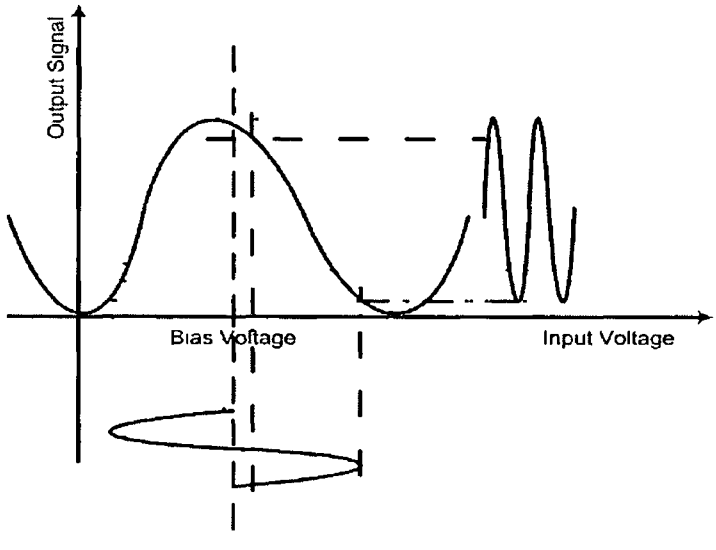

Figure 3-15 2f generation using MZM

By choosing the bias voltage $\varepsilon = 1$ and adjusting the modulator drive current we can generate an RF signal at a frequency that is four times the modulating signal If the bias voltage is set to 1 then the odd components are suppressed The optical spectrum consists of an optical carrier at Ω and two sidebands separated by 2ω from the central component By modifying the drive voltage α the central spectral element can also be suppressed This happens for $\alpha \cong 1\ 53$ [19] As a result we obtain a spectrum consisting of only two sidebands separated by 4ω, which will mix in the photodiode to generate signal at frequency equal to 4ω This method is called a 4f generation

In both cases (2f and 4f generation) the two sidebands are correlated, which means that the quality of the generated signal does not depend on the phase noise of the optical signal but mainly on the quality of the drive generator used for modulation This also means that 2f and 4f methods are capable of generating very high quality RF signals at frequencies well beyond the bandwidth of the external modulator

3 2 1 Simulation of 2f and 4f generation

2f and 4f generation have been simulated using VPI Transmission Maker The simulation model is shown in *Figure 3-16*

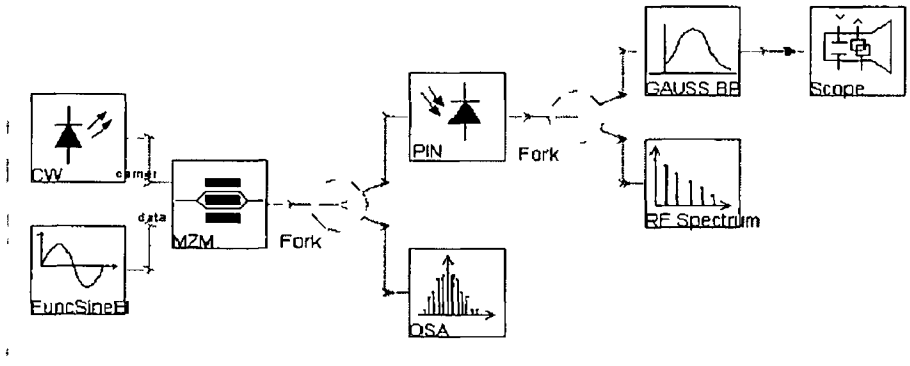

Figure 3-16 *Simulation model - 2f and 4f generation*

The light from a continuous wave (CW) source is passed through the MZM A 10 GHz sine wave is applied to the electrical input of the MZM The sine wave has a bias voltage of 0 V and 1 V and an amplitude of 1 V and 1 53 V for 2f and 4f generation respectively The output of the MZM is split between an optical spectrum analyzer (OSA) (*Figure 3-17* (a) and (b)) and a photodiode

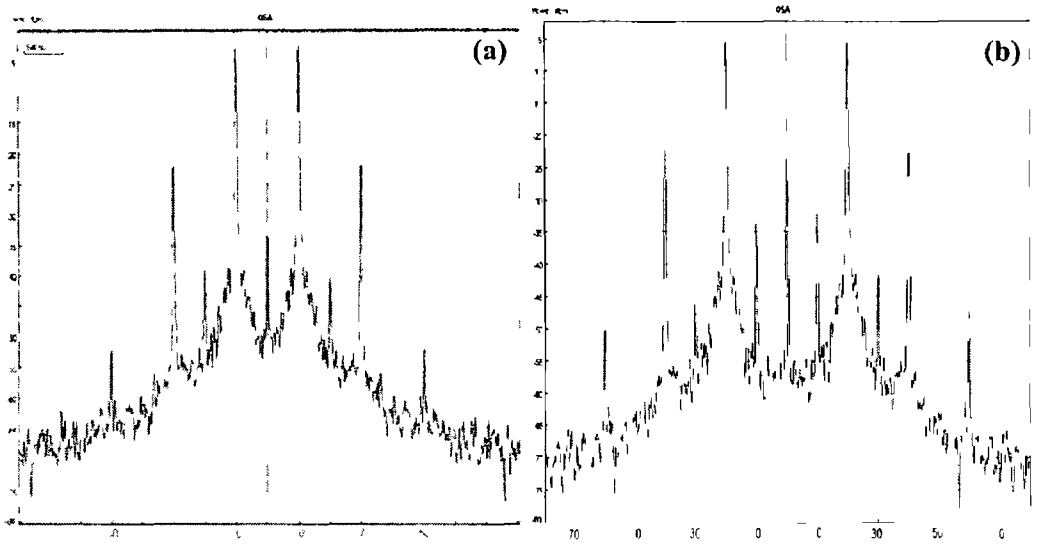

Figure 3-17 Optical spectrum (a) 2f generation (b) 4f generation

One can see from *Figure 3-17* that for 2f and 4f generation the optical spectrum consists of two main elements at ±10 GHz and ±20 GHz respectively and that the optical carrier is suppressed in both cases The RF spectrum of the detected electrical signal is displayed using an RF spectrum analyzer (*Figure 3-18* and *Figure 3-19*)

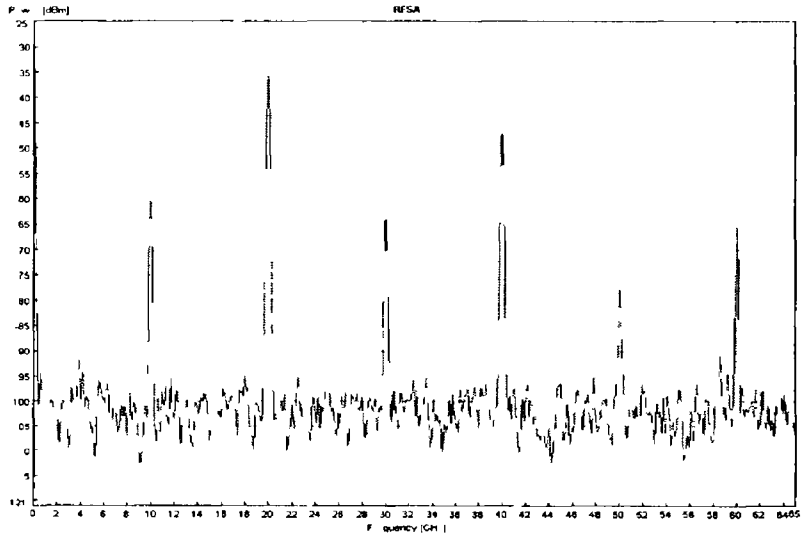

Figure 3-18 Electrical spectrum - 2f generation

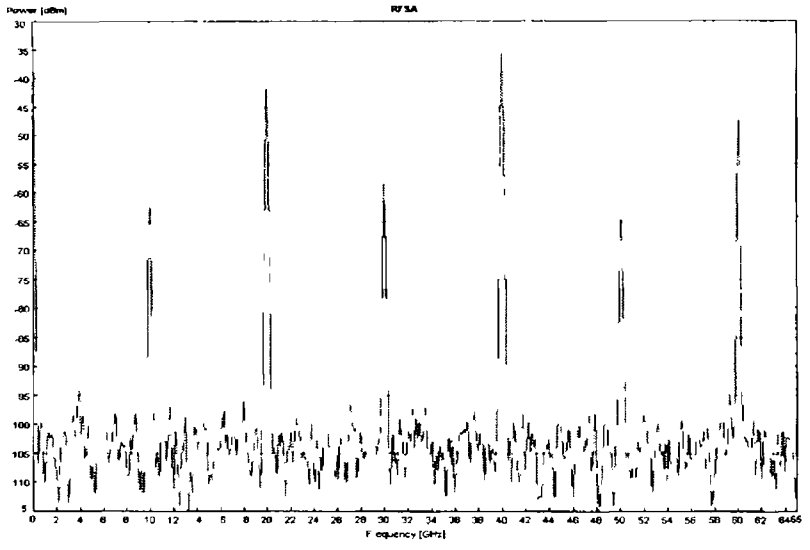

Figure 3-19 Electrical spectrum - 4f generation

The electrical spectrum consists of many components, as a result of the mixing between the optical side bands Hence in order to obtain the desired signal electrical filtering is necessary The RF carrier in the time domain, after filtration, is presented in *Figure 3-20*

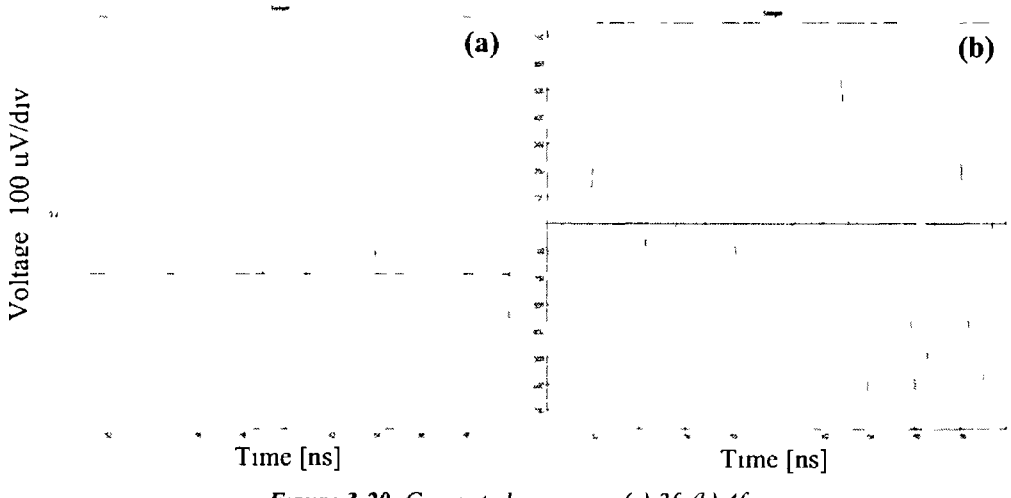

Figure 3-20 Generated sine wave (a) 2f (b) 4f

3 3 Heterodyning

Heterodyning or optical beating is yet another method of generating RF signals that is free from dispersion caused fading This technique is based on the principle that when two coherent optical carriers are incident on a high-speed photodiode, the signal obtained at the output of the detector would have a frequency that is equal to the difference between the two carriers This is due to the fact that a mixing process

takes place in the detector The result of mixing two sine waves at frequencies f_1 and f_2 would be the sum of two sine waves at frequencies f_1- f_2 and f_1+ f_2 The optical beating is capable of producing signals with 100% modulation depth, but it suffers from phase noise, if the two carriers are not correlated In this situation the generated RF signal will have linewidth of the order of combined spectral widths of the two optical modes Essentially what this means is that in order to generate a high purity RF signal, a laser with a very narrow linewidth is needed e g gas laser [24] In the case of semiconductor lasers the typical value of the laser's linewidth ranges from 10 – 100 MHz [25] The linewidth of an RF signal generated by heterodyning can be decreased by reducing the laser spectral width The latter could be achieved with the help of an external cavity and electrical or optical feedback techniques to control and lock frequency or phase Nevertheless, systems using narrow linewidth lasers suffer from the effects of Stimulated Brillouin Scattering (SBS) [14, 15], which ultimately limits the maximum power in the fiber [19] On the other hand controlling the frequency or the phase of the signal increases the cost and complexity of the system

The quality of the generated signal using optical mixing can be improved if the two modes were correlated i e the phase noise of the optical carriers would be cancelled out during the mixing process in the detector and the RF signal obtained at the output would have a very narrow linewidth (order of few hertz) Numerous techniques to correlate the optical waves have been proposed This correlation could be achieved by using the feed forward technique [26], an optical phase-locked loop (OPLL) [27] and sideband injection locking [33] It is important to note that a combination of the latter techniques is also possible The OPLL consists of a phase detector, a microwave reference oscillator and a loop filter The signal generated by heterodyning is compared with the signal from the reference source in the phase detector The resulting phase error is fed back to the slave laser, which is then forced to track the master laser [28] The main challenge in the realisation of OPLL is the need for wide-band electronics, since the linewidth of semiconductor lasers are relatively large The required bandwidth of the feedback is determined by the sum of the laser linewidths Because the PLL receiver has only a limited bandwidth, which is much smaller than the bandwidth of data signal, it provides only a limited tracking of the RF carrier The residual phase jitter between the carrier and the reference

employed for demodulation will increase the CNR required to achieve a desired BER and produce an error floor [29]

Another problem that has to be addressed is the frequency stability of the generated signal The stabilization of optical waves is not sufficient for radio/fiber requirements Rather than stabilising the optical wavelength, the difference frequency could be stabilized This could be achieved using either an optical frequency locked loop (OFLL) [30] or opto-electronic automatic frequency control loop (AFC) Equally good results could be obtained by using the PLL and injection-locking techniques, which as mentioned before can be utilised to suppress the phase noise [31]

The experiments illustrating the phase noise problems and ways to overcome it have been described in [31] First the millimeter-wave carrier was generated using two different lasers, one of which was directly modulated with a 140 Mb/s data signal The RF signal received at the output of the photodiode had a hnewidth of 4 MHz This proves that heterodyning of two separate lasers, without any phase cancellation is not a suitable method for the generations of millimeter-wave signals

If two optical carriers are generated in the same cavity, their phase noise is expected to be correlated Lima *et al* [32] describe an experiment involving a Distributed Feed - Back laser (DFB) This laser had its phase shift in the Bragg grating, ensuring single mode oscillation, removed In this case the laser generated two modes with one on each side of the Bragg frequency, separated by the stop band of the filter Such a dual-mode laser has been used to generate millimeter-wave signals The mode separation was 0 48 nm, which corresponds to a beating frequency of around 57 GHz The RF signal obtained had a linewidth of 150 MHz, which shows that the two modes were uncorrelated

The two experiments described above show that some special arrangements have to be used in order to eliminate the phase noise in the heterodyning process, especially if carriers generated this way are to be used in future radio/fiber systems

One of the simplest techniques of achieving the phase correlation between the laser modes involves phase locking of millimeter-wave signals by subharmonic modulation of the laser This is realized by applying a drive signal to a laser The locking process can be explained as follows direct modulation of the laser with a

subharmonic signal of the desired RF signal generates multiple side bands on each of the modes When one of the side bands belonging to one laser mode overlaps the neighbouring mode then this overlapping side band provides the injection-locking signal for that mode Because each mode has side bands, both modes will be injection-locked Locking causes most of the power to be transferred to the locking sideband, making it possible to achieved injection-locking using a subharmonic of the required RF frequency [33] Heterodyning with subharmonic phase locking is capable of producing RF signals that exhibit high power and purity This is simple and cheap essentially because there is no need for a high-speed signal generator since locking can be achieved with a subharmonic of the RF carrier [34] Wake *et al* [35] report on generating a 60 GHz signal with a linewidth that is less than 10 Hz and phase noise less than –73 dBc/Hz at an offset of 10 kHz This was achieved using a dual-mode DFB laser injection-locked by the ninth harmonic of the desired beat signal Another advantage of injection-locking is that the modulating frequency does not have to be the exact subharmonic of the beat signal Locking ranges of 500 MHz for multisection DFB laser has been reported [33] This allows for compensation of any inaccuracy in adjusting the mode spacing, to obtain the required frequency The authors in [33] also show that the frequency of the beat signal can be tuned between 40 and 60 GHz by varying the individual contact bias currents, and in range of 1 GHz at each of these frequencies by changing single contact current

In the experiments mentioned above the modulation depths varied within a range of 10-20% This is due to the high power at the fundamental drive frequency and is an unavoidable consequence of subharmonic injection locking as opposed to fundamental injection-locking [33]

Generation of an RF carrier using a dual-mode laser requires a specially fabricated laser This can be avoided if a mode-locked laser is used [36] Sato *et al* [37] demonstrate a method of generating millimeter-waves using a DBR laser integrated with an Electro-Absorption Modulator (EAM) By driving the modulator at a frequency corresponding to the mode spacing of the laser, the mode-locking occurs Furthermore, since the EAM is capable of doubling the modulating frequency, the modulator can be driven at half of the desired RF frequency Mode-locking ensures the dual-mode operation of a laser and a phase correlation of both modes The authors in [37] report on the generation of a 60 GHz carrier with –78 dBc/Hz phase

noise at an offset of 100 kHz and a modulation depth of 90% This method overcomes the problem of low modulation depth since no fundamental drive frequency is present in the locking signal

A recent report by A J Vieira *et al* [38] demonstrates another method of generating millimeter-wave signals using a mode-locked laser The experiment describes a microchip laser that is situated in a millimeter-wave cavity, whose length was chosen to match the axial mode spacing of the laser and the desired RF frequency The laser's modes are locked by an electrical signal coupled into the cavity using a small loop antenna The tuning of the generated frequency can be achieved by scaling the length of the cavity The electrical signal generated using the above-described laser had a phase noise of −110 dBc/Hz at an offset of 10 kHz The main advantages of this method, according to the authors, are simplicity, compactness, high level of integration of millimeter-wave and optic components and good performance The cost of the system based on this type of transmitter can be further reduced by using a subharmonic frequency of the RF signal to lock the modes

3 3 1 Heterodyning - simulation

Millimeter-wave generation by heterodyning was simulated using the VPI package The generation as a result of beating between two correlated and uncorrelated sources was considered as different cases *Figure 3-21* illustrates the simulation model for the case, when the RF carrier was generated using two independent laser diodes

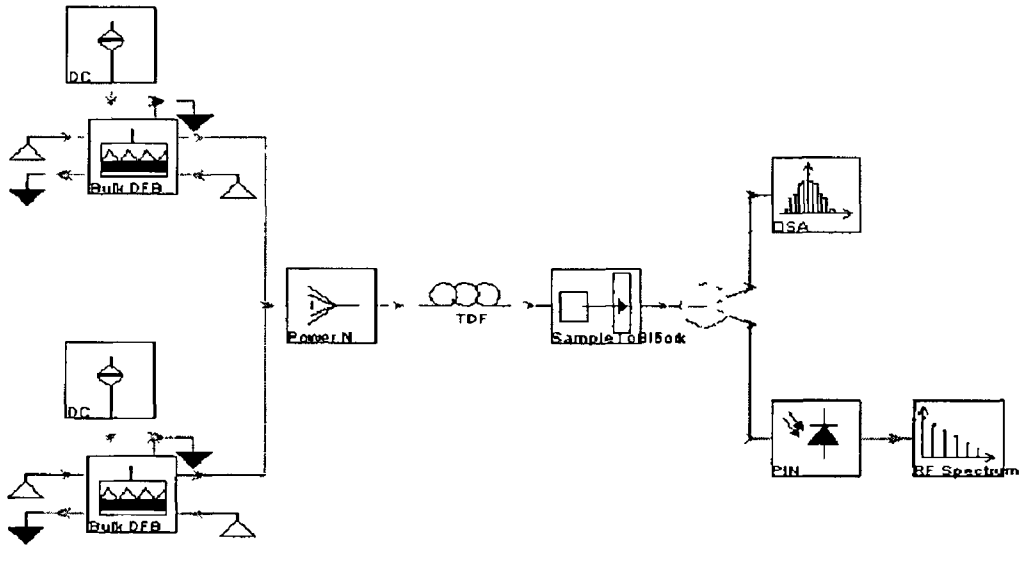

Figure 3-21 Heterodyning using two lasers - simulation model

The lasers were biased at 50 mA DC bias current The outputs of the lasers were combined using a power combiner and transmitted over 2 km Standard Single Mode Fiber (SSMF) Output signal form the fiber was split between optical spectrum analyser and a photodiode The spectrum of the detected electrical signal was then displayed using an electrical spectrum analyser *Figure 3-22* shows the optical spectrum at the output of the coupler The wavelengths of lasers were set to be 40 GHz apart

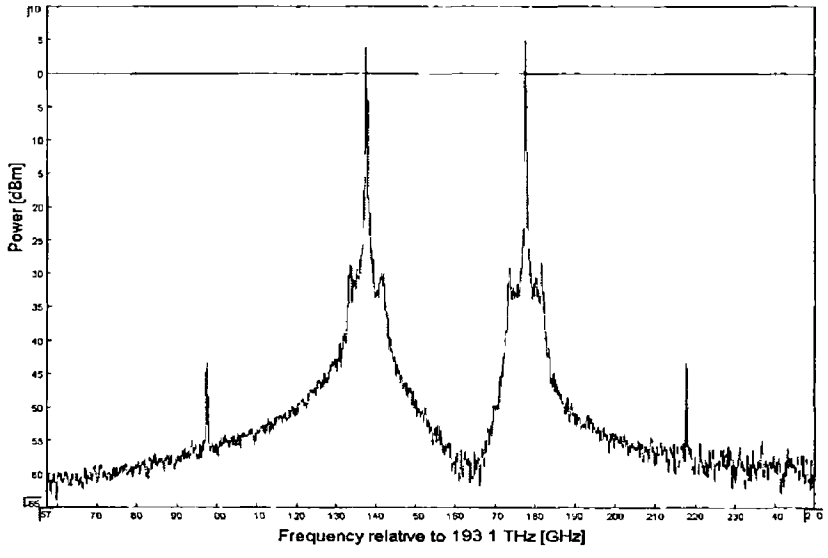

Figure 3-22 *Combined optical spectrum - uncorrelated lasers*

As mentioned in the previous section, an RF signal generated by the beating of two uncorrelated modes (generated by two independent lasers) has a spectral width equal to the sum of the linewidths of the lasers used for heterodyning In the simulation lasers had linewidths of around 17 MHz each *Figure 3-23* present the RF spectrum of the generated radio carrier

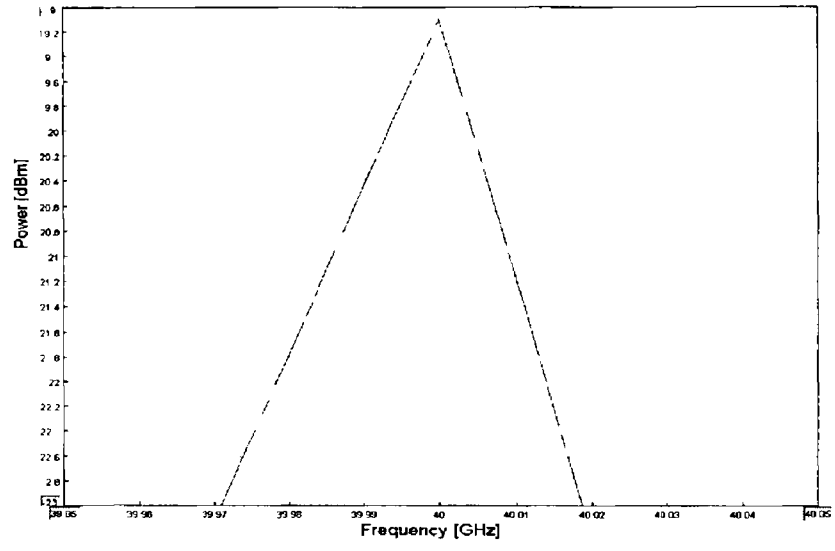

Figure 3-23 Electrical spectrum - lasers linewidth 40 MHz

From *Figure 3-23* the quality of the RF signal could be seen to be rather poor, solely due to the spectral width being approximately 40 MHz

The simulation results prove that heterodyning of two independent lasers is not suitable for the generation of high quality RF carriers and that the signal obtained at the output of the pin is determined by the linewidth of the laser modes used for the generation

Having established the fact above, the next step was to investigate, whether using side-band injection locking would lead to the generation of higher quality RF signals The model used to perform this simulation is shown in *Figure 3-24* The simulation model is very similar to one from *Figure 3-21* This time though the side-band injection locking was used to correlate two DFB lasers

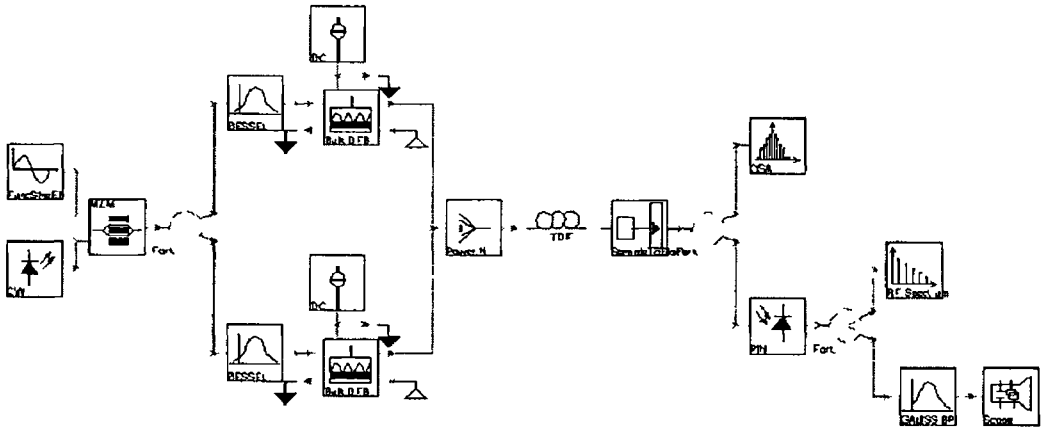

Figure 3-24 Heterodyning using bimodal laser - simulation model

Light from a CW laser was externally modulated using 20 GHz electrical signal By biasing the MZM at its null point the frequency multiplication was achieved The output of the MZM consisting of two modes separated by 40 GHz (see *Figure 3-17* (a)) was split and the modes were separated using two Band Pass (BP) optical filters Each mode was then injected into a different laser providing the locking signals [39, 40] The optical spectrum of the lasers after the power combiner is *Figure 3-25*

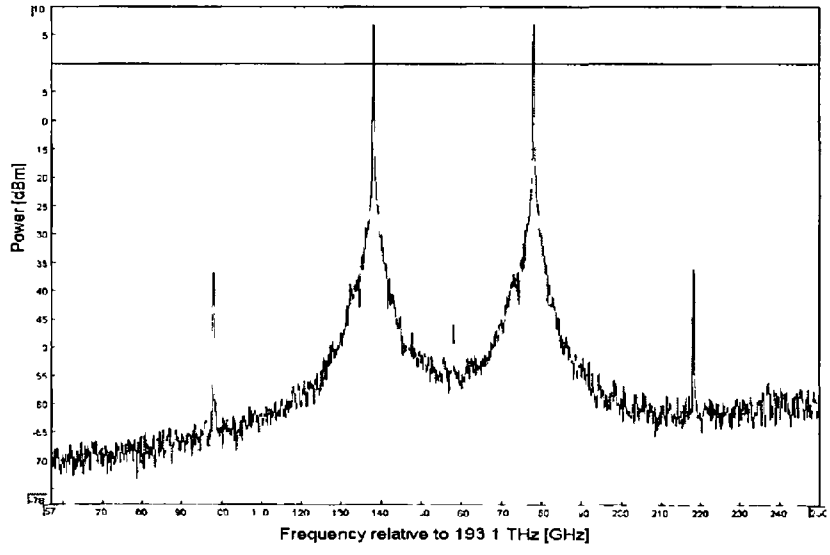

Figure 3-25 *Optical spectrum of injection-locked lasers*

The spectral widths of the modes were again around 17 MHz The electrical spectrum of the received signal after filtration is shown in *Figure 3-26*

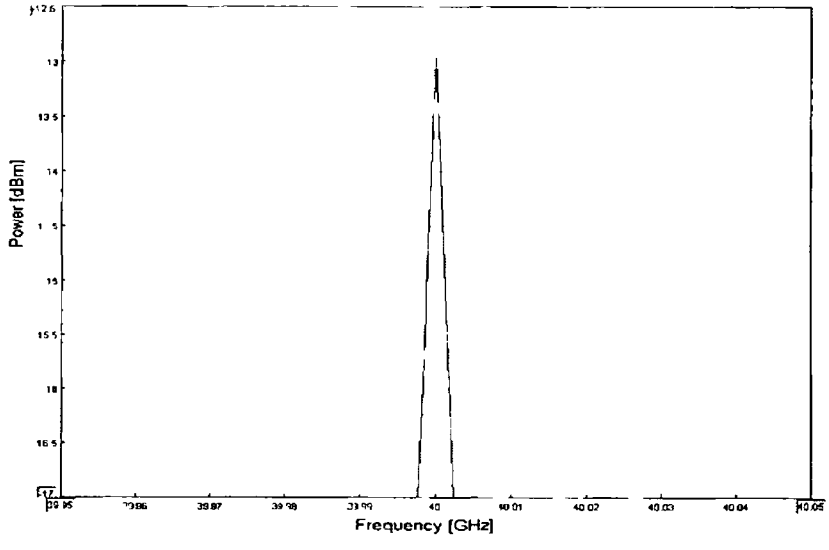

Figure 3-26 *Electrical spectrum of the generated RF carrier*

From *Figure 3-26* it can be seen that quality of the signal generated using heterodyning of two modes from a single laser is much better than that of the

independent lasers The spectral width in this case is around 3 5 MHz, much lower than the linewidth of the lasers

3 4 Optical frequency conversion

This method makes the use of the fact that any physical component of a system has a nonlinear transfer characteristic such that it manifests in creation of new frequency components in the output signal A lot of effort is put in the reduction of the scale of the component nonlinearity since harmonics and Inter-Modulation Distortion (IMD) degrade the performance of a system However, this feature could also be used advantageously in order to generate new frequencies for example higher frequency signals using only low speed signal generators The main components used for frequency conversion in radio/fiber systems are photodiodes and external modulators

In photodiodes the nonlinearity, which can be used for RF generation is caused by saturation of the photodetector When the incident optical power falling on the detector increases and the reverse bias of the diode decreases, the response of the detector is distorted When two optical carriers, each one modulated with a different frequency, fall on the detector with a nonlinear response, the mixing between the electrical signals occurs and components $f_1 \pm f_2$ are generated If one of the signals carries data, the data signal will be upconverted to a higher frequency band [41 - 43]

In the case of external modulators, the nonlinearity used for optical mixing and frequency conversion come about due to their sinusoidal transfer function Usually for analog systems the external modulator is biased at the most linear part of the transfer function to minimize the power in the generated harmonics and intermodulation products On the other hand, biasing the modulator at the minimum or maximum transmission point can maximize the frequency conversion By applying two electrical signals to the modulator optical mixing can by realised This can be used to achieve both up- and downconversion of the signals [44, 45]

3 5 Remote upconversion using heterojunction bipolar phototransistor

Heterojunction bipolar phototransistors (photoHBT) can perform as a photodetectors with gain, optically injection locked oscillators and mixers When placed in a RAU

the photoHBT can be used for detection and remote upconversion of data sent from the CS using an Intermediate Frequency (IF) The base-collector junction of a photoHBT is photosensitive, allowing an optical signal to be detected Mixing is achieved by applying a Local Oscillator (LO) signal to the third terminal of the transistor [25] The output signal of the transistor consists of mixing products of the received signal and the LO (at frequencies $f_{IF} \pm n*f_{LO}$), because photoHBT is inherently a nonlinear device High conversion efficiency can be achieved even for higher order harmonics This is due to the internal gain of the transistor A phototransistor can also be employed in the uplink to downconvert the incoming signal from a Mobile Station (MS) to allow a simple low frequency return path [46, 47] Experimental and theoretical investigation of an optoHBT can be found in [48, 49]

3.6 Comparison of different methods

The choice of a particular method for the generation of RF signals will have a serious impact on system cost and flexibility Each of the methods described above has its advantages and disadvantages Hence the final decision, which one to choose is rather difficult This section presents a brief comparison of all the methods mentioned above

Direct and external modulation are the most common and oldest ways of generating optical microwave signals The main advantages of direct modulation is its low cost, the main problem associated with it is the bandwidth limitation The experiments presented in this chapter show that by using external injection this problem could be overcome at the expense of using an additional laser On the other hand resonant modulation is free from this hindrance The main difficulty here lies in obtaining enough power Also this method is suitable only for transmission of narrowband signals, since the bandwidth of the resonantly enhanced laser dose not exceed 1 GHz External modulation brings about high insertion loss of the modulator In the case of 1f generation a high-speed modulator is required, which increases the cost of system realisation This can be overcome by using 2f or 4f generation at the price of high driving voltage, which is required to overdrive the modulator

All above-mentioned methods involve intensity modulation, which generates Double Side Band (DSB) signals As mentioned in Chapter 2 this format suffers from dispersion effects of the fiber and transmission of such signals requires additional

arrangements (see Chapter 4) to overcome this problem Another disadvantage of these methods (except 2f and 4f generation) is that a high speed RF signal generator is required to produce the radio carrier On the other hand, a very important advantage of intensity modulation is its flexibility in regard to the choice of frequency A laser as well as an external modulator can generate any frequency as long as it is within their respective bandwidth capabilities The exception here is the resonant modulation, for which the frequency of the generated signal is determined by the length of the external cavity

The remaining methods described in this chapter are new and their practical implementation would be much more difficult As mentioned before heterodyning is one of the most promising ways for generating high-speed optical signals It is very flexible and dispersion resistant [23] It is also cheap, but there are still many difficulties in realising a hybrid system based on heterodyning First of all achieving dual mode operation of a laser requires the usage of either three lasers (to lock the modes), or two lasers, one of which has to be directly or externally modulated Mode locking gives the flexibility in choosing the RF frequency, which is to be generated Heterodyning can also be realised with a use of an injection locked bimodal laser, but this requires special design and limits the range of frequencies that could be produced in this way Other important difficulties include stability problems (small drift in wavelength of the generated light results in large changes in generated RF signal) and phase noise cancellation

Generation of millimeter-wave signals using frequency conversion has one important disadvantage This involves the distribution of optical or electrical power over a large range of harmonic frequencies, which limits the modulation depth at the desired frequency [33, 50] This obviously reduces the efficiency of the system Transmission of many different optical components is also spectrally inefficient

The main method used for the generation of RF signals in this thesis is direct modulation essentially due to its simplicity and cost efficiency Hence the following chapters will mainly focus on the characterisation of this technique and its applications

References

[1] A Yariv "Optical Electronics in Modern Communications", Oxford University Press, Oxford 1997

[2] J M Liu *et al* "Modulation Bandwidth, Noise and Stability of a Semiconductor Laser Subject to a Strong Injection Locking", *IEEE Photon Technol Lett*, vol 9, pp 1325–1327, 1997

[3] F Mogensen *et al*, "Locking Conditions and Stability Properties for a Semiconductor Laser with External Light Injection", *IEEE J Quantum Electron*, vol 21, pp 784-793, 1985

[4] J B Georges *et al* "Multichannel Millimeter Wave Subcarrier Transmission By Resonant Modulation of Monolithic Semiconductor Lasers", *IEEE Photon Technol Lett* vol 7, pp 431-433, 1995

[5] Z Hu *et al* "Bandwidth Enhancement and Chirp Reduction in DBR Lasers by Strong External Light Injection", *CLEO 2000*, pp 99-100, 2000

[6] X J Meng *et al* "Experimental demonstration of modulation bandwidth enhancement in distributed feedback lasers with external light injection," *Electron Lett*, vol 34, pp 2031-2032, 1998

[7] G Yabre "Effect of relatively strong light injection on the chirp-to-power ratio and the 3 dB bandwidth of directly modulated semiconductor lasers," *J Lightwave Technol*, vol 14, pp 2367-2373, 1996

[8] J Wang *et al* "Enhancement of Modulation Bandwidth of Laser Diodes by Injection Locking", *IEEE Photon Technol Lett* vol 8, pp 34–36, 1996

[9] Z Hu *et al* "40-GHz Optical Pulse Generation Using Strong External Light Injection of a Gain-Switched High-Speed DBR Laser Diode", *IEEE Photon Technol Lett*, vol 15, pp 1767-1769, 2003

[10] C G Lim *et al* "Nonlinear Dynamics of Optically Injected Self-Pulsating Laser Diodes", *IEEE J Quantum Electron*, vol 37, pp 699-706, 2001

[11] A. Uchida *et al.* "High-Frequency Broad-Band Signal Generation Using a Semiconductor Laser With a Chaotic Optical Injection", *IEEE J. Quantum Electron.*, vol. 39, pp. 1462-1467 2003

[12] T.B Simpson *et al.* "Double locked laser diode for microwave photonic applications", *IEEE Photon. Technol. Lett.*, vol. 11, pp. 1476-1478, 1999.

[13] O. Frazao *et al.* "Tunable optical oscillator based on a DFB-MQW laser and a fiber loop reflector," *IEEE Transactions on Ultrasonics, Ferroelectrics and Frequency Control,* vol. 46, pp. 1341-1342, 1999

[14] H. Burkhard *et al.* "Ultra low phase noise in multigigahertz oscillations of injection tracked DFB lasers," *SPIE*, vol. 2994, pp.636–646, 1997.

[15] G. Yabre *et al.*" Noise Characteristics of Single-Mode Semiconductor Lasers Under External Light Injection", *IEEE J. Quantum Electron.*, vol. 36, pp. 385-393, 2000

[16] R. Nagarajan *et al.* "Resonantly Enhanced Semiconductor Laser for Efficient Transmission of Millimeter Wave Modulated Light", *IEEE Photon. Technol. Lett.*, vol.5, pp.4-6, 1993

[17] J. B. Georges *et al.* "Optical Transmission of Narrow-Band Millimeter-Wave Signals By Resonant Modulation of Monolithic Semiconductor Lasers", *IEEE Photon. Technol. Lett.*, vol.6, pp.568-570, 1994

[18] J. M. Senior "Optical Fiber Communications – Principles and Practice", Prentice Hall, London 1985

[19] B. Wilson *et al.* "Analogue Optical Fiber Communications", IEE, London 1995

[20] T. Kuri *et al.* "Fiber-Optic Millimeter-Wave Downlink System Using 60 GHz-Band External Modulator", *J. Lightwave Technol.*, vol.17, pp.799-806, 1999

[21] A. Stohr *et al.* "Chirp Optimized 60 GHz Millimeter-Wave Fiber-Optic Transmission Incorporating EA-Modulator", *Proc. European Conference on Optical Communications*, vol. 1, pp. 669-670, 1998

[22] K. Kitayama *et al.* "Error-Free Optical 156 Mb/s Millimeter-Wave Wireless Transport Through 60 GHz External Modulation", *OFC'98*, San Jose, 1998

[23] R Hofstetter *et al* "Dispersion Effects in Optical Millimeter-Wave System Using Self-Heterodyne Method for Transport and Generation", *IEEE Trans Microwave Theory Tech* vol 43, pp 667-669, 1995

[24] G J Simonis *et al* "Optical Generation, Distribution and Control of Microwaves Using Laser Heterodyne", *IEEE Trans Microwave Theory Tech*, vol 38, pp 667-669, 1990

[25] B Wilson *et al* "Analogue Optical Fiber Communications", IEE, London 1995

[26] R A Griffin *et al* "Optical millimeter-wave generation with high spectral purity using feed-forward optical field modulation", *Electron Lett*, vol 34, pp 364-366, 1998

[27] G R Lin *et al* "Demonstration and Optimization of an Optoelectronic Phase-Locked Phase Shifter for Optical Microwave Signals", *IEEE Photon Technol Lett*, vol 12, pp 1555-1557, 2000

[28] L N Langley *et al* "Packaged Semiconductor Laser Optical Phase-Locked Loop (OPLL) for Photonic Generation, Processing and Transmission of Microwave Signals", *IEEE Trans Microwave Theory Tech*, vol 47, pp 1257-1264, 1999

[29] R A Griffin *et al* "System Capacity for Millimeter-Wave Radio-Over-Fiber Distribution Employing an Optically Supported PLL", *J Lightwave Technol*, vol 17, pp 2480-2487, 1999

[30] J O'Reilly *et al* "Remote Delivery of Video Services Using mm-Wave and Optics", *J Lightwave Technol* vol 12, pp 369-375, 1994

[31] R P Braun *et al* "Optical Microwave Generation and Transmission Experiments in the 12- and 60- GHz Region for Wireless Communications", *IEEE Trans Microwave Theory Tech* vol 46, pp 320-330, 1998

[32] C R Lima *et al* "Compact Optical Millimeter-Wave Source Using a Dual-Mode Semiconductor Laser", *Electron Lett*, vol 31, pp 364-366, 1995

[33] D Wake *et al* "Optical Generation of Millimeter-Wave Signals for Fiber-Radio Systems Using a Dual-Mode DFB Semiconductor Laser", *IEEE Trans Microwave Theory Tech*, vol 43, pp 2270-2276, 1995

[34] G Grosskopf *et al* "Optical Millimeter- Wave Generation and Wireless Data Transmission Uing a Dual-Mode Laser", *IEEE Photon Technol Lett*, vol 12, pp 1692-1694, 2000

[35] D Wake *et al* "Transmission of 60-GHz Signals Over 100 km of Optical Fiber Using a Dual-Mode Semiconductor Laser Source", *IEEE Trans Microwave Theory Tech*, vol 8, pp 578-580, 1996

[36] D Novak *et al* "Millimeter-Wave Signal Generation Using Pulsed Semiconductor Laser", *Electron Lett*, vol 34, pp 1430-1431, 1994

[37] K Sato *et al* "Optical Millimeter-Wave Generation by Dual-Mode Operation of Semiconductor Modelocked Laser", *Electron Lett*, vol 36, Feb 2000

[38] A J Vieira *et al* "A Mode-Locked Microchip Laser Optical Transmitter for Fiber Radio", *IEEE Trans Microwave Theory Tech*, vol 49, pp 1882-1887, 2001

[39] R P Braun *et al* "Optical Feeding of Baser Station in Millimeter-Wave Mobile Communications", *ECOC 98*, Madrid, Spain 1998

[40] M Ogusu *et al* "60 GHz Millimeter-Wave Source Using Two-Mode Injection-Locking of a Fabry-Perot Slave Laser", *Microwave and Wireless Components Lett*, vol 11, pp 101-103, 2001

[41] M Tsuchiya *et al* "Nonlinear Photodetection Scheme and Its System Applications to Fiber-Optic Millimeter-Wave Wireless Down-Links", *IEEE Trans Microwave Theory Tech*, vol 47, pp 1342-1350, 1999

[42] Q Z Liu *et al* "Experimental Investigation of Fiber Optic Microwave Link with Monolithic Integrated Optoelectronic Mixing Receiver", *IEEE Trans Microwave Theory Tech* vol 43, pp 2357-2360, 1995

[43] G Maury *et al* "Microwave-Frequency Conversion Methods by Optical Interferometer and Photodiode", *IEEE Trans Microwave Theory Tech*, vol 45, pp 1481-1485, 1997

[44] C K Sun *et al* "Efficient Microwave Frequency Conversion Using Photonic Link Signal Mixing", *IEEE Photon Technol Lett*, vol 8, pp 154-156, 1996

[45] A C Lindsay *et al* "Photonic Mixers for Wide Bandwidth RF Receiver Applications", *IEEE Trans Microwave Theory Tech*, vol 43, pp 2311-2317, 1995

[46] Y Betser *et al* "A Single-Stage Three-Terminal Heterojunction Bipolar Transistor Optoelectronic Mixer", *J Lightwave Technol*, vol 16, pp 605-609, 1998

[47] H Sawada *et al* "An Experimental Study on a Self-Oscillating Up-Converter that Uses a Heterojunction Bipolar Transistor", *IEEE Trans Microwave Theory Tech*, vol 47, pp 1515-1521, 1999

[48] J Lasri *et al* "HBT Optoelectronic Mixer at Microwave Frequencies Modelling and Experimental Characterization", *J Lightwave Technol* vol 17, pp 1423-1428, 1999

[49] C Gonzalez *et al* "HBT Phototransistor for Remote Upconversion in Hybrid Fibre Radio Distribution Systems", *ECOC 2000*, Munich, Germany

[50] D Novak *et al* "Signal Generation Using Pulsed Semiconductor Laser for Application in Millimeter-Wave Wireless Links", *IEEE Trans Microwave Theory Tech* vol 43, pp 2257-2262, 1995

4 Radio/Fiber System Based on Externally Injected Laser Transmitter

The generation of millimeter-wave signals using various techniques was described in detail in the previous chapter Direct modulation is seen to be one of the simplest and most cost effective amongst these methods One of the major limitations experienced in using this technique is due to the insufficient inherent modulation bandwidth of the laser diode However, it has already been shown that this could be overcome by using external light injection Hence in this chapter the experimental realisation of a simple radio/fibre system employing external light injection is presented

4 1 Single Channel System

The experimental set-up to examine the use of a directly modulated laser diode with external injection in a hybrid radio/fibre system is shown in *Figure 4-1*

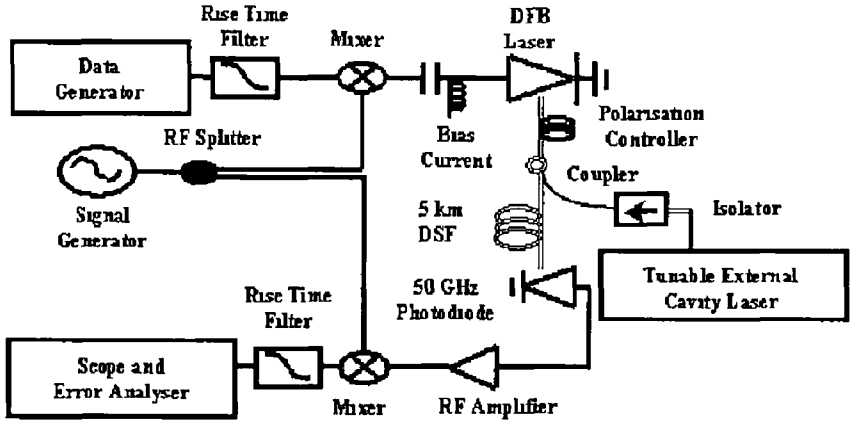

Figure 4-1 Experimental set-up for radio/fiber system using directly modulated laser with external injection

Initially, an Anritsu Pulse Pattern Generator (PPG) was used to generate a Non-Return to Zero (NRZ) Pseudo Random Bit Sequence (PRBS) at 155 Mbit/s The signal was then filtered using a 117 MHz rise-time filter in order to limit its spectral width The resulting electrical spectrum is shown in *Figure 4-2*

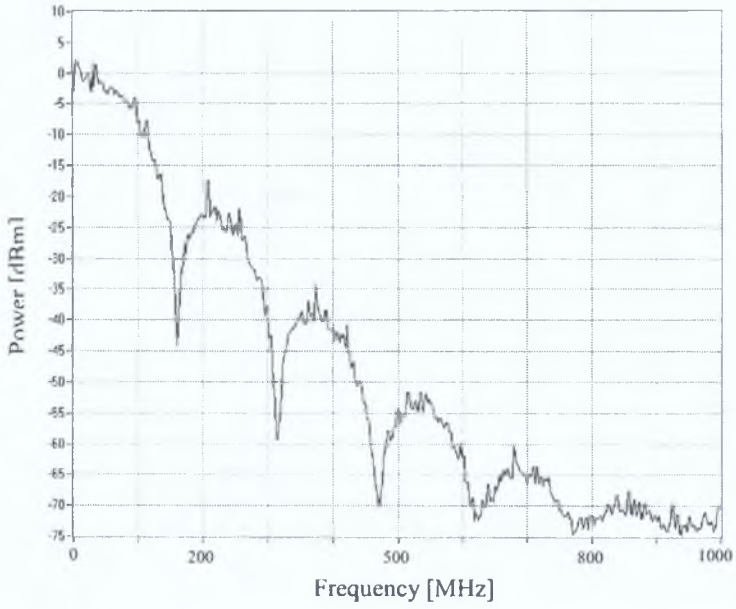

Figure 4-2: *Electrical spectrum of the data signal from the pattern generator*

The filtered signal was then mixed with an 18 GHz RF-carrier to generate a Binary Phase Shift Keyed (BPSK) data signal (*Figure 4-3*). The RF carrier was generated with the use of a 20 GHz signal generator (HP83731B) that had a maximum output power of 20 dBm.

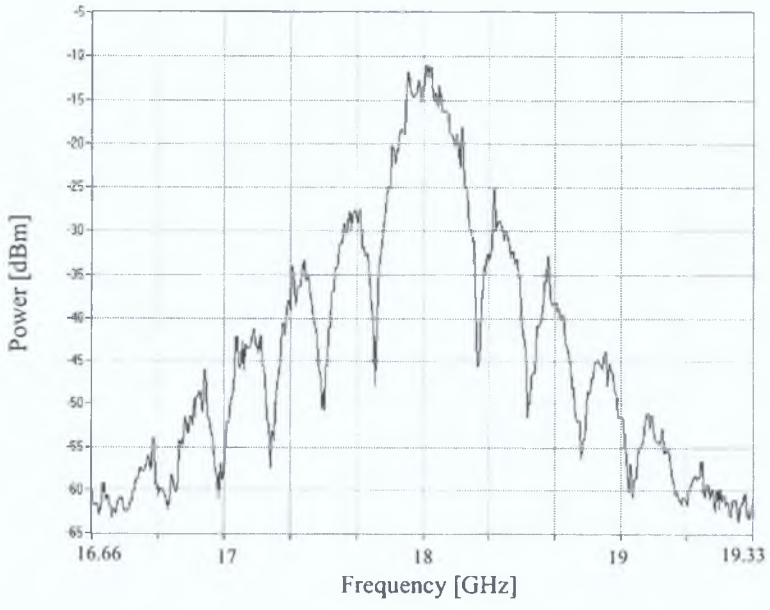

Figure 4-3: *Electrical spectrum of the data signal mixed with signal from Local Oscillator*

The upconverted data signal was then used to directly modulate a 1543 nm NTT Distributed Feed-Back (DFB) laser (KELD 1551 CCC_1). Basic characterisation of the laser was performed before the laser was used in the experiment. The output

power vs current dependence is shown in *Figure 4-4* Using the P/I curve the threshold current was determined to be 24 5 mA

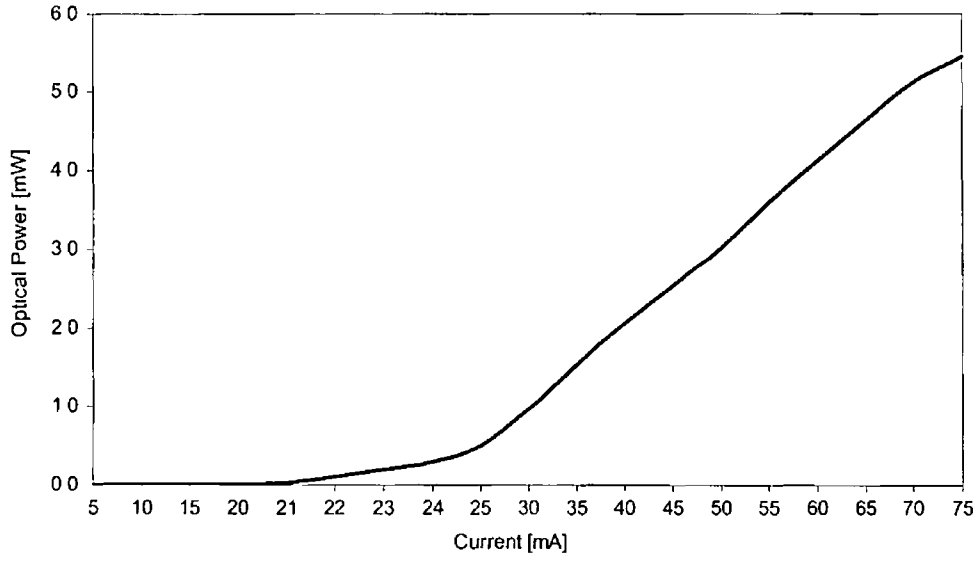

Figure 4-4 *Output power vs bias current for laser used in experiments*

The frequency response of the device was characterised using a HP vector Network Analyser The response is shown in *Figure 4-5* (a)

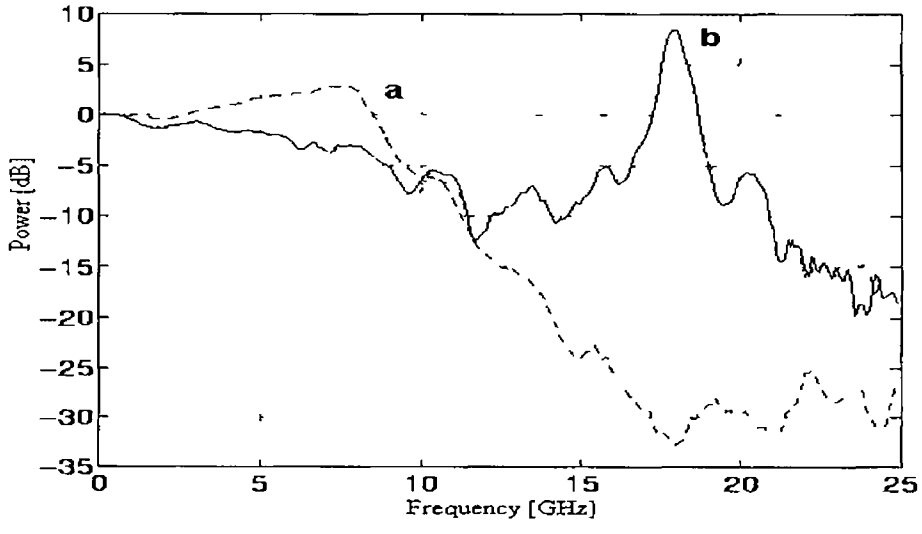

Figure 4-5 *Modulating response of the laser (a) free running (b) under external injection*

The 18 GHz RF data signal was applied in turn to both the free running laser and the laser under external injection External injection was realised (as described in Chapter 3) using a tunable External Cavity Laser (ECL) diode (HP8168F) The ECL had a resolution of 1 pm and a maximum output power of 5 mW across the whole range of tunability As outlined in Chapter 3 the external injection greatly enhances

the modulation response of the laser and in this work an injection level was used that optimized the response at the operating frequency of 18 GHz (injection power 5 dBm) In both cases (free running conditions and external injection) the RF data signal was combined with a DC bias current of 60 mA with the use of a 40 GHz bias tee The resulting optical microwave data signal from the laser (*Figure 4-6*) was amplified with the use of an Erbium Doped Fiber Amplifier (EDFA) The EDFA had a gain of 28 dB and a saturation output power of 14 dBm The amplified signal was then coupled into 3 km of Dispersion-Shifted Fibre (DSF) and finally detected with the use of a high-speed photodiode The latter had a bandwidth of about 50 GHz and a responsivity of 0 62 A/W The effect of propagation along the DSF did not have a great influence on the system performance since the total dispersion of such a fiber at 1550 nm is negligible (3 ps/nm km)

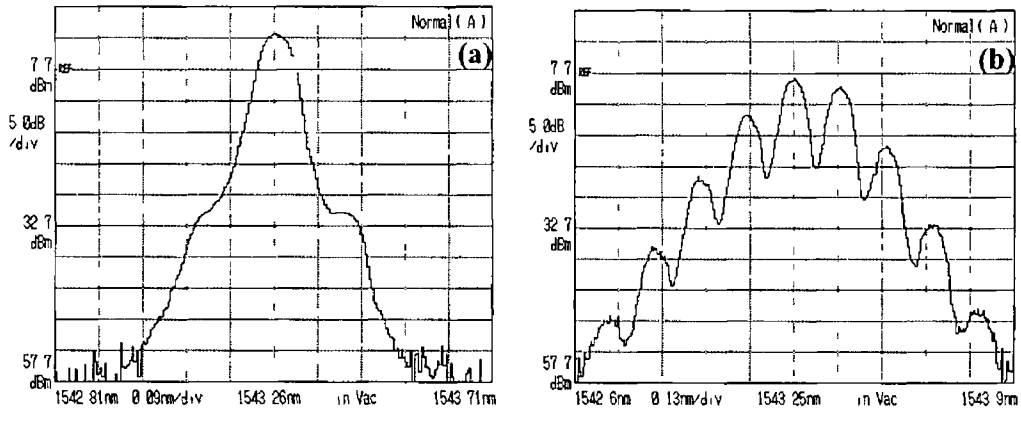

Figure 4-6 *Optical spectrums of the laser (a) in free running conditions (b) under external injection*

In a complete system the output signal of the detector would be transmitted through an RF antenna to the mobile network stations where the data would be received by down-converting the incoming signal using a Local Oscillator (LO) However, the experiment was focused on the optical part of the system, hence the down conversion takes place after the photodiode, by mixing the data signal with an 18 GHz LO After the detector the RF carrier was amplified using an amplifier (Agilent 83017A) The amplifier had a bandwidth of 26 GHz, gain of 25 dB and maximum output power of 15 dBm The downconverted data signal was then amplified by using another amplifier (Picosecond 5840) that had an operational frequency that ranges between 80 kHz and 10 GHz, gain of 22 dB and a maximum output power of 12 dBm The resulting 155 Mbit/s data signal was then displayed on the oscilloscope as well as fed into the Anritsu error analyser to determine the Bit-

Error-Rate (BER) of the received signal *Figure 4-7* displays the received eye diagrams for the cases when the directly modulated laser was (a) free running, and (b) had an external injection level of 5 dBm from the ECL The received optical power in both cases was -12 dBm to ensure that variation in received power does not play a part in the enhancement/degradation of the eye diagram *Figure 4-7* (a) clearly shows that the eye is almost completely closed However, the eye in *Figure 4-7* (b) is wide and fully open Hence we can conclude that there is a major improvement in the system performance when external injection is employed

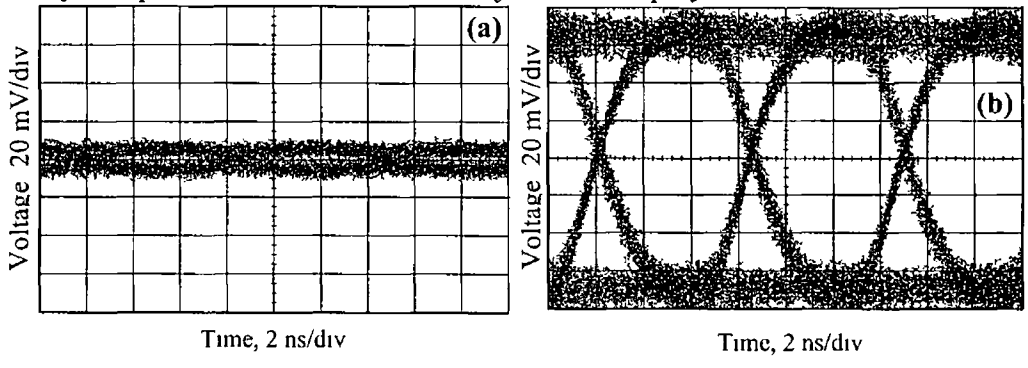

Figure 4-7 *Received eye diagrams of 155 Mbit/s signal from the optically fed microwave system using (a) free running laser (b) laser with the external injection level of 5 dBm*

In order to carry out the BER measurements the optical power falling on the detector was varied with the aid of a variable optical attenuator This yielded values of BER at different received optical powers Here again the measurements were carried out for both cases (free running and external injection) These results were then plotted as shown in ***Figure 4-8***

The enhancement in the frequency response obtained by injecting the light from the master laser (*Figure 4-5* (b)) manifests itself as an improvement in system performance, which is visible in ***Figure 4-8*** The 14 dB improvement corresponds to a 28 dB increment in the electrical modulation response This is less than would be expected (38 dB) from the enhanced electrical frequency response at the operating frequency of 18 GHz shown in *Figure 3 7* This may be attributed to the fact that the external injection reduces the laser threshold, and thus increases the average output power from the laser [1] This additional power is a DC component, which does not improve the BER of the signal Also the self-pulsation of the laser may introduce additional noise, which affects the BER

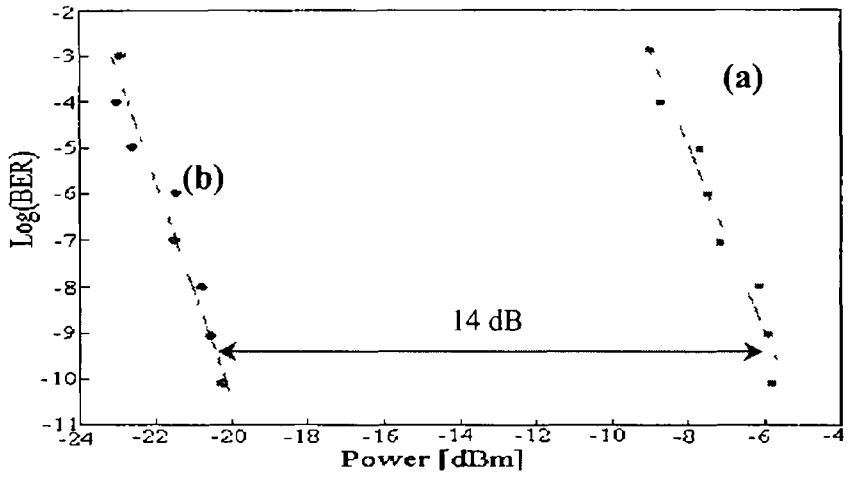

Figure 4-8 BER against received optical power of 155 Mbit/s signal from the optically fed microwave system using a) free running laser b) laser with an external injection level of 5 dBm

The results obtained demonstrate that external light injection enhances the performance of a single channel hybrid radio/fiber system Because the millimeter-wave systems are expected to utilise Sub-Carrier Multiplexing (SCM) it was important to verify, whether external injection can support the generation of multiple channels If the self-pulsation frequency was locked to only one of modulating frequencies, a laser with external injection could not be used for multichannel systems The next section aids in the validation of the latter statement

4 2 Two channel system

4 2 1 Data transmission

In order to verify the usefulness of external light injection for multichannel transmission a two-channel system was built The experimental set-up used is shown in *Figure 4-9* This set up is very similar to the single channel one from *Figure 4-1* A filtered 155 Mbit/s NRZ data stream from an Anritsu pattern generator was split using an RF coupler Each one of the two data streams was then mixed with a different RF-carrier (18 6 GHz and 19 GHz), resulting in two BPSK data signals The RF data signals were then combined in another RF coupler, and the resulting multi-carrier signal was used to directly modulate the DFB laser The two RF carriers could be applied either to the free running laser or to the laser diode under external injection (injection power 5 dBm) In both cases the RF data signal was combined with a DC bias current of 60 mA The resulting optical microwave data signal from the laser was then passed through 3 km of DSF before being detected with a 50 GHz pin photodiode

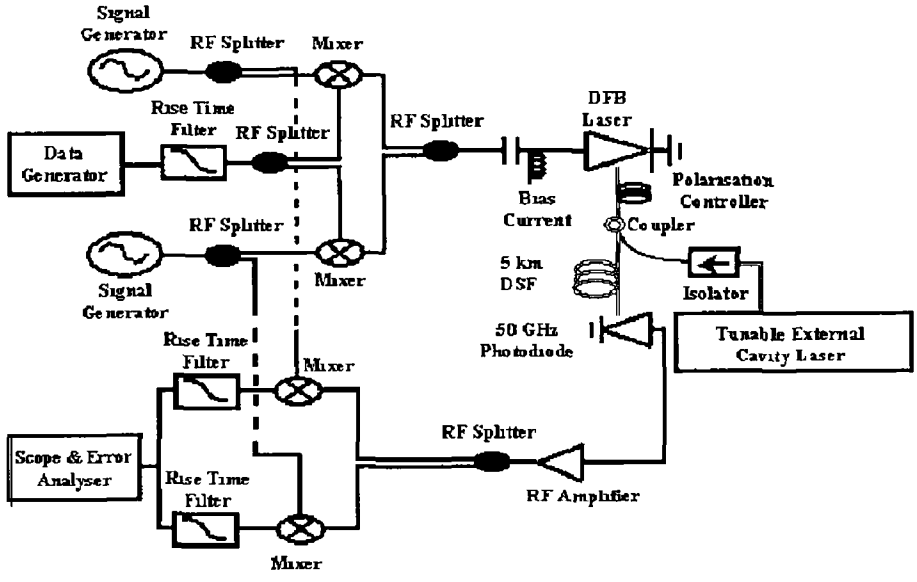

Figure 4-9 Two channel system - experimental set-up

The RF spectrum of the combined electrical channels used to modulate the transmitter is presented in *Figure 4-10*

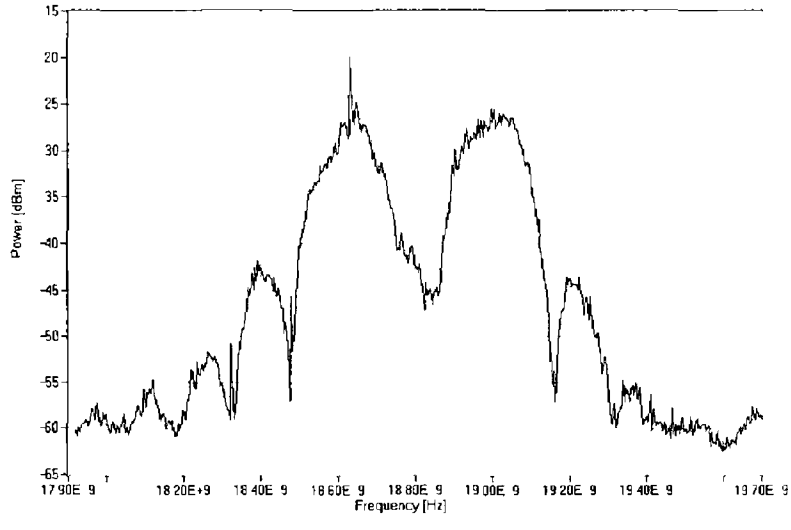

***Figure 4-10** RF spectrum of the modulation signal*

The electrical spectra of the resulting detected signal without and with injection are shown in *Figure 4-11* (a) and (b) respectively

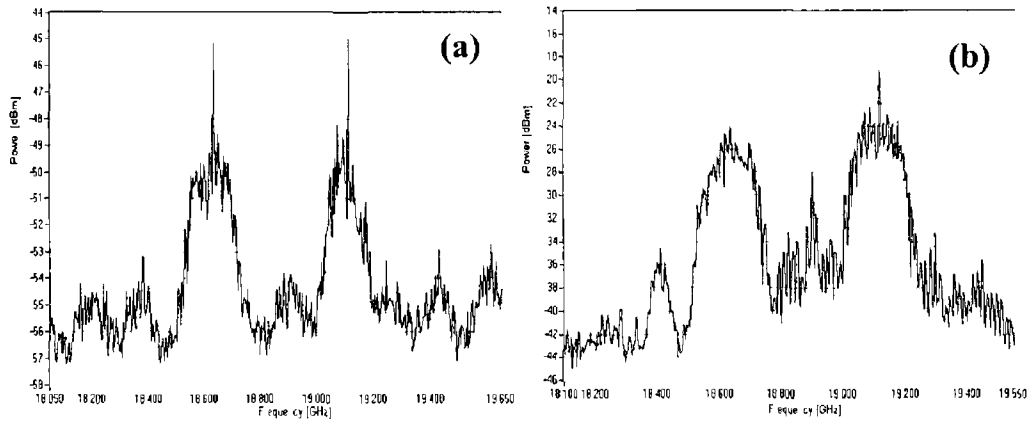

Figure 4-11 Spectra of the detected signal (a) without injection (b) with injection

From the electrical spectra it can be seen that external injection has significantly increased the received RF signal power The 18 6 GHz signal is 23 dB and 19 GHz signal 25 dB stronger than for the free running case The detected signal was than split using an RF coupler and each data channel was downconverted by mixing the incoming signal with a signal from the appropriate signal generator After the downconversion process the adjacent RF channels and the LO signal are still present These unwanted components were then filtered out by using a 117 MHz low-pass filter The improvement can also be seen in the temporal version of the signal The eye diagrams of the downconverted data channels are shown in *Figure 4-12 Figure 4-12* (a) shows the eye diagram of the signal generated by externally injected laser, while *Figure 4-12* (b) eye for free running laser The received optical power in this case was –3 dBm

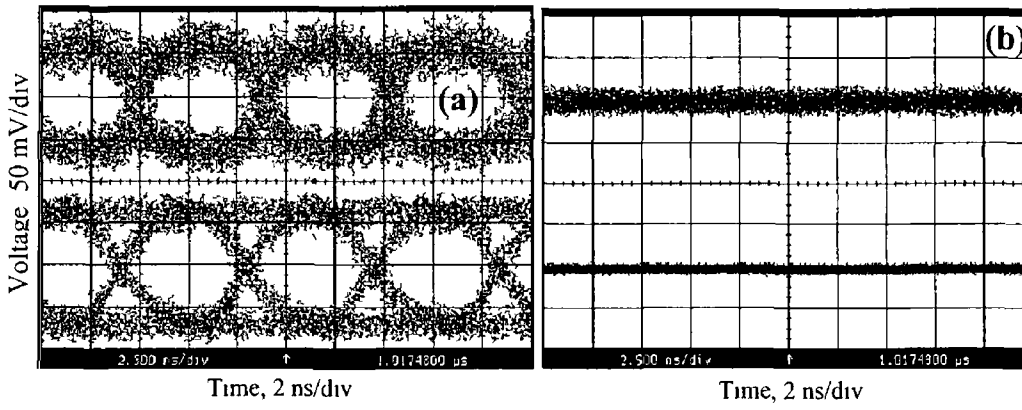

Figure 4-12 Received eye diagrams (a) laser with external injection (b) free running laser

The eye diagram in *Figure 4-12* (a) is clearly open, while in *Figure 4-12* (b) it is completely closed The final verification of the system performance was done by carrying out BER measurements *Figure 4-13* illustrates the BER as a function of

received optical power The circles denote the BER for 18 6 GHz data, while the squares BER for 19 GHz signal In the case of the free running laser the quality of the signal was very poor Hence the lowest BER that could be measured was 10^{-5} The curve for lower BER values had to be extrapolated, which is indicated by the broken line Also it can be seen that the quality of the two data channels was different (difference of around 2 5 dB for laser with external injection) This was due to the poorer quality of the 19 GHz carrier, which was generated using a sweep generator

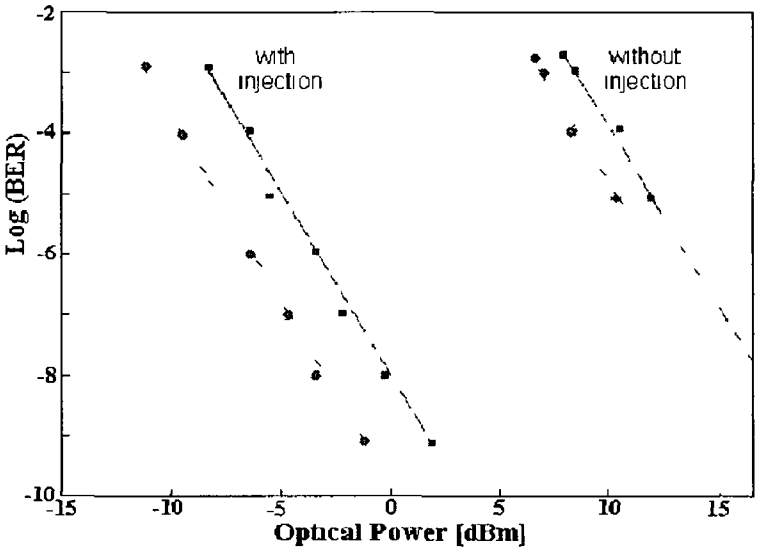

Figure 4-13 BER vs received optical power with and without injection (circles - 18 6 GHz squares - 19 GHz)

From the *Figure 4-13* it can be seen that external light injection improved the BER of both data channels In case of 18 6 GHz this improvement was an equivalent of around 20 dB and in case of 19 GHz around 17 dB

The experiment described above proves that external light injection is capable of enhancing the quality of more than one signal simultaneously From this we can conclude that the technique of generating multiple RF carriers using externally injected lasers is viable The next chapter comprises more detail investigation of multiple channel generation using direct modulation This includes the nonlinear distortion characterisation

4 2 2 Two-tone test

An important parameter of the described system is the Dynamic Range (DR) This could be defined as the maximum range of powers that a system can receive

correctly The verification of the DR of a system could be performed by carrying out a basic two-tone test on the system in question The DR could be measured, from the results of this two-tone test, by finding the difference in power between the received signal and the IMD signal, when the IMD signal reaches the noise floor of the overall system A high DR is especially important in the radio/fiber system due to large variations in the received powers of the signals transmitted by the Mobile Stations (MS) (near-far effect)

In order to measure the DR of our system, the laser was directly modulated with two carriers at frequencies of 18 and 18 4 GHz The two-tone test was performed for the laser with and without injection and the results are shown in *Figure 4-14* and *Figure 4-15* respectively The power of the detected signal and the IMD_3 component was measured, as the power of the modulating signal was varied

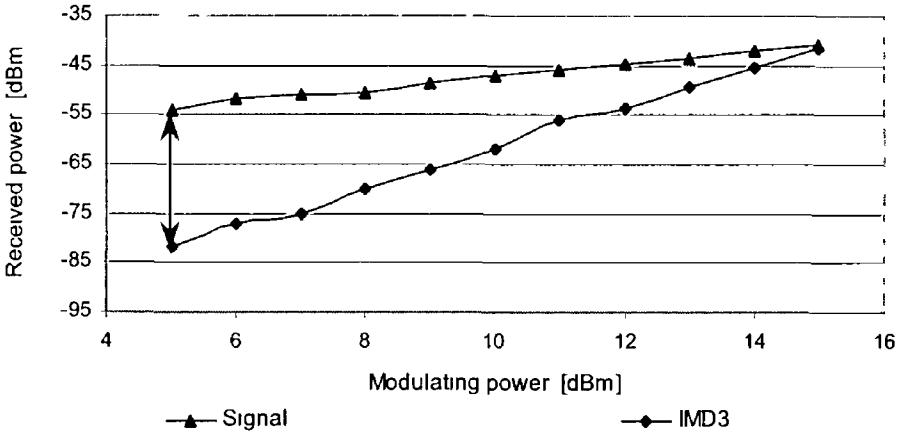

Figure 4-14 *Two-tone measurement - laser with external injection*

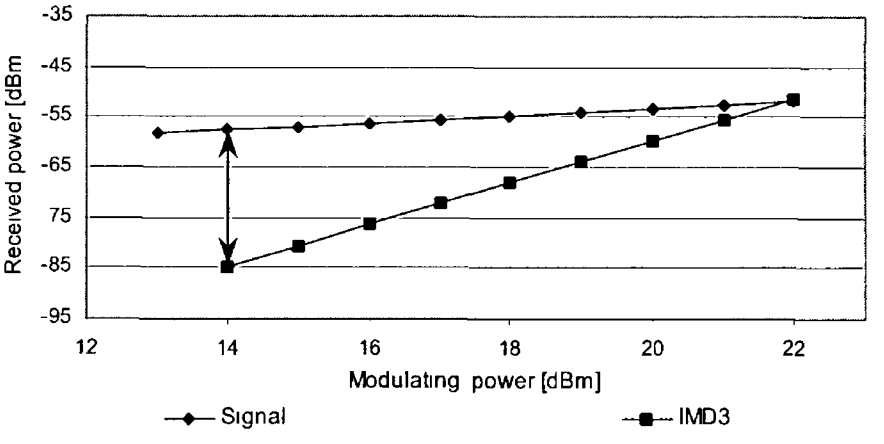

Figure 4-15 *Two-tone measurement - free running laser*

For the free running laser the DR was 28 dB (the noise floor was –85 dBm) On the other hand for the externally injected laser the DR was limited not by the noise floor but by the minimum modulating power that is required to obtain a stable carrier (suppress the self-pulsation) As mentioned earlier (in Chapter 3), this power was 5 dBm Thus from *Figure 4-14* it can be seen that the minimum output power was – 82 dBm This then gives a DR of around 27 8 dB

In both cases the DR was very poor In the case of the free running laser it was due to the fact that laser was operating well beyond its bandwidth while for the externally injected laser the main limitation was the requirement for the modulating power to exceed 5 dBm to generate a stable RF carrier

4 3 Chromatic Dispersion in Millimetre-wave Transmission Systems

The performance of an optical system strongly depends on the fiber dispersion, which limits the bandwidth-distance product of the link In digital systems dispersion causes a linear degradation of the transmitted signal due to pulse broadening as the signal propagates in the transmission fiber Chromatic dispersion is caused by the fact that refractive index of glass changes depending on the wavelength of light Different frequencies of the light travel in the fiber with different speeds because the velocity of the light depends on the refractive index The effect of chromatic dispersion becomes more important as the spectral width of the data signal increases [2, 3]

4 3 1 Effect of the chromatic dispersion on the millimeter-wave transmission

In analogue millimetre-wave systems dispersion can have much more serious effect on the system performance then in other systems In radio/fiber systems the radio carrier is generated remotely, in the CS and then transmitted via fiber to a RAU Modulation of the optical carrier normally generates two main components in the optical spectrum that are equi-distant from the light carrier by the radio frequency, which may be in the range of 2 – 200 GHz The space between these side bands equals twice the radio frequency These components are affected by chromatic dispersion, which cause them to travel at different speeds This introduces a phase

difference between them The larger the distance between the frequency components (higher modulation frequency), the faster the change When the signal is detected using a photodiode, each side band beats with the optical carrier to give an electrical signal at the modulation frequency All the RF components that are generated in this way are summed together at the output of the detector If the upper and lower side bands have opposite phases, the components created by them will interfere destructively thereby causing the output signal to fade [4] Because of the sinusoidal nature of the optical carrier, the phase difference between side bands changes continually between 0 and 2π radians as the signal travels along the fiber This means that the power of the received RF signal will fade and rise as a function of transmission length [5]

It can be shown that for small modulation depths the detected signal power of the RF carrier is approximately proportional to [6]

$$P = \cos^2\left(\frac{\pi D\lambda^2 L f^2}{c}\right), \qquad \textbf{Equation 4-1}$$

where D – chromatic dispersion,

λ - the optical wavelength,

c – speed of the light,

L – length of the fiber

f – modulating frequency

Equation 4-1 shows that the phase of the output signal of the fiber depends on the RF frequency If the signal transmitted over a fiber consists of two or more frequency components, each of them will reach the output of the fiber with a different phase That means that in the photo-detector these waves will beat together and interfere constructively or destructively, depending on their phases For a simple sinusoidal wave, complete extinction of the signal will take place when the phase difference between frequency components equals 180° (90° for each side band relatively to the optical carrier) The transmission distance at which the first complete extinction occurs can be calculated from [7]

$$L = \frac{c}{2D\lambda^2 f^2} \quad \text{for} \quad \frac{\pi D\lambda^2 L f^2}{c} = \frac{\pi}{2}, \qquad \textbf{Equation 4-2}$$

For a millimeter-wave carrier at 18 GHz transmitted on an optical wavelength of 1550 nm over a standard fiber with a chromatic dispersion of 17 ps/km nm the signal

will fade for the first time after propagating over 11 335 km of fiber As mentioned before this is a cyclic behaviour and the periodic length (ΔL) could be found using the following formula

$$\Delta L = \frac{c}{D\lambda^2 f_c^2}, \quad \text{for} \quad \frac{\pi D\lambda^2 L f^2}{c} = \pi, \qquad \textbf{Equation 4-3}$$

From the formula above one can see that the transmission distance is inversely proportional to fiber dispersion (1/D dependence) It can also be seen that the frequency of signal fading increases with the square of the modulation frequency An increase in either dispersion or carrier frequency significantly limits the obtainable transmission distance Using the formula above a plot of the RF power of a received signal against the fiber length is presented in *Figure 4-16*

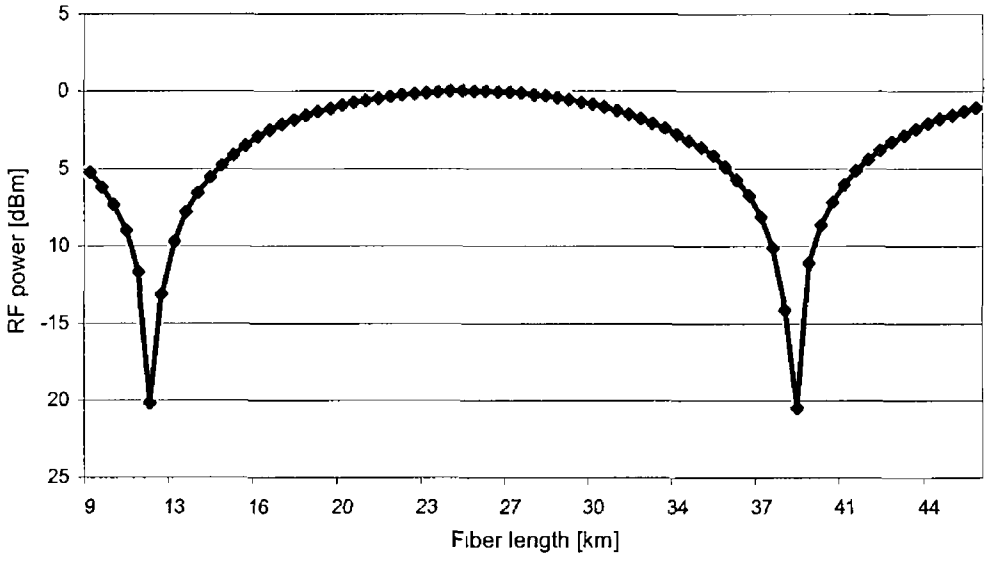

Figure 4-16 *Theoretical plot of RF power as a function of fiber length*

4 3 2 Overcoming the chromatic dispersion – SSB Modulation

The influence of chromatic dispersion can be overcome by employing the Single Side Band (SSB) modulation [8] In most systems using direct or external modulation of the laser the signal generated consists of an optical carrier and the two side bands equally spaced from the carrier by the modulating frequency This type of modulation is known as Double Side Band (DSB) In mm-wave systems, because of the significant distance between both side bands, the influence of chromatic dispersion on system performance can be very serious and can significantly limit the length of the optical link This problem can be overcome by ensuring that there is

only one side band travelling along the fiber In systems employing the external modulation a SSB signal could be achieved by using a dual-drive modulator In this type of device the modulating signal is split into two branches before being applied to the modulator The phase of one of the branches is shifted by 90° in regards to the original signal [8 - 10] For the direct modulation the only way of achieving a SSB signal is by using an optical filtering A Band-Stop Filter (BSF), which will filter out one of the side bands, could be used However in practice modulation results in more than two sidebands being generated because it is not a perfectly linear process The components created as a result of transmitter nonlinearity, interfere with the signal in the photodiode Although they carry much less power than the main sidebands these components still cause degradation of the data signal Hence the BSF has to be substituted with a Band-Pass Filter (BPF), which will allow only one sideband and the optical carrier to propagate along the fiber [4, 11 - 13]

4 3 3 Experimental investigation of dispersion

The dispersion induced fading of the signal was investigated experimentally by measuring the power of the RF signal for different fiber lengths The experimental set-up used is shown in *Figure 4-17*

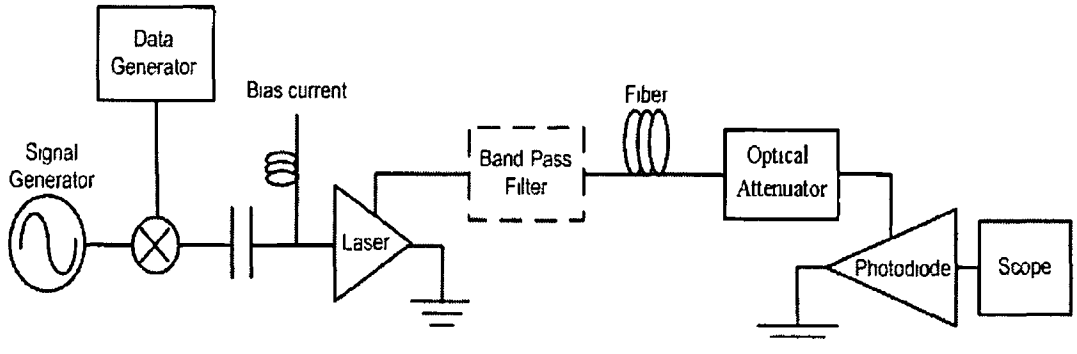

***Figure 4-17** Transmission of DSB and SSB signals over the fiber -experimental set-up*

In the experiment the 1550 nm laser diode, biased at 60 mA, was directly modulated by 155 Mb/s data upconverted to 18 GHz The output signal from the laser was first transmitted through the fiber An optical attenuator was used to ensure that equal power level fell on the photodiode, regardless of the length of the fiber used Downconversion of the received signal requires constant tracking of the phase of the incoming signal and adjusting the phase of the LO in accordance with the signal Such an action is required due to fluctuations in the phase of the signal travelling

along the fiber (due to changes of the temperature, polarisation and other factors) Lack of phase tracking equipment made it difficult to measure the BER of the received signal The performance of the system was thus verified by measuring the peak-to-peak voltage of the signal on the scope screen The results were plotted as a function of fiber length for two cases

1 signal travels through the fiber in DSB format
2 BPF is inserted into link after the laser to select out just the carrier and one side band

Optical spectra of the DSB and SSB signals are shown in *Figure 4-18* and *Figure 4-19* respectively

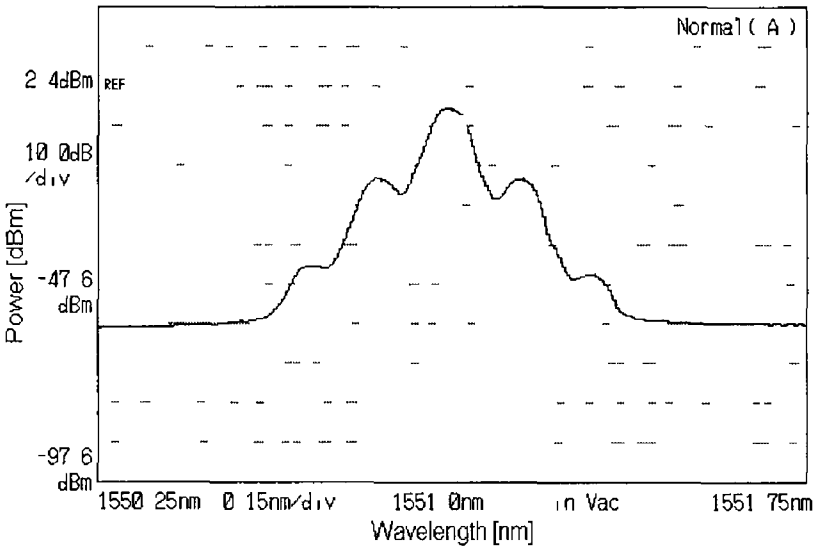

Figure 4-18 *Optical spectrum of the DSB signal*

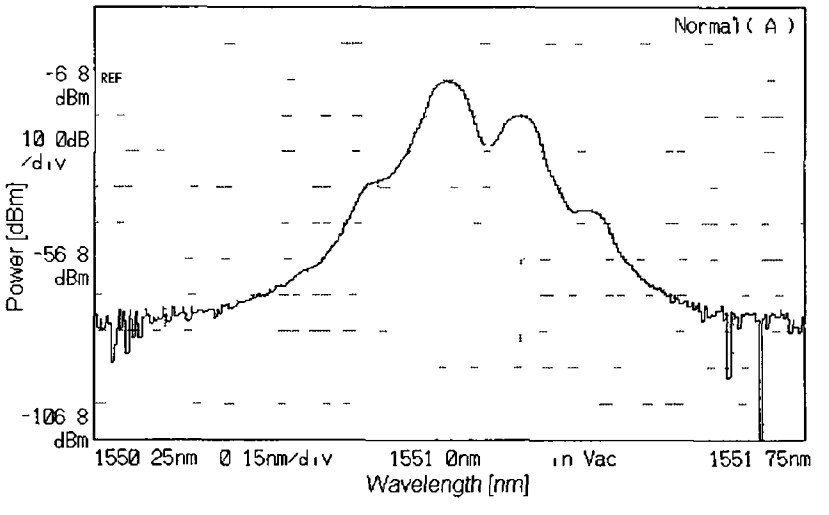

Figure 4-19 *Optical spectrum of the SSB signal*

From *Figure 4-19* (b) it can be seen that the side band is not completely removed This is due to insufficient sharpness of the filter response (*Figure 4-20*)

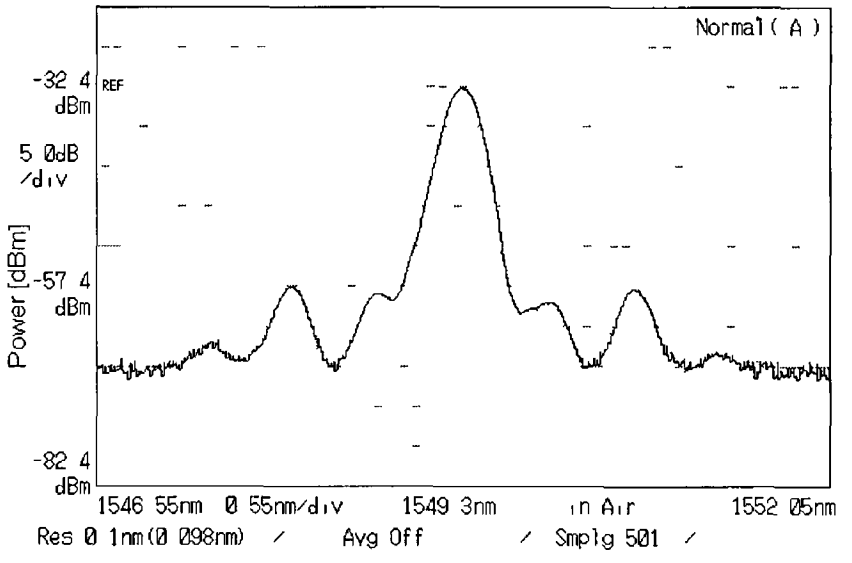

Figure 4-20 *Frequency response of the filter*

Figure 4-21 presents the dependence of the power of the received RF signal on the fiber length for two cases mentioned above signals in DSB (diamonds) and SSB format (circles) Eye diagrams of a received signal for three different fiber lengths 11, 23 and 37 km can also be seen as an inset in *Figure 4-21* These lengths are the length for which the 18 GHz signal travelling along the fiber has the lowest (complete fading), highest and intermediate power respectively From *Figure 4-21* it is clear that by converting the DSB signals, which are generated by intensity modulation of the laser, into SSB format one can overcome the dispersion induced fading

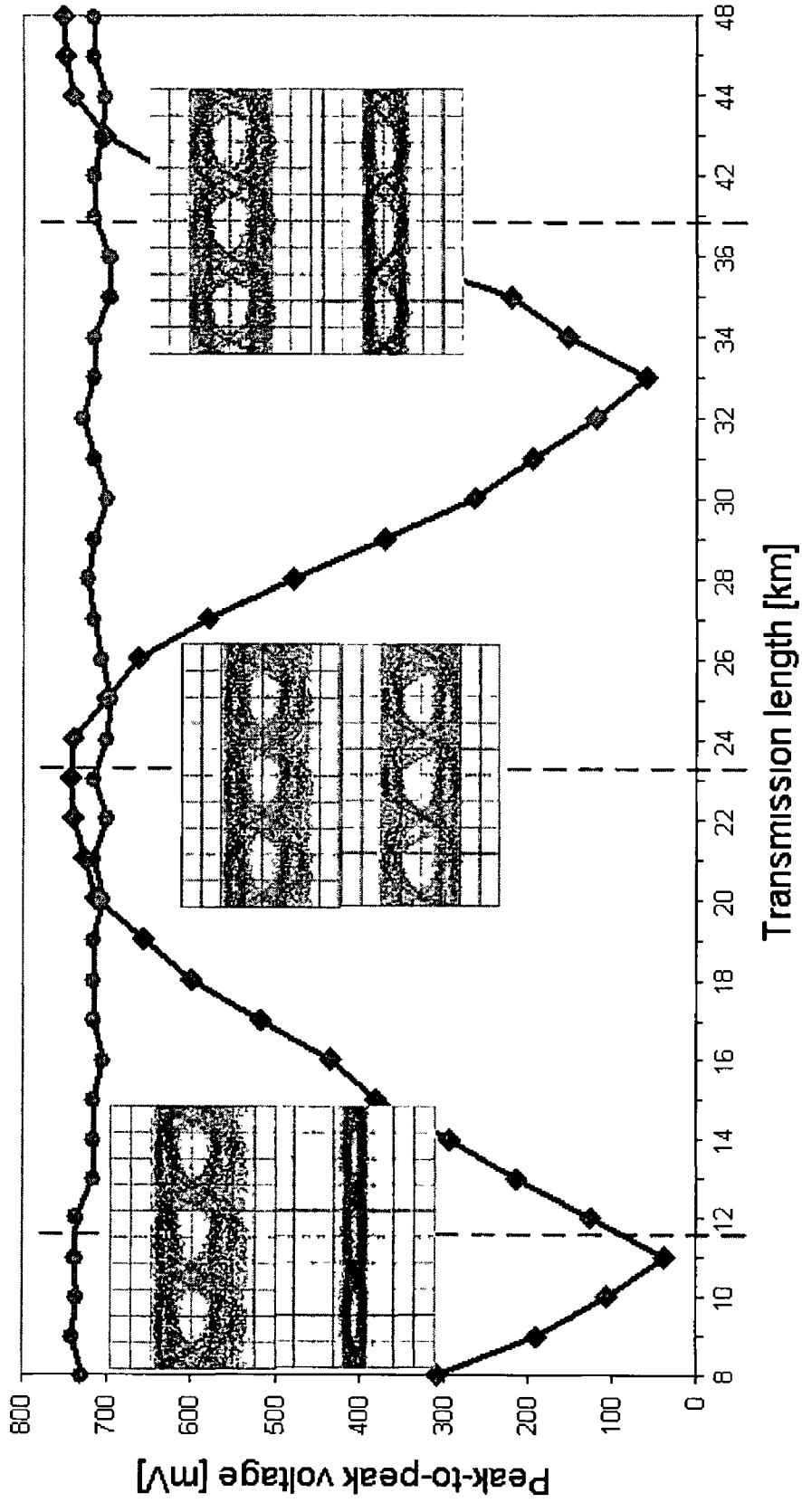

Figure 4-21 Signal amplitude as a function of fiber length for DSB (diamonds) and SSB (circles) signal

References

[1] C H Henry *et al* "Locking Range and Stability of Injection Locked 1 54 μm InGaAsP Semiconductor Lasers", *IEEE J Quantum Electron*, vol 21, pp 784-793, 1985

[2] J M Senior "Optical Fiber Communications – Principles and Practice", Prentice Hall, London 1985

[3] G Keiser "Optical Fiber Communications", McGraw-Hill Higher Education, London, 2000

[4] E Vourch *et al* "Lightwave Single Sideband Wavelength Self-Tunable Filter Using an InP Fe Crystal for Fiber-Wireless Systems", *IEEE Photon Technol Lett*, vol 14, pp 1-3, 2002

[5] H Schmuck "Comparison of Optical Millimetre-Wave Systems Concepts With Regard to Chromatic Dispersion", *Electronics Lett* Vol 31, pp 18481849, 1995

[6] J Park *et al* "Fiber Chromatic Dispersion Effects on Multichannel Digital Millimeter-Wave Transmission", *IEEE Photon Technol Lett*, vol 8, pp 1716-1718, 1996

[7] U Gliese *et al* "Chromatic Dispersion in Fiber-Optic Microwave and Millimeter-Wave Links", *IEEE Trans Microwave Theory Tech*, vol 44, pp 1716-1724, 1996

[2] G H Smith *et al* "Overcoming Chromatic-Dispersion Effects in Fiber-Wireless Systems Incorporating External Modulators", *IEEE Trans Microwave Theory Tech*, vol 46, pp 1410-1415, 1998

[9] R Hui *et al* "Subcarrier Multiplexing for High-Speed Optical Transmission", *IEEE Lightwave Technol*, vol 20, pp 417-427, 2002

[10] M Sieben *et al* "Optical Signal Sideband Transmission for Dispersion Avoidance and Electrical Dispersion Compensation in Microwave Sub-carrier and Baseband Digital Systems", *Electronics Lett* Vol 33, pp 972-973, 1997

[11] T Kuri *et al* "Fiber-Optic Millimeter-Wave Downlink System Using 60 GHz-Band External Modulator", *IEEE Lightwave Technol* vol 17, pp 799-806, 1999

[12] K Kitayama *et al* "Dispersion Effects of FBG Filter and Optical SSB Filtering in DWDM Millimeter-Wave Radio-Fiber Systems", *IEEE Lightwave Technol*, vol 20, pp 1397-1407, 2002

[13] C Marra *et al* "Wavelength-Interleaved OADMs Incorporating Optimized Multiple Phase-Shifted FBGs for Fiber-Radio Systems", *IEEE Lightwave Technol*, vol 21, pp 32-39, 2003

5 Multichannel System

It is expected that future hybrid systems will divide the available RF spectrum into many frequency bands [1, 2] This will allow the system designers to make use of Subcarrier Multiplexing (SCM) or Orthogonal Frequency Multiplexing (OFDM) These techniques are used in high capacity multi-path environments in order to overcome multi-path fading effects and to simplify the complexity of the radio links and the management of the available spectral bandwidth [3 - 5] In addition to the use of SCM and OFDM, it is also expected that hybrid radio/fiber distribution networks may employ Wavelength Division Multiplexing (WDM) in order to allow different Remote Antenna Units to be fed with a common optical fiber [6, 7]

The following section examines two multiplexing techniques (electrical) used in multichannel systems SCM and OFDM

5 1 Multiplexing techniques used in multichannel systems

5 1 1 Subcarrier Multiplexing

SCM has been widely utilized in Cable TV systems, radio and satellite applications It provides low cost and highly bandwidth efficient transmission [8] Recently it has been considered as one of the methods to increase the bandwidth utilization in optical systems Furthermore, the building of hybrid WDM/SCM systems and employing SCM to generate multiple radio carriers using a single laser diode for radio-fiber systems has been proposed [9] In an optical SCM system individual data channels are upconverted to a desired RF frequency, combined together and used to modulate light The latter could be achieved by performing either direct or external modulation The use of SCM brings about many advantages one of them being the ability to transmit many channels using one optical transmitter These channels are completely independent of each other since they are carried by separate RF frequencies This in turn allows the transmission of many different formats and types of data within a system without the need for signal conversion or clock rate adjustment Another advantage of SCM is that all channels would be available at all points and nodes [10]

SCM is orthogonal to Time Division Multiplexing (TDM) and WDM This means that SCM could be combined with either of these techniques The WDM/SCM system is especially attractive because of better utilization of the available spectrum [11-13]

The attained spectral efficiency is due to WDM being a well-established technique that results in the increase of system capacity and SCM enhancing the system efficiency and flexibility even further SCM achieves the latter by employing Bandwidth Efficient Modulation (BEM) formats, pulse shaping, Forward-Error Correction (FEC) coding and Single Side Band (SSB) modulation [10]

Quadrature Amplitude Modulation (QAM) is one of the most common higher-order modulations used in SCM In this type of modulation scheme, the value of an information bit is encoded using not only the amplitude of the signal but also its phase By doing so, multiple bits can be transmitted in a single signalling interval A typical example would be the case of a QAM using four bits per symbol (4-QAM) Here each transmitted symbol represents two information bits, identifying one of four different symbols (Q_n), depending on the phase and amplitude as shown in *Figure 5-1* This translates into much lower clock rates (decreasing the required speed of electronics) and into an ability to transmit more information within the available bandwidth Thus these types of modulations are referred to as BEM [10]

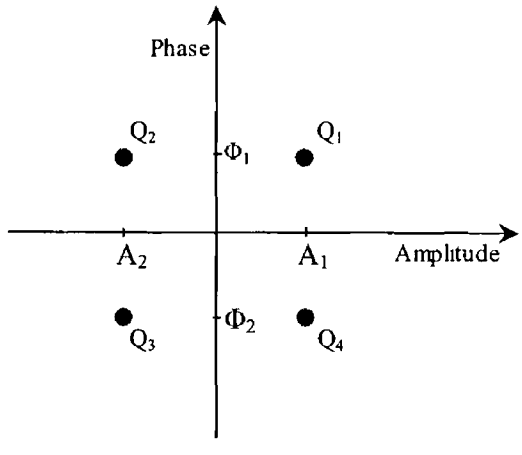

***Figure 5-1** 4 QAM amplitude-phase plane*

In addition to the utilization of BEM, Digital Signal Processing (DSP) could also be employed in SCM systems The shape of the pulse is changed in order to concentrate most of the signal energy in a minimum frequency band This reduces the required spacing between channels thus enhancing the spectral efficiency of the system However, sending more information during each period increases the likelihood of error The performance of systems using QAM is enhanced by using Forward Error Correction (FEC) coding algorithms at the transmitter and a linearization process at the demodulator [14, 15] The first measure taken decreases the optical power

necessary to close the link while the second reduces distortion introduced by fiber nonlinearity [16, 17]

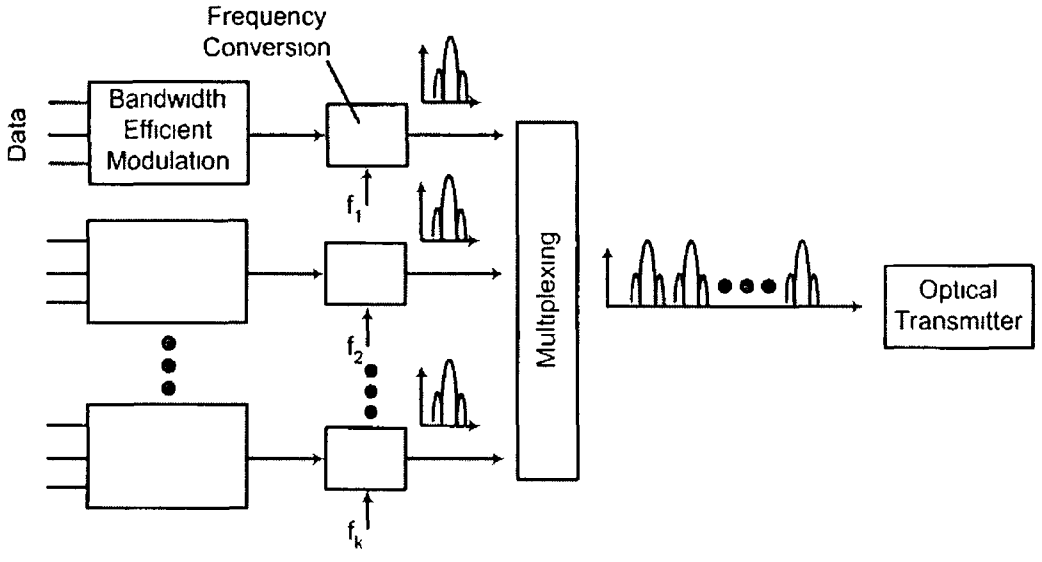

Figure 5-2 SCM - basic configuration

The block diagram of a typical SCM transmitter is shown in *Figure 5-2* Initially the data signal undergoes BEM The next stage of the signal processing is frequency conversion During this phase each data channel is upconverted to a different frequency band All the channels are then multiplexed in the frequency domain The combined signal is used to modulate the laser diode and the modulated light is then sent over optical fiber to the destination

As mentioned before the usage of BEM decreases the bandwidth requirements of the system This could be further reduced by employing SSB modulation on the optical part of the transmitter One of the side bands could easily be filtered out since the data is spectrally spaced by a large amount from the optical carrier (depending on the RF carrier) This results in the spectral occupation being almost halved (*Figure 5-3*)

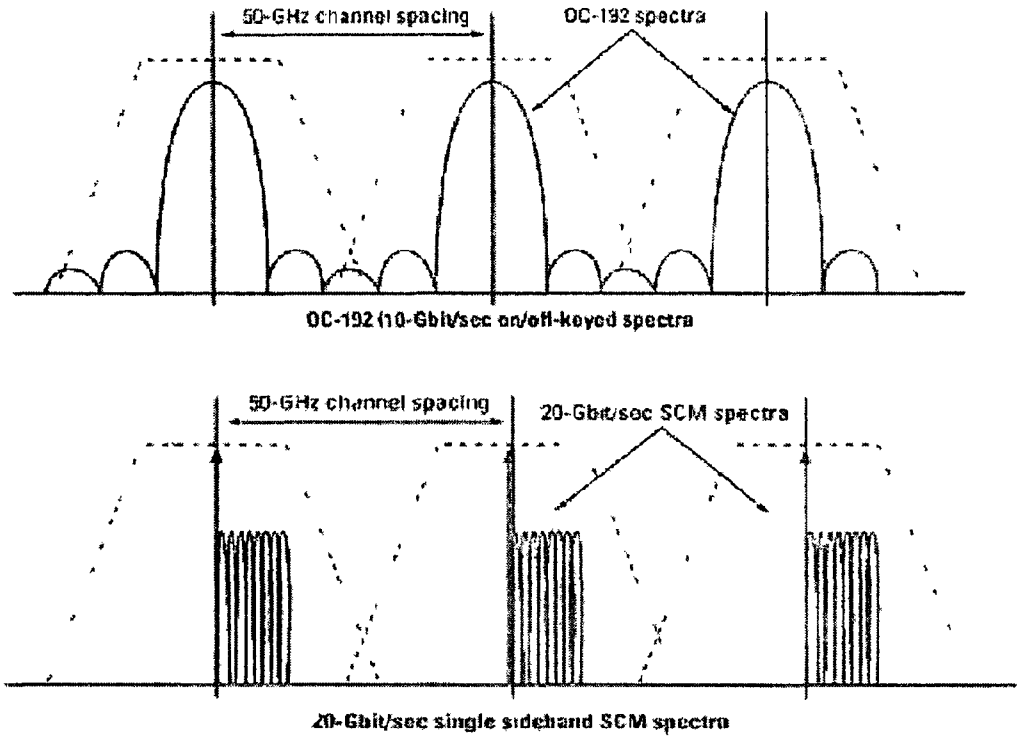

Figure 5-3 Employment of SSB modulation increases spectral efficiency of the system [18]

SSB not only reduces the bandwidth of the signal, but also minimizes the effect of chromatic dispersion Distance (restricted by dispersion) over which the data can be sent would be limited only by the single channel symbol rate Since the latter is relatively low transmission over very long lengths of fibers is possible Though SSB does not increase the system tolerance to Polarization–Mode Dispersion (PMD), the inherent bandwidth of the SCM limits the impact of PMD [18]

As shown before, SCM provides an additional dimension of multiplexing, which increases the efficiency and flexibility of optical transport networks SCM divides the available spectrum into many channels by using different frequency bands In TDM the data from each channel is combined together by assigning one time slot for each channel As a result the TDM circuits operate at an aggregate data rate of all the multiplexed channels In SCM, each channel is upconverted to a different Intermediate Frequency (IF) Subsequently they are combined together and then used to modulate a laser In such a scenario the circuits operate only at the individual channel data rate (*Figure 5-4*)

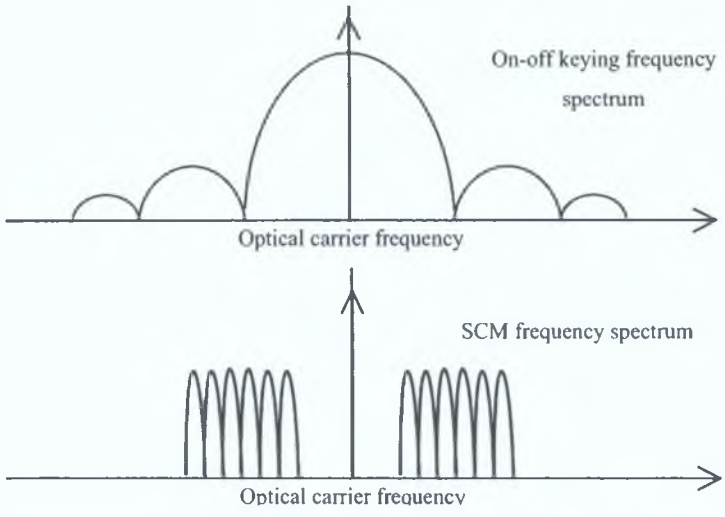

Figure 5-4: Optical spectral efficiency of SCM system in comparison to TDM system

Simplicity and cost efficiency of the receiver end of a system are other advantages that are encountered. In order to receive a particular channel the optical signal has to be detected using a photodiode, mixed with a signal from the appropriate signal generator, and finally filtered using a low-pass filter. Equally important is that each channel can be detected at any point of the system [10].

While SCM is used to carry different channels on different frequencies in order to add flexibility and reduce the cost of a telecommunication system, the goal of employing OFDM is different.

5.1.2 Orthogonal Frequency Division Multiplexing

OFDM is a special case of multicarrier transmission, where a single data stream is transmitted over a number of lower rate subcarriers [19]. This technique finds its application in broadband wireless systems, for which the delay spread becomes a real problem [20]. The shorter the bit period, the more severe the Inter-Symbol Interference (ISI). This limitation could be overcome by employing OFDM, where the bits generated by one source are split into a few streams at a lower bit rate. Each of these streams is sent to the user on a different radio carrier. By increasing the bit period, the signal becomes less sensitive to propagation delays in the radio channel. Additionally, introducing a temporal guard-band in every OFDM symbol can almost completely eliminate the ISI [19]. To improve the frequency utilisation data streams are sent using a set of frequencies, which are orthogonal to each other. Hence the data can be sent using overlapping frequencies without suffering from interference. At the receiver a convolution of the incoming signal with a desired frequency is performed.

At the output of the receiver only data carried by this frequency will be present since the convolution of all other carriers will result in zero output (due to the frequencies being orthogonal)

On the whole, OFDM is very advantageous for high-speed radio systems since it allows higher bit rates to be transmitted even in environments with high delay spreads and at the same time it is spectrally efficient [21, 22]

5 2 Distortions associated with multicarrier transmission

In order to make use of all the advantages of the techniques described above one needs an optical transmitter capable of generating multiple RF carriers Linearity is the main criteria used in evaluating the sources for multiple carrier generation If a signal consisting of many frequencies is applied to an ideally linear transmitter, the output signal will consist only of the frequency components corresponding to the input signal In reality each device has a nonlinear transfer function, which means that mixing products will be present in the output signal These additional spectral components are one of the sources of distortion They interfere with the desired signal reducing its quality and thereby degrade the overall system performance

5 2 1 Sources of distortion

The RF to optic conversion could be carried out by direct or external modulation However, both these techniques suffer from interference caused by mixing products In the case of direct modulation mixing products result from static and dynamic nonlinearity of the laser Static nonlinearity is caused by an imperfect power-versus-current (PI) characteristic of the laser [23] Distortions caused by this kind of nonlinearity dominate in low frequency applications On the other hand, in broadband systems using frequencies near the relaxation resonance frequency, the main problem is the dynamic nonlinearity This type of nonlinearity is caused by the coupling between photons and electrons in the laser cavity [24 - 26]

In the case of external modulation, distortion is caused by the nonlinear transfer characteristic of the modulator (sinusoidal dependence – as shown *Figure 5-21*) [27] There are two main types of Inter-Modulation Distortions (IMD) caused by the above-mentioned nonlinearity One is Second order Harmonic Distortions (SHD), which appear at frequencies $2f_1$, $2f_2$, $f_1+ f_2$, and the other is third order IMD (IMD_3), which

can be found at frequencies $2f_2 \pm f_1$ $f_1+f_2+f_3$ $f_1+f_2-f_3$ etc In hybrid radio/fiber systems the frequency band occupied by the channels is much smaller then the carrier frequency Thus SHD do not have much of an impact on the system since they fall outside the above-mentioned signal spectral band On the contrary, the IMD_3 components fall directly in-band with the data channels thereby seriously limiting system performance There is no way to filter those components out, hence other methods have to be employed in order to reduce their impact on the quality of the signal

5 2 2 Methods of combating distortion in multichannel systems

The nonlinearity can be suppressed using predistortion [28, 29], electro-optic feedback and feed-forward compensation techniques The electronics required for the predistortion process for broadband systems are not readily available thereby restricting the usage of such electrical methods Consequently the electro-optic schemes become more favourable [30]

In the case of direct modulation of a laser, the nonlinearity increase when the modulation frequency approaches the Relaxation Oscillation Frequency (ROF) [31] By increasing the ROF of a laser the power of the IMD_3 components could be significantly reduced This increment can be achieved by using external light injection [24] Another method of suppressing the nonlinear distortion in directly modulated lasers was proposed by Jung *et al* [32] This novel method exploits the fact that the phase of the generated light depends on the bias current By parallel modulation of two lasers biased at different, carefully chosen bias currents, distortion products having opposite phases could be generated By combining the output signals from both the lasers, a 20 dB suppression of IMD_3 was achieved by the authors

The above-mentioned techniques of combating IMD_3 have a couple of disadvantages One such drawback involves the requirement of additional hardware, which increases the cost of the system Another hitch is that these techniques only overcome the distortion generated by the optical transmitter In hybrid radio/fiber systems both optical and electrical devices produce IMD_3 components Electrical amplifiers, antennas etc are all nonlinear devices that would produce IMD and thus degrade the signal quality To avoid distortion due to IMD_3 generated by both electrical and optical system components, a special frequency assignment scheme could be used

Essentially this entails assigning particular frequency carriers to different BS's in such a way that the IMD_3 components do not fall onto any of the signal channels in use [33] This does not require a large amount of hardware and can greatly improve the quality of the signal Nevertheless, as the number of carriers increases so does the number of IMD_3 generated by these carriers Thus the number of IMD_3-free channels becomes very small (e g for 62 channels there are only 9 IMD_3-free channels) In such a case rather than excluding all the channels that are affected by IMD, one could eliminate only the channels with the highest amount of IMD_3 Simple and efficient frequency assignment algorithms can be found in [33, 34]

5 3 Multichannel system – experiments

The performance of the multichannel system based on direct and external modulation was experimentally verified

5 3 1 Five-channel system based on direct modulation

The process of generating multiple RF channels using direct modulation has been experimentally verified using a five-channel system Experiments with multiple channels allowed the characterization of the nonlinearity of the laser diode and its dependence on the modulation frequency Hence the following cases were examined

1 Laser with external injection modulated at a frequency close to relaxation frequency

2 Free running laser modulated at a frequency close to relaxation frequency

3 Free running laser modulated at a frequency where the laser modulation response is flat

It should be noted that the power of the modulating signal was kept constant (at 11 dBm) throughout the experiments described in the following section, as any change in the signal amplitude could have a great impact on the effect of the transmitter nonlinearity

5 3 1 1 Five-channel system based on an externally injected laser

The experimental set-up used is shown in *Figure 5-5*

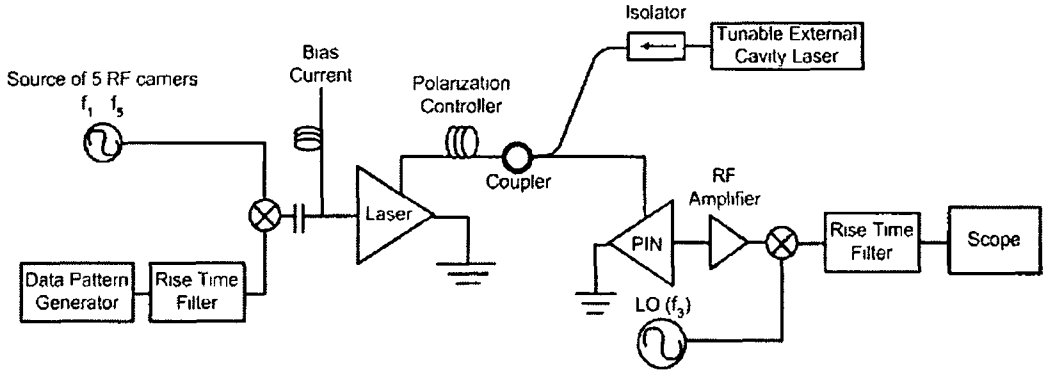

Figure 5-5 Experimental set-up of a five-channel system based on an externally injected laser

Initially, a 155 Mb/s Pseudo Random Bit Sequence (PRBS) from an Anritsu pattern generator was upconverted to five RF carriers (centre frequency 18 5 GHz) A 117 MHz rise-time filter was used prior to mixing in order to limit the spectral width of the data signal The SCM signal was combined with 60 mA of bias current and then applied to a commercially available NTT Distributed Feed-Back (DFB) laser (KELD 1551 CCC_1) External injection was realized the same way as mentioned in the previous experiments (Chapter 3) The injection power was set to 5 dBm, which resulted in the maximum response of the laser occurring around 18 GHz The output signal of the laser was then detected using a 50 GHz photodiode The detected signal was then amplified and the central channel was downconverted The latter was achieved by mixing the SCM signal with the LO, which was set to 18 5 GHz (f_3 as in *Figure 5-5*) After filtering out all the unwanted components, the desired data signal was analyzed with the aid of a digital sampling oscilloscope and the Bit Error Rate (BER) was measured using an Anritsu error analyzer

The initial experimental procedure involved finding the feasible channel spacing, which would be used throughout the subsequent experiments This was achieved by measuring the BER vs received optical power for different values of spacing between the channels At this juncture it is vital to note that there is a trade off between the performance and the spectral efficiency of the system From *Figure 5-6* it can be seen that about –12 dBm is required to achieve an acceptable BER of 10^{-9} at a spacing of 400 MHz A further increase of the channel spacing does reduce the required power, however this is achieved at the expense of system spectral efficiency Hence it was concluded that 400 MHz was the channel spacing that yielded reasonable system performance and spectral efficiency

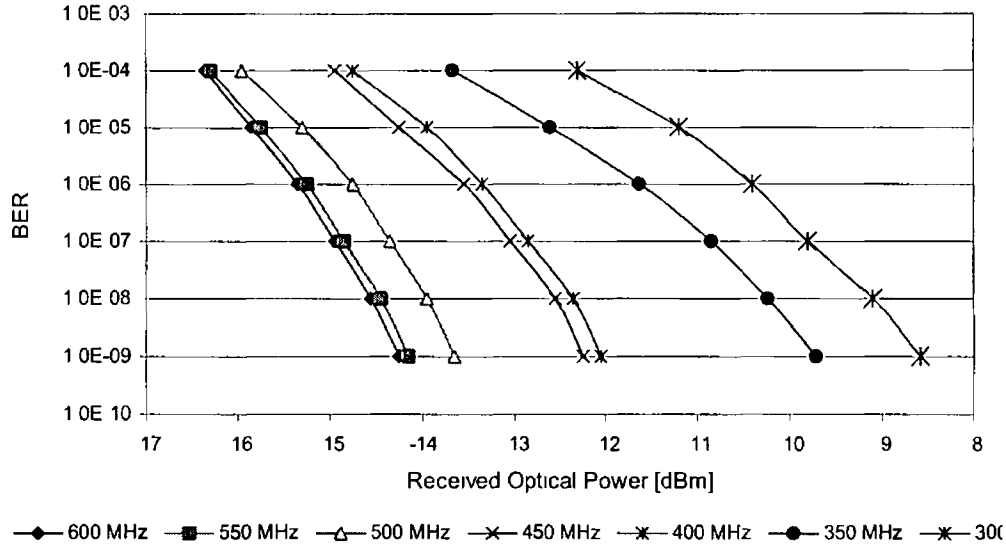

Figure 5-6 BER as a function of received optical power for different channel spacing

The effect on laser nonlinearity was examined by measuring BER of the central data channel for equal and unequal channel spacing When the distance between all SCM channels is the same, the IMD_3 products fall exactly in the centre of the data band This is the worst-case scenario, since the centre of the signal (around the carrier) carries the majority of the power However, the IMD_3 could be shifted by moving the two extreme channels (ch 1 and ch 5) away from their adjacent channels Shifting the IMD_3 towards the edges of the data band reduces the interference and enhances the system performance The change in BER as the channel spacing is varied could be treated as a measure of the laser nonlinearity In the experiment the channel spacing between three central channels was kept constant at 400 MHz The spacing between the first and second channels and the fourth and fifth channels was varied from 400 MHz to 550 MHz at intervals of 50 MHz This resulted in IMD_3 falling at a distance of 0 to 150 MHz away from the centre of the data channel It is important to note that the improvement in system performance is only due to the removal of IMD_3 and not due to reduction of adjacent channel interference The fact that the adjacent channel interference does not change is because only the extreme channels are moved while the measurement of the BER is carried out on the central channel The eye diagrams of the downconverted central channel with IMD_3 (a) 50 and (b) 150 MHz away from the centre of the channel for received optical power of −18 dBm are shown in *Figure 5-7* As expected the eye in *Figure 5-7* (a) is noisier in comparison to the eye shown in *Figure 5-7* (b)

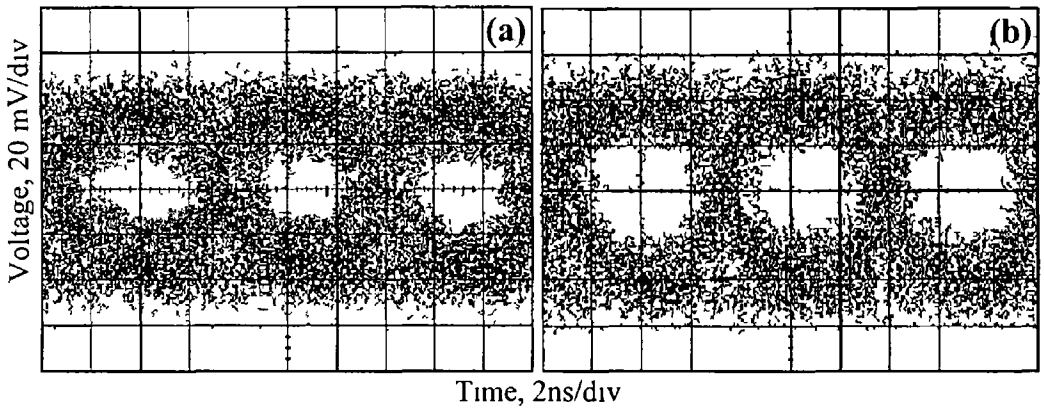

Figure 5-7 Eye diagrams for IMD's at (a) 50 MHz (b) 150 MHz – received optical power –18 dBm

The effect of IMD_3 on system performance was quantified by measuring the BER as a function of the received optical power and is shown in *Figure 5-8*

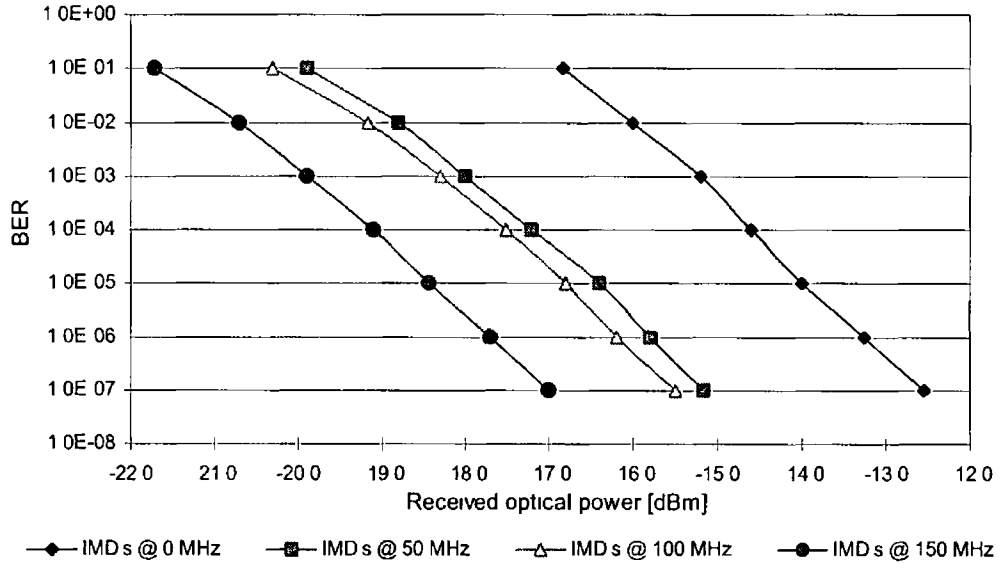

Figure 5-8 Influence of IMD s on system performance

From *Figure 5-7* and *Figure 5-8* it can be seen the IMD_3 has a strong influence on the performance of a system based on an externally injected laser From the plot above (*Figure 5-8*) it can be seen that this performance improves by 4 5 dB when the IMD_3 are almost completely removed (150 MHz away from centre of the channel) The effect of the laser nonlinearity could also be seen in the electrical spectrum of the detected SCM signal (*Figure 5-9*) Significant mixing products are clearly visible at frequencies both lower and higher than the data signals This implies that the response of the laser with external injection is highly nonlinear around the relaxation frequency Such a degree of nonlinearity could be expected since the relaxation peak in the frequency response of an externally injected laser is very high and steep

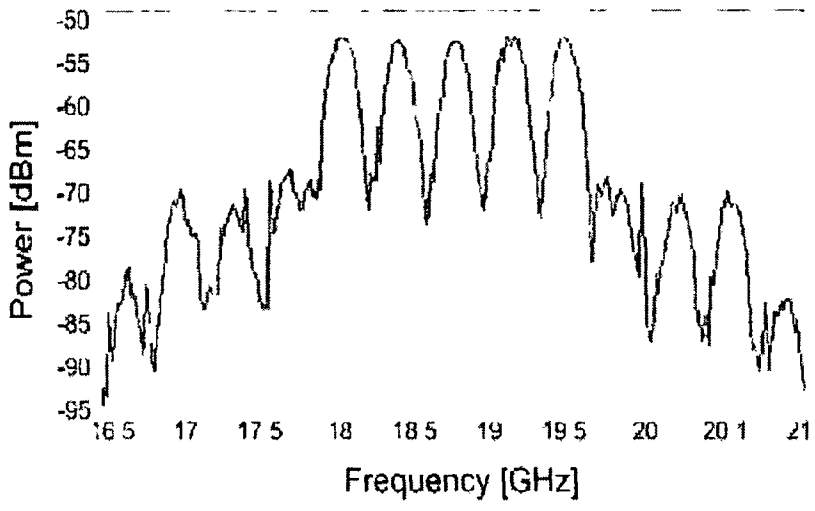

Figure 5-9 Electrical spectrum of SCM signal - laser with external injection - equal channel spacing

It should be noted that in most devices, a nonlinear frequency response does not imply that the device is nonlinear Nevertheless, in the case of a laser the resonance peak is an effect of nonlinear interactions between electrons and photons Thus the stronger the nonlinearity the higher the resonance peak

In order to compare the nonlinearity of an externally injected laser with a free running one, further experiments were performed Five-channel system based on a free running 8 5 GHz DFB chip laser

5 3 1 2 Free running laser modulated at relaxation frequency

First the IMD_3 generated by a free running laser modulated at a frequency around its relaxation oscillation was investigated The set-up used for all the experiments described in this section is shown in *Figure 5-10*

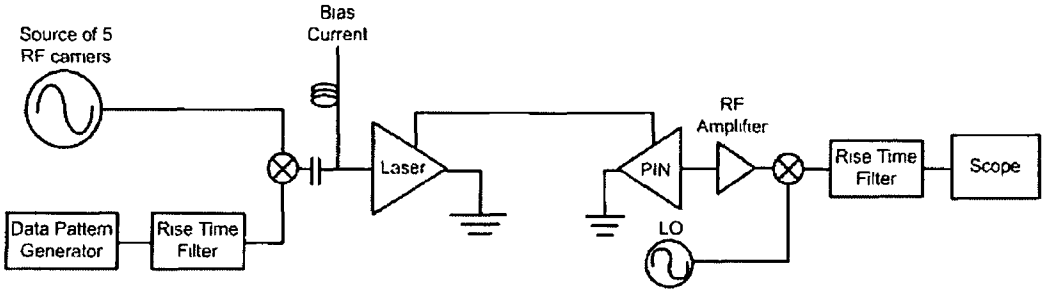

Figure 5-10 Five-channel system based on free running laser

The DFB laser (KELD 1551 CCC_1) used here was the same as that used in the external injection case In free running conditions this laser had its relaxation frequency around 8 5 GHz Hence this frequency was chosen for the central channel The same channel spacing that was used before is employed here as well (400 MHz)

As in the previous section 5 3 1 1 the channel spacing between the extreme channels was varied from 400 MHz to 550 MHz at intervals of 50 MHz The eye diagrams when the IMD_3 falls at 50 MHz and 150 MHz away from centre of the data channel are shown in *Figure 5-11* (a) and (b) respectively (received optical power –11 dBm)

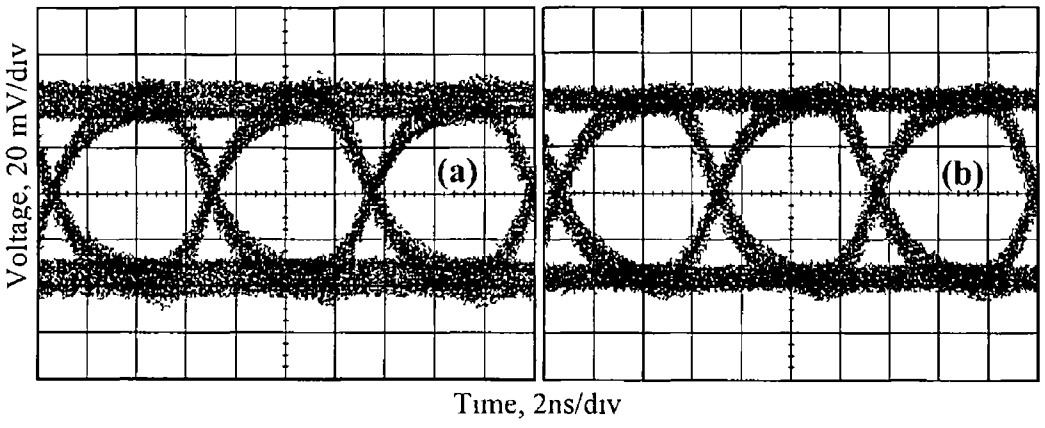

Figure 5-11 *Eye diagrams for IMD's at (a) 50 MHz (b) 150 MHz- received optical power – 11 dBm*

The build-up of the noise, caused by IMD's, can be seen to be higher in *Figure 5-11* (a) than in *Figure 5-11* (b) Another interesting aspect that could be noticed is that the influence of the nonlinearity seems to be much lower in comparison to the externally injected laser (rationale for this is already explained in section 5 3 1 1) Here again the effect of IMD_3 was determined by measuring the BER as a function of the received optical power *Figure 5-12* illustrates this plot of the BER against the optical power, when the IMD_3 are moved away from centre of the data channel

As already observed from the eye diagrams, the system improvement due to removal of IMD_3 is much smaller for the free running laser Here the improvement in performance is around 0 3 dB, which is much less than the 4 5 dB improvement achieved in the externally injected laser

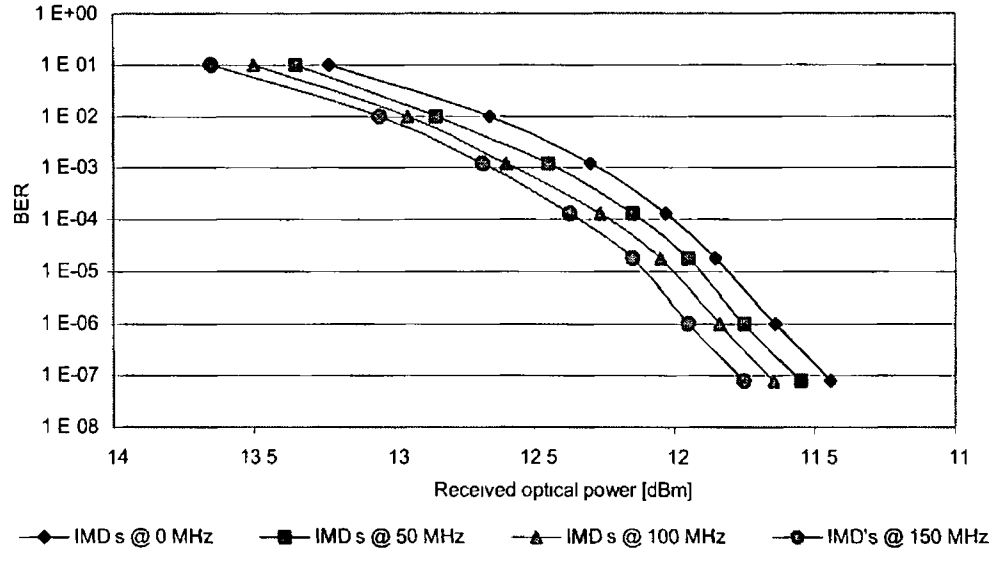

Figure 5-12 Influence of IMD_3 – free running laser modulated at relaxation frequency

5 3 1 3 Free running laser modulated at flat part of the frequency response

Further verification of the dependence of nonlinearity of a laser on the modulating frequency is carried out here The previously described experiment is repeated at a frequency where the modulating signal falls on the flat part of the laser frequency response The frequency chosen was 6 GHz The eye diagrams of the received central data channel for IMD's at 50 and 150 MHz are shown in *Figure 5-13* (a) and (b) respectively The same trend is seen here in the eye diagrams in that *Figure 5-13* (a) is more noisy than *Figure 5-13* (b) (received optical power -9 dBm)

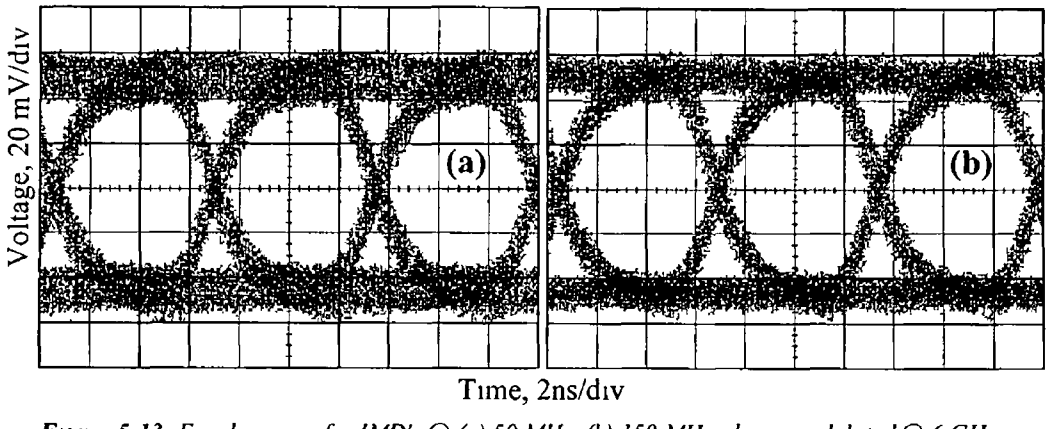

Figure 5-13 Eye diagrams for IMD's @ (a) 50 MHz (b) 150 MHz - laser modulated @ 6 GHz - received optical power –9 dBm

The BER plot for different distances of IMD_3 from centre of data channel is shown in *Figure 5-14*

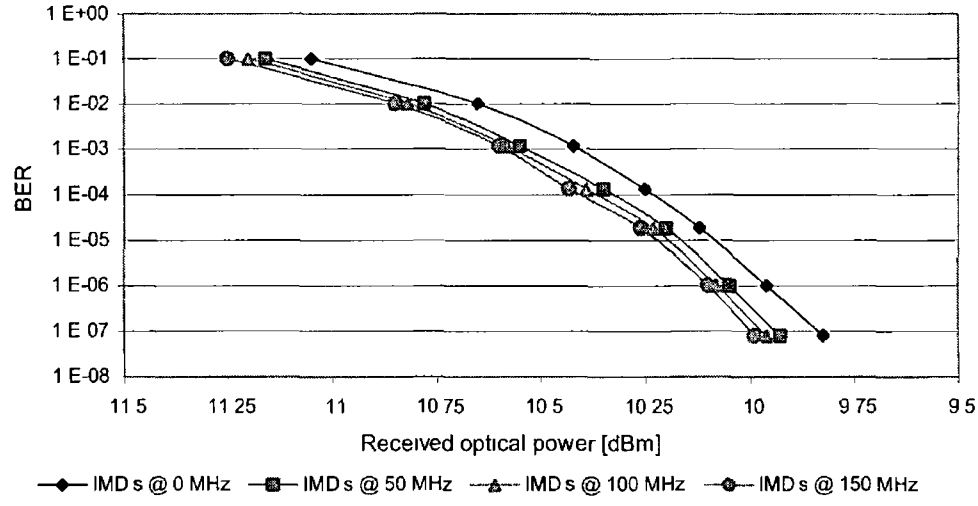

Figure 5-14 1 MD_3 influence - laser modulated at 6 GHz

As in the previous case the power penalty induced by laser nonlinearity is very small and equals around 0 2 dB By comparing *Figure 5-12* and *Figure 5-14* one can see that for the DFB laser used in the experiment the IMD_3 are very low even when the laser is modulated at its relaxation oscillation frequency This is not the case for all lasers The reason for this is due to different lasers exhibiting variable levels of nonlinearity The latter was clarified by carrying out the same experimental procedures, as in this section, using a higher speed packaged DFB laser

5 3 1 4 Five-channel system based on a free running 21 GHz packaged DFB laser

A high-speed DFB Multi-Quantum-Well (MQW) laser (KELD 1552 SSC) from NTT Electronics was used here in order to verify the statement made in the previous section (different lasers yielding dissimilar levels of the nonlinearity) The frequency response of this high-speed laser when biased at 60 mA is shown in *Figure 5-15* The same set of experiments, as described in the previous section, were performed (modulation frequency set close to the relaxation frequency and at the flat part of the frequency response) The two points marked on the plot are the modulating frequency used for the experiments As can be seen the triangle denotes the modulation at the flat part of the response (6 GHz), while the circle represents the modulation close to the relaxation frequency (14 8 GHz)

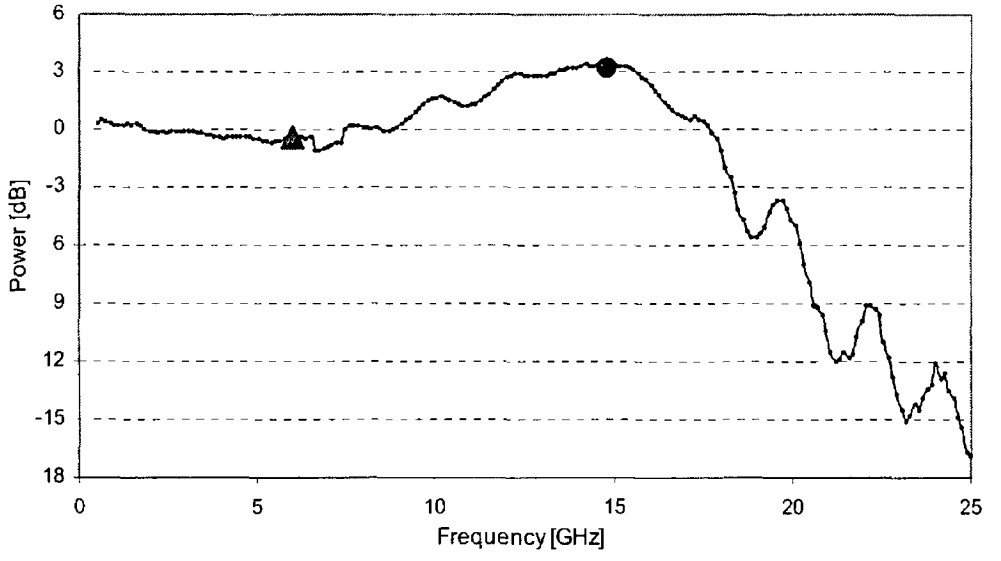

Figure 5-15 Frequency response of the NTT Electronics laser

The BER versus received optical power plot obtained for the modulation frequency set close to the relaxation peak is shown in *Figure 5-16*

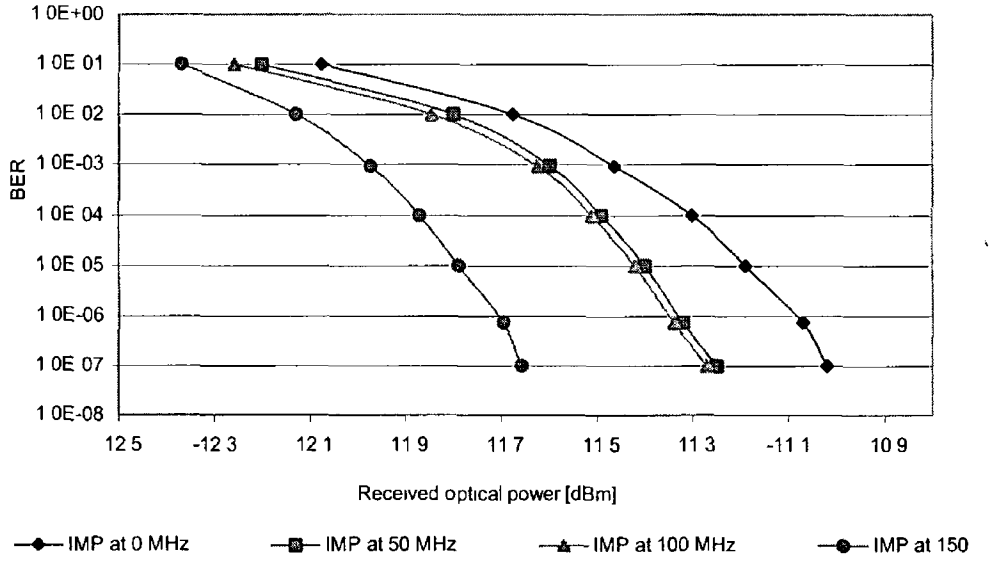

Figure 5-16 Influence of IMD's for laser modulated at relaxation frequency

The BER against received optical power plot obtained from the flat part of the frequency response of the laser is illustrated in *Figure 5-17*

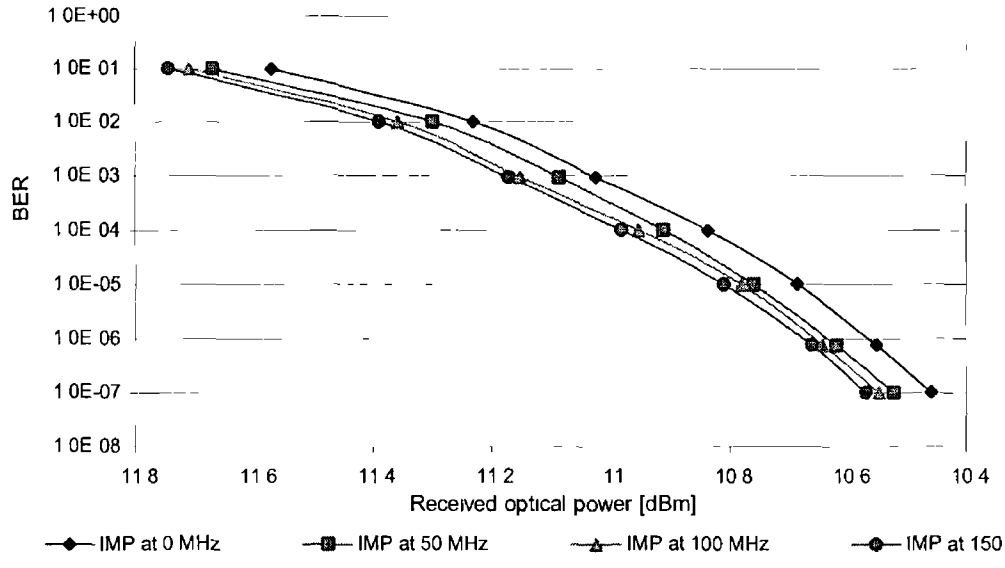

Figure 5-17 Influence of IMD3 on system performance - laser modulated @ 6GHz

From *Figure 5-16* it can be seen that the difference in system performance when the IMD_3 are moved away from the centre of the data channel is around 0 7 dB while in *Figure 5-17* this difference is less than 0 2 dB The difference in the level of the nonlinearity depending on the modulating frequency could also be noticed when comparing the RF spectra of the detected signals

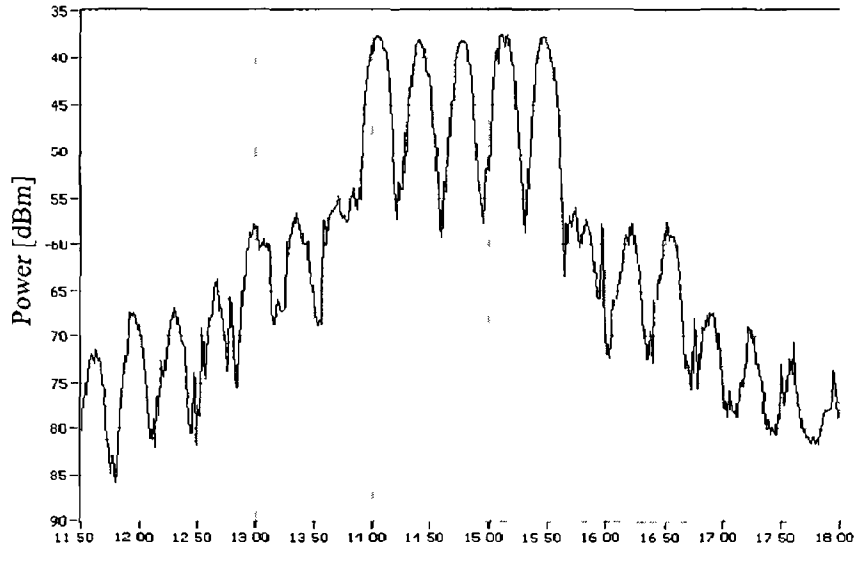

Figure 5-18 RF spectrum of the detected signal- modulating frequency close to relaxation oscillation

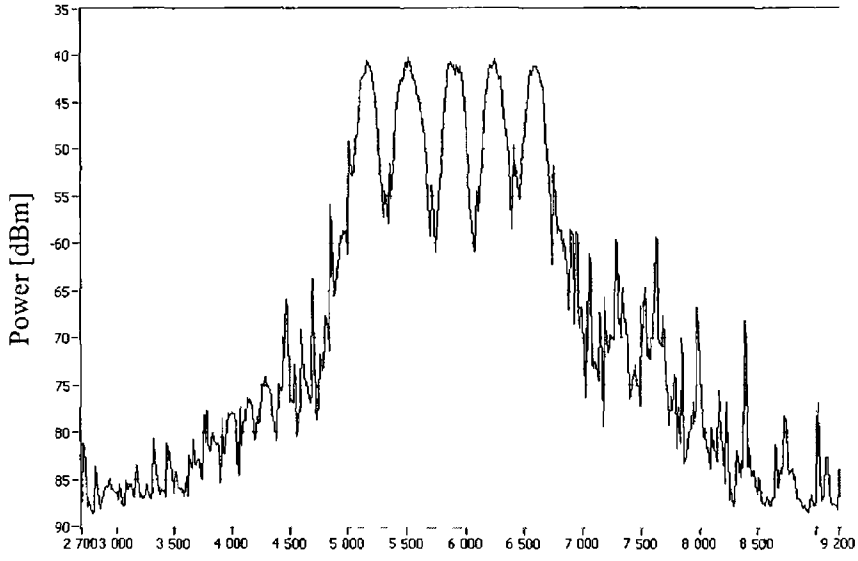

Figure 5-19 RF spectrum of the detected signal - laser modulated at the flat part of the frequency response

In the case of *Figure 5-18* the multiple mixing products are clearly visible The unwanted spectral components are around 20 dB lower than the data signals However, in *Figure 5-19* it can be seen that laser operation is much more linear Hence the mixing products at frequencies below the data band are well suppressed It is important to note that some mixing products are present for frequencies above the modulating frequencies

The degradation of system performance becomes worse as the number of channels increases For a system transmitting tens of channels using one wavelength the IMD_3 would pose a real problem In order to overcome this obstacle some sort of linearization scheme (see section 5 2 2) must be used [28]

5 3 2 Five-channel system based on external modulator

One of the alternative techniques (as mentioned in Chapter 3) that could be used to generate millimeter-wave signals in an optical way involves the use of an external modulator The reasons for carrying out experiments in this section are twofold Firstly, it would aid in the analysis of the level of the nonlinearity associated with the external modulator technique Secondly, it would serve as a comparator between the two techniques (direct and external modulation) to show which of them suffers more from the nonlinearity The experimental set-up that was used to generate optical millimeter-wave signals involving an external modulator is shown in *Figure 5-20*

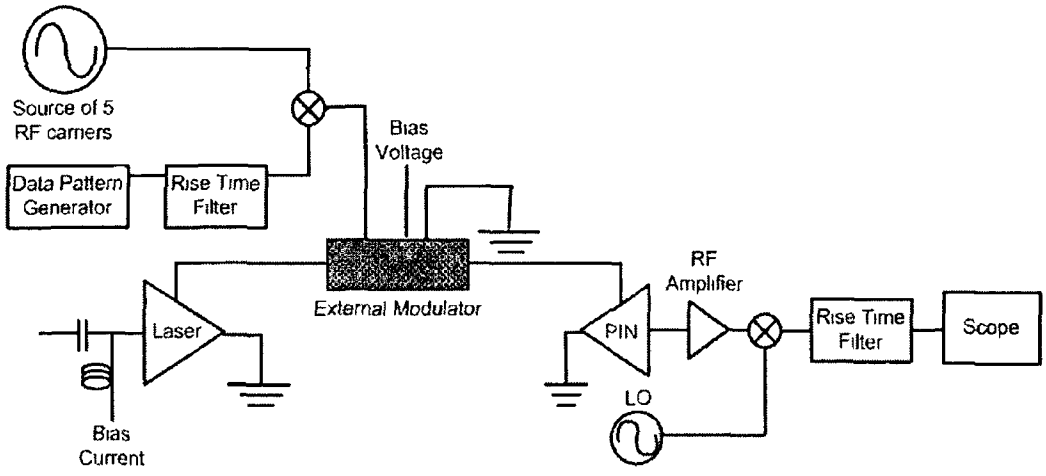

Figure 5-20 Five channel system based on external modulator - experimental set-up

An EOspace external modulator with a modulation bandwidth of 18 GHz was used Its transfer characteristic is shown in *Figure 5-21* In the experiment the modulator was biased at 2 V, which ensured that the device was operated at one of the most linear part of its transfer characteristic

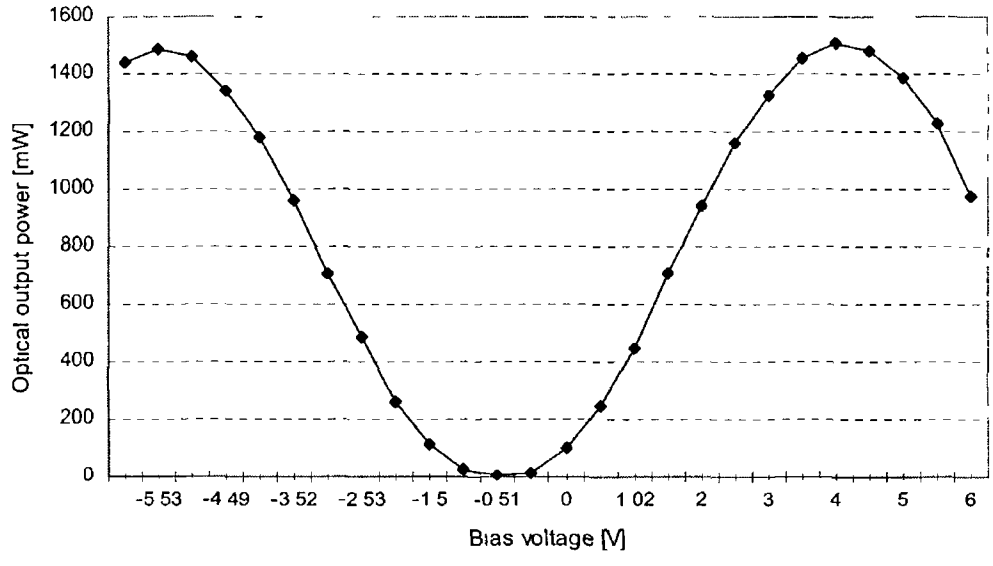

Figure 5-21 Transfer characteristic of the external modulator

The experimental procedure conducted here was similar to that of the direct modulation section In this case though the laser was used as a source of CW light The output of the diode was then modulated externally with the five data channels The optical signal was then detected using a photodiode after which it was amplified Subsequently the central channel was downconverted by mixing with a signal from the LO

The channel spacing was set to 400 MHz as this was found to be an optimum value The electrical spectrum of the detected SCM signal is shown in *Figure 5-22*

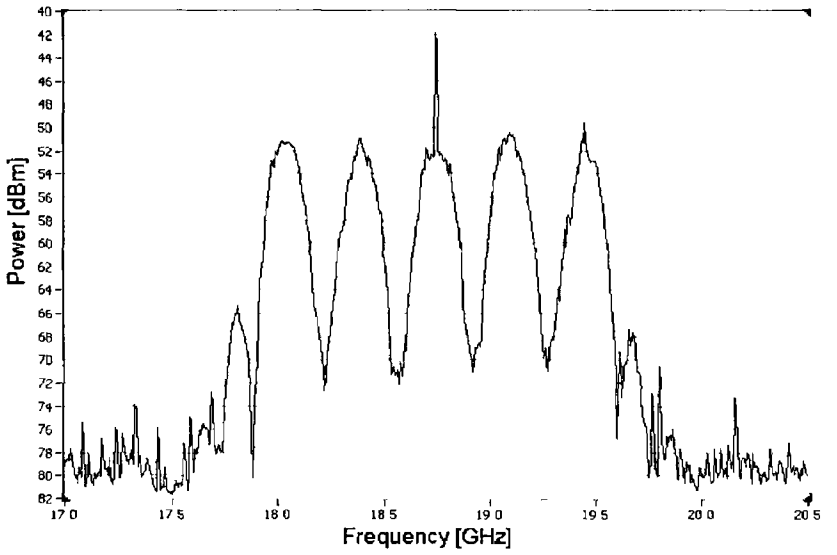

Figure 5-22 *Electrical spectrum of SCM signal*

It is quite clear from the electrical spectrum in *Figure 5-22*, that there are less mixing products than in the case of the spectrum in *Figure 5-9* This suggests that the external modulation technique is more linear when compared to the direct modulation of an externally injected laser However, the level of nonlinearity associated with the external modulation technique is closely comparable to that of the free running case

Subsequent to establishing the fact that this technique is less susceptible to nonlinear effects in comparison to the direct modulation of an externally injected laser, BER measurements for the verification of the IMD_3 influence on system performance were carried out The channel spacing for the two extremes channels were then varied and the BER rate against the received optical power was measured (as described in previous experiments within this chapter) The BER as a function of the received optical power is plotted and shown in *Figure 5-23*

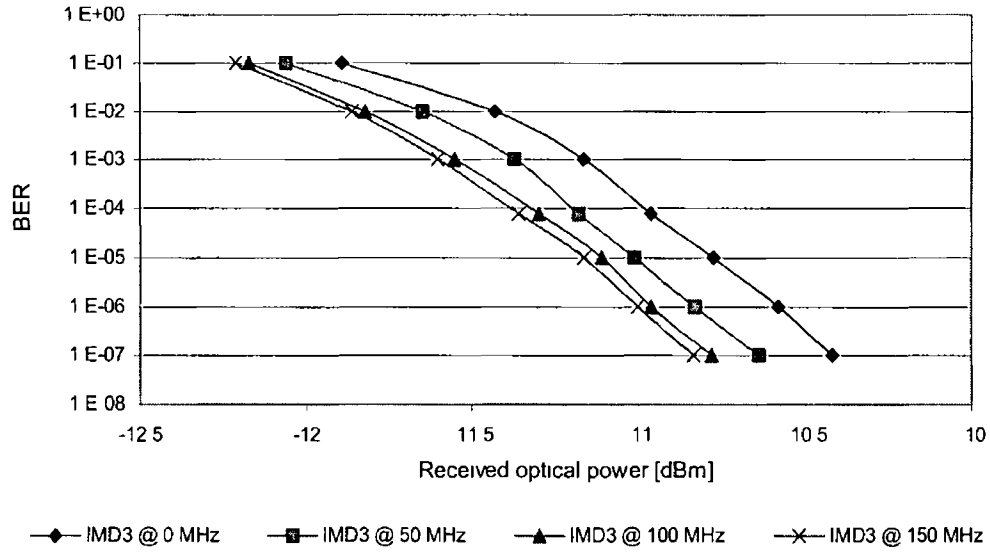

Figure 5-23 Influence of IMD_3 - system based on external modulator

From the *Figure 5-23* it can be seen that the systems performance worsens due to IMD_3 by around 0 4 dB The power penalty here is much smaller than that of the externally injected laser However, it is very similar to the values obtained in the case of the directly modulated free running lasers It is important to note that the performance of the system based on external modulation strongly depends on the amplitude of the modulating signal Thus an increase in the power of the RF signal could severally degrade the BER of the received signal due to generated IMD_3

5 4 WDM/SCM transmission system

The final step in building the optical part of a hybrid radio/fiber system entailed the simultaneous employment of two multiplexing techniques namely WDM and SCM One of the objectives of this experiment was to test the adjacent channel interference between the WDM channels Different schemes of demultiplexing the optical channels were another aim

One of the main problems encountered in hybrid radio/fiber systems is the need for an optical SSB signal at the base-station in order to overcome dispersion effects in the transmission fiber [35] Previous work in this area has used either complex signal generation techniques to produce optical SSB signals, followed by simple optical filtering at the Remote Antenna Unit [3, 4], or a complicated demultiplexing technique using a Fabry-Perot etalon and an Array Waveguide Grating (AWG) to select out just one carrier and one side-band from the WDM/SCM signal [5] In this

section a simpler and cheaper method to overcome dispersion caused fading is demonstrated It is shown that by the correct use of a simple Bragg filter at the receiver BS, not only is the selection of one of the wavelengths made possible, but also the elimination of one the sidebands in order to overcome dispersion effects in the transmission fiber is achieved [36]

The experimental set-up used is shown in *Figure 5-24*

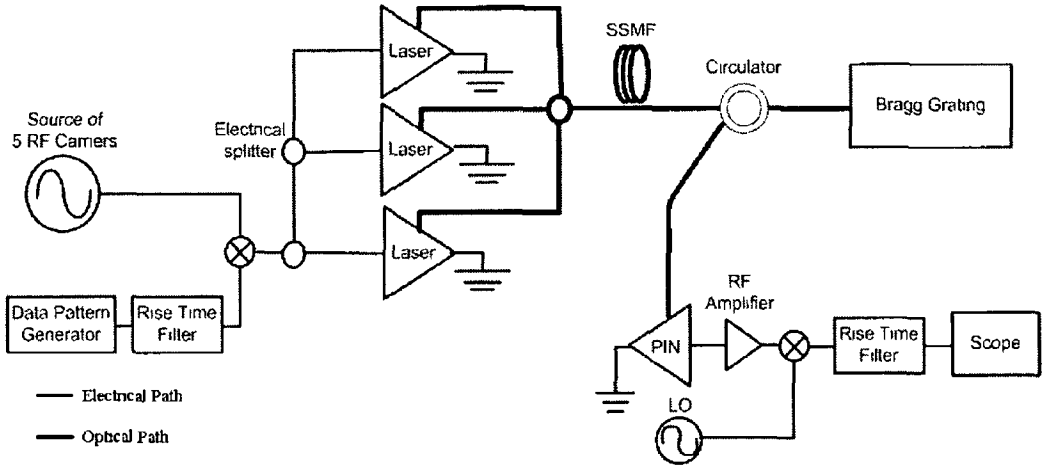

Figure 5-24 *WDM/SCM experimental set-up*

The lasers used were all high-speed devices from NTT Electronics (Appendix B) The composite SCM signal (consisting of five data channels) was split into three and used to directly modulate the transmitters Electrical attenuators were used in order to ensure that all modulating signals had equal powers Each of the SCM signals was transmitted over a different length of cable (20, 45 and 130 cm) in order to decorrelate the signals applied to different lasers All the lasers had a 3-dB bandwidth of around 18 GHz and a central wavelength of about 1550 nm at 20°C By varying the temperature control the emission frequency could be changed The operating wavelengths were set to 1549 9, 1550 3, and 1550 7 nm All lasers were biased at 60 mA The output of the lasers were combined together using a 4x1 optical coupler The appropriate wavelength channel was then demultiplexed from the WDM signal using a circulator in conjunction with a Fiber Bragg Grating (FBG) The FBGs used are designed specifically for WDM systems with 50 GHz spacing, and have reflection bandwidths of around 0 35 nm The reflection and transmission profiles of the filter are shown in *Figure 5-25* (a) and (b) respectively

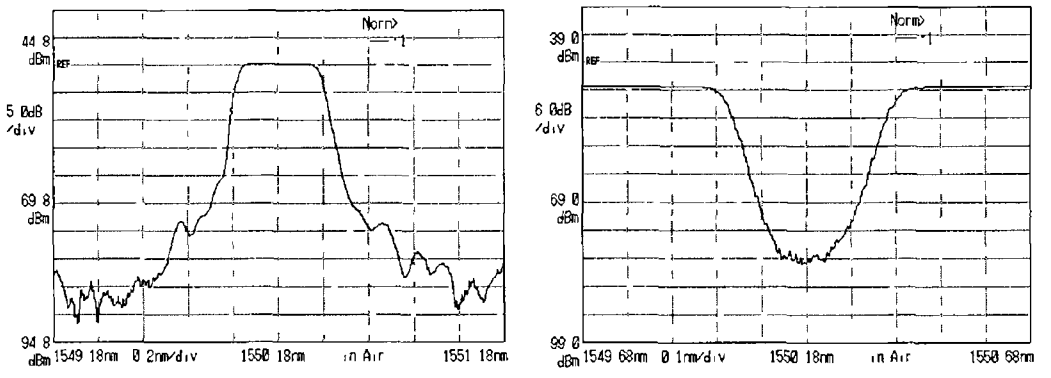

Figure 5-25 Bragg grating profiles (a) reflection (b) transmission

After filtering out one of the optical wavelength channels the signal was then detected using a 50 GHz pin diode As in the previous experiments the detected signal was downconverted by mixing with the LO The down-converted signal (central channel of the 5-channel RF data signal) was then passed through a low-pass filter to ensure that only the required base-band signal is examined using a 50 GHz oscilloscope and an error analyzer

Figure 5-26 displays the 3-channel optical data signal after passing through the optical coupler

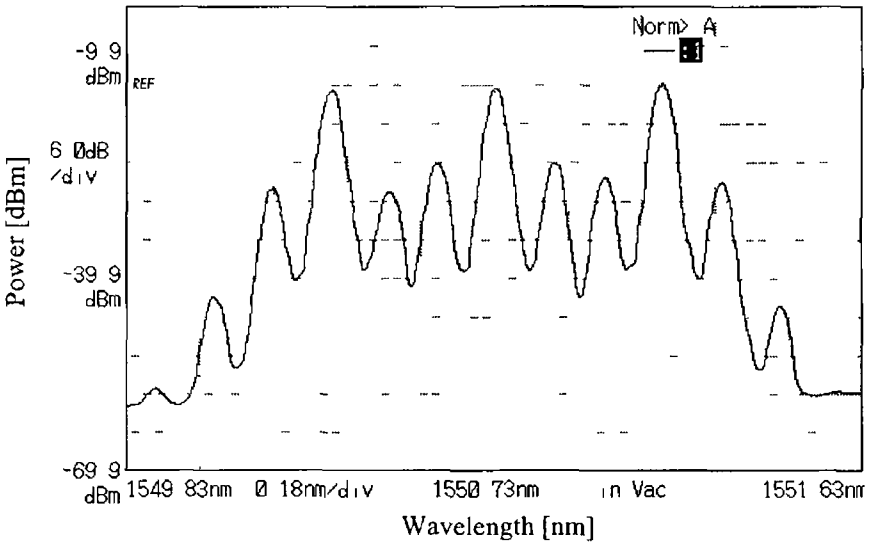

Figure 5-26 Optical spectrum of the WDM/SCM signal

In order to select out only one carrier and one side-band of the central optical channel the positioning of the Bragg filter is vital The latter is done in such a way that the central carrier is at the longest wavelength that is correctly reflected by the Bragg filter The Bragg filter having a sharp cut-off, ensures that only one-side band is

reflected The reflected signal is illustrated in *Figure 5-27* and it can clearly be seen that only one-side band of the central channel is reflected by the filter

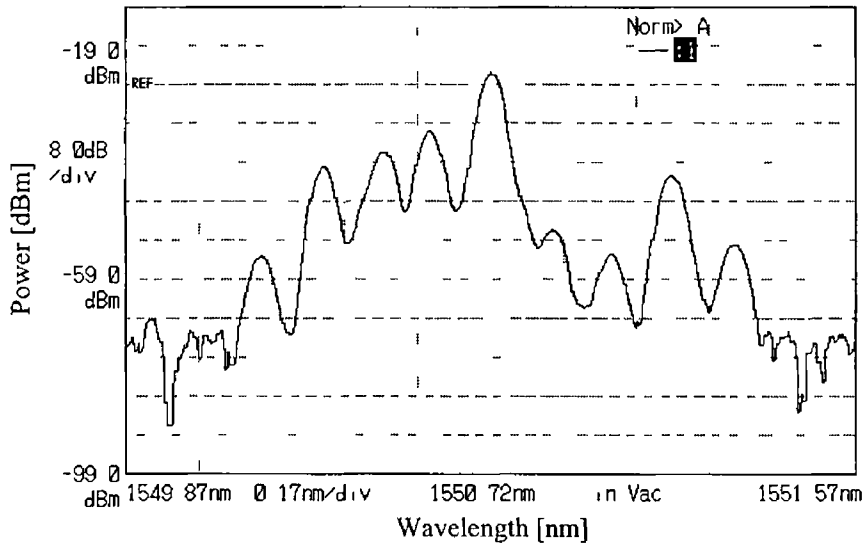

Figure 5-27 Demultiplexed central WDM channel

In addition, the filter also selects out one of the side-bands from the lower wavelength optical channel, and suppresses the carrier of this channel by 20 dB relative to the power in the central channel The longer wavelength optical channel is suppressed by 23 dB relative to the central channel

On filtering out the central wavelength channel as described above, the optical signal is received with the aid of a high speed pin diode and then down-converted by mixing it with a 18 5 GHz LO The unwanted components were filtered out with a use of the rise-time filter *Figure 5-28* displays the received eye diagrams of both (a) back-to-back case and (b) the demultiplexed WDM case for the central channel when the received power is about –10 dBm

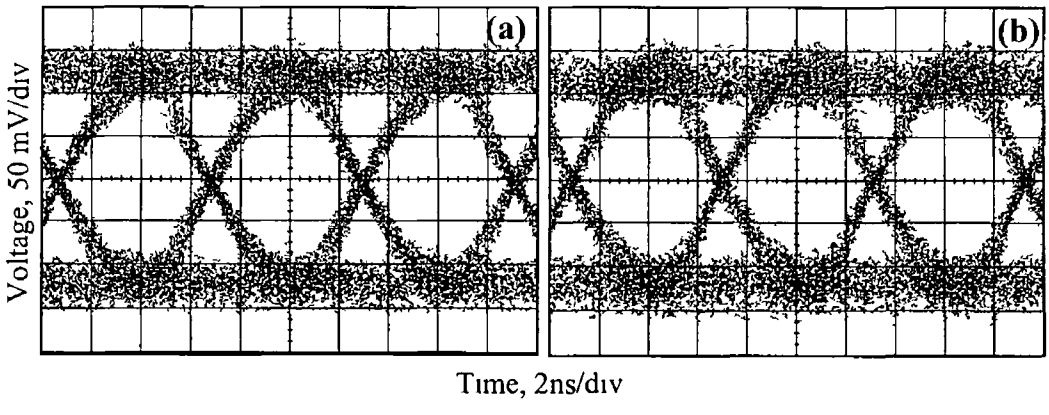

Figure 5-28 Received eye diagrams of 155 Mbit/s data signal (a) back-to-back set-up and (b) after demultiplexing of WDM signal for central optical channel

To completely characterize the system performance two stages of BER vs received optical power measurements were carried out (for the down-converted 155 Mbit/s data signal at an RF carrier frequency of 18 5 GHz (central WDM channel)) *Figure 5-29* displays both the system performance of the three optical channels multiplexed together and also the back-to-back performance of the central wavelength channel It can be seen from this plot that the degradation in system performance is only in the order of 0 4 dB This impairment is caused by the interference from the adjacent optical channels The negligible effect of the channel demultiplexing is also clear from the eye diagrams shown in *Figure 5-28* (a & b)

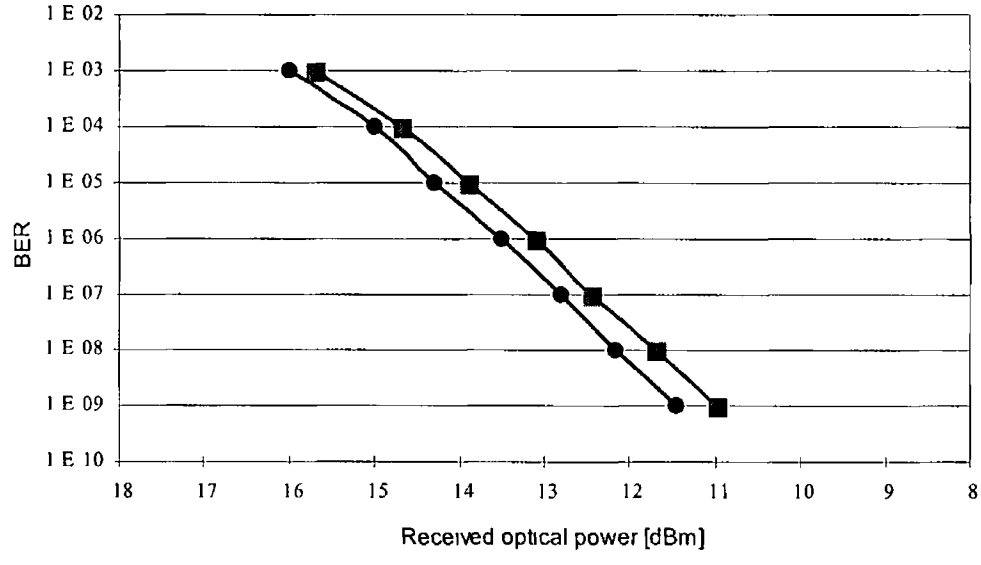

Figure 5-29 *BER vs received optical power for central optical channel demultiplexed from WDM system (squares) central optical channel back-to-back case (circles)*

To confirm that the demultiplexing technique used does indeed overcome dispersion effects in transmission fiber, a 12 km length of Standard Single Mode Fiber (SSMF) was inserted after the optical coupler that combines the three wavelength signals This fiber length has been determined to yield minimal received power of the DSB optical signal due to fiber dispersion effects (for the modulating frequency of 18 GHz) *Figure 5-30* displays the received eye diagrams after propagation through the transmission fiber followed by demultiplexing, detection, and down-conversion of the (a) SSB and (b) DSB signal

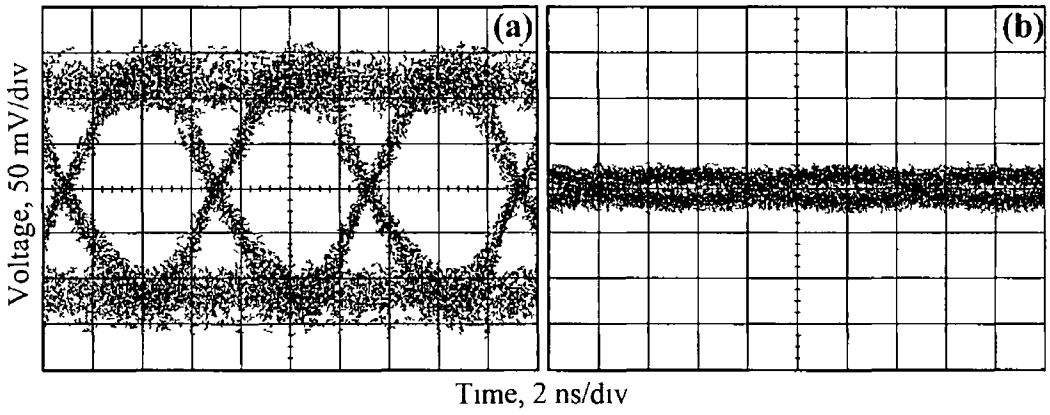

Figure 5-30 Received eye diagrams of 155 Mbit/s data signal after propagation of WDM/SCM signal through 12 km of standard fiber with Bragg filter positioned to (a) select single side band optical signal (b) select double side band optical signal

The received optical power level is −10 dBm By comparing *Figure 5-30* (a) with the eye diagrams in *Figure 5-28* one can see that the degradation in system performance due to the fiber is negligible The Bragg filter was then positioned in such a way that the carrier of the central wavelength channel was at the centre of the filter's reflection band In this case the filter selected out the complete DSB optical signal, and the received eye confirms how the fiber dispersion greatly affects the system performance (*Figure 5-30*(b))

The results presented show that by correct positioning of the Bragg filter relative to the optical channel to be demultiplexed, it would be possible to select out only the carrier and one side band in order to overcome dispersion effects in the distribution fiber In this scenario the degradation in system performance due to interference between the optical data channels after demultiplexing is negligible This work shows that it may not be a necessity to generate SSB at the transmitter in a radio/fibre system incorporating WDM technology, as correct optical filtering at the receiver RAU may be used to overcome system limitations imposed by DSB generation at the transmitter

5 4 1 Wavelength interleaving

The method of combating dispersion and demultiplexing a signal using a single filter at the receiver has one major disadvantage in that the spectral efficiency is very poor Sending a DSB signal over the fiber means that the WDM channels have to be separated by more than twice the highest modulating frequency At the receiver, in order to avoid dispersion caused fading, only one of the side-bands is detected The

effect of this drawback could be significantly reduced by employing a process called wavelength interleaving In systems using this method the channel spacing between the WDM channels is reduced to values that are less than twice the RF frequency The different possible multiplexing schemes are schematically presented in *Figure 5-31* [37]

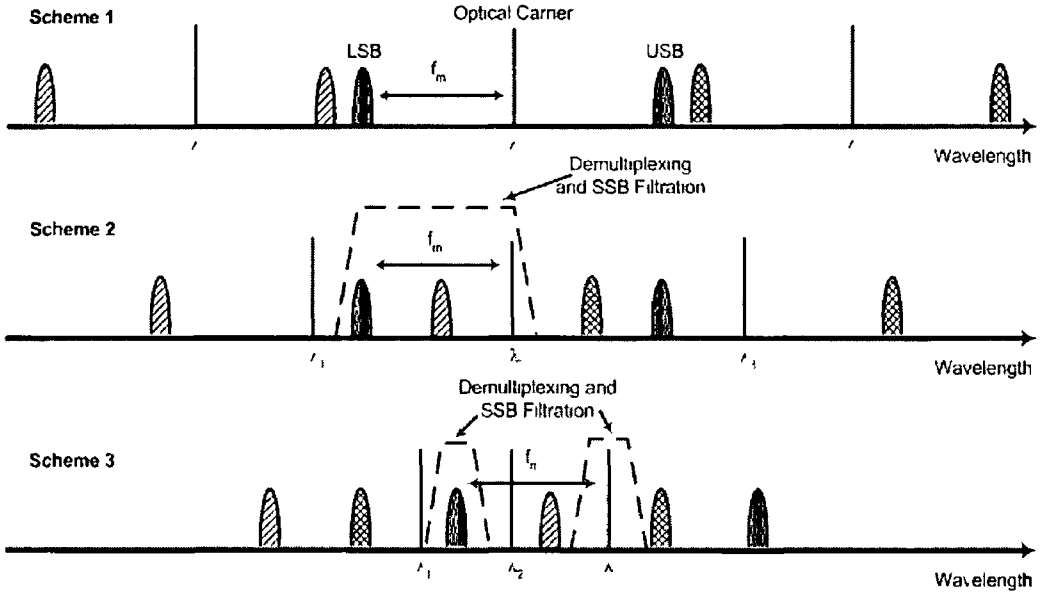

Figure 5-31 Different schemes of WDM channel allocation

Scheme 1 in *Figure 5-31* presents the conventional channel allocation in WDM/SCM systems Scheme 2 illustrates the case when the channel spacing fulfils the condition $f_{RF} < \Delta\lambda < 2f_{RF}$, where f_{RF} is the radio carrier frequency and $\Delta\lambda$ is the channel spacing If this relationship is preserved the demultiplexing and SSB filtering could be performed using a single Bragg grating as was presented in the previous section In case of scheme 3 ($\Delta\lambda < f_{RF}$) in order to demultiplex the WDM signal a specially designed filter or two filters in a cascaded arrangement must be used to choose one side-band and the optical carrier [38] In this scenario the wavelength drift and frequency of the RF carrier have to be monitored closely to ensure correct demultiplexing [39, 40] Even though scheme 3 is spectrally efficient it brings about a lot of complexity (additional components, monitoring etc) Hence scheme 2 was chosen because of its simplicity and cost efficiency

The chosen scheme of interleaving was then employed in the WDM/SCM system experiment The BER was measured as the wavelength channel spacing was varied The result is illustrated in *Figure 5-32*

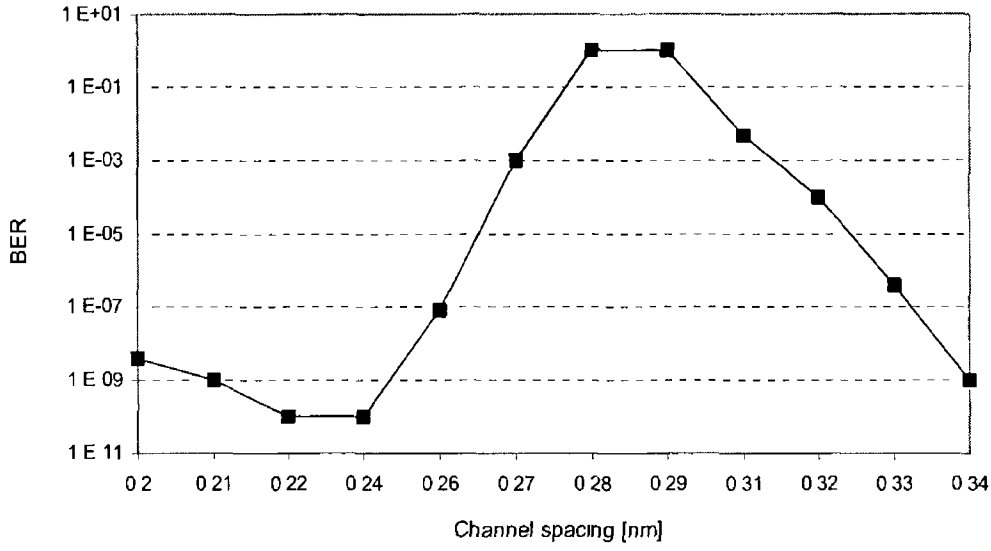

***Figure 5-32** BER vs channel spacing*

From the plot it can be seen that BER is low when the channel spacing is greater than twice the RF frequency ($\Delta\lambda > 2f_{RF}$) The BER gets worse as the channel spacing approaches 0 29 nm This value of $\Delta\lambda$ corresponds to the frequency of around $2\,f_{RF}$ For such a channel spacing the side-bands from the adjacent WDM channels start interfering The BER improves again when the $\Delta\lambda$ reaches 0 26 nm At this point the channel spacing is such that the WDM channels are wavelength interleaved Similar levels of system performance are achieved between 0 26 nm and 0 2 nm (range of 0 06 nm) as can be seen in *Figure 5-32* After that BER increases rapidly (not shown in the plot) This rapid degradation of the signal quality is due to the imperfection of the filter response (not square) When the channel spacing is reduced below 0 2 nm, the adjacent WDM carrier starts leaking through the pass band, making the detection of the signal impossible This happens even though the optical carrier and the adjacent side-band do not overlap The experiment shows that the minimum channel spacing between WDM channels will be ultimately defined by the roll-off of the filter response

Figure 5-33 shows the optical spectrum of the demultiplexed signal when the channel spacing was set to 0 23 nm The limited resolution of the spectrum analyzer (0 05 nm) did not allow distinguishing side-bands for lower values of $\Delta\lambda$

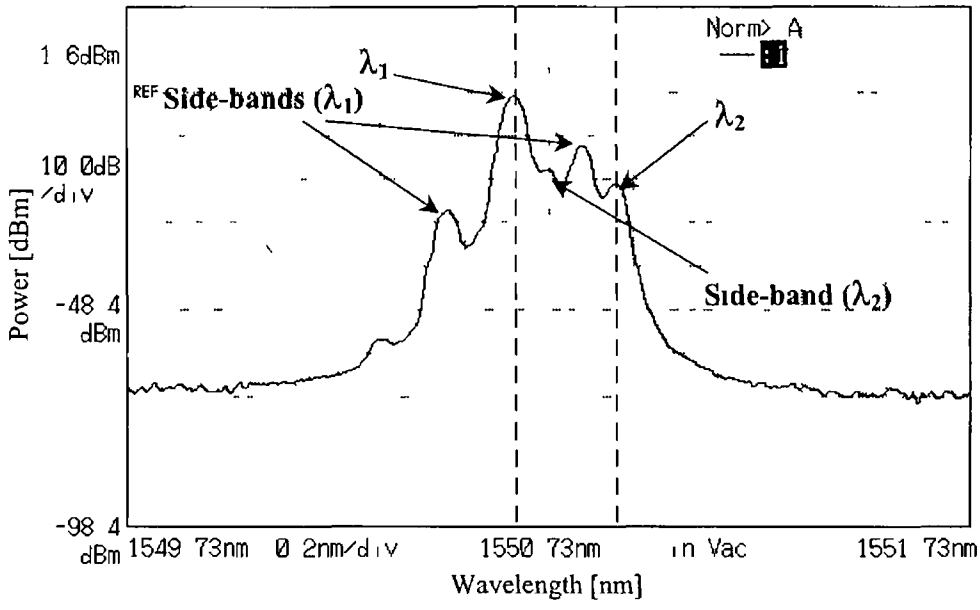

Figure 5-33 Optical spectrum of the demultiplexed signal (channel spacing = 0 24 nm)

From the plot above it can be seen that the lower side band of λ_1 is suppressed by around 15 dB in comparison with upper one λ_2 on the other hand is more than 20 dB lower than λ_1

The experiments presented in this chapter show that WDM/SCM system could be realized in a simple and cost effective way by using an FBG at the receiver to demultiplex the incoming signal and to combat dispersion caused fading This method could be used even when wavelength interleaving is used in order to increase the spectral efficiency of the system

References

[1] W I Way "Subcarrier Multiplexed Lightwave System Design Considerations for Subscriber Loop Applications", *J Lightwave Technol*, vol 7, pp 1806-1818, 1989

[2] O K Tonguz *et al* "Personal Communications Access Networks Using Subcarrier Multiplexed Optical Links", *J Lightwave Technol*, vol 14, pp 1400-1408, 1996

[3] G H Smith *et al* "A Millimeter-Wave Full-Duplex Fiber-Radio Star-Tree Architecture Incorporating WDM and SCM", *IEEE Photon Technol Lett*, vol 10, pp 1650-1652, 1998

[4] E Vourch, *et al* "A WDM Fiber-Radio Experiment Incorporating a Wavelength Tunable Single-Side-Band Filter", *Proc Microwave Symposium Digest, 2002 IEEE MTT-S International,* vol 3 , pp 1703 –1706, Seattle, USA, 2002

[5] H Toda *et al* "DWDM Demultiplexing with 25 GHz Channel Spacing for 60 GHz Band Radio-on-Fibre Systems", *Proc European Conference on Optical Communications,* vol 3, Paper 8 2 4, Copenhagen, Denmark, 2002

[6] A Stohr *et al* "Full-Duplex 60 GHz Fiber Optic Transmission", *Electron Lett*, vol 35, pp 1653-1655, 1999

[7] K Kitayama *et al* "Dispersion Effects of FBG Filter and Optical SSB Filtering in DWDM Millimeter-Wave Fiber-Radio Systems", *J Lightwave Technol*, vol 20, pp 1397-1407, 2002

[8] R Olshansky *et al* "Subcarrier Multiplexed Lightwave Systems for Broadband Distribution", *J Lightwave Technol*, vol 7, pp 931-943, 1991

[9] W Lin *et al* "A Reliable Architecture for Broad-Band Fiber-Wireless Access Networks", *IEEE Photon Technol Lett*, vol 15, pp 344-346, 2003

[10] T Wolcott *et al* "Subcarrier multiplexing more than just capacity", *Lightwave*, July 2001

[11] E J Tyler *et al* "Toward Terabit-per-Second Capacities Over Multimode Fiber Links Using SCM/WDM Techniques", *J Lightwave Technol*, vol 21, pp 3237-3242, 2003

[12] N K Shankaranarajanan *et al* "WDM/subcarrier-FDMA Lightwave Networks Limitations Due to Optical Beat Interference", *J Lightwave Technol*, vol 9, pp 1329-1342, 1989

[13] R Ramaswami *et al* "A Packet-Switched Multihop Lightwave Network Using Subcarrier and Wavelength Division Multiplexing", *IEEE Trans Comm*, vol 42, pp 1198-1211, 1994

[14] K Wesolowski "Mobile Communication Systems", John Wiley & Sons Ltd, 2002

[15] H Al-Raweshidy "Radio over Fiber Technologies for Mobile Communications Networks", Artech House, London 2002

[16] T Wolcott *et al* "SCM complements DWDM, increases capacity", *WDM Solutions*, 2001

[17] S Haykin "Telecommunications Systems", John Wiley & Sons, INC , New York 1994

[18] T Wolcott *et al* "Optical subcarrier multiplexing squeezes more capacity from bandwidth", *Lightwave*, 2000

[19] R van Nee *et al* "OFDM for Wireless Multimedia Communications", Artech House Publishers, Boston, London 2000

[20] Y Sun "Bandwidth-efficient wireless OFDM", *IEEE J on Selected Areas in Comm*, vol 19, pp 2267 – 2278, 2001

[21] W A C Fernando *et al* "Performance of coded OFDM with higher modulation schemes", *1998 International Conference on Comm Technol Proceedings*, vol 2, pp 5-7,1998

[22] V Nangia, *et al*," Experimental broadband OFDM system field results for OFDM and OFDM with frequency domain spreading" *Proceedings Vehicular Technology Conference*, vol 1, pp 223 – 227, 2002

[23] P Hill *et al* "A 20-Channel Optical Communication System Using Subcarrier Multiplexing FOR the Transmission of Digital Video Signals", *J Lightwave Technol*, vol 8, pp 554-560, 1990

[24] X J Meng *et al* "Improved Intrinsic Dynamic Distortions in Directly Modulated Semiconductor Lasers by Optical Injection Locking", *Trans on Microwave Theory and Tech*, 1999

[25] B Wilson *et al* "Analogue Optical Fibre Communications", IEE, London 1995

[26] T Darcie *et al* "Lightwave Subcarrier CATV Transmission Systems", *IEEE Trans Microwave Theory Tech*, vol 38, pp 524 – 533, 1990

[27] E Bravi *et al* "Experimental Confirmation of the Theoretical Analysis of Distortion Effects in Analog Externally Modulated Lightwave Systems", *IEEE Photon Technol Lett*, vol 12, pp 1061-1063, 2000

[28] R Sadhwani *et al* "Adaptive CMOS Predistortion Linearizer for Fiber-Optic Links", *J Lightwave Technol*, vol 21, pp 3180-3193, 2003

[29] S L Woodward *et al* "Optimizing Subcarrier-Multiplexed WDM Transmission Links", *J Lightwave Technol*, vol 22, pp 773-778, 2004

[30] X J Meng *et al* "Electro-optical Predistortion Technique for Linearization of Mach-Zehnder Modulators", *Electron Lett*, vol 37, pp 1545-1547, 2001

[31] J Chen *et al* "Linearity and Third-Order Intermodulation Distortion in DFB Semiconductor Lasers", *IEEE J Quantum Electron* vol 35, pp 1231-1237, 1999

[32] H D Jung *et al* "Nonlinear Distortion Suppression in Directly Modulated DFB-LD by Dual-Parallel Modulation", *IEEE Photon Technol Lett*, vol 14, pp 980-982, 2002

[33] C K Chan *et al* "Efficient Frequency Assignment Scheme for Intermodulation Distortion Reduction in Fiber-Optic Microcellular systems", *Electron Lett* vol 30, pp 1831-1832, 1994

[34] Y Akaiwa *et al* "Application of Channel Segregation for Automatic Channel Selection Free from Intermodulation Interference", *7th International Symposium on Personal, Indoor and Mobile Radio Communications*, vol 3 pp 1235-1238, 1996

[35] G H Smith *et al* "Overcoming Chromatic – Dispersion Effects in Fibre-Wireless Systems Incorporating External Modulators", *IEEE Trans Microwave Theory Tech*, vol 45, pp 1410 – 1415, 1997

[36] C Marra *et al* "Optical SSB Modulation using Fiber Bragg Gratings and the Impact of Grating Dispersion on Transmission Performance", *International Topical Meeting on Microwave Photonics*, pp 93-96, Long Beach 2001

[37] K Kitayama *et al* "Dispersion Effects of FBG Filter and Optical SSB Filtering in DWDM Millimeter-Wave Fiber-Radio System", *J Lightwave Technol*, vol 20, pp 1397-1407, 2002

[38] C Lim *et al* "Capacity Analysis for WDM Fiber-Radio Backbones with Star-Tree and Ring Architecture Incorporating Wavelength Interleaving", *J Lightwave Technol*, vol 21, pp 3308-331, 2003

[39] C Marra *et al* "Wavelength-Interleaved OAMDs Incorporating Optimized Multiple Phase-Shifted FRBs for Fiber-Radio Systems", *J Lightwave Technol*, vol 21, pp 32-39, 2003

[40] C Lim *et al* "Technique for increasing Optical Spectral Efficiency in Millimetre-Wave WDM Fibre-Radio", *Electron Lett*, vol 37, pp 1043-1045, 2001

6 Modelling of a Radio/Fiber System

The design of photonic systems has reached a stage in which simulations are no longer a luxury, but a necessity [1] The hybridization of radio and optical networks and the exponential growth in the number of channels[1] operating with channel spacings that are reduced to a few times the channel bit rate bring about new problems In order to solve these problems and achieve optimized operation of high-speed optical links, many design variables have to be assessed This assessment could be addressed with the help of software design tools [2] Just as Electronic Design Automation (EDA) tools have become an essential part of the semiconductor and electronics industry, Photonic Design Automation (PDA) tools have brought in huge advances in the optical communications world Matlab (a high performance software environment) and Virtual Photonics Incorporated – Transmission Maker ((VPI - TM) a PDA) are employed as the modelling tools in this work

This chapter consists of the simulations[2]that confirm the multi-channel experimental results obtained in the previous chapter Transmission over fiber was also modelled[3] here, giving an insight into the effects of fiber characteristics on the propagating signal The latter is especially important since the same could not have been experimentally verified (using long lengths of fiber) due to drifting of the phase of the transmitted signal

6 1 SCM System based on a directly modulated laser

The performance of the system based on a directly modulated laser was modelled using Matlab The first stage of the modelling process, in this section, looks at the improvement in system performance brought about by external injection The subsequent simulation step involved the examination of third order Inter-Modulation Distortions (IMD_3) influence on system performance in a five-channel system The latter was carried out with both the free running as well as the externally injected laser

---

[1] DWDM
[2] Using MATLAB
[3] Using VPI

6 1 1 Improvement of performance – Free running versus externally injected laser

A fully lumped laser model in terms of three ordinary differential equations (for phase, electron and photon concentrations), commonly known as the laser rate equations, is well established [3, 4] Hence the above-mentioned method was chosen to model the laser in this work The laser rate equations for the single mode laser with external injection are

$$\frac{dN(t)}{dt} = \frac{I(t)}{qV} - \frac{N(t)}{\tau_n} - g_0\left(N(t) - N_{om}\right)S(t), \qquad \textbf{Equation 6-1}$$

$$\frac{dS(t)}{dt} = \Gamma g_0\left(N(t) - N_{om}\right)S(t) - \frac{S(t)}{\tau_p} + \Gamma\beta\frac{N(t)}{\tau_n} + 2K_c\sqrt{S_{inj}S(t)}\cos(\varphi(t)), \qquad \textbf{Equation 6-2}$$

$$\frac{d\phi(t)}{dt} = \frac{\alpha}{2}\left(\Gamma g_0(N(t) - N_{om}) - \frac{1}{\tau_p}\right) - \Delta\omega - K_c\sqrt{\frac{S_{inj}}{S(t)}}Sin(\phi(t)), \qquad \textbf{Equation 6-3}$$

where

N – carrier number in the active volume,

I – is the drive current,

e – electron charge,

V – volume of the active layer,

τ - carrier lifetime,

g_0 – gain slope constant,

N_{om} – carrier density at threshold,

S – photon density,

Γ - optical confinement factor,

τ_p – photon lifetime,

β - spontaneous emission coefficient,

K_c - coupling coefficient for the injected light,

S_{inj} - photon density of the injected light

φ(t) – phase of the light,

α - linewidth enhancement factor,

$\Delta\omega = \varpi - \omega_{inj}$ - detuning frequency between the slave and master laser

The Matlab code for the system model is presented in Appendix C The parameters used for the laser model are given in the table below

g_0	1e-12
N_{om}	1 4e23
V	11e-17
τ_p	2e-11
τ_n	0 3e-9
Γ	0 35
β	0 0
q	1 6e-19
α	6 8
$\Delta\omega$	$2\pi\Delta f$
S_{inj}	varied
K_c	2 5e11
Ar	03e-12 m^2
c	3e8 ms^{-1}
n	3 63
h	6 625e-34
f	1 935e14 Hz
R	0 32

Table 6-1 *Laser model parameters*

The power - current (P/I) dependence for the single mode laser modelled (free running case) is shown in *Figure 6-1* From the P/I curve one can see that the laser threshold current is around 18 mA

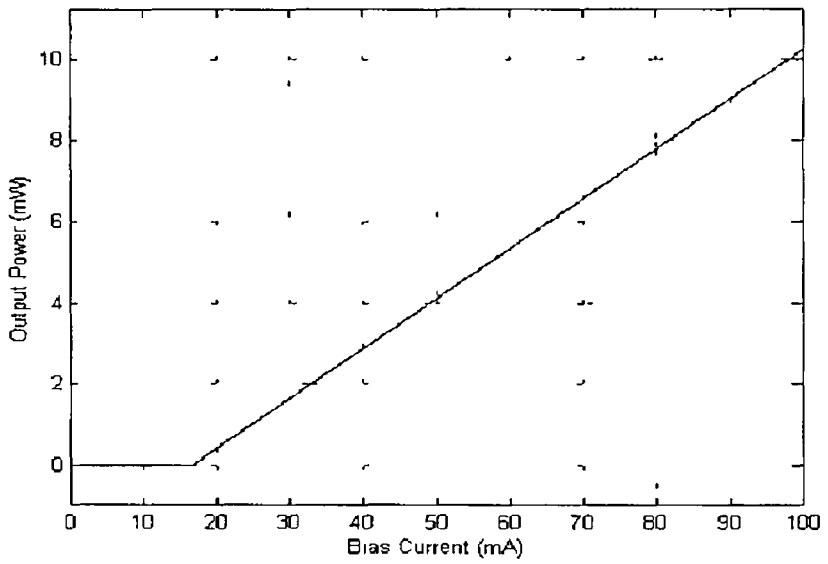

Figure 6-1 Laser P/I curve

The bias current for the simulation was chosen to be 60 mA The frequency response of the laser at this bias is shown in *Figure 6-2* The free running case is depicted by curve (a) while the external injection case is portrayed by curve (b) The injection ratio for the latter was set to be $S_{inj}/S = 0\ 04$

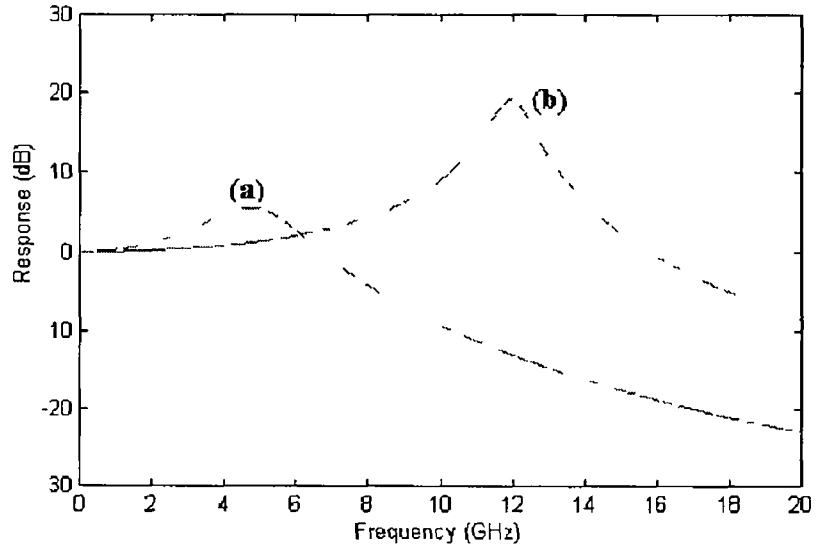

Figure 6-2 Frequency response of (a) free running laser (b) laser under external injection

From the plot it can be seen that the modulation bandwidth of the free running laser is around 7 GHz, while external injection increases the modulation bandwidth up to around 16 GHz (ROF @ ~ 12 GHz) Another important point to be noted is that the relaxation oscillation peak in case of external injection is around 12 dB higher than for the free running laser

The central RF frequency was chosen to be 12 GHz, to make use of the enhanced response at this frequency The simulations were performed for two cases a single channel and a multichannel system

Single channel system

First a single channel system was modelled A 140 Mb/s data stream was upconverted to 12 GHz and used to directly modulate the laser

The output signal of the laser was detected using a photodiode It was modelled as a simple optoelectronic conversion with the addition of noise For simplicity, thermal noise was considered but shot noise was ignored The equation for thermal noise is given as

$$\sigma_{th}^{2} = \frac{4kTf_0}{R}, \qquad \textbf{Equation 6-4}$$

where k is Boltzmann's constant, T is the temperature in degrees Kelvin, R is the receiver impedance, and f_0 is the receiver bandwidth Noise is random in nature so it cannot be predicted what it will do to the signal To model the noise in this system it was assumed that the noise had zero mean and a Gaussian distribution These assumptions allows the noise model to be greatly simplified A responsivity of 0 6 A/W was used

The RF spectrum of the modulating signal is shown in *Figure 6-3*

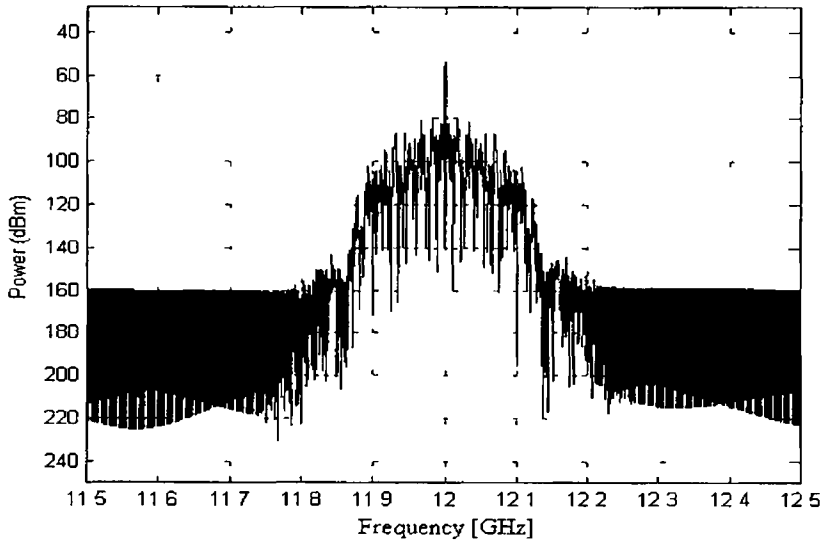

Figure 6-3 Electrical spectrum of the modulating signal - single channel system

This signal was first applied to the free running laser and subsequently to the laser under the external injection The detected RF spectra of signals generated by the free

running and externally injected laser are shown in *Figure 6-4* and *Figure 6-5* respectively

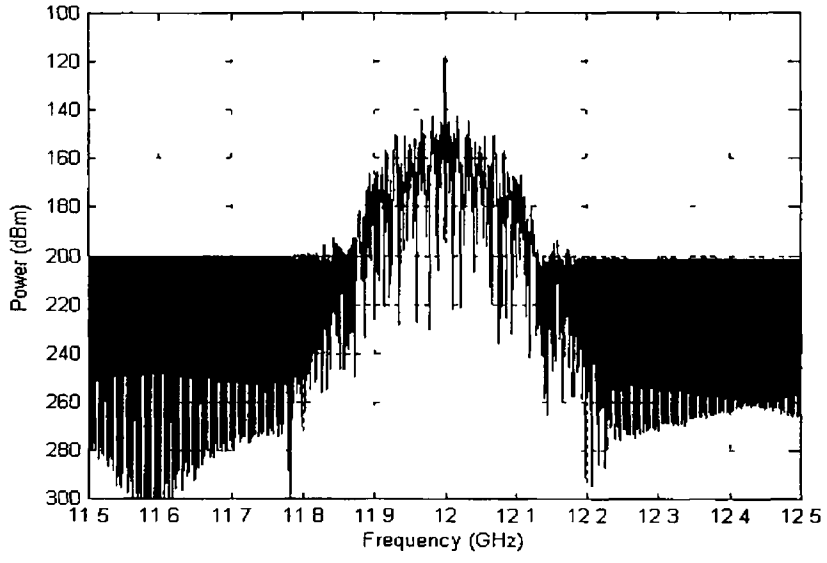

Figure 6-4 *Electrical spectrum of the detected signal - free running laser*

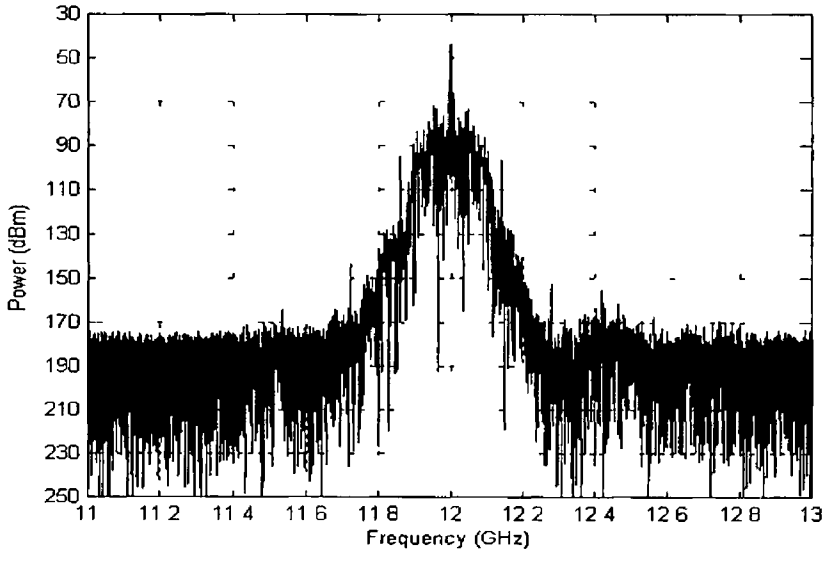

Figure 6-5 *Electrical spectrum of the detected signal - laser with external injection*

From the figures above it can be seen that the signal generated by the externally injected laser is much stronger than that of the free running laser The corresponding eye diagram of the downconverted signal for the free running laser and laser under external injection are shown in *Figure 6-6* and *Figure 6-7* respectively

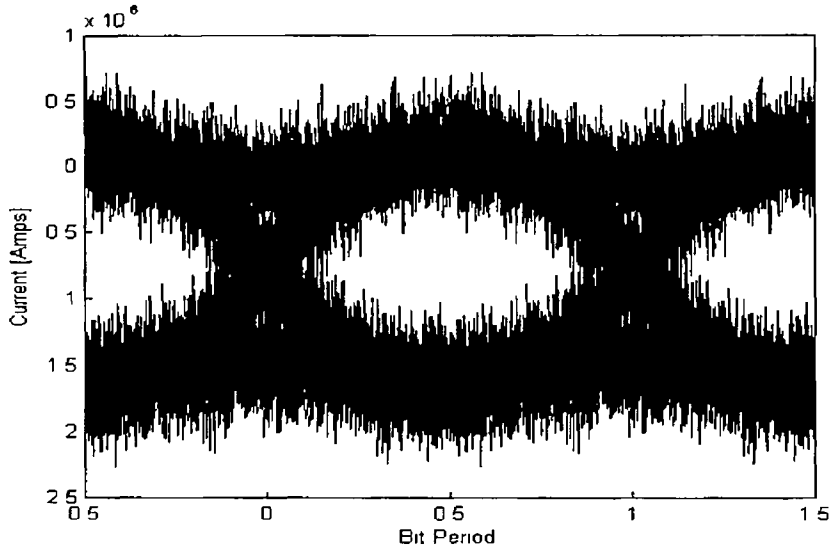

Figure 6-6 Eye diagram - free running laser

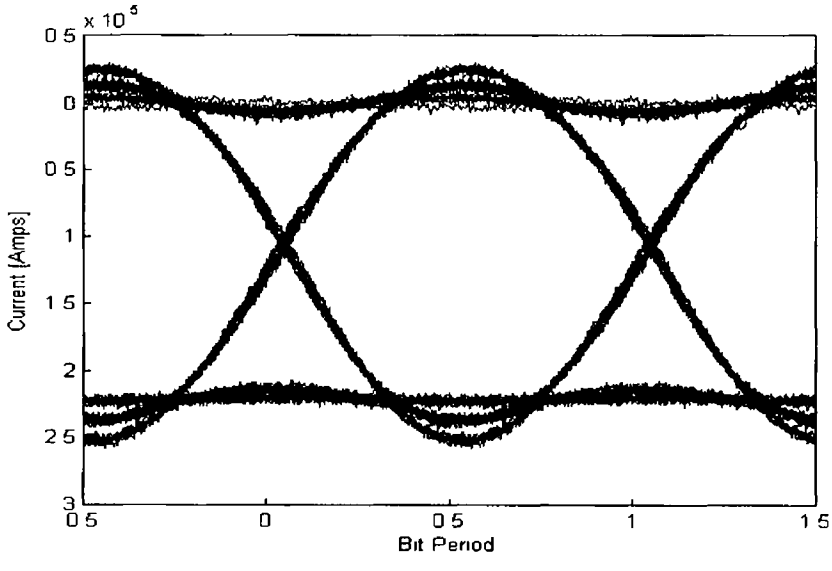

Figure 6-7 Eye diagram - externally injected laser

In both cases the received optical power was –17 dBm In case of the free running laser the eye height is less than 1μA, while for the externally injected laser the eye height exceeds 20 μA

To quantify the improvement in system performance brought about by external light injection, BER measurements were performed The equation used to calculate the BER in the model was

$$BER = \frac{1}{4}\left[erfc\left(\frac{\overline{I_{(1)}} - I_D}{\sqrt{2}\sigma_1} \right) + erfc\left(\frac{I_D - \overline{I_{(0)}}}{\sqrt{2}\sigma_0} \right) \right], \qquad \textbf{Equation 6-5}$$

where $\overline{I_{(1)}}$ is the mean of the current when the signal is high

$\overline{I_{(0)}}$ is the mean of the current when the signal is high low

σ_1 is the standard deviation of the current when the signal is high

σ_0 is the standard deviation of the current when the signal is low

The resultant plot of the BER versus received optical power for the free running laser and laser under external injection is shown in *Figure 6-8*

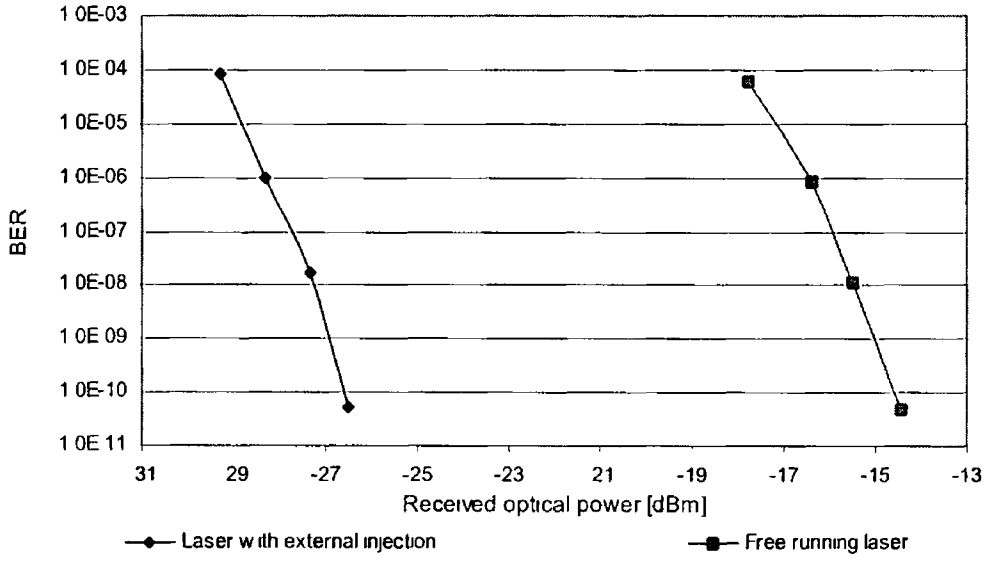

Figure 6-8 *BER vs received optical power free running laser (squares) externally injected laser (diamonds)*

From *Figure 6-8* it can be seen that external injection improves the system performance by around 12 dB (in terms of optical power) It corresponds to a 24 dB increase in electrical power, which is less than that observed in the frequency response of the laser (around 30 dB - *Figure 6-2*) The difference could be attributed mainly to two factors Firstly, as mentioned in Chapter 4 1, external injection decreases the threshold current of the laser This results in an increase in the power due to DC, thus decreasing the improvement in system performance Secondly, signals generated by externally injected lasers are noisier than signals generated by the free running lasers Both these features result in this response increment not being directly reflected in the improvement in system performance

Five channel system

In case of the multichannel system five PRBS data streams each at 140 Mb/s were amplitude modulated onto five RF carriers The channel spacing between the carriers

was set to 400 MHz (carriers ranging from 11 2 to 12 8 GHz) The spectrum of the modulating signal is shown in *Figure 6-9*

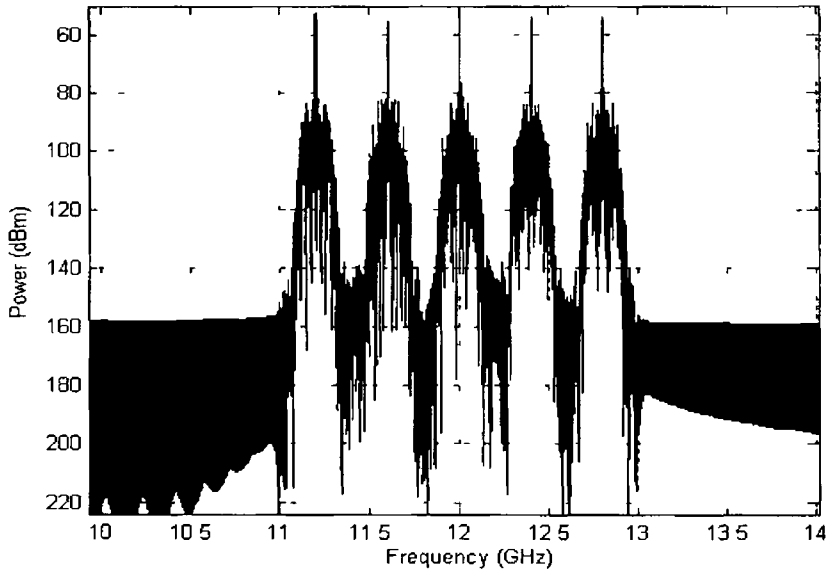

Figure 6-9 *Electrical spectrum of the modulating SCM signal*

As in the previous section the combined SCM signal was initially applied to the free running laser and subsequently to the laser under external injection The detected spectra and the resulting eye diagrams were used to compare the difference in performance between the two simulation cases The disparity between them was then quantified with the aid of a plot of the BER versus received power

The electrical spectrum of the detected SCM signal generated by a free running laser is shown in *Figure 6-10*

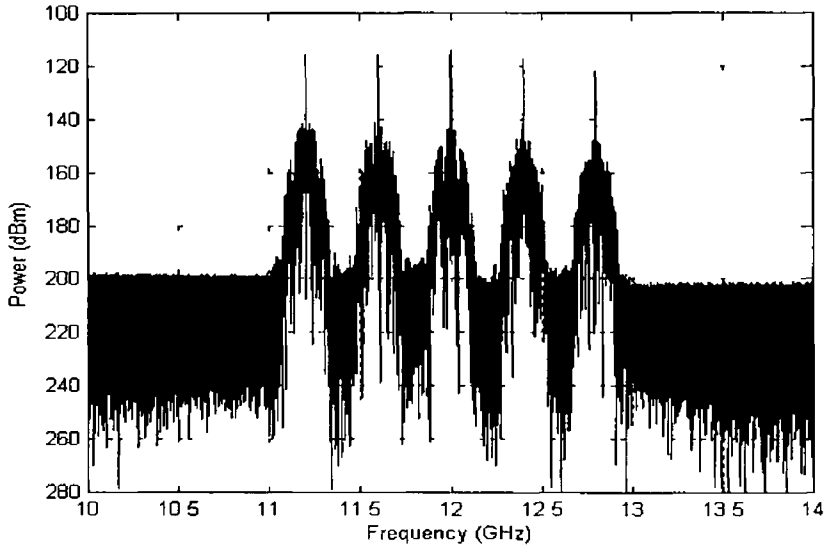

Figure 6-10 Electrical spectrum of the detected signal - free running laser

The eye diagram of the received and downconverted central channel again of the free running laser is shown in *Figure 6-11*

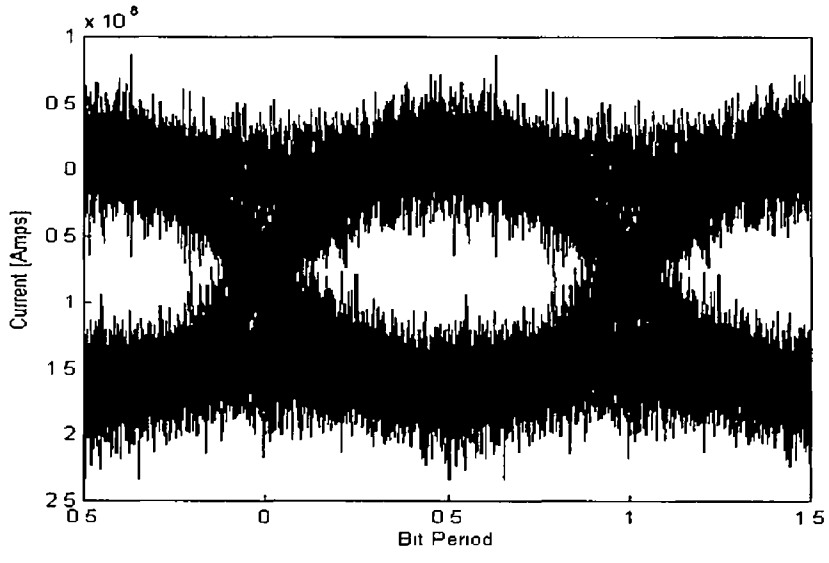

Figure 6-11 Eye diagram - free running laser

The received optical power was about – 17 dBm From the figure it can be seen that the eye height is around 0 75 μA

Figure 6-12 shows the electrical spectrum of the received SCM signal generated by the externally injected laser

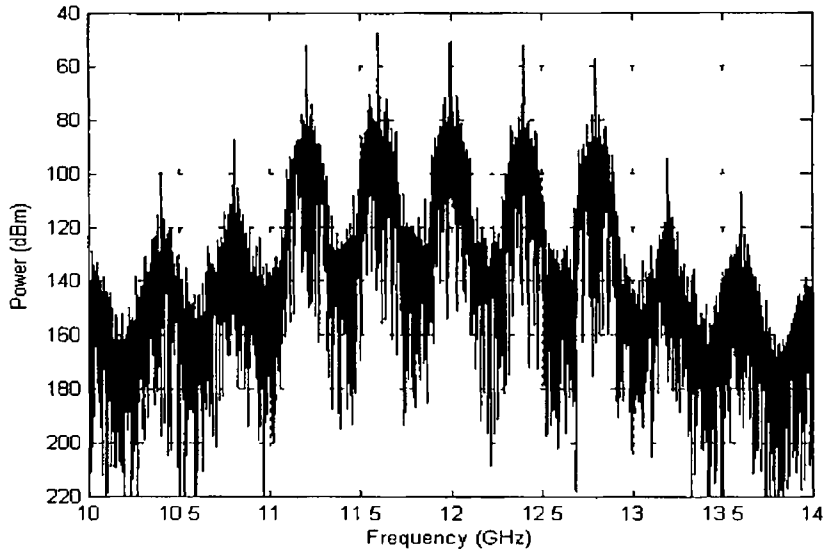

Figure 6-12 Electrical spectrum of the detected signal – laser under external injection

In comparison to *Figure 6-10* there are many more frequency components present in the signal generated by the laser under external injection These components are the mixing products of the input RF signals and are caused by the nonlinearity of the laser Their presence suggests that when the laser transmitter is subjected to external light injection, it becomes much more nonlinear than in the free running condition This was also indicated by the height of the resonance peak in the modulation response of the laser with injection At this juncture it is necessary to reiterate that in most devices, a nonlinear frequency response does not mean that the device is nonlinear Nevertheless, in the case of a laser the resonance peak is an effect of nonlinear interactions between electrons and photons Thus the stronger the nonlinearity the higher the resonance peak

The above-mentioned mixing products would have a negative influence on system performance since they could fall directly into the signal band and consequently cannot be filtered out Another important fact to be noted, as mentioned in Chapter 5, is that the effect of laser nonlinearity becomes more severe as the number of carriers and their amplitudes increase However in spite of the shortcomings, the power in the signal is much higher This could be attributed to the response of the laser being comparatively higher than the free running case at the modulating frequency

Figure 6-13 presents the eye diagram of the downconverted central channel generated by the laser under external injection As in the previous case the detected optical power was – 17 dBm It can be seen that the height of the eye is much bigger in comparison to the free running case The eye height can be estimated to be around

15 μA, which again reflects the fact that the power in the signal is higher here when compared with the free running case

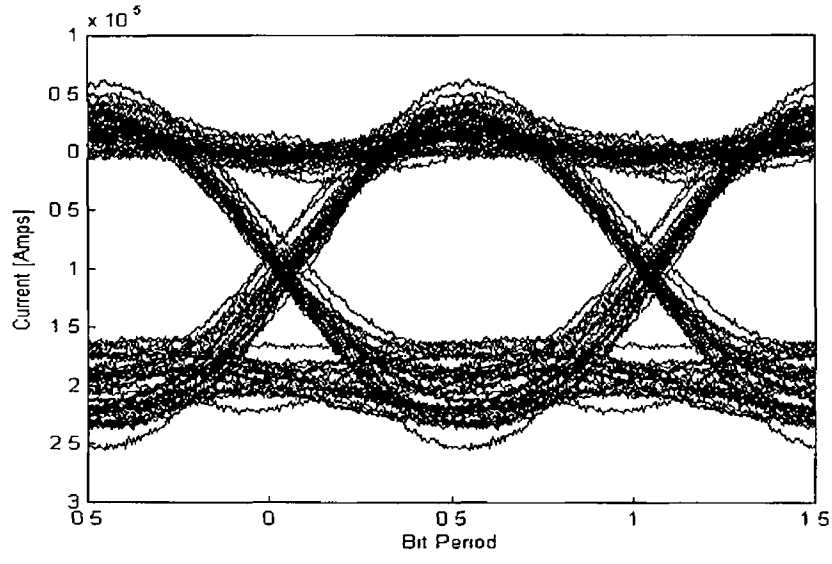

Figure 6-13 Eye diagram - laser under external injection

As mentioned earlier, the quantification of the differences in the performance of the system based upon the free running and externally injected laser was performed by carrying out BER vs received optical power measurements for both cases The BER was measured for the central SCM channel since it is the channel with the highest number of mixing products falling into its band The results are shown in *Figure 6-14*

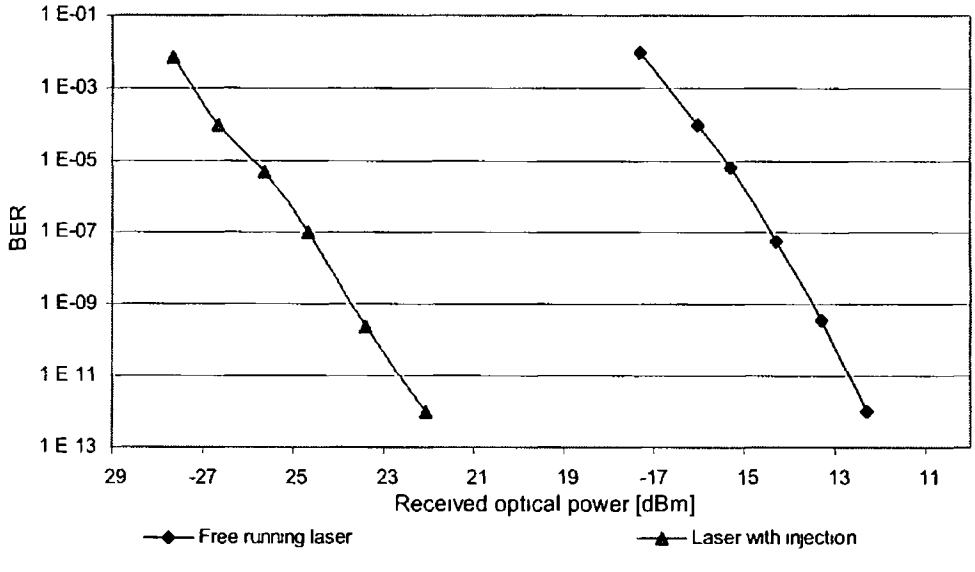

Figure 6-14 BER vs received optical power for the central SCM channel free running laser (diamonds) laser under external injection (triangles)

From the *Figure 6-14* one can see that the external injection improves system performance by around 10 dB This is improvement in terms of the optical power, which corresponds to 20 dB in electrical power Again this is significantly less than what could be expected in comparison to the difference between the frequency responses of the free running and externally injected laser shown in *Figure 6-2* (30 dB improvement at 12 GHz) It is also less than the single channel case This disparity could be attributed to a few aspects First of all the reasons given in the previous section (increase in DC power and in noise) apply here as well Secondly, the frequency response is plotted by modulating the laser with one frequency at a time and measuring the power of the detected signal Thus the actual increase in response for a laser modulated with multiple carriers (simultaneously) may be different than that for single carrier modulation Finally and most importantly, since the laser becomes more nonlinear with external injection, the mixing products resulting from laser nonlinearity will distort the received signal These IMD_3 products will reduce system performance of the externally injected transmitter much more severely than in case of a free running laser

The following section looks at the increase in laser nonlinearity in more detail

6 1 1 1 Influence of laser nonlinearity on system performance

Laser modulated at 12 GHz

In order to verify how mixing products influence system performance, the channel spacing between the extreme carriers (first & second and fourth & fifth) was varied from 400 MHz to 600 MHz using a step interval of 50 MHz The effect of IMD_3 was established by measuring BER for the central SCM channel As mentioned before this channel suffers the most from mixing products Varying the channel spacing moves the IMD_3 products away from the centre of the detected channel thereby reducing their influence IMD_3 components are most harmful when they fall in the centre of the signal band since the majority of the signal energy is concentrated around the carrier (centre of the signal band) The removal of IMD_3 from the signal band can be noticed by looking at *Figure 6-15* and *Figure 6-16* These figures illustrate the electrical spectra of the detected SCM signal with the central channel (laser with external injection) switched off By doing so, the mixing products falling in band with the filtered signal can be seen clearly *Figure 6-15* shows the spectrum

when all the channels are equally spaced The mixing products fall exactly at 12 GHz and they are only around 30 dB below the carrier level

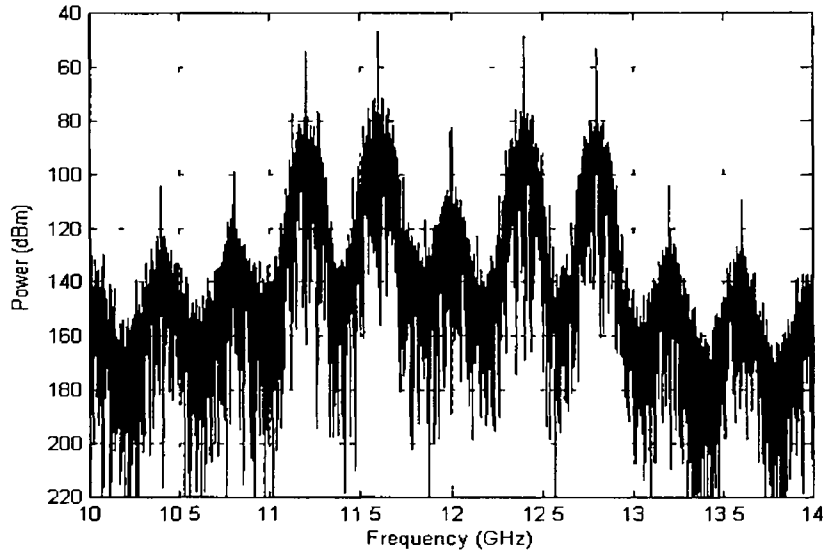

Figure 6-15 *Electrical spectrum of detected signal with even channel spacing (central channel switched off)*

Figure 6-16 on the other hand shows the spectrum when the channel spacing between the extreme channels is 500 MHz For such channel spacing the IMD_3 components fall 100 MHz away from centre of the signal band

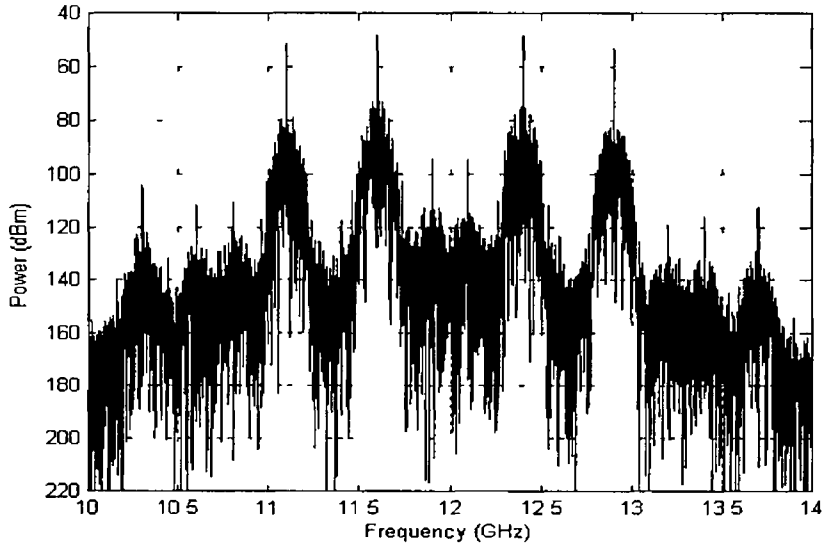

Figure 6-16 *Electrical spectrum of detected signal with uneven channel spacing (central channel switched off)*

The BER was measured with different channel spacing in order to quantify the influence of IMD_3 on system performance The tests were performed for both the free running laser and the laser under external injection The results are shown in *Figure 6-17* and *Figure 6-18* respectively

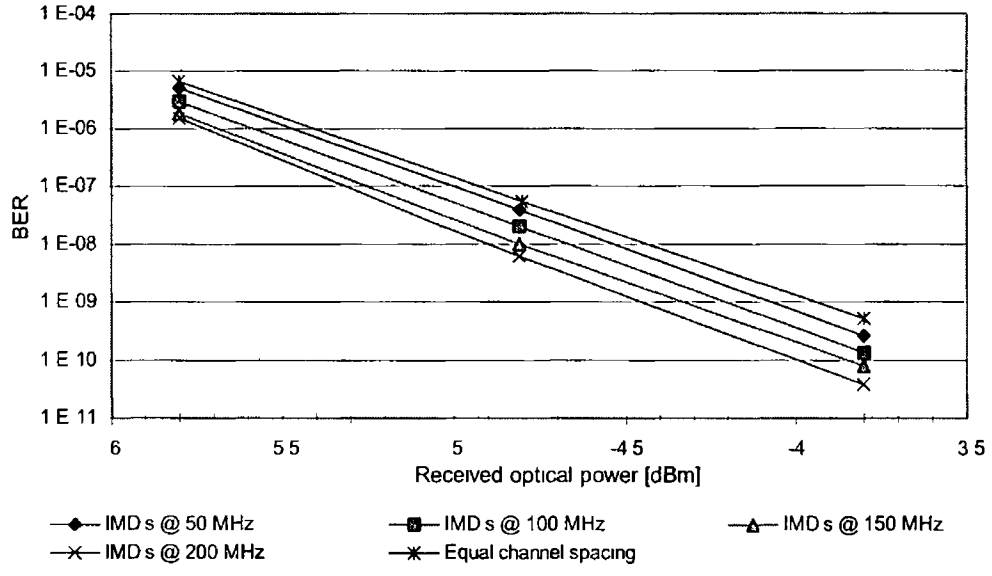

Figure 6-17 Influence of IMD_3 on system performance - free running laser

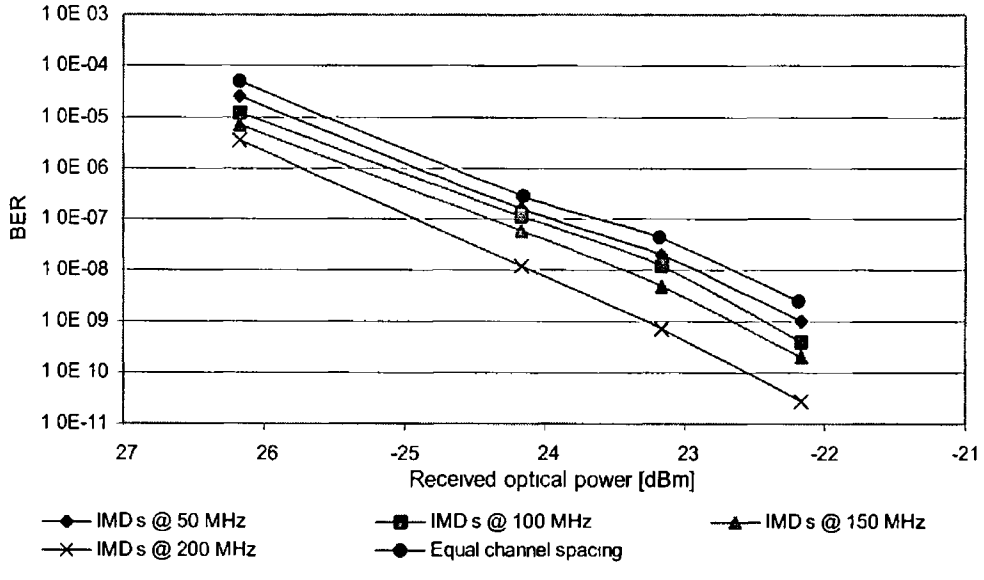

Figure 6-18 Influence of IMD_3 on system performance - externally injected laser

From the figures above, it can be seen that the performance of the system based on the free running laser could be improved by around 0 4 dB by removing the IMD_3 components from the signal band In the case of the laser with external injection this improvement is around 1 5 dB The biggest improvement is achieved when the channel spacing between the extreme channels is changed from 550 to 600 MHz This could be ascribed to the fact that the IMD_3 products are completely removed from the signal bandwidth

Laser modulated at 5 GHz

The same measurements were performed here for the free running laser modulated at its relaxation frequency This was done in order to verify whether laser nonlinearity actually increases with external injection[4] The relaxation oscillation frequency of the simulated laser was found to be at about 5 GHz The electrical spectrum of the detected signal when the central channel is switched off for channel spacings of 400 and 500 MHz (even and uneven spacing) is shown in *Figure 6-19* and *Figure 6-20* respectively

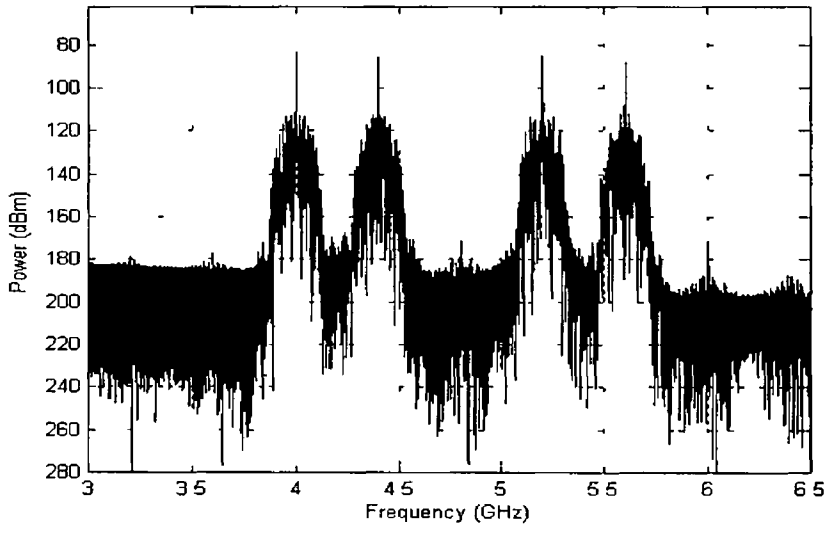

Figure 6-19 Electrical spectrum of laser modulated at relaxation frequency - even channels spacing

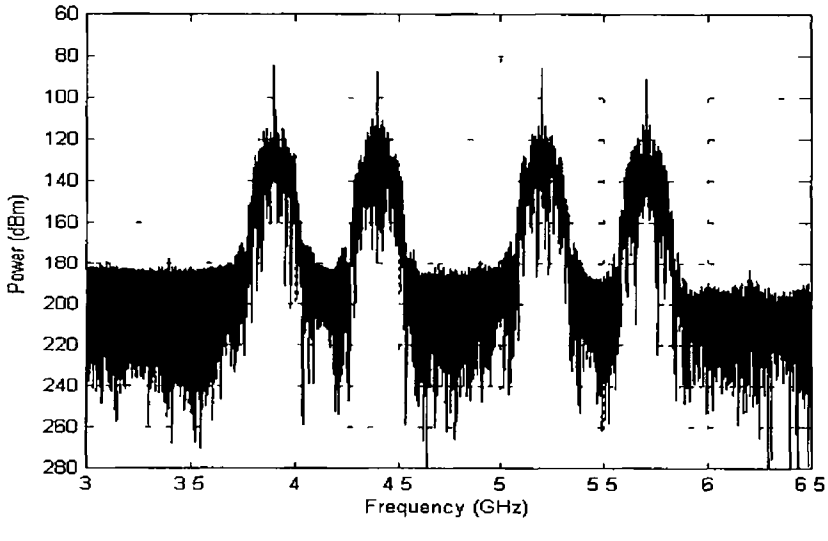

Figure 6-20 Electrical spectrum of laser modulated at relaxation frequency - uneven channels spacing

[4] Where the modulation was also carried out at the relaxation oscillation frequency

The IMD_3 are more than 80 dB below the carrier level as can be seen from *Figure 6-19* It can be seen from both figures that the IMD_3 products for the free running laser are higher when modulated at the relaxation frequency than when it is modulated away from oscillation frequency However, it is also important to note that the IMD_3 components of both cases above are lower (~ 50 dB) than those of the laser under external injection (shown in *Figure 6-15*)

The BER vs received optical power for free running laser modulated at its relaxation oscillation frequency is presented in *Figure 6-21*

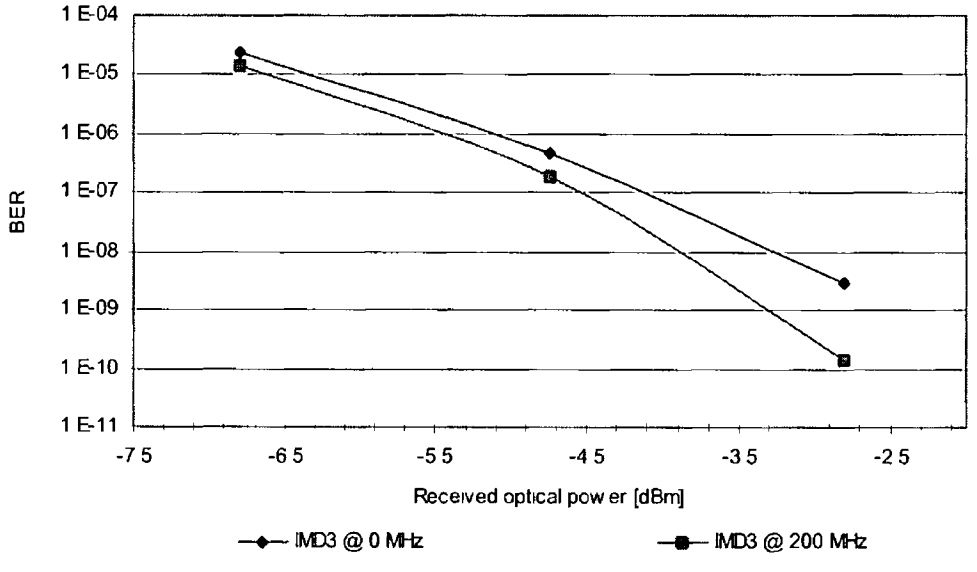

Figure 6-21 *Influence of IMD_3 on system performance for free running laser modulated at relaxation frequency*

Removal of the IMD_3 components from the signal band improves the system performance as revealed in *Figure 6-21* In aiming to achieve a BER of 10^{-8} in the case of even channel spacing a power penalty of 0 6 dB is incurred in comparison to the case when the IMD_3 products are completely removed from the signal band (extreme channels spaced by 600 MHz) This penalty is higher than that sustained in the case of the free running laser modulated at 12 GHz (0 4 dB)[5], but less than the case where the laser with external injection is modulated at 12 GHz (1 5 dB)[6]

The results presented above confirm that as the modulating frequency approaches the relaxation frequency, the power of the mixing products increases This phenomenon has important implications especially in regard to multichannel systems where the

[5] *Figure 6-17*
[6] *Figure 6-18*

impact of the nonlinearity proves to be crucial as regards system performance. The results obtained and the power penalty trends show that external light injection increases nonlinearity in the laser transmitter. Furthermore, the simulations results obtained here are in good agreement with experimental results presented in Chapter 4.

The modelling in this section has established the dependence of the nonlinearity on the modulating frequency and external injection and the subsequent degradation in multichannel system performance. The following section focuses on the influence of fiber nonlinearity on these multichannel systems.

6.2 Multichannel transmission over the fiber

The response of any dielectric to lightwaves is nonlinear. Nevertheless, as long as the signal power in a fiber is at a low level, fiber can be considered as a linear system. When the optical power in a fiber increases, the nonlinear effects become non negligible. These nonlinear effects in fiber may have a significant impact on the performance of WDM optical communication systems [5, 6].

When considering multichannel transmission, it is vital to realise that apart from taking into account the nonlinearity of the transmitter, the degradation of the signal due to the nonlinear characteristic of the fiber has also to be taken into consideration. Even though the power for individual channels is low the total power of the WDM/SCM signal for a large numbers of channels can exceed 100 mW, hence the effect of fiber nonlinearity can still be observed [7].

In the hybrid radio/fiber system employing WDM and SCM there are two groups of interactions that have to be taken into account: interactions between SCM carriers and interactions between WDM channels [8]. While the distortion due to propagation of multiple optical channels along the fiber are well known and studied, extent of the mixing between channels and degradation of the signal due to SCM transmission is still relatively unknown. The influence of fiber nonlinearity on the hybrid radio/fiber system employing WDM/SCM could be especially severe since data is transmitted in an analog form, which is much more sensitive to noise and distortion than the digital signals [9].

The most important types of nonlinearity that could affect WDM/SCM systems are Four Wave Mixing (FWM) [10, 11], Cross-Phase Modulation (XPM) [12] and Stimulating Raman Scattering (SRS) [13]. FWM falls into a broad class of harmonic

mixing processes It causes two or more frequencies to combine to generate emission at a different frequency, which is the sum or difference of the signals that are mixed [14] These newly generated waves, which are effectively intermodulation products, can cause crosstalk in a multichannel system, if the channels are equally spaced [15] The efficiency of FWM depends on the degree of optical phase matching This means that the distortion caused by FWM would depend on fiber dispersion and channel spacing (higher dispersion and larger channel spacing causes faster walk-off between wavelengths) [16] FWM thus will degrade the performance of a hybrid radio/fiber system especially due to its small channel spacing

XPM is caused by a variation in the refractive index of glass due to a variation in the intensity of light travelling along the fiber The amplitude modulation of one channel thus causes a phase modulation of the signal carried by other channels This phase modulation is then converted into intensity modulation by fiber dispersion [15, 17] XPM increases with the number of channels and becomes stronger when the channel spacing is reduced [15]

SRS is caused by light interfering with molecular vibrations Scattered light is generated at longer wavelengths than that of the incident light Hence SRS causes the transfer of energy to a different frequency band The newly created signals cause crosstalk, thereby degrading the performance of a WDM system [15] In WDM/SCM systems the subcarriers comprises of only a small fraction of the total optical power thus the main source of distortion due to SRS would be the interaction between subcarriers and optical carriers (not between subcarriers in different WDM channels) The strength of SRS crosstalk depends on fiber dispersion (decreases for higher dispersion) and on the subcarrier frequency as a result of the subcarrier walk-off due to dispersion [8,18] In the case of SRS, the crosstalk increases when the channel spacing increases

The effects of fiber nonlinearity increase as the optical power launched into the fiber increases Introducing new channels also degrades system performance since it usually means increasing the power and also the number of mixing products generated e g by FWM Furthermore, a higher optical modulation index causes more signal distortion [19] Finally, even for relatively low optical power travelling along the fiber, the effects of fiber-induced distortion could become significant if the signal propagates over long distances, since nonlinear effects accumulate along the fiber

The effects of fiber nonlinearity on SCM and WDM/SCM signals were simulated using the VPI-TM The results obtained are shown in the forthcoming section

6 2 1 SCM transmission over the fiber

Initial work here involved the characterization of the laser used in the model The module parameters and the frequency response of this laser module are shown in *Figure 6-22* and respectively *Figure 6-23*

LaserRateEqSM.vtms - Parameter Editor

Name LaserRateEqSM.vtms

ID LaserRateEqSM.vtms

Description

Laser Rate Equations (Single Mode)

Name	Value	Unit
Physical		
EmissionFrequency	193 1e12	Hz
SampleRate	SampleRateDefault	Hz
PowerNorm	5 0e 3	W
BiasToThreshold	2 0	
ModulToThreshold	0 0	
Length	300e-6	m
Width	3e 6	m
Height	0 2e 6	m
OptConfinement	0 5	
CarrierLifetime	2 10e-09	s
DifferentialGain	3 3e 20	m^2
IndexToGainCoupl	6 0	
NonlinearGain	0 03	
GroupIndex	4 0	
OutputCoupling	3798 11	1/m
InternalLosses	2873 00	1/m
SpontEmissFactor	1 11298	
InversionFactor	2 0	
Numerical		
MaxStepsNumber	100000	
RelativeAccuracy	1e 6	
InitialStepWidth	10e-12	s
MinimumStepWidth	0 0	s
Enhanced		
RandomNumberSeed	0	
OutputDataType	Blocks	
Active	On	
Scheduler		
Simulation Domain	SDF	

Figure 6-22 Laser module parameters

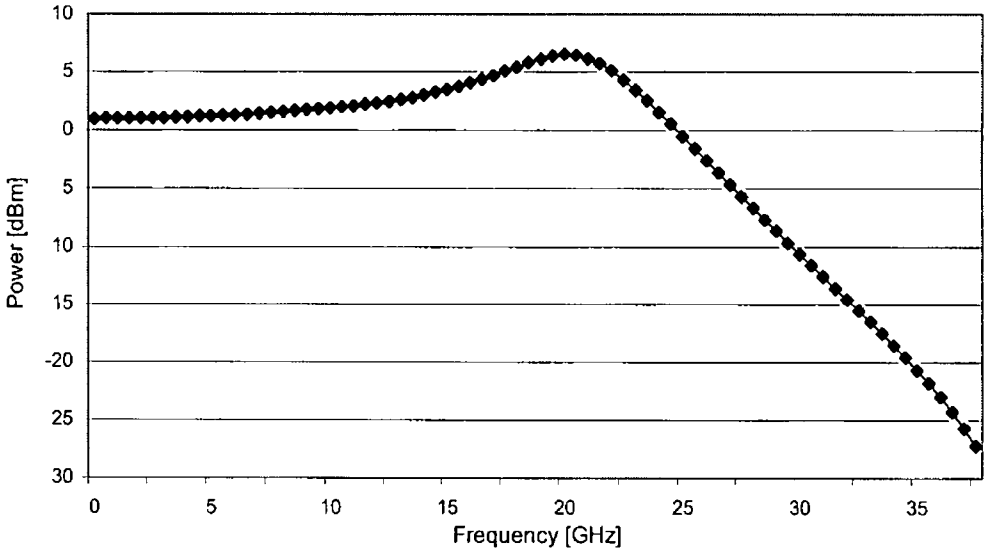

Figure 6-23 *Frequency response of laser used in the simulation*

From this figure it can be seen that the laser bandwidth was around 26 GHz The modulation frequency was then chosen close to the relaxation oscillation peak of the laser (~ 20 GHz) The laser was biased at five times its threshold current with the ratio of the modulation amplitude to the threshold current set to one

The simulation model used to verify the influence of fiber transmission on an SCM signal is shown in *Figure 6-24*

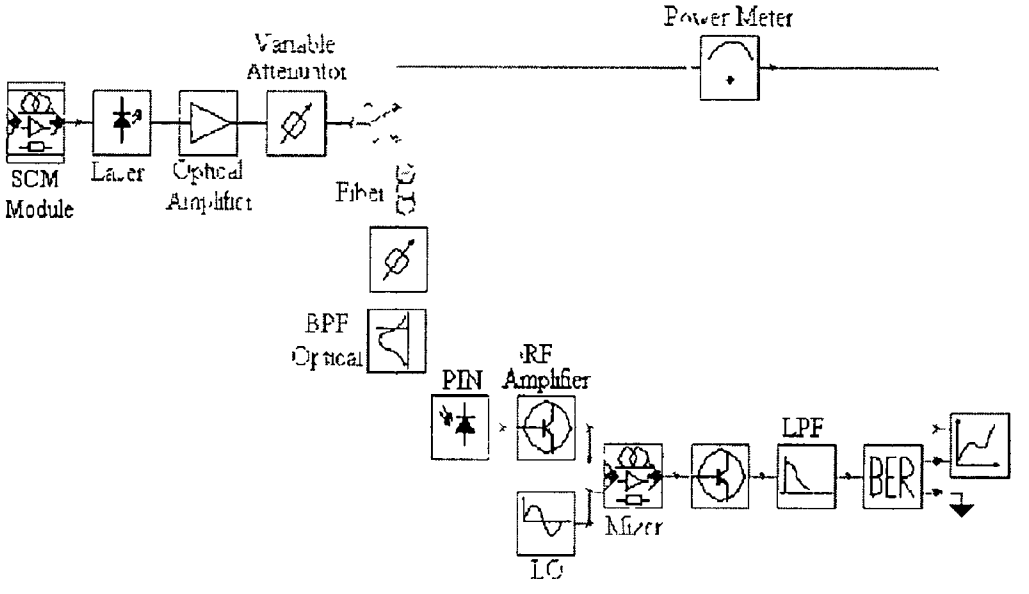

Figure 6-24 *Simulation model*

Figure 6-25 presents an insight into the SCM module used in the simulation

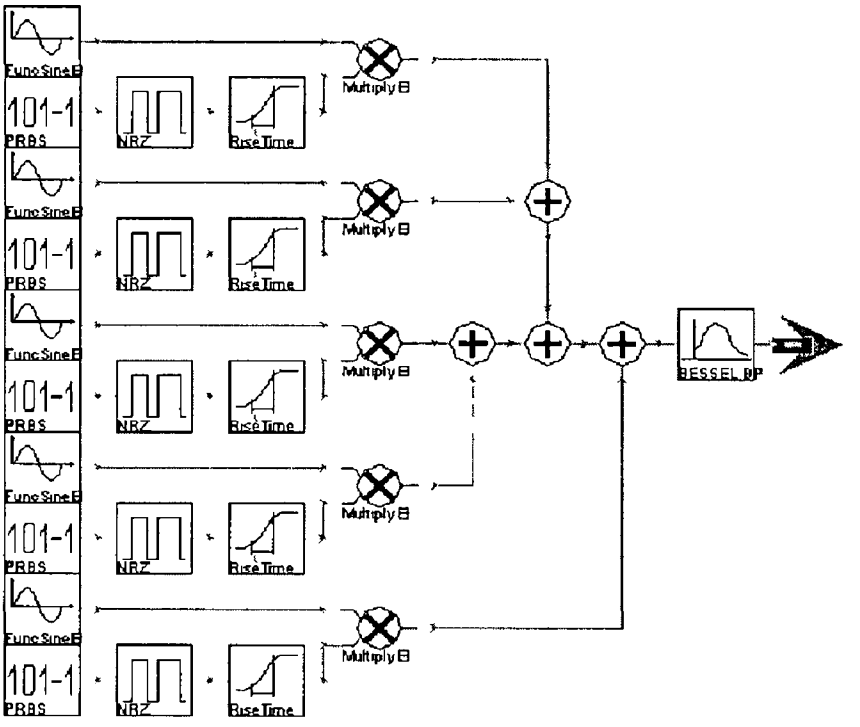

Figure 6-25 SCM module

The parameters of the photodiode and fiber modules are shown in *Figure 6-27* and *Figure 6-26* respectively

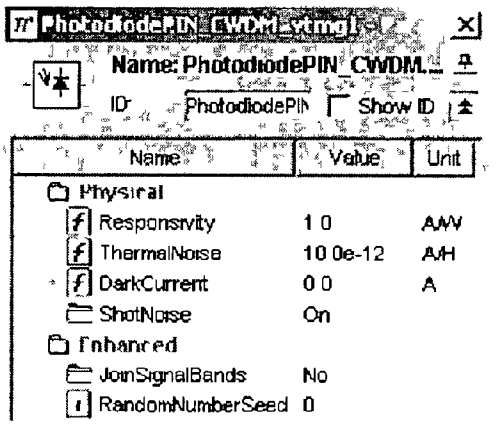

Figure 6-26 Parameters of the pin module used

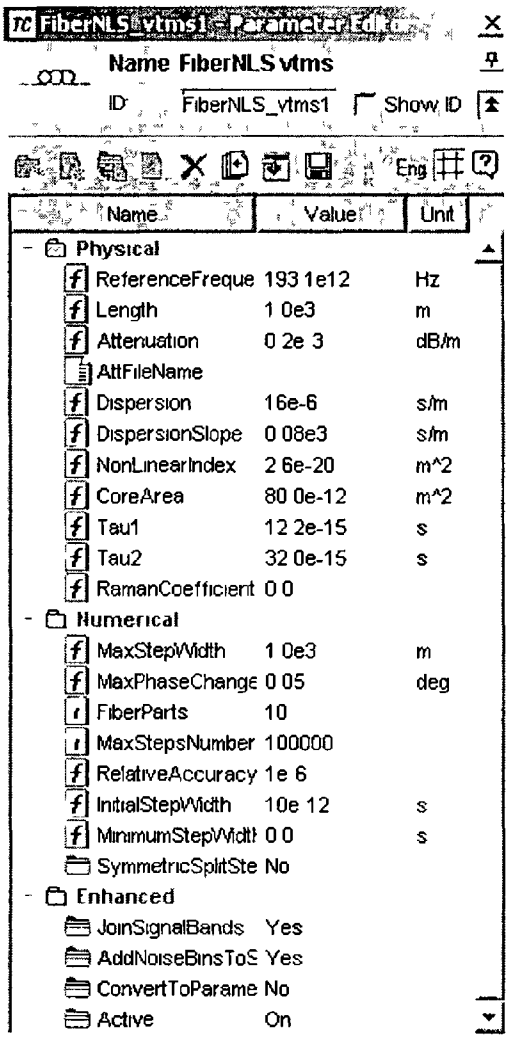

Figure 6-27 Parameters of the fiber module used

Five data channels consisting of a PRBS module followed by Non-Return-to-Zero (NRZ) coder and rise-time filter were upconverted to five different RF frequencies ranging from 19 2 to 20 8 GHz (see *Figure 6-25*) The upconverted data channels were then combined together and used to directly modulate the laser

The optical spectrum of the generated SCM signal is shown in *Figure 6-28*

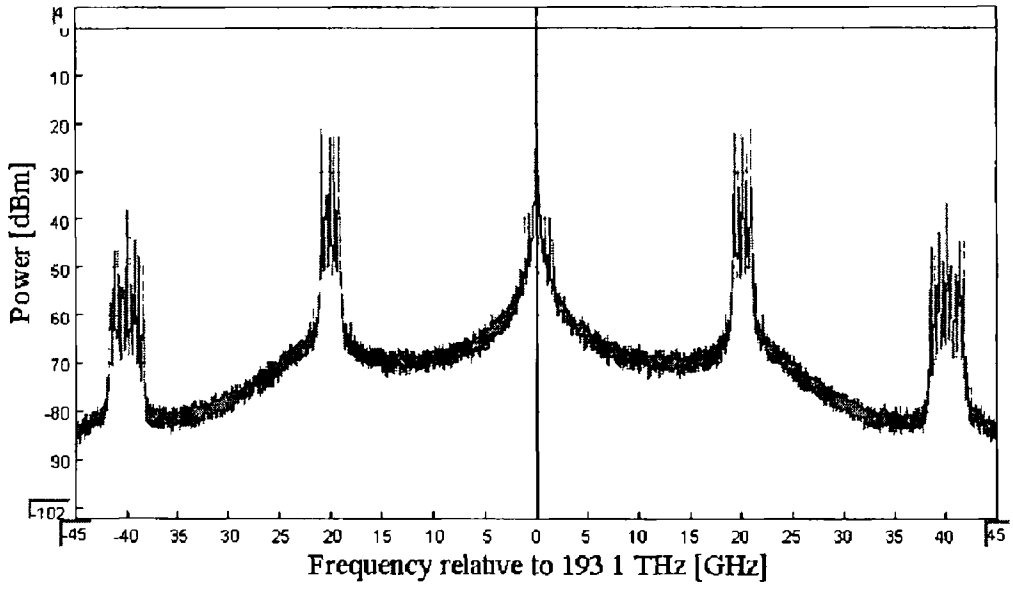

Figure 6-28 Optical spectrum of the SCM signal

The five RF channels are clearly visible in *Figure 6-28* In addition, a second pair of side bands together with some mixing products are also visible These extra components do not cause signal degradation in case of a single wavelength system, since they can be easily filtered out in the optical domain[7] However, these components can cause a significant interference if many optical channels (WDM) are to be transmitted

The optical signal from the transmitter was then amplified using an EDFA Two variable optical attenuators were used, one to vary the optical power launched into the fiber while the other to vary the power falling on the detector The output signal of the fiber was converted into SSB format using an optical BPF and is shown in *Figure 6-29*

[7] Also possible to be filtered in the electrical domain

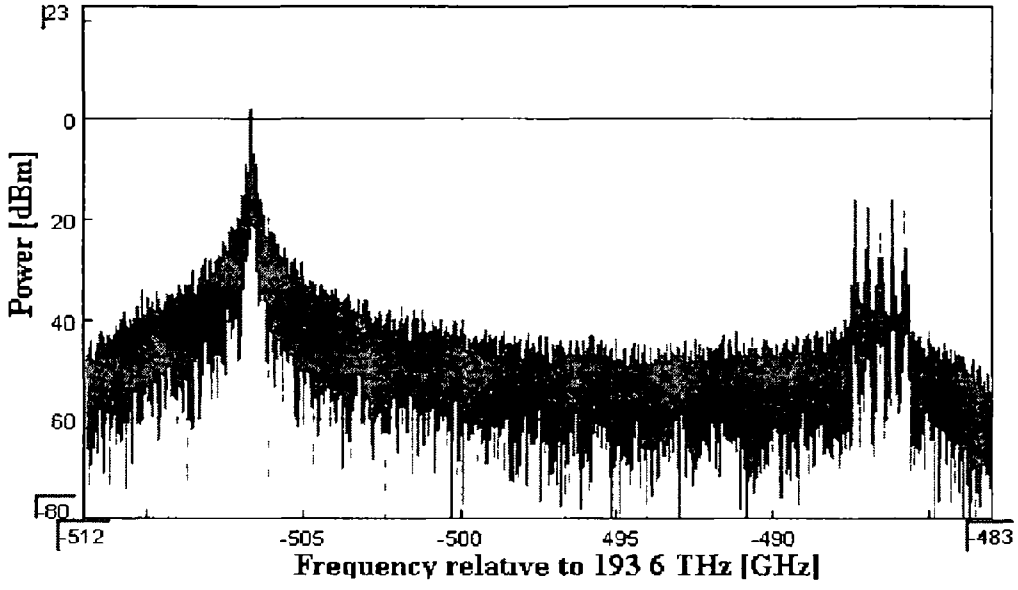

Figure 6-29 The output of the fiber after optical filtering

The received signal was then amplified and the central SCM channel was downconverted by mixing the signal with the signal from the LO Subsequently the downconverted data was filtered out and its quality was verified by performing the BER measurements The detected SCM signal is shown in *Figure 6-30*

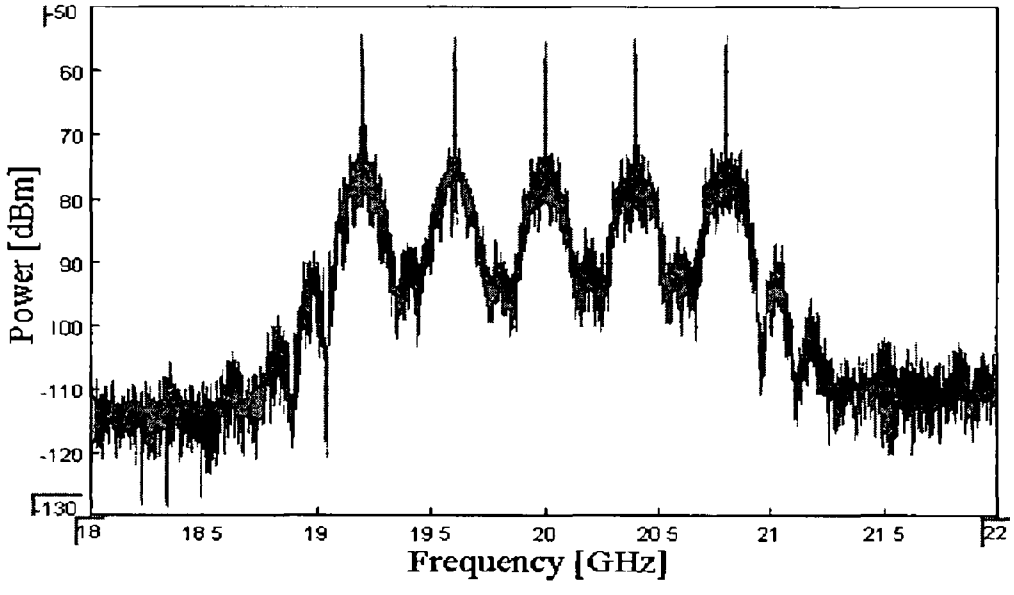

Figure 6-30 RF spectrum of the detected signal

It could be seen (*Figure 6-30*) that there are hardly any observable mixing products outside the signal band From this it could be inferred that the laser has a low level of nonlinearity In order to verify this statement, BER measurements were performed

for the central channel at different spacings between the extreme channels The results obtained are presented in *Figure 6-31*

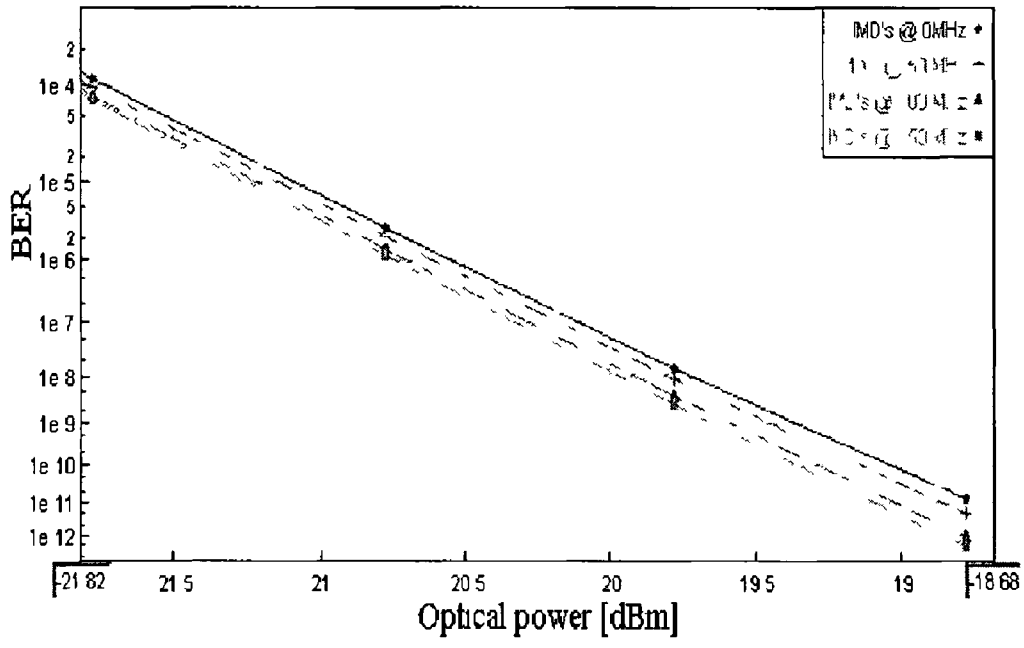

Figure 6-31 *Influence of IMD's for laser modulated at relaxation frequency*

The system performance in order to achieve a BER of 10^{-9} is improved by only 0 3 dB even with the complete removal of IMD_3 components from the signal band This confirms that the laser is more linear than the devices characterised earlier (experiments and simulations)

In order to verify the influence of fiber induced distortion on SCM system performance the fiber length in the model was set to 20 km The optical power launched into the fiber was varied by modifying the attenuation (using an optical attenuator) before the fiber To ensure a constant level of power falling on the detector another optical attenuator was used at the output of the fiber The resultant BER dependence on the optical power injected into the fiber is shown in *Figure 6-32* The power falling on the detector was maintained at 60 μW

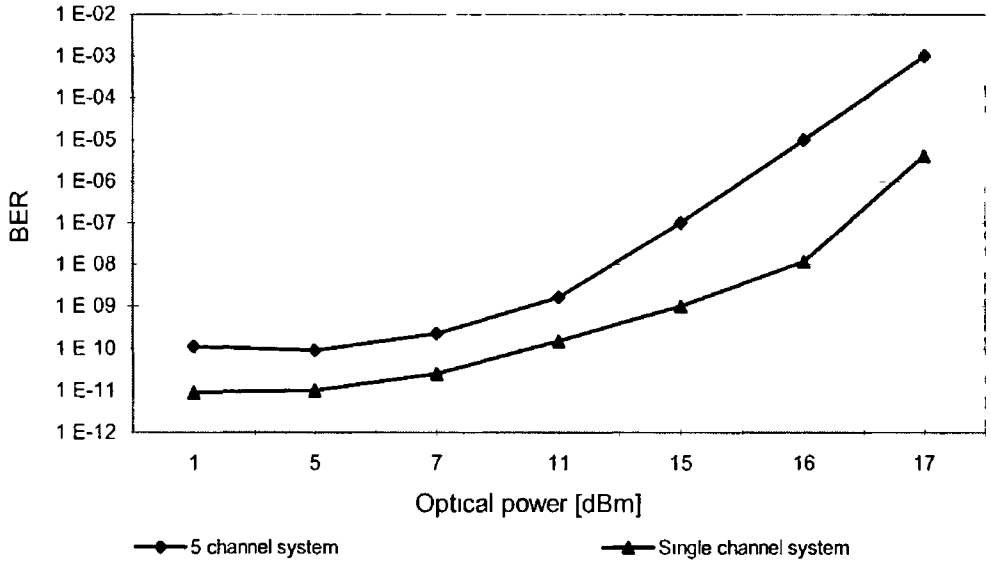

Figure 6-32 BER vs input optical power for 20 km fiber link

From *Figure 6-32* it can be seen that the system performance remains unchanged as the optical input power increases to 11 dBm Above this value rapid signal degradation is observed The received eye diagrams of the detected central SCM channel at a power level of 7 and 16 dBm are shown in *Figure 6-33* and *Figure 6-34* respectively

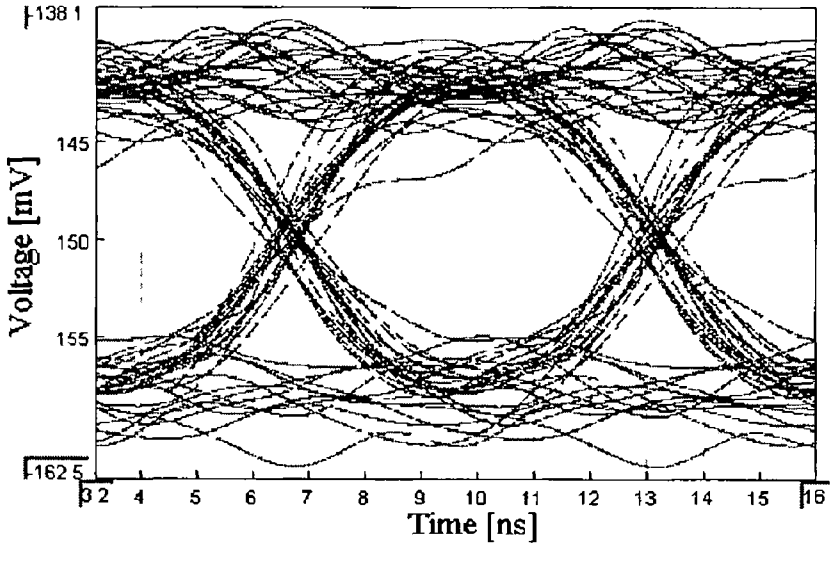

Figure 6-33 Eye diagram of the central SCM channel for 7 dBm optical power level

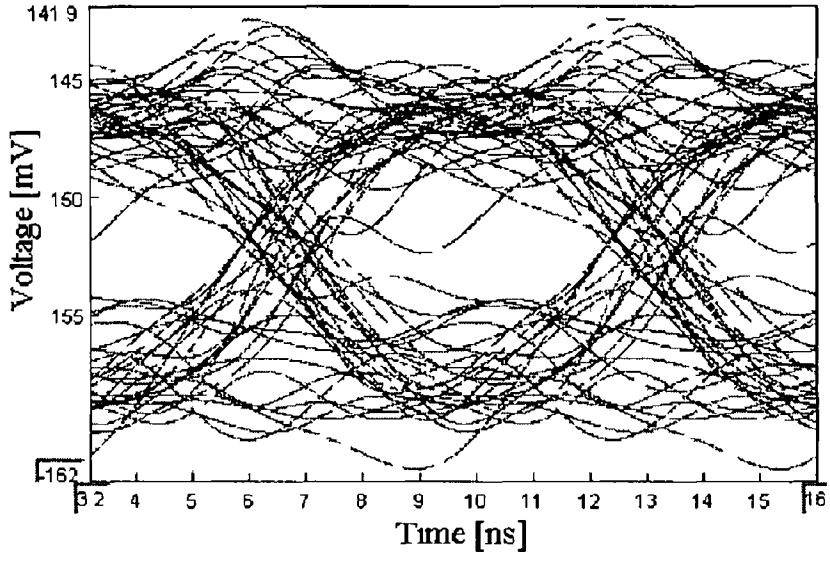

Figure 6-34 Eye diagram of the central SCM channel for 16 dBm optical power level

Figure 6-32 also presents the BER versus the optical power launched into the fiber for a single channel at a solitary wavelength In this case a lower BER is achieved for low levels of optical power This could be attributed to the fact that the single channel system is free from IMD_3 The BER remains low until the power exceeds 15 dBm Further increase in optical power travelling along the fiber degrades the system performance in a similar manner to that of the SCM system Self-Phase Modulation[8] (SPM) is the main source of distortion for the single channel system The difference in power levels at which the system performance become degraded shows that the optical SCM signals suffer more from fiber nonlinearity than the single channel systems even if only a single wavelength channel is transmitted This proves that fiber nonlinearity cause interactions between the SCM channels, which result in signal degradation It is expected that increasing the number of SCM channels would cause the system performance to degrade even faster

6 2 2 WDM/SCM transmission over the fiber

The simulation model used in investigating the impact of fiber nonlinearity on a WDM/SCM system is shown in *Figure 6-35* It is very similar to the model used in the previously described simulation (*Figure 6-24*) The major difference in this case is the increase in the number of optical channels to five The output of the lasers were

[8] SPM causes phase modulation of the signal due to a variation in the refractive index of glass, which in turn is a result of a variation in the intensity of light travelling along the fiber

combined together using a passive optical coupler The central SCM channel carried by the central wavelength was chosen for BER measurements since this is the channel, which suffers the most from nonlinear distortions

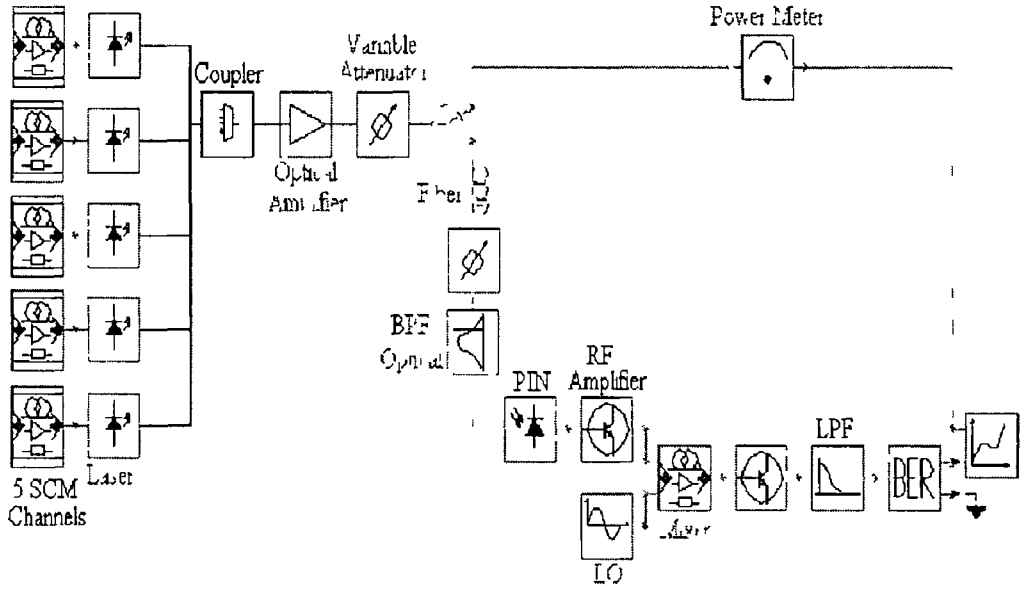

Figure 6-35 WDM/SCM system - simulation model

Initially the fiber length was set to 1 km in order to eliminate any distortion that could be brought about by the fiber characteristics The optical spectrum of the five combined optical channels is shown in *Figure 6-36*

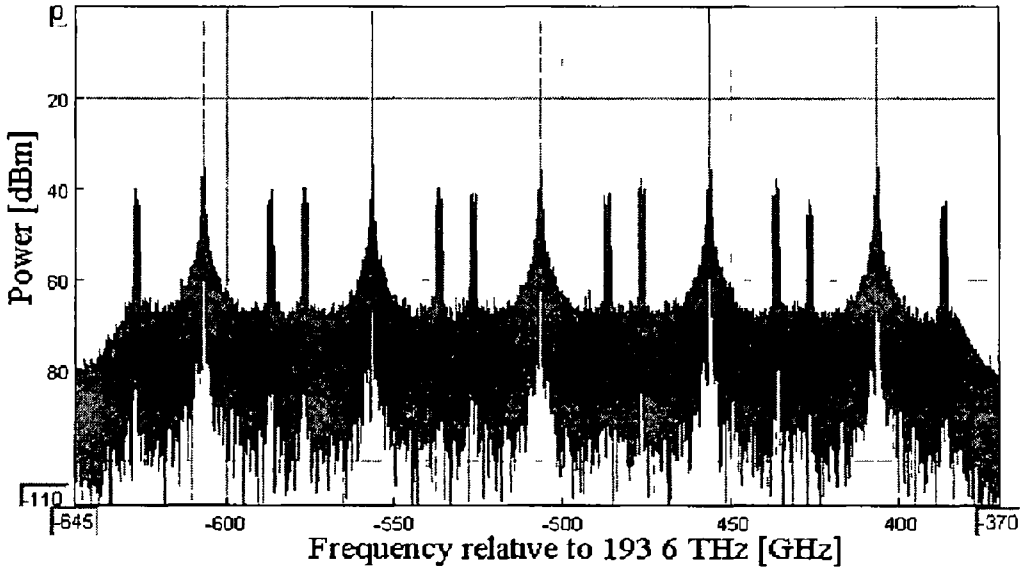

Figure 6-36 Optical spectrum of WDM/SCM signal

The channel spacing was initially set to 50 GHz This was big enough to accommodate DSB signals and still leave a 10 GHz clearance between the side bands

of neighbouring WDM channels Such a configuration is not bandwidth efficient, since at the receiver only one side band is needed Thus if the signal was converted to SSB format at the transmitter, the spectral efficiency (channel spacing) could be improved (reduced) by a factor of two, while keeping the same optical power falling at the receiver Nevertheless, an SSB format is not achievable by direct modulation One possible solution to this problem involves the employment of wavelength interleaving (as explained in Chapter 5) This technique allows the reduction of the channel spacing to a value lower than twice the modulating frequency Thus by employing such a technique the spectral efficiency of the system could be improved without the need for SSB conversion at the transmitter The optical spectrum of the optically filtered central channel in a 25 GHz spaced WDM system is shown in *Figure 6-37*

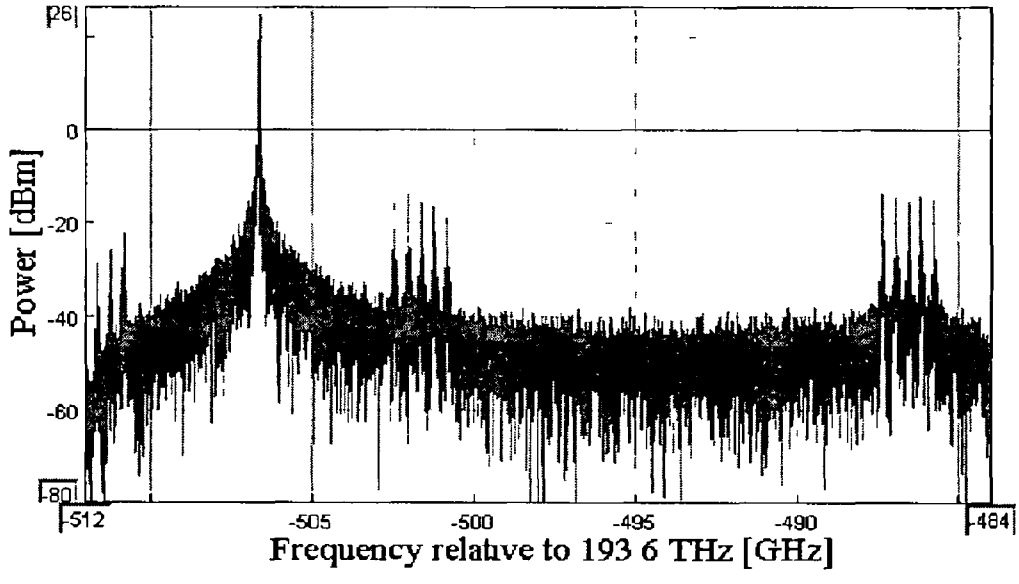

***Figure 6-37** Optical spectrum of the demultiplexed central WDM channel for 25 GHz channel spacing*

The side bands of the adjacent WDM channels can be seen at distance of 5 GHz on either side of the optical carrier These side bands will beat with the optical carrier at the receiver generating extra electrical components at 5 GHz, which can easily be filtered out The electrical spectrum of the detected signal is shown in *Figure 6-38* The 5 GHz as well as the 25 GHz components (caused by mixing between adjacent optical carriers) are clearly visible

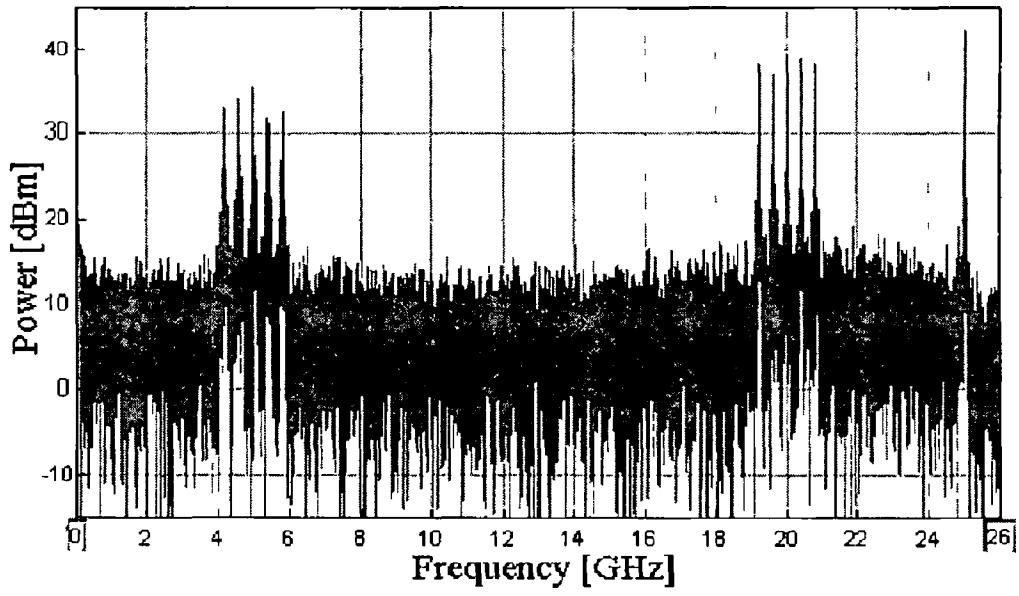

Figure 6-38 Detected RF spectrum of the central WDM channel (25 GHz channel spacing)

In order to find the minimum channel spacing that can be used without causing signal degradation, the BER was measured as a function of WDM channel spacing These measurements were performed for three different cases Initial measurements were carried out for the first SCM channel since this channel would be the first to suffer from crosstalk when the wavelengths are interleaved Secondly BER for the last SCM channel was measured with the wavelength channel spacing varied between the range of 42 to 55 GHz Finally the BER for the central SCM channel with a spacing variation of 22 – 55 GHz was also measured The results are presented in *Figure 6-39*

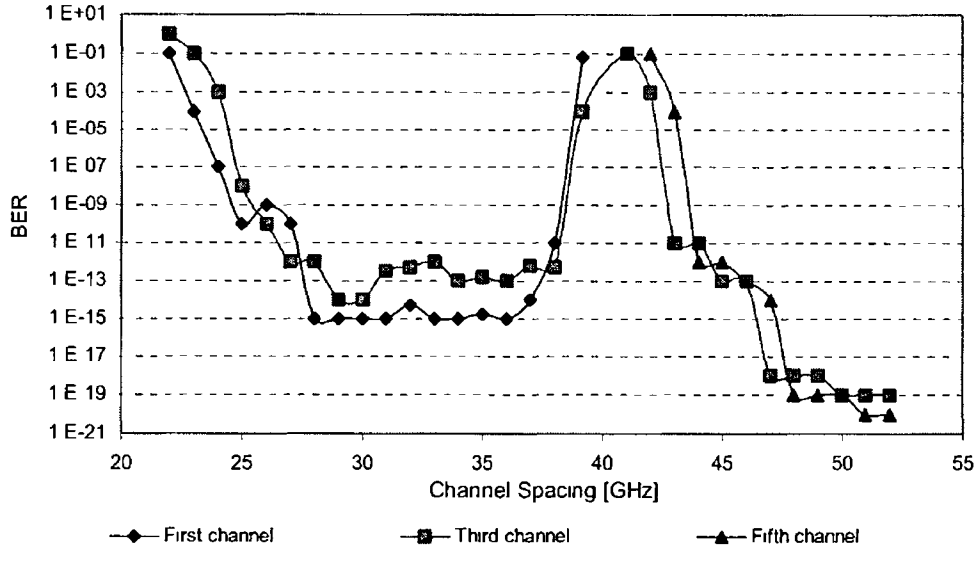

Figure 6-39 BER vs WDM channel spacing for first channel (diamonds) central channel (squares) and fifth channel (triangles)

From the figure above it can be seen that if wavelength interleaving is employed the channel spacing can be reduced to a range within 25 and 38 GHz Two factors set the lower limit for the channel spacing first is the sharpness of the filter response If the roll-off of the filter is not steep enough, then crosstalk could occur between the SCM signal and optical carrier The phase noise of the laser is the second factor that limits the channel spacing The transfer function of the optical BPF used in the simulation is shown in *Figure 6-40*

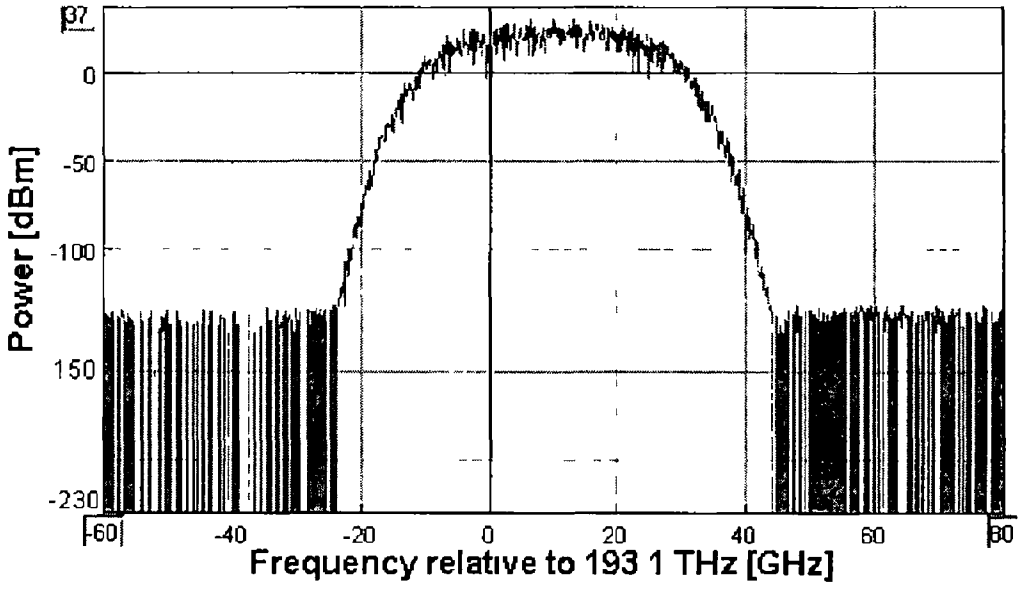

Figure 6-40 *Optical filter response*

The filter used had 3 dB bandwidth of 20 GHz while the 20 dB cut-off was about 37 GHz Such a filter should allow closer placement of the WDM channels The factor, as regards this simulation, which ultimately limited the minimum channels spacing was the phase noise of the laser As the channel spacing decreases, the SCM signal moves closer to the optical carrier of the adjacent channel From *Figure 6-37* it can be seen that by reducing channel spacing by 2 GHz would increase noise in the signal band by 5 dB Reducing the spacmg by 3 GHz would increase the noise by 10 dB This noise degrades the quality of the signal, which in turn makes the channel spacing of 25 GHz unfeasible

Figure 6-39 also illustrates the BER vs the channel spacing without wavelength interleaving being employed (channel spacing greater than twice the RF frequency) Here the BER was measured for the highest frequency (fifth SCM channel) of the SCM carrier In this case the minimum channel spacing is determined by interference between SCM signals from adjacent WDM channels In order to achieve a BER

lower than 10^{-9} a channel spacing of 44 GHz is required It can be seen that channel spacings ranging between 38 to 44 GHz cannot be used At these values the side bands of neighbouring optical channels overlap resulting in an unacceptable BER The optical and electrical spectrum of the demultiplexed signal at a channel spacing of 44 GHz is shown in *Figure 6-41* and *Figure 6-42* respectively

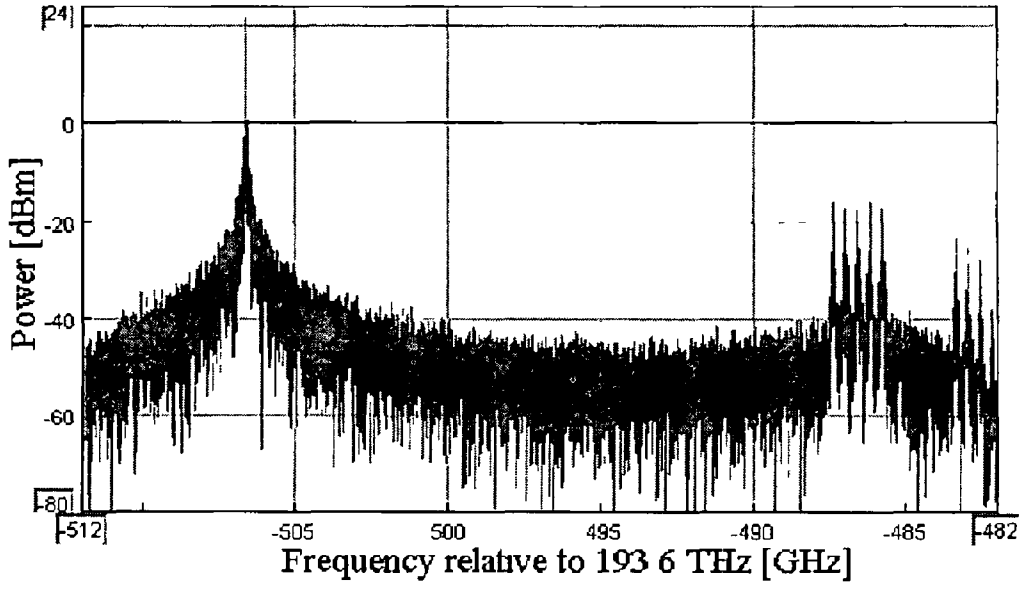

Figure 6-41 Optical spectrum of the demultiplexed central WDM channel (44 GHz channel spacing)

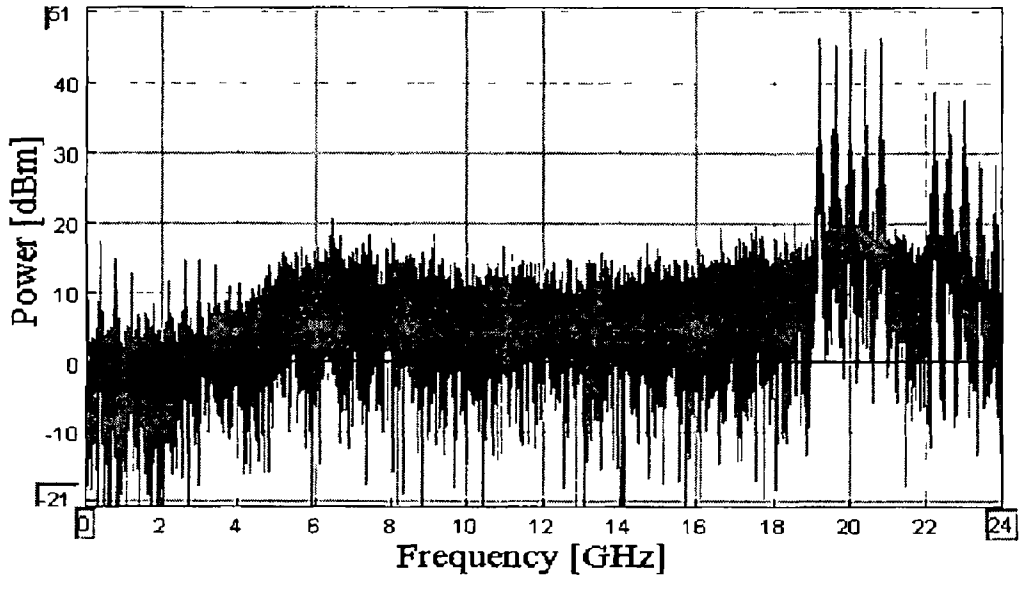

Figure 6-42 Detected RF spectrum of the central WDM channel (44 GHz channel spacing)

The optical spectrum in *Figure 6-41* contains not only the upper side band of the desired signal but also a part of the lower side band that belongs to the adjacent WDM signal These signals beat at the receiver with the optical carrier to generate new frequency components at 24 GHz as seen in *Figure 6-42* After the

downconversion of the desired signal, an electrical rise time filter could be used to remove these unwanted components

The remainder of this chapter concentrates on the influence of fiber nonlinearity on a WDM/SCM system The simulations were performed with a modulating frequency of 20 GHz and the channel spacing set to 50 GHz (no wavelength interleaving)

The fiber length in the simulation model was set to 20 km in order to verify how an increase in the optical power launched into a fiber influences the quality of the signal As in section 6 2 1 the optical power launched into the fiber was varied using an optical attenuator placed before the fiber The power falling on the detector was maintained constant with the help of another attenuator situated before the receiver The BER of the central electrical channel that belongs to the central WDM channel was plotted as the fiber input power was varied and is displayed in *Figure 6-43*

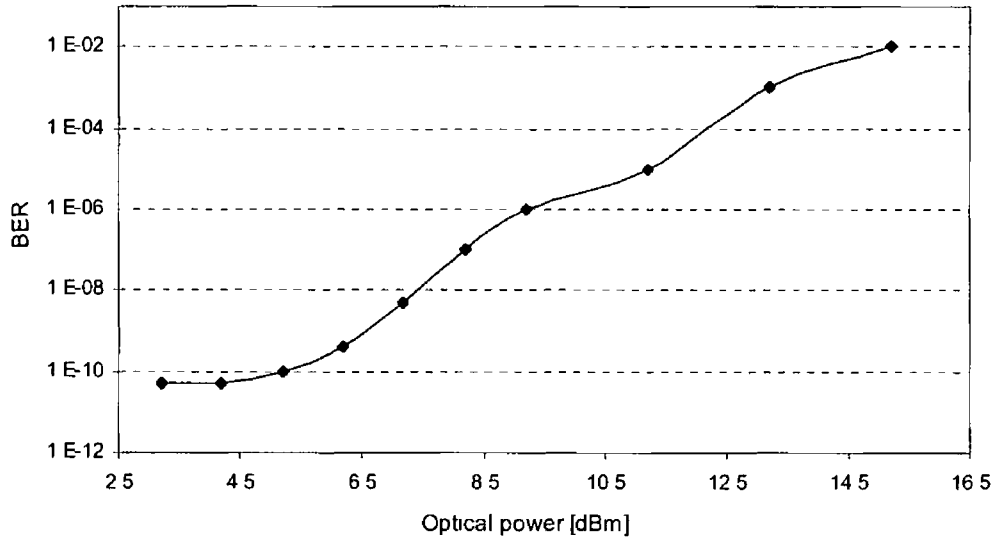

Figure 6-43 *BER vs fiber input power for central WDM channels for 50 GHz channel spacing*

From *Figure 6-43* it can be seen that when optical power launched into the fiber is relatively low (below 5 dBm) the quality of the signal remains unchanged Nevertheless, as the power increases above 6 dBm, the BER gets degraded In comparison to *Figure 6-32* it can be noticed that the power at which the degradation of the signal becomes visible is much lower for the WDM/SCM than for the SCM system This result tends to confirm the previous statement that the influence of fiber induced distortion increases with the number of channels propagating over the fiber Finally the eye diagrams of the downconverted signal for fiber input power of 7 and 15 dBm are presented in *Figure 6-44* and *Figure 6-45* respectively

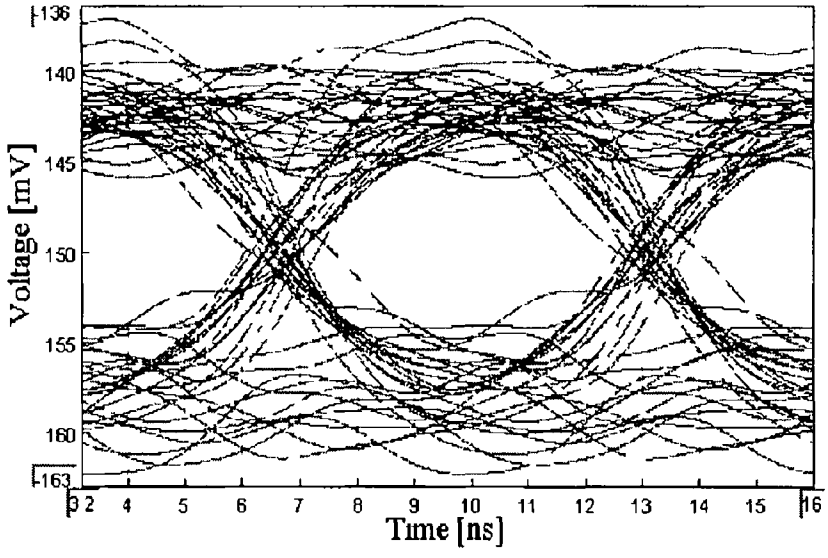

Figure 6-44 Eye diagram of the central WDM central SCM channel after propagation over 20 km of fiber (fiber input power 7 dBm)

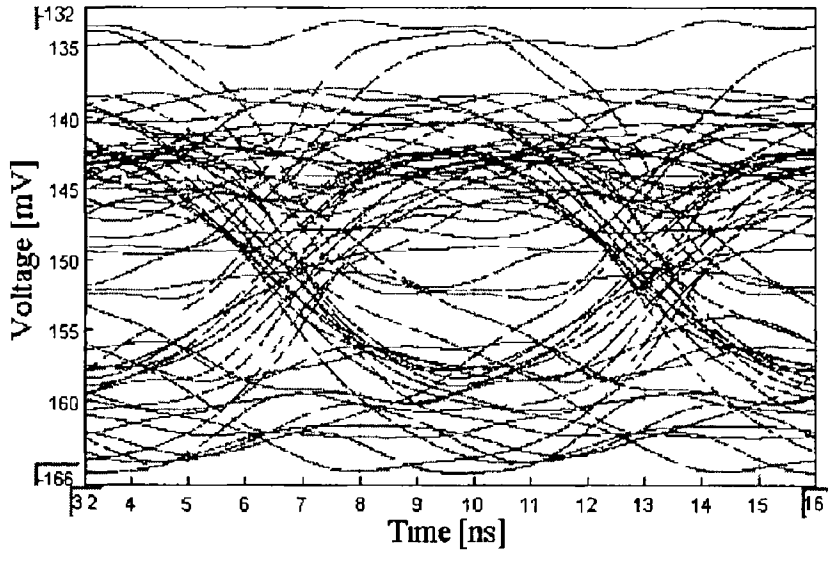

Figure 6-45 Eye diagram of the central WDM central SCM channel after propagation over 20 km of fiber (fiber input power 15 dBm)

The results presented above illustrate the system degradation due to fiber nonlinearity This issue has an equally important impact as dispersion caused fading of RF signals in the transmission of signals using a hybrid radio/fiber system employing the WDM/SCM techniques The results obtained prove that fiber induced distortion becomes an important problem even when only one optical channel carrying SCM signals is transmitted over the fiber In order to minimize the degradation of a signal due to fiber nonlinearity, the WDM/SCM system has to be carefully designed by taking various influencing parameters into account This

involves choosing optimum power levels, optical modulation indices, channel spacing and modulating frequency since all these factors could have a huge impact on system performance

References

[1] A Lowery *et al* " Multiple Signal Representation Simulation of Photonic Devices, Systems and Networks", *IEEE J Sel Topics Quan Electron*, vol 6, pp 282-296, 2000

[2] A J Lowery *et al* "Computer-Aided Photonics Design", *IEEE Spectrum*, vol 34, pp 26-31, 1997

[3] W R Smith *et al* "Mathematical Modelling of Electrical –Optical Effects in Semiconductor Laser Operation", *SIAM J Appl Math*, Vol 61, No 6, pp 2122–2147, 2001

[4] J Huang "Gain and Saturation in Semiconductor Lasers", *Opt Quantum Electron*, Vol 25, pp 369–390, 1993

[5] A R Chraplyvy, "Limitations on Lightwave Communications Imposed by Optical Fibre Non-linearities," *IEEE J of Lightwave Technol*, vol 8, pp 1548-1557, 1990

[6] A R Chraplyvy *et al* "What is the Actual Capacity of Single Mode Fibres in Amplified Lightwave Systems," *IEEE Photon Technol Lett*, vol 5, pp 666–668, 1993

[7] B Wilson *et al* "Analogue Optical Fiber Communications", IEE, London 1995

[8] F Yang *et al* "Nonlinear Crosstalk and Two Countermeasures in SCM-WDM Optical Communication Systems", *J Lightwave Technol*, vol 18, pp 512-519, 2000

[9] M R Phillips *et al* "Optical Fiber Nonlinearities in 1550 nm Analog Transmission Systems", *ECOC'99*

[10] K Nosu, "Optical FDM Network Technologies (1st Ed)," Artech house, 1997

[11] J Zweck and C R Menyuk, "Analysis of Four Wave Mixing between Pulses in High Data Rate Quasi-Linear Sub-Channel Multiplexed Systems," *Opt Lett*, vol 27, pp 1235-1237, 2002

[12] H J Thiele *et al*, "Transmission Limitation in Optical WDM Networks due to Cross Phase Modulation" *IEE Colloquium-Multiwavelength Optical Networks Devices, Systems and Network Implementations,* pp 10/1 – 10/4, 1998

[13] A Tomita, "Cross Talk Caused by Stimulated Raman Scattering in Single Mode Wavelength Division Multiplexed Systems," *Opt Lett*, vol 8, pp 412-414, 1983

[14] J Hecht "Understanding Fiber Optics", Prentice-Hall International (UK) Ltd, 2002

[15] G P Agrawal "Nonlinear Fiber Optics", 2nd Edition, Academic Press, 1989

[16] G Keiser "Optical Fiber Communications", McGraw-Hill Higher Education, London 2000

[17] Z Wang *et al* "Effects of Cross-Talk Modulation in Wavelength-Multiplexed SCM Video Transmission Systems", *Electron Lett*, vol 31, pp 1591-1592, 1995

[18] Z Wang *et al* "Performance Limitations Imposed by Stimulated Raman Scattering in Optical WDM SCM Video Distribution Systems", *IEEE Photon Technology Lett*, vol 7, pp 1492-1494, 1995

[19] G K Gopalakrishnan *et al* "Experimental Study of Fiber Induced Distortion in Externally Modulated 1550 nm Analogue CATV Links", *Electron Lett*, vol 32, pp 1309-1310, 1996

Conclusions

As the demand for broadband mobile services such as video-on-demand and mobile computing increases, so does the need to develop high capacity mobile communication networks which are capable of delivering broadband signals to remote areas "over the air" Microwave and millimeter wave fiber/radio systems are a very attractive option to realize such broadband networks In these hybrid radio/fiber systems, the microwave or millimeter wave data signals are modulated onto an optical carrier at a central location, and then distributed to remote Remote Antenna Units using optical fiber The Remote Antenna Units then transmit the microwave/millimeter-wave signals over small areas using microwave antennas Such an architecture should prove to be highly cost efficient, since it allows sharing the transmission and processing equipment (remotely located in the central control station) between many Remote Antenna Units

The realisation of future radio/fiber systems presents a challenge to the system designers almost at every stage Problems associated with these systems include the generation of high frequency optical signals, transmission of these signals over the fiber with minimum distortion and finally delivering the high bit data rate signals over the air to both stationary and mobile users are very important issues This work concentrated on the two first challenges

Initial investigations were carried out on the generation of optical millimeter wave signals There have been many methods proposed to achieve the above-mentioned goal and most of them have been discussed in detail in Chapter 3 This involved looking at their main advantages and disadvantages Prominence was then given to a simple and reliable technique (amongst the listed methods), which involves the direct modulation of a laser diode to generate millimeter-wave optical signals However, one of the shortcomings in using this method is associated with the generation of high frequencies This difficulty is brought about by the limited (insufficient) modulation bandwidth of currently available commercial laser diodes One effective technique for overcoming the above-mentioned limitation was then examined, namely external light injection into the directly modulated laser This fairly novel concept was then verified by carrying out simulations and experiments The results obtained exhibited that the

inherent modulation bandwidth of the laser could be enhanced by a factor of around three, thereby allowing high frequency signals to be generated in this manner

The usefulness of the direct modulation of an externally injected laser to be employed in a radio/fiber system was verified by building a signal channels system based upon an externally injected laser In the experiment, a single mode DFB laser with inherent modulation bandwidth of around 8 GHz was directly modulated with a 155 Mb/s data signal upconverted to 18 GHz The experimental results showed a 14 dB improvement in the performance of the system using the external injection, when compared with the free running case

The subsequent investigations led to scrutinizing the performance of an externally injected laser when it was modulated with multiple carriers This is an important issue in future hybrid radio/fiber systems, since they are expected to use Sub-Carrier Multiplexing (SCM) to deliver data signals to many users utilizing single laser transmitter The use of SCM technology not only assists in cutting down cost but also renders many of its other advantages to the overall radio/fiber system Experiments and simulations employing a two-channel system based on an externally injected laser were performed to quantify the BER as a function of the received optical power This yielded a 17 dB improvement for one and 20 dB improvement for the other channel The disparity in the performance between the two channels arose from the fact that the quality of the signal generated differed (different signal generators used) The achievement of such a result tended to prove that external light injection could be used effectively to support multichannel transmission At this juncture an in-depth analysis was carried out on millimeter-wave transmitters to determine the influence of laser nonlinearity on multiple channel system performance Initial investigation involved five-channel system based on an externally injected laser Results obtained here showed that the power penalty incurred due to Inter-Modulation Products (IMD_3) was 4 5 dB (worst-case scenario) Further measurements were carried out on a free running laser at the flat part and the peak of its frequency response Amongst the above-mentioned cases the system based on externally injected laser suffered the most from IMD_3

Another multiplexing technique, which is likely to be employed in future radio/fiber systems, is Wavelength Division Multiplexing (WDM) In a system that utilises WDM, a single fiber could be used to feed many RAU at the same time In this scenario each RAU would be assigned one wavelength channel to carry the data

traffic for users communicating with this RAU by means of SCM To examine such a multi-wavelength - multi-channel network, a WDM/SCM system was built One of the issues, which was looked at experimentally was the verification of the influence of adjacent channel interference (WDM channels) Another aspect examined, within the same context of this work, was the possibility of employing the wavelength interleaving technique The SCM channels in hybrid radio/fiber systems would occupy a relatively small fraction of spectrum in comparison to the RF carrier frequency Spacing the wavelength channels in the same way as is done in other WDM systems (channels spacing > twice the modulating frequency) would not be spectrally efficient (large slice of unused spectrum between optical carrier and SCM channels) In order to improve the spectral efficiency the channel spacing between WDM channels could be reduced to values lower than the radio frequency Such an arrangement is known as wavelength interleaving The experiments performed proved that this technique is a viable way to reduce the required spectrum for system transmission without compromising the system performance By measuring BER for different channel spacing it has been established that the optimal channel spacing for an RF frequency of 18 GHz is 0 2 nm (25 GHz) (for the given filter)

The effect of propagation over fiber on the radio signals has also been examined This mainly involved the investigation of dispersion caused fading of Double Side Band (DSB) radio signals propagating along a fiber Direct modulation of a laser with a high frequency signal results in two side bands being generated These side bands experience different phase shifts (due to dispersion being dependent of wavelength) while propagating along the fiber When the signal is detected by the photodiode each side band beats with the optical carrier to produce two electrical RF signals These two components are then combined together to produce the received output signal (electrical) If the side bands were out of phase the RF components generated by them would interfere destructively in the photodiode causing the output signal to fade This phenomenon makes it unfeasible to transmit high frequency DSB signals over large distances of fiber This problem could be overcome by using Single Side Band (SSB) modulation However, SSB signals cannot be generated using the direct modulation Hence SSB conversion would have to be performed to avoid signal degradation if one is to employ the direct modulation technique The experiments performed have proved that by simply employing an optical Band Pass Filter (BPF), a DSB signal generated by a directly modulated laser could be converted into an SSB format

The investigation of the propagation of the radio signals over fiber also involved the verification of nonlinear effects in the fiber on a multichannel system This was done using the Virtual Photonics Inc Transmission Maker simulation package First the influence of fiber nonlinearity on the single wavelength SCM system was verified The results show that even though there is only one wavelength channel propagating over fiber, the fiber nonlinearity cause significant crosstalk between the SCM channels resulting in degradation of system performance This degradation becomes even more serious when additional wavelength channels are appended WDM/SCM system design requires a careful choice of several system parameters due to fiber-induced distortion Some parameters that would have strong bearing on system design are the optical power level, channels spacing, number of channels etc

The demultiplexing of the WDM/SCM signal and its influence on system performance was also examined The manner in which demultiplexing could be performed would depend on the network architecture For a ring network, where the wavelengths designated for particular RAU are dropped as the signal travels along the loop, utilisation of an optical Fiber Bragg Grating (FBG) in conjunction with an optical circulator is an attractive option The possibility of using a single filter to perform both the demultiplexing and conversion of a signal into SSB format were examined This proves to be a cost effective and simple solution since it avoids the use of optical BPF at the transmitter site This method would have to be used in conjunction with the wavelength interleaving technique to ensure optimal spectral efficiency In the experiments performed a reflective FBG was used to demultiplex the required WDM channel and to filer out only one side band, converting the demultiplexed signal into an SSB format The above-mentioned not only gave a very small power penalty (0 4 dB) but also proved to be a feasible method of overcoming the dispersion caused fading of the signal

Appendix A

Rate Equations – Steady State Solution

The rate equations for a single mode laser diode with injection are as follows By simply setting the external injection term S_{inj} to zero the equations revert back to the free running form

$$\frac{dN(t)}{dt} = \frac{I(t)}{qV} - \frac{N(t)}{\tau_n} - g_0(N(t) - N_{om})S(t) \qquad \text{A 1}$$

$$\frac{dS(t)}{dt} = \Gamma g_0(N(t) - N_{om})S(t) - \frac{S(t)}{\tau_p} + \Gamma\beta\frac{N(t)}{\tau_n} + 2K_c\sqrt{S_{inj}S(t)}\cos(\varphi(t)) \qquad \text{A 2}$$

$$\frac{d\phi(t)}{dt} = \frac{\alpha}{2}\left(\Gamma g_0(N(t) - N_{om}) - \frac{1}{\tau_p}\right) - \Delta\omega - K_c\sqrt{\frac{S_{inj}}{S(t)}}Sin(\phi(t)) \qquad \text{A 3}$$

For simplicity, in the further calculations the spontaneous emission factor is neglected

The steady state solutions can be obtained by setting the left-hand side of the equations (A 1) – (A 3) to zero

$$0 = \frac{I_0}{qV} - \frac{N_0}{\tau_n} - g_0(N_0 - N_{om})S_0 \qquad \text{A 4}$$

$$0 = \Gamma g_0(N_0 - N_{om})S_0 - \frac{S_0}{\tau_p} + 2K_c\sqrt{S_{inj}S_0}\cos(\varphi_0) \qquad \text{A 5}$$

$$0 = \frac{\alpha}{2}\left(\Gamma g_0(N_0 - N_{om}) - \frac{1}{\tau_p}\right) - \Delta\omega - K_c\sqrt{\frac{S_{inj}}{S_0}}Sin(\phi_0) \qquad \text{A 6}$$

Manipulating (A 6) gives

$$K_c\sqrt{\frac{S_{inj}}{S_0}}\sin(\varphi_0) = \frac{\alpha}{2}\left[\Gamma g_0(N_0 - N_{om}) - \frac{1}{\tau_p}\right] - \Delta\omega \qquad \text{A 7}$$

Squaring both sides

$$K_c^2 \frac{S_{inj}}{S_0} \sin^2(\varphi_0) = \left[\left(\frac{\alpha\Gamma g_0(N_0 - N_{om})}{2} - \frac{\alpha}{2\tau_p}\right) - \Delta\omega\right]^2 \qquad \text{A 8}$$

Manipulating (A 5)

$$2K_c\sqrt{S_{inj}S_0}\cos(\varphi_0) = \Gamma g_0(N_0 - N_{om})S_0 - \frac{S_0}{\tau_p} \qquad \text{A 9}$$

Multiply by $\frac{\sqrt{S_0}}{\sqrt{S_0}} = 1$

$$2K_c S_0\sqrt{\frac{S_{inj}}{S_0}}\cos(\varphi_0) = \frac{S_0}{\tau_p} - \Gamma g_0(N_0 - N_{om})S_0 \qquad \text{A 10}$$

Dividing across by S_0

$$2K_c\sqrt{\frac{S_{inj}}{S_0}}\cos(\varphi_0) = \frac{1}{\tau_p} - \Gamma g_0(N_0 - N_{om}) \qquad \text{A 11}$$

Squaring both sides and dividing by 4

$$K_c^2 \frac{S_{inj}}{S_0}\cos^2(\varphi_0) = \frac{1}{4}\left(\frac{1}{\tau_p} - \Gamma g_0(N_0 - N_{om})\right)^2 \qquad \text{A 12}$$

Adding (A 8) and (A 12) gives

$$K_c^2 \frac{S_{inj}}{S_0}\left(\sin^2(\varphi_0) + \cos^2(\varphi_0)\right) = \left[\left(\frac{\alpha\Gamma g_0(N_0 - N_{om})}{2} - \frac{\alpha}{2\tau_p}\right) - \Delta\omega\right]^2 + \frac{1}{4}\left(\frac{1}{\tau_p} - \Gamma g_0(N_0 - N_{om})\right)^2 \qquad \text{A 13}$$

Using the relationship $\cos^2\theta + \sin^2\theta = 1$ gives

$$K_c^2 \frac{S_{inj}}{S_0} = \left[\left(\frac{\alpha\Gamma g_0(N_0 - N_{om})}{2} - \frac{\alpha}{2\tau_p}\right) - \Delta\omega\right]^2 + \frac{1}{4}\left(\frac{1}{\tau_p} - \Gamma g_0(N_0 - N_{om})\right)^2 \qquad \text{A 14}$$

Manipulation of (A 4) yields an expression for S_0 as follows

$$\frac{\frac{I_0}{qV}-\frac{N_0}{\tau_n}}{g_0(N_0-N_{om})}=S_0 \quad \text{A 15}$$

Substituting the expression for S_o from (A 15) into (A 14) yields after much manipulation, a following expression in N_o which can be solved very simply in Matlab

$$aN_0^3+bN_0^2+cN_0+d=0 \quad \text{A 16}$$

where

$$a=\frac{(\Gamma g_0)^2}{4\tau_n}\left(\frac{\alpha^2}{4}-1\right) \quad \text{A 17}$$

$$b=\frac{1}{4\tau_n}\left(2(\Gamma g_0)^2 N_{om}+\frac{2\Gamma g_0}{\tau_p}+\frac{(\Gamma g_0\alpha)^2}{2}N_{om}+\frac{\Gamma g_0\alpha^2}{2\tau_p}+\Delta\omega\Gamma g_0\alpha\right)+ \quad \text{A 18}$$

$$+\frac{I_0}{4qV}\left((\Gamma g_0)^2+\frac{(\Gamma g_0\alpha)^2}{4}\right)$$

$$c=-\frac{I_0}{4qV}\left(2(\Gamma g_0)^2 N_{om}+\frac{2\Gamma g_0}{\tau_p}+\frac{(\Gamma g_0\alpha)^2}{2}N_{om}+\frac{\Gamma g_0\alpha^2}{2\tau_p}+\Delta\omega\Gamma g_0\alpha\right)-\frac{(N_{om}\Gamma g_0)^2}{4\tau_n}+$$

$$-\frac{2N_{om}\Gamma g}{4\tau_n\tau_p}-\frac{(\Gamma g_0\alpha)^2}{16\tau_n}N_{om}^2-\frac{N_{om}\Gamma g\alpha^2}{4\tau_n\tau_p}-\frac{\Delta\omega\Gamma g_0\alpha}{4\tau_n}N_{om}-\frac{1}{\tau_p^2}-\frac{\alpha^2}{4\tau_p^2}-\frac{\Delta\omega\alpha}{\tau_p}+ \quad \text{A 19}$$

$$-\Delta\omega^2-K_c^2 S_{inj} g_0$$

$$d=\frac{I_0}{4\tau_p qV}\Gamma g_0 N_{om}\left(\Gamma g_0 N_{om}+\frac{2}{\tau_p}+\frac{\Gamma g_0\alpha^2}{4}N_{om}+\frac{\alpha^2}{\tau_p}+\Delta\omega\alpha\right)+ \quad \text{A 20}$$

$$+\frac{I_0}{4\tau_p qV}\left(\frac{1}{\tau_p}+\frac{\alpha^2}{4\tau_p}+\Delta\omega\alpha+\Delta\omega^2\tau_p\right)+K_c^2 S_{inj} g_0 N_{om}$$

Dynamic solutions

The dynamic solutions of the laser rate equations (A 1) – (A 3) can be found by using small signal analysis In such an approach the assumption is made that the variable changes slightly from its DC value Thus the variables in the equations (A 1) – (A 3) consists of an DC and AC components

$$I(t) = I_0 + \Delta I e^{j\varpi_m t} \quad \text{A 21}$$

$$S(t) = S_0 + \Delta S e^{j\varpi_m t} \quad \text{A 22}$$

$$N(t) = N_0 + \Delta N e^{j\varpi_m t} \quad \text{A 23}$$

$$\phi(t) = \phi_0 + \Delta\phi e^{j\varpi_m t} \quad \text{A 24}$$

Where I_0, S_0, N_0 and φ_0 denote the steady state values of the current, photon and carrier density and phase respectively

Substituting the above expressions to the laser rate equations yields the following

$$\frac{d(N_0 + \Delta N e^{j\varpi_m t})}{dt} = \frac{I_0 + \Delta I e^{j\varpi_m t}}{qV} - \frac{N_0 + \Delta N e^{j\varpi_m t}}{\tau_n} - g_0\left(N_0 + \Delta N e^{j\varpi_m t} - N_{om}\right)(S_0 + \Delta S e^{j\varpi_m t}) \quad \text{A 25}$$

$$\frac{d(N_0)}{dt} + \frac{d\Delta N e^{j\varpi t}}{dt} = \frac{I_0}{qV} + \Delta I e^{j\varpi t} - \frac{N_0}{\tau_n} - \Delta N e^{j\varpi t} - g_0(N_0 - N_{om})S_0 - g_0(N_0 - N_{om})\Delta S e^{j\varpi t} - g_0 \Delta N e^{j\varpi t} - g_0 \Delta N e^{j\varpi t}\Delta S e^{j\varpi t} \quad \text{A 26}$$

The term

$$\frac{dN_0}{dt} = \frac{I_0}{qV} - \frac{N_0}{\tau_n} - g_0\left(N_0 - N_{om}\right)S_0 \quad \text{A 27}$$

is a steady solution for the carrier density N_0 is a constant thus the above equation equals zero and can be removed from (A 26) By doing so and dividing both sides of (A 26) by $e^{j\varpi_m t}$ one obtains

$$\frac{1}{e^{j\varpi_m t}}\frac{d(\Delta N e^{j\varpi_m t})}{dt} = \frac{\Delta I}{qV} - \frac{\Delta N}{\tau_n} - g_0\left(N_0 - N_{om}\right)\Delta S - g_0 \Delta N S_0 \quad \text{A 28}$$

Since

$$\frac{d\Delta N e^{j\varpi_m t}}{dt} = j\varpi_n \Delta N e^{j\varpi_n t} \quad \text{A 29}$$

(A 28) can be rewritten as

$$j\omega\Delta N = \frac{\Delta I}{qV} - \frac{\Delta N}{\tau_n} - g_0\left(N_0 - N_{om}\right)\Delta S - g_0 \Delta N S_0 \quad \text{A 30}$$

The term $g_0\left(N_0 - N_{om}\right)$ can be substituted using the steady state solution to rate equations

$$g_0\left(N_0 - N_{om}\right) = \frac{1}{\Gamma\tau_p} - 2K_c\frac{\sqrt{S_{inj}S_0}}{\Gamma S_0}\cos\phi_0 \quad \text{A 31}$$

Inserting (A 31) to (A 30) yields

$$j\omega\Delta N = \frac{\Delta I}{qV} - \frac{\Delta N}{\tau_n} - \frac{\Delta S}{\Gamma\tau_p} + 2K_c\frac{\sqrt{S_{inj}S_0}}{\Gamma S_0}\cos\phi_0\Delta S - g_0\Delta N S_0 \qquad \text{A 32}$$

Similarly the photon density can be written as

$$\frac{d(S_0+\Delta S e^{j\varpi_m t})}{dt} = \Gamma g_0\left(N_0+\Delta N e^{j\varpi_m t} - N_{om}\right)(S_0+\Delta S e^{j\varpi_m t}) \qquad \text{A 33}$$

$$+ 2K_c\sqrt{S_{inj}S_0+\Delta S e^{j\varpi_m t}}\cos(\varphi_0+\Delta\varphi e^{j\varpi_m t})$$

Using the trigonometric identities one can write

$$\cos\left(\varphi_0+\Delta\varphi e^{j\varpi_m t}\right) = \cos\varphi_0\cos\left(\Delta\varphi e^{j\varpi_m t}\right) - \sin\varphi_0\sin\left(\Delta\varphi e^{j\varpi_m t}\right) \qquad \text{A 34}$$

Because $\left(\Delta\varphi e^{j\varpi_m t}\right)$ is a small one can write

$$\cos\left(\Delta\varphi e^{j\varpi_m t}\right)\approx 1$$

$$\sin\left(\Delta\varphi e^{j\varpi_m t}\right)\approx \Delta\varphi e^{j\varpi_m t}$$

Thus (A 34) can be rewritten as

$$\cos\varphi_0\cos\left(\Delta\varphi e^{j\varpi_m t}\right) - \sin\varphi_0\sin\left(\Delta\varphi e^{j\varpi_m t}\right) \approx \cos\varphi_0 - \Delta\varphi e^{j\varpi_m t}\sin\varphi_0 \qquad \text{A 35}$$

Thus the last term in (A 33) can be written as

$$\Rightarrow 2K_c\left(\cos\varphi_0 - \Delta\varphi e^{j\varpi_m t}\sin\varphi_0\right)\sqrt{S_{inj}S_0+\Delta S e^{j\varpi_m t}} \qquad \text{A 36}$$

Furthermore

$$\sqrt{S_{inj}S_0+S_{inj}\Delta S e^{j\varpi_m t}} = \sqrt{S_{inj}S_0}\sqrt{1+\frac{S_{inj}\Delta S e^{j\varpi_m t}}{S_{inj}S_0}} \approx \sqrt{S_{inj}S_0}\sqrt{1+\frac{\Delta S e^{j\varpi_m t}}{S_0}} \qquad \text{A 37}$$

Because $\Delta S e^{j\varpi_m t}$ is small one can add a term $\left(\frac{\Delta S e^{j\varpi_m t}}{2S_0}\right)^2$ to the last expression in equation above ($\left(\frac{\Delta S e^{j\varpi_m t}}{2S_0}\right)\approx 0$) Thus one can write

$$\sqrt{1+2\frac{\Delta S e^{j\varpi_m t}}{2S_0}+\left(\frac{\Delta S e^{j\varpi_m t}}{2S_0}\right)^2} = \sqrt{\left(1+\frac{\Delta S e^{j\varpi_m t}}{2S_0}\right)^2} = 1+\frac{\Delta S e^{j\varpi_m t}}{2S_0} \qquad \text{A 38}$$

Thus (A 36) can be written as follows

$$\Rightarrow 2K_c\left(\cos\varphi_0 - \Delta\varphi e^{j\varpi_m t}\sin\varphi_0\right)\left(\sqrt{S_{inj}S_0} + \sqrt{S_{inj}S_0}\frac{\Delta S e^{j\varpi_m t}}{2S_0}\right) \qquad \text{A 39}$$

$$\Rightarrow 2K_c\sqrt{S_{inj}S_0}\cos\varphi_0 + 2K_c\sqrt{S_{inj}S_0}\frac{\Delta S e^{j\varpi_m t}}{2S_0}\cos\Delta\varphi e^{j\varpi_m t} \qquad \text{A 40}$$

$$-2K_c\sqrt{S_{inj}S_0}\Delta\varphi e^{j\varpi_m t}\sqrt{S_{inj}S_0}\sin\varphi_0 - 2K_c\sqrt{S_{inj}S_0}\frac{\Delta S e^{j\varpi_m t}}{2S_0}\Delta\varphi e^{j\varpi_m t}\sin\varphi_0$$

$$\frac{d(S_0)}{dt} + \frac{d(\Delta S)}{dt} = \Gamma g_0\left(N_0 - N_{om}\right)S_0 + \Gamma g_0\left(N_0 - N_{om}\right)\Delta S$$
$$+\Gamma g_0\Delta N(S_0) + \Gamma g_0\Delta N\Delta S - \frac{S_0}{\tau_p} - \frac{\Delta S}{\tau_p}$$
$$+ 2K_c\sqrt{S_{inj}S_0}\cos\phi_0 + \frac{\sqrt{S_{inj}S_0}}{2S_0}\cos\phi_0\Delta S$$
$$-2K_c\sin\phi_0\Delta\phi\sqrt{S_{inj}S_0} - 2K_c\sin\phi_0\Delta\phi\frac{\sqrt{S_{inj}S_0}}{2S_0}\Delta S \qquad \text{A 41}$$

The steady state equation for photon density is as follows

$$\frac{dS_0}{dt} = \Gamma g_0\left(N_0 - N_{om}\right)S_0 - \frac{S_0}{\tau_p} + 2K_c\sqrt{S_{inj}S_0}\cos(\varphi_0) \qquad \text{A 42}$$

As is case of (A 27) this term is equal zero, hence the (A 41) reduces to

$$\frac{d\Delta S e^{j\varpi_m t}}{dt} = \Gamma g_0(N_0 - N_{om})\Delta S e^{j\varpi_m t} + \Gamma g_0 S_0\Delta N e^{j\varpi_m t} - \frac{\Delta S e^{j\varpi_m t}}{\tau_p}$$
$$+ 2K_c\frac{\sqrt{S_{inj}S_0}}{2S_0}\Delta S e^{j\varpi_m t}\cos\varphi_0 - 2K_c\sqrt{S_{inj}S_0}\Delta\varphi e^{j\varpi_m t}\sin\varphi_0 \qquad \text{A 43}$$

Inserting (A 31) to (A 43), performing the derivation and dividing both sides by $e^{j\varpi_m t}$ yields

$$j\omega\Delta S = \left(\frac{1}{\Gamma\tau_p} - 2K_c\frac{\sqrt{S_{inj}S_0}}{\Gamma S_0}\cos\phi_0\right)\Gamma\Delta S + \Gamma g_0\Delta N S_0 - \frac{\Delta S}{\tau_p}$$
$$+2K_c\frac{\sqrt{S_{inj}S_0}}{2S_0}\cos\phi_0\Delta S - 2K_c\sin\phi_0\sqrt{S_{inj}S_0}\Delta\phi$$

$$j\omega\Delta S = \frac{\Delta S}{\tau_p} - 2K_c\frac{\sqrt{S_{inj}S_0}}{S_0}\cos\phi_0\Delta S + \Gamma g_0\Delta N S_0 - \frac{\Delta S}{\tau_p}$$
$$+2K_c\frac{\sqrt{S_{inj}S_0}}{2S_0}\cos\phi_0\Delta S - 2K_c\sin\phi_0\sqrt{S_{inj}S_0}\Delta\phi \qquad \text{A 44}$$

Grouping the terms yields

$$j\omega\Delta S = \Gamma g_0\Delta N S_0 - 2K_c\frac{\sqrt{S_{inj}S_0}}{2S_0}\cos\phi_0\Delta S - 2K_c\sin\phi_0\sqrt{S_{inj}S_0}\Delta\phi \qquad \text{A 45}$$

Finally the phase equation for the small signal modulation can be written as follows

$$\frac{d\left(\phi_0 + \Delta\varphi e^{j\varpi_m t}\right)}{dt} = \frac{\alpha}{2}\left(\Gamma g_0(N_0 + \Delta N e^{j\varpi_n t} - N_{om}) - \frac{1}{\tau_p}\right) - \Delta\omega$$
$$- K_c\sqrt{\frac{S_{inj}}{S_0 + \Delta S e^{j\varpi_m t}}}Sin\left(\phi_0 + \Delta\varphi e^{j\varpi_m t}\right) \qquad \text{A 46}$$

Similarly to (A 34) and (A 38) the last term in the equation above can be written as

$$\sin\left(\phi_0 + \Delta\phi\right) = \left(\sin\phi_0\cos\Delta\phi + \cos\phi_0\sin\Delta\phi\right) \approx \left(\sin\phi_0\ 1 + \cos\phi_0\Delta\phi\right) \qquad \text{A 47}$$

$$\sqrt{\frac{S_{inj}}{S_0 + \Delta S e^{j\varpi_m t}}} = \frac{\sqrt{S_{inj}}}{\sqrt{S_0 + \Delta S e^{j\varpi_m t}}} = S_{inj}^{\frac{1}{2}}\left(S_0 + \Delta S e^{j\varpi_m t}\right)^{-\frac{1}{2}} \qquad \text{A 48}$$

$$= S_{inj}^{\frac{1}{2}}\left(S_0^{-\frac{1}{2}} - S_0^{-\frac{3}{2}}\Delta S e^{j\varpi_m t}\right) = \sqrt{S_{inj}}\left(\frac{1}{\sqrt{S_0}} - \frac{1}{2\sqrt{S_0^3}}\Delta S e^{j\varpi_m t}\right)$$

The final term in (A 46) can be written as

$$-K_c\sin\phi_0 - K_c\Delta\varphi e^{j\varpi_m t}\cos\phi_0\left(\frac{\sqrt{S_{inj}}}{\sqrt{S_0}} - \frac{\sqrt{S_{inj}}}{2\sqrt{S_0^3}}\Delta S e^{j\varpi_m t}\right) = -\frac{\sqrt{S_{inj}}}{\sqrt{S_0}}K_c\sin\phi_0$$
$$+\frac{\sqrt{S_{inj}}}{2\sqrt{S_0^3}}K_c\sin\phi_0 - \frac{\sqrt{S_{inj}}}{\sqrt{S_0}}K_c\Delta\varphi e^{j\varpi_m t}\cos\phi_0 + \frac{\sqrt{S_{inj}}}{2\sqrt{S_0^3}}K_c\Delta\varphi e^{j\varpi_m t}\cos\phi_0 \qquad \text{A 49}$$

Thus (A 46) can be written as follows

$$\frac{d(\phi_0)}{dt}+\frac{d\left(\Delta\varphi e^{j\varpi_m t}\right)}{dt}=\frac{\alpha}{2}\Gamma g_0(N_0-N_{om})+\frac{\alpha}{2}\Gamma g_0\Delta N e^{j\varpi t}-\frac{\alpha}{2\tau_p}-\Delta\omega$$

$$-\frac{\sqrt{S_{inj}}}{\sqrt{S_0}}K_c\sin\phi_0+\frac{\sqrt{S_{inj}}}{2\sqrt{S_0^{\,3}}}K_c\Delta S e^{j\varpi_m t}\sin\phi_0-\frac{\sqrt{S_{inj}}}{\sqrt{S_0}}K_c\Delta\varphi e^{j\varpi_m t}\cos\phi_0 \qquad \text{A 50}$$

$$+\frac{\sqrt{S_{inj}}}{2\sqrt{S_0^{\,3}}}K_c\Delta\varphi e^{j\varpi_m t}\Delta S e^{j\varpi_m t}\cos\phi_0$$

The steady state version of the equation above is

$$\frac{d(\phi_0)}{dt}=\frac{\alpha}{2}\left(\Gamma g_0(N_0-N_{om})-\frac{1}{\tau_p}\right)-\Delta\omega-K_c\sqrt{\frac{S_{inj}}{S_0}}Sin(\phi_0) \qquad \text{A 51}$$

As is case of (A 27) and (A 42) this term is equal zero, hence it can be removed from (A 51) Additionally, term $\frac{\sqrt{S_{inj}}}{2\sqrt{S_0^{\,3}}}K_c\Delta\varphi e^{j\varpi_m t}\Delta S e^{j\varpi_m t}\cos\phi_0$ (very small) can also be neglected Therefore (A 51) reduces to

$$\frac{d\left(\Delta\varphi e^{j\varpi_m t}\right)}{dt}=\frac{\alpha}{2}\Gamma g_0\Delta N e^{j\varpi_m t}+\frac{\sqrt{S_{inj}}}{2\sqrt{S_0^{\,3}}}K_c\Delta S e^{j\varpi_m t}\sin\phi_0-\frac{\sqrt{S_{inj}}}{\sqrt{S_0}}K_c\Delta\varphi e^{j\varpi_m t}\cos\phi_0 \qquad \text{A 52}$$

After dividing by $e^{j\varpi_m t}$ one obtains the final version of the equation (A 52)

$$\frac{d(\Delta\phi)}{dt}=\frac{\alpha}{2}\left(\Gamma g_0(\Delta N)\right)+K_c\frac{\sqrt{S_{inj}}}{\sqrt{4S_0^{\,3}}}\sin\phi_0\Delta S-K_c\frac{\sqrt{S_{inj}}}{\sqrt{S_0}}\cos\phi_0\Delta\phi \qquad \text{A 53}$$

So the linearized laser rate equations are as follows

$$j\omega\Delta N=\frac{\Delta I}{qV}-\frac{\Delta N}{\tau_n}-\frac{\Delta S}{\Gamma\tau_p}+2K_c\frac{\sqrt{S_{inj}S_0}}{\Gamma S_0}\cos\phi_0\Delta S-g_0\Delta N S_0 \qquad \text{A 54}$$

$$j\omega\Delta S=\Gamma g_0\Delta N S_0-2K_c\frac{\sqrt{S_{inj}S_0}}{2S_0}\cos\phi_0\Delta S-2K_c\sin\phi_0\sqrt{S_{inj}S_0}\Delta\phi \qquad \text{A 55}$$

$$j\omega\Delta\phi=\frac{\alpha}{2}\Gamma g_0\Delta N+K_c\frac{\sqrt{S_{inj}}}{\sqrt{4S_0^{\,3}}}\sin\phi_0\Delta S-K_c\frac{\sqrt{S_{inj}}}{\sqrt{S_0}}\cos\phi_0\Delta\phi \qquad \text{A 56}$$

Letting $X=2K_c\sqrt{S_{inj}S_0}\cos\phi_0$ and $Y=K_c\sqrt{\frac{S_{inj}}{S_0}}\sin\phi_0$

$$j\omega\Delta N = \frac{\Delta I}{qV} - \frac{\Delta N}{\tau_n} - \frac{\Delta S}{\Gamma\tau_p} + \frac{X}{\Gamma S_0}\Delta S - g_0\Delta N S_0 \qquad \text{A 57}$$

$$j\omega\Delta S = \Gamma g_0 S_0 \Delta N - \frac{X}{2S_0}\Delta S - 2K_c\sqrt{S_{inj}S_0}\sin\phi_0\Delta\phi$$

$$\Rightarrow j\omega\Delta S = \Gamma g_0 S_0 \Delta N - \frac{X}{2S_0}\Delta S - 2K_c\sqrt{S_{inj}S_0}\frac{\sqrt{S_0}}{\sqrt{S_0}}\sin\phi_0\Delta\phi$$

$$\Rightarrow j\omega\Delta S = \Gamma g_0 S_0 \Delta N - \frac{X}{2S_0}\Delta S - 2K_c S_0\sqrt{\frac{S_{inj}}{S_0}}\sin\phi_0\Delta\phi$$

$$\Rightarrow j\omega\Delta S = \Gamma g_0 S_0 \Delta N - \frac{X}{2S_0}\Delta S - 2S_0 Y\Delta\phi \qquad \text{A 58}$$

$$j\omega\Delta\phi = \frac{\alpha}{2}\Gamma g_0\Delta N + K_c\frac{\sqrt{S_{inj}}}{\sqrt{4S_0^{\,3}}}\sin\phi_0\Delta S - K_c\frac{\sqrt{S_{inj}}}{\sqrt{S_0}}\cos\phi_0\Delta\phi$$

$$\Rightarrow j\omega\Delta\phi = \frac{\alpha}{2}\Gamma g_0\Delta N + K_c\frac{\sqrt{S_{inj}}}{\sqrt{S_0}}\frac{\sqrt{1}}{\sqrt{4S_0^{\,2}}}\sin\phi_0\Delta S - K_c\frac{\sqrt{S_{inj}}}{\sqrt{S_0}}\frac{\sqrt{S_0}}{\sqrt{S_0}}\cos\phi_0\Delta\phi$$

$$\Rightarrow j\omega\Delta\phi = \frac{\alpha}{2}\Gamma g_0\Delta N + \frac{K_c}{2S_0}\frac{\sqrt{S_{inj}}}{\sqrt{S_0}}\sin\phi_0\Delta S - K_c\frac{\sqrt{S_{inj}S_0}}{S_0}\cos\phi_0\Delta\phi$$

$$\Rightarrow j\omega\Delta\phi = \frac{\alpha}{2}\Gamma g_0\Delta N + \frac{1}{2S_0}K_c\frac{\sqrt{S_{inj}}}{\sqrt{S_0}}\sin\phi_0\Delta S - 2K_c\frac{\sqrt{S_{inj}S_0}}{2S_0}\cos\phi_0\Delta\phi$$

$$\Rightarrow j\omega\Delta\phi = \frac{\alpha}{2}\Gamma g_0\Delta N + \frac{Y}{2S_0}\Delta S - \frac{X}{2S_0}\Delta\phi \qquad \text{A 59}$$

Tidying (A 57), (A 58), and (A 59)

$$\left[j\omega + \frac{1}{\tau_n} + g_0 S_0\right]\Delta N + \left[\frac{1}{\Gamma\tau_p} - \frac{X}{\Gamma S_0}\right]\Delta S + [0]\Delta\phi = \frac{\Delta I}{qV} \qquad \text{A 60}$$

$$\left[-\Gamma g_0 S_0\right]\Delta N + \left[j\omega + \frac{X}{2S_0}\right]\Delta S + [2S_0 Y]\Delta\phi = 0 \qquad \text{A 61}$$

$$\left[-\frac{\alpha}{2}\Gamma g_0\right]\Delta N + \left[-\frac{Y}{2S_0}\right]\Delta S + \left[j\omega + \frac{X}{2S_0}\right]\Delta\phi = 0 \qquad \text{A 62}$$

Putting into matrix form yields the following

$$\begin{pmatrix} j\omega + a_{11} & a_{12} & a_{13} \\ a_{21} & j\omega + a_{22} & a_{23} \\ a_{31} & a_{32} & j\omega + a_{33} \end{pmatrix}\begin{pmatrix} \Delta N \\ \Delta S \\ \Delta\phi \end{pmatrix} = \begin{pmatrix} \Delta I/qV \\ 0 \\ 0 \end{pmatrix} \qquad \text{A 63}$$

where

$$a_{11} = \frac{1}{\tau_n} + g_0 S_0 \quad a_{12} = \frac{1}{\Gamma \tau_p} - \frac{X}{\Gamma S_0} \quad a_{13} = 0$$

$$a_{21} = -\Gamma g_0 S_0 \qquad a_{22} = \frac{X}{2S_0} \qquad a_{23} = 2S_0 Y$$

$$a_{31} = -\frac{\alpha}{2}\Gamma g_0 \qquad a_{32} = \frac{-Y}{2S_0} \qquad a_{33} = \frac{X}{2S_0}$$

and

$$X = 2K_c\sqrt{S_{mj} S_0}\,Cos(\phi_0)$$

$$Y = K_c\sqrt{\frac{S_{mj}}{S_0}}\,Sin(\phi_0)$$

The frequency response is $\frac{\Delta S}{\Delta I}$ and to obtain this one must eliminate the other two time varying components from the set of equations (A 61) will be used as the main equation and remove the two terms for it by substitution

So to remove $\Delta\phi$ one takes (A 62)

$$\left[j\omega + \frac{X}{2S_0}\right]\Delta\phi = \left[\frac{Y}{2S_0}\right]\Delta S + \left[\frac{\alpha}{2}\Gamma g_0\right]\Delta N$$

Letting $O = j\omega + \frac{X}{2S_0}$ one obtain

$$\Delta\phi = \frac{\frac{Y\Delta S}{2S_0} + \frac{\alpha}{2}\Gamma g_0 \Delta N}{O} \qquad \text{A 64}$$

Subbing (A 64) into (A 61) then gives

$$\left[-\Gamma g_0 S_0\right]\Delta N + \left[j\omega + \frac{X}{2S_0}\right]\Delta S + \left[2S_0 Y\right]\left[\frac{\frac{Y\Delta S}{2S_0} + \frac{\alpha}{2}\Gamma g_0 \Delta N}{O}\right] = 0 \qquad \text{A 65}$$

$$\left[-\Gamma g_0 S_0\right]\Delta N + \left[j\omega + \frac{X}{2S_0}\right]\Delta S + \left[\frac{Y^2\Delta S}{O} + \frac{S_0 Y \alpha \Gamma g_0 \Delta N}{O}\right] = 0 \qquad \text{A 66}$$

Regrouping terms yields an expression in ΔS without $\Delta\phi$

$$\left[-\Gamma g_0 S_0 + \frac{S_0 Y \alpha \Gamma g_0}{O}\right]\Delta N + \left[j\omega + \frac{X}{2S_0} + \frac{Y^2}{O}\right]\Delta S = 0 \qquad \text{A 67}$$

Now ΔN needs to be eliminated from (A 67) so taking (A 60)

$$\left[j\omega + \frac{1}{\tau_n} + g_0 S_0\right]\Delta N = \frac{\Delta I}{qV} + \left[-\frac{1}{\Gamma \tau_p} + \frac{X}{\Gamma S_0}\right]\Delta S \qquad \text{A 68}$$

Letting $P = j\omega + \frac{1}{\tau_n} + g_0 S_0$ we obtain

$$\Delta N = \frac{\frac{\Delta I}{qV} + \left[-\frac{1}{\Gamma \tau_p} + \frac{X}{\Gamma S_0}\right]\Delta S}{P} \qquad \text{A 69}$$

Substituting (A 69) into (A 67) yields

$$\left[-\Gamma g_0 S_0 + \frac{S_0 Y \alpha \Gamma g_0}{O}\right]\left[\frac{\frac{\Delta I}{qV} + -\frac{\Delta S}{\Gamma \tau_p} + \frac{X \Delta S}{\Gamma S_0}}{P}\right] + \left[j\omega + \frac{X}{2S_0} + \frac{Y^2}{O}\right]\Delta S = 0 \qquad \text{A 70}$$

Multiplying out

$$0 = \left[j\omega + \frac{X}{2S_0} + \frac{Y^2}{O}\right]\Delta S + \frac{S_0 Y \alpha \Gamma g_0 \Delta I}{PqVO} - \frac{S_0 Y \alpha g_0 \Delta S}{OP\tau_p} + \frac{Y \alpha g_0 X \Delta S}{PO} - \frac{\Delta I \Gamma g_0 S_0}{PqV} + \frac{\Delta S g_0 S_0}{P\tau_p} - \frac{X \Delta S g_0}{P} \qquad \text{A 71}$$

Grouping all ΔS terms

$$\left[j\omega + \frac{X}{2S_0} + \frac{Y^2}{O} - \frac{S_0 Y \alpha g_0 \Delta S}{OP\tau_p} + \frac{Y \alpha g_0 X \Delta S}{PO} + \frac{\Delta S g_0 S_0}{P\tau_p} - \frac{X \Delta S g_0}{P}\right]\Delta S = \frac{\Delta I \Gamma g_0 S_0}{PqV} - \frac{S_0 Y \alpha \Gamma g_0 \Delta I}{PqVO} \qquad \text{A 72}$$

Dividing both sides by the coefficient of ΔS yields

$$\Delta S = \frac{\frac{\Delta I \Gamma g_0 S_0}{PqV} - \frac{S_0 Y \alpha \Gamma g_0 \Delta I}{PqVO}}{j\omega + \frac{X}{2S_0} + \frac{Y^2}{O} - \frac{S_0 Y \alpha g_0 \Delta S}{OP\tau_p} + \frac{Y \alpha g_0 X \Delta S}{PO} + \frac{\Delta S g_0 S_0}{P\tau_p} - \frac{X \Delta S g_0}{P}} \qquad \text{A 73}$$

Factoring the numerator leaves the equation used in the Matlab code to plot the modulation response

$$\Delta S = \frac{\frac{\Delta I \Gamma g_0 S_0}{PqV}\left[1 - \frac{Y\alpha}{O}\right]}{j\omega + \frac{X}{2S_0} + \frac{Y^2}{O} - \frac{S_0 Y \alpha g_0 \Delta S}{OP\tau_p} + \frac{Y\alpha g_0 X \Delta S}{PO} + \frac{\Delta S g_0 S_0}{P\tau_p} - \frac{X \Delta S g_0}{P}} \qquad \text{A 74}$$

S_0 and ϕ_0 are known from the Steady state solution ω is the frequency range over which we wish to plot the modulation response ΔI is simply the amplitude of the modulating sine wave and every other term is a constant Hence one can plot the modulation response

Appendix B

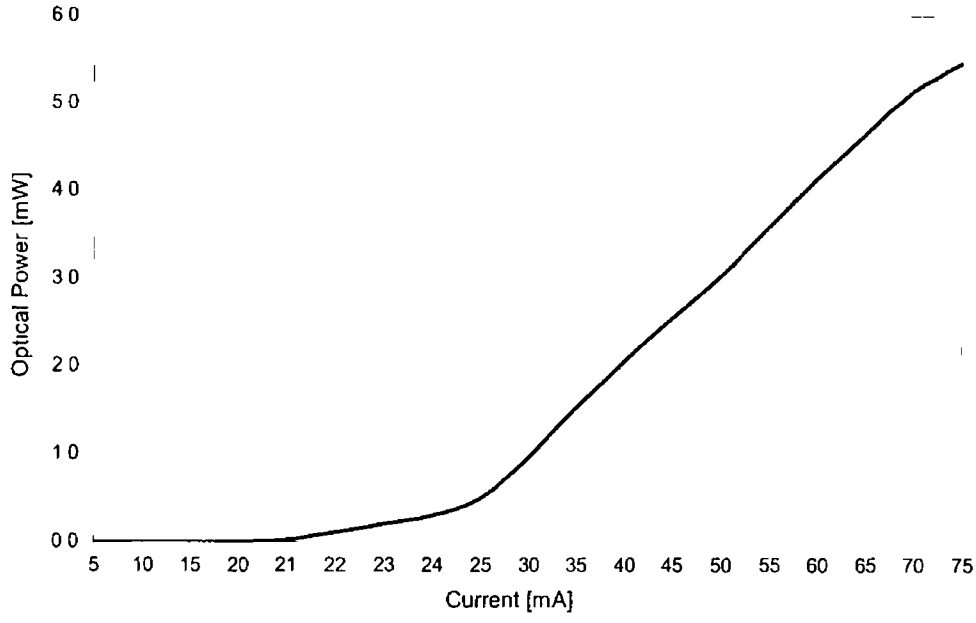

Figure 1 PI curve for 1 5 NTT DFB (KELD 1551 CCC_1)

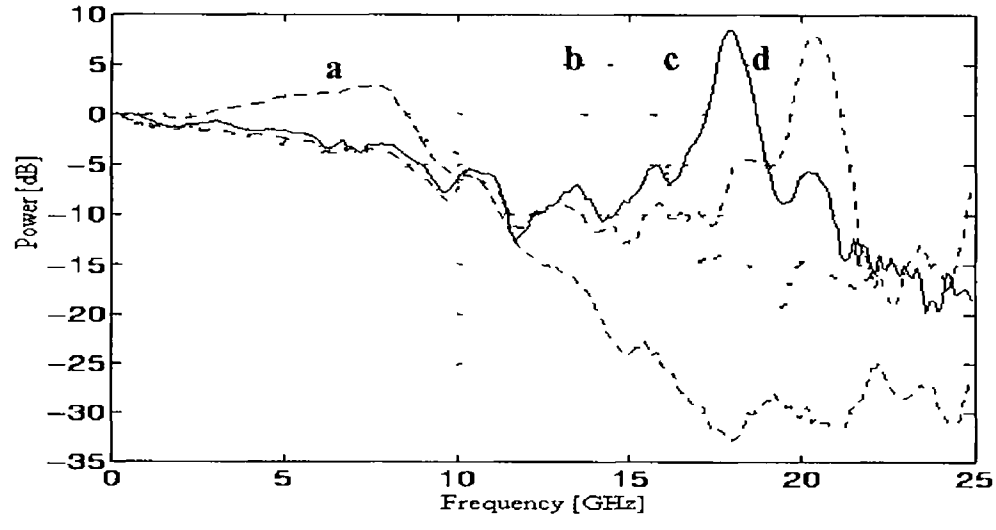

Figure 2 Frequency response of 1 5 NTT DFB (KELD 1551 CCC_1) (a) free running with injection level set to (b) 4 dBm (c) 5 dBm (d) 6 dBm

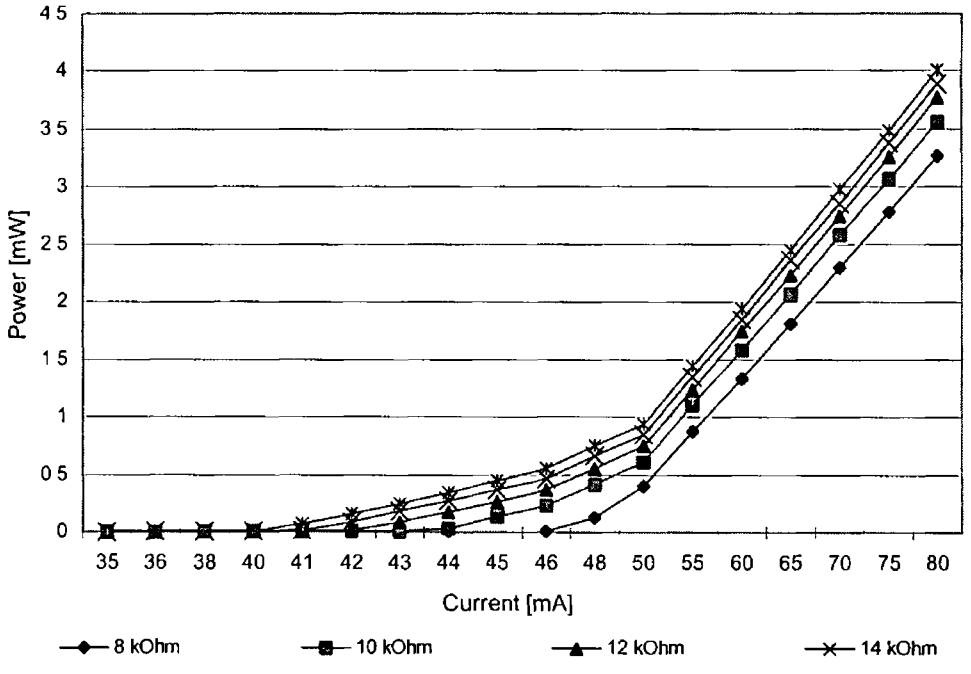

Figure 3 PI curve for1 5 MQW DFB (KELD 1552 SSC) for different temperatures

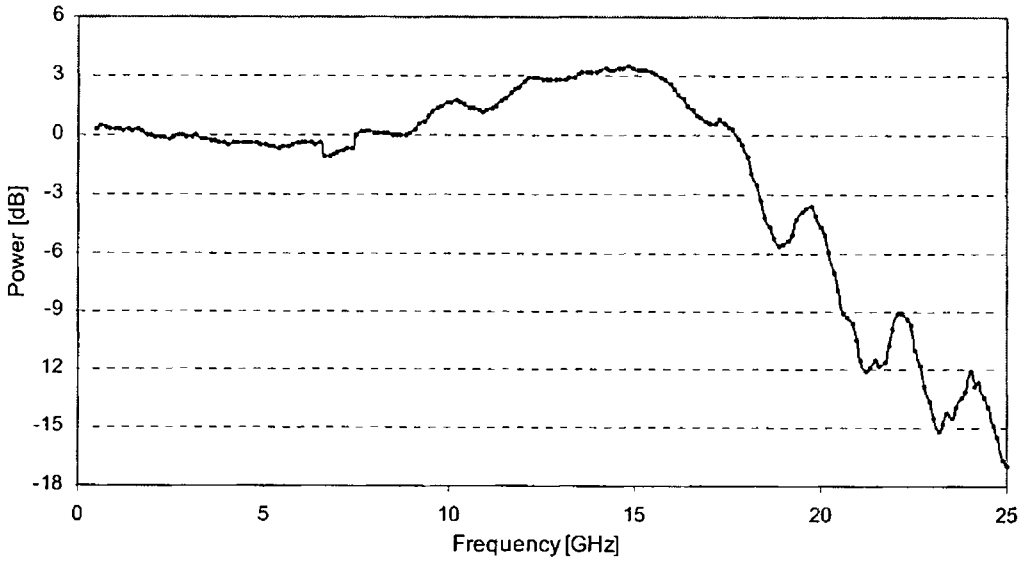

Figure 4 Frequency response of 1 5 MQW DFB (KELD 1552 SSC)

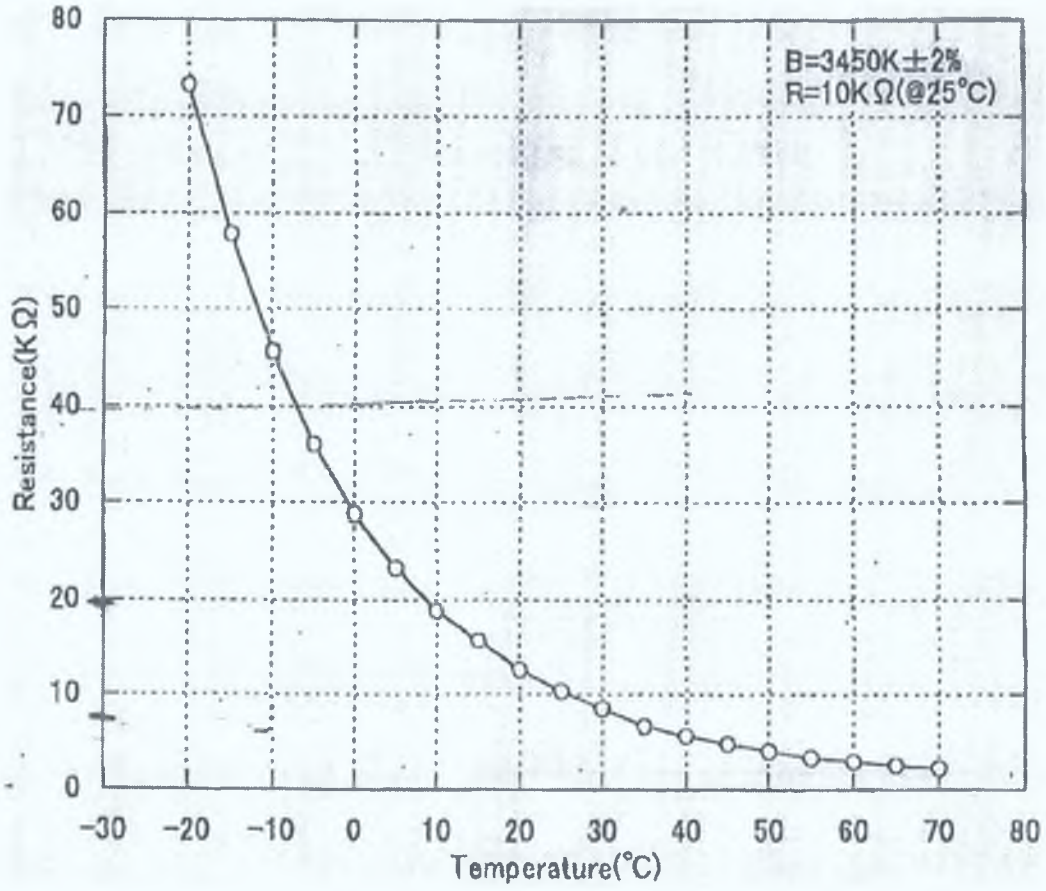

Figure 5: *Temperature vs. resistance for 1.5 MQW DFB (KELD 1552 SSC)*

Appendix C

Steady state solution to rate equations

```
function dp = Rate_Equations(Si)

%%%%%%%%%%%%%%%%%%%%%%%%%%%%%%%%%%%%%%%%%%%%%%%%%%%%%%%%%%%%%%%%%%%%%%%%%%%%
%%%%This program finds the steady state solution to laser rate
equations
%%It then plots the Output Power as a function of Bias current and
the %%Modulation Response as a function of Frequency
%%%%%%%%%%%%%%%%%%%%%%%%%%%%%%%%%%%%%%%%%%%%%%%%%%%%%%%%%%%%%%%%%%%%%%%%%%%%
%%

clear

%%%%%%%%%%Laser Parameters%%%%%%%%%%%%%
g0 = 1e-12,              % Differential gain coeff
Nom = 1 4e23,            % Transparency density (m^-3)
V = 11e-17,              % Volume of active layer
tp = 2e-11,              % Photon lifetime (s)
tn =  3e-9,              % Carrier recombination lifetime
OCF = 0 35,              % Mode confinement factor
B = 0 0000,              % Beta, spontaneous emission factor
q = 1 6e-19,             % Charge of electron (C)
alpha = 6 8,             % Linewidth Enhancement Factor
Ac = 8e-3,               % Amplitude of carriers
I_bias = 70e-3,          % Bias Current
deltaf = -5 5e9          % Frequency Detuning
deltaw = 2*pi*deltaf,    %Convert frequency to radians
Kc = 2 5e11,             %Injected light coulping coefficient
if Si == 0,
   deltaw = 0,           %it there's no injection then ignore the
end                      %detuning in the phase equation


h = 6 625e-34,     % Plancks constant
R = 0 32,          % Reflectivity in cavity
c = 3e8,           % Speed of light
n = 3 63,          % Refractive index
Ar =  03e-12,      % Area of the active region
lamda = 1550e-9,   % Wavelength of output light
f_laser = c/lamda,% Frequency of the output light
responsivity = 0 6, % Responsivity of the detector

fml = 1e7,            %Data Modulation Rate
bitperiod = 1/fml,    %Data bit period Period = 1/f
numcarriers = 5,      %number of subcarriers

%%%%%%%%%%%%%%%%%%%%%%%%%%%%%%%%%%%%%%%%%%%%%%%%%%%%%%%%%%%%%%%%%%%%%%%%%%%%
%%%%%%%%%%%%%%%%%%%
%THIS SECTION CALCULATES THE STEADY STATE VALUES FOR PHOTON AND
CARRIER %DENSITY AND INITIAL PHASE AND USES THEM TO CALCULATE THE
SMALL SIGNAL %RESPONSE OF THE LASER
%%%%%%%%%%%%%%%%%%%%%%%%%%%%%%%%%%%%%%%%%%%%%%%%%%%%%%%%%%%%%%%%%%%%%%%%%%%%
%%%%%%%%%%%%%%%%%%
```

```
%TO OBTAINE N0 (STADY STATE VALUE FOR CARRIER DENSITY) ROOTS OF THE
%FOLLOWING EQUATIONS HAVE TO BE FOUND
% a_var*N0^3 + b_var*NO^2 + c_var*N0 + d_var = 0
%%%%%%%%%%%%%%%%%%%%%%%%%%%%%%%%%%%%%%%%%%%%%%%%%%%%%%%%%%%%%%%%%
%%%%%%%%%%%%%%%%
C=OCF*g0,
E=I_bias/(q*V),


a_var = -(C^2+C^2*alpha^2/4)/(4*tn),

b_var=1/(4*tn)*(2*C^2*Nom+2*C/tp+C^2*alpha^2/2*Nom+C*alpha^2/(2*tp)+
+deltaw*C*alpha)+E/4*(C^2+C^2*alpha^2/4)

c_var=-E/4*(2*C^2*Nom+2*C/tp+C^2*alpha^2/2*Nom+C*alpha^2/(2*tp)+
+deltaw*C*alpha)-1/(4*tn)*(Nom*C*(Nom*C+2/tp+C*alpha^2/4*Nom+
+alpha^2/tp+deltaw*alpha)+1/tp^2+alpha^2/(4*tp^2)+deltaw*alpha/tp+del
taw^2)-Kc^2*Si*g0

d_var=E*C*Nom/4*(C*Nom+2/tp+C*alpha^2/4*Nom+alpha^2/tp+deltaw*alpha)+
+E/(4*tp^2)+E*alpha^2/(16*tp^2)+deltaw*E*alpha/(4*tp)+
+E*deltaw^2/4+Kc^2*Si*g0*Nom


%Get the roots of the above equation
N0_eq = [a_var b_var c_var d_var],
N0_Roots = roots(N0_eq)
N0 =(N0_Roots(3)),                  %N0, the steady state carrier
density

%S0 THE STEADY STATE PHOTON DENSITY IS CALCULATED USING THE NO
OBTAINED %ABOVE
S0 = ((I_bias*tn)- (N0*q*V))/(tn*g0*(N0-Nom)*q*V)

% Injection Ratio
ratio = Si/S0

if Si == 0,
   Phi0 = 0,
else
Phi0 = asin((-alpha/(2*tp) - (deltaw) + ((alpha/2)*OCF*g0*(N0-
Nom)))/(Kc*sqrt(Si/S0))),
end

freq = [10e6 10e6 20e9],      %RANGE OF FREQUENCIES TO PLOT THE
RESPONSE
wm = 2*pi*freq,

%%%%%%%%%%%%%%%%%%%%%%%%%%%%%%%%%%%%%%%%%%%%%%%%%%%%%%%%%%%%%%%%%
%%%%%%%%%%%%%%%%%%%
%%CALCULATE THE SMALL SIGNAL RESPONSE AND PLOT THE MODULATION
RESPONSE %%OF THE LASER
%%%%%%%%%%%%%%%%%%%%%%%%%%%%%%%%%%%%%%%%%%%%%%%%%%%%%%%%%%%%%%%%%
%%%%%%%%%%%%%%%%%%%
```

```
X = 2*Kc*sqrt(S1*S0)*cos(Ph10),
Y = Kc*sqrt(S1/S0)*sin(Ph10),
O = (j *wm + (X/(2*S0))),
P = (j *wm + (1/tn) + g0*S0),

if S1 == 0
s1 = -((Ac/(q*V))*g0*S0*OCF) /(wm ^2 - (wm) *(1*g0*S0) +
(wm) *(1/(tn)) - (g0*S0)/tp),
end
if S1 > 0
   s1 = (((OCF*Ac*g0*S0) /(P *q*V)) *(1 - Y*alpha /O)) /((j *wm) +
        (X/(2*S0)) + (Y^2 /O) + (X*Y*alpha*g0 /(P *O))-
        (S0*Y*alpha*g0 /(P *O*tp))-(X*g0 /P) + (g0*S0 /(P *tp))),
end

%%%%%%%%% Plot Resonance Freq  %%%%%%%%%
figure(2),
s = abs(s1),              %Get absolute values of the change in
                          photon          %density
logs = 20*log10(s/Ac),    %Get the log of change in photon number
                          with %respect to change
                          %in input current (The modulation response)
norms = logs - logs(1),   %Normalise it to the first value
plot(freq *1e-9,norms),   % and plot
axis([0 20 -30 40]),
title('Modulation Response'),
xlabel('Frequency (GHz)'), ylabel('Response (dB)'),
hold on, grid,

for I_bias = [0  0001 100e-3] %Each current value to take the power
at
a_var = -(C^2+C^2*alpha^2/4)/(4*tn),

b_var=1/(4*tn)*(2*C^2*Nom+2*C/tp+C^2*alpha^2/2*Nom+C*alpha^2/(2*tp)+
+deltaw*C*alpha)+E/4*(C^2+C^2*alpha^2/4)

c_var=-E/4*(2*C^2*Nom+2*C/tp+C^2*alpha^2/2*Nom+C*alpha^2/(2*tp)+
deltaw*C*alpha)-1/(4*tn)*(Nom*C*(Nom*C+2/tp+C*alpha^2/4*Nom+
+alpha^2/tp+deltaw*alpha)+1/tp^2+alpha^2/(4*tp^2)+deltaw*alpha/tp+del
taw^2)-Kc^2*S1*g0


d_var=E*C*Nom/4*(C*Nom+2/tp+C*alpha^2/4*Nom+alpha^2/tp+deltaw*alpha)+
+E/(4*tp^2)+E*alpha^2/(16*tp^2)+deltaw*E*alpha/(4*tp)+E*deltaw^2/4
+Kc^2*S1*g0*Nom
%Get the roots of the above equation
N0_eq = [a_var b_var c_var d_var],
N0_Roots = roots(N0_eq),
N0 =(N0_Roots(3)),                %N0, the steady state carrier
density

S0 =((I_bias*tn)- (N0*q*V))/(tn*g0*(N0-Nom)*q*V),

%From the photon density the power can be obtained and then plotted
Pout = S0 *c /(2*OCF*n)*h*f_laser*Ar*(1-R),
   figure(100),
   plot(I_bias*1000,Pout*1000,'k'),
   axis([0 100 0 16])
   title('Plot of "P vs I" Curve'),
```

```
 xlabel('Bıas Current (mA)'), ylabel('Output Power (mW)'),
   grıd, hold on,
end
```

SCM system

```
%%%%%%%%%%%%%%%%%%%%%%%%%%%%%%%%%%%%%%%%%%%%%%
%%%%%%%%%%%%%%%%%%%%%%%%%%%%%%%%%%%%%%%%% This Program
models the transmission of a multichannel data signal %% over optical
fiber  The laser is modelled by solving the optical rate equations
using the ODE-45 function in Matlab
%%%%%%%%%%%%%%%%%%%%%%%%%%%%%%%%%%%%%%%%%%%%%%%%%%%%%%%%%%%%%%%%%%%%
%%

clear all   % clears all variables

% defines the global variables
global Ar Nom OCF tp B q V numcarriers spacing moding_sig
input_signal sample_number span fc1 Ac A I_bias tn g0 x fm1 TFinal Fs
numbits f Tex bitsequence Ts filtered_moding_sig bitvalue deltaw
alpha Si Kc f,

%%%%%%%%%Laser Parameters%%%%%%%%%%%
g0 = 1e-12,        % Differential gain coefficient
Nom = 1 4e23,      % Transparency density (m^-3)
V = 11e-17,        % Volume of active layer
tp = 2e-11,        % Photon lifetime (s)
tn =  3e-9,        % Carrier recombination lifetime
OCF = 0 35,        % Mode confinement factor
B = 0 0000,        % Beta, spontaneous emission factor
q = 1 6e-19,       % Charge of electron (C)
alpha = 6 8,       % Linewidth Enhancement Factor
Ac=6e-3,
A = [3 2e-3 2 9e-3 0e-3 3e-3 3 2e-3],          % Amplitude of carriers
I_bias = 70e-3,    % Bias Current
deltaf = -11e9,    % Frequency Detuning
deltaw = 2*pi*deltaf, %Convert frequency to radians
Si =30e20,         %Injection Level (Injected photon density)
Kc = 2 5e11,       %Injeted light coulping coefficient
if Si == 0,
   deltaw = 0,     %it there's no injection then ignore the detuning
in
end                % the phase equation

h = 6 625e-34,     % Plancks constant
R = 0 32,          % Reflectivity in cavity
c = 3e8,           % Speed of light
n = 3 63,          % Refractive index
Ar =  03e-12,      % Area of the active region
lamda = 1550e-9,   % Wavelength of output light
f_laser = c/lamda,% Frequency of the output light
responsivity = 0 6, % Responsivity of the detector

fm1 = 140e6,          %Data Modulation Rate
bitperiod = 1/fm1,    %Data bit period Period = 1/f
numcarriers = 5,      %number of subcarriers

%%%%%%%%%%%%%%%%%%%%%%%%%%%%%%%%%%%%%%%%%%%%%%%%%%%%%%%%%%%%%%%%%%%%
%%%% THIS SECTION USES THE RATE_EQUATIONS FUNCTION TO OBTAIN THE
CARRIER %% DENSITY, CALCULATES THE PHI0 AND S0 AND PLOT THE FREQUENCY
RESPONSE %% OF THE LASER
%%%%%%%%%%%%%%%%%%%%%%%%%%%%%%%%%%%%%%%%%%%%%%%%%%%%%%%%%%%%%%%
N0=Rate_Equations(Si)
```

```
% S0 the steady state photon density is worked out by rearranging the
% carrier density rate equation
S0 = ((I_bias*tn)- (N0*q*V))/(tn*g0*(N0-Nom)*q*V)

% Injection Ratio
ratio = S1/S0

% Output power is worked out using Photon Density
%Pout = S0 *c /(2*OCF*n)*h*f_laser*Ar*(1-R),

if S1 == 0,
   A=[6e-3 6e-3 6e-3 6 3e-3 6 4e-3],   %CARRIER AMPLITUDES FOR FREE
   Phi0 = 0,                           % RUNNING LASER
else
Phi0 = asin((-alpha/(2*tp) - (deltaw) + ((alpha/2)*OCF*g0*(N0-
Nom)))/(Kc*sqrt(S1/S0))),
end

%%%%%%%%%%%%%%%%%%%%%%%%%%%%%%%%%%%%%%%%%%%%%%%%%%%%%%%%%%%%%%%%%%%%%%%%%%%%
%%
%% THIS SECTION IS WHERE THE DATA CHANNELS WHICH MODULATE THE LASER
ARE %% SET UP AND MODULATED ONTO THE LASER
%%%%%%%%%%%%%%%%%%%%%%%%%%%%%%%%%%%%%%%%%%%%%%%%%%%%%%%%%%%%%%%%%%%%%%%%%%%%
%%

%RANDOM BIT SEQUENCE
numbits = 100,
bitsequence = Random_Bit_Allocator(fm1, numbits, numcarriers),
numbits = size(bitsequence,2),

fc1 = 11 2e9,      % Frequency of 1st carrier (Hz)
spacing = 0,       % Carrier spacing      defined later on
span = 1 6e9,      % Freq  Span occupied by combined carriers

Fs = 29 96e9,         % Sampling Frequency
TFinal = numbits*bitperiod, % Time for full pattern
Ts = 1/Fs,         % time interval

channel_BW =  7*fm1, % Filter Bandwidth

% Noise parameters
k = 1 3807e-23,
T = 295,
M = 1,
F = 1,
Imp = 50,
numsamples = (TFinal*Fs) + 1,

% Set up thermal noise
thermal_noise = (sqrt((4*k*T*channel_BW)/Imp)*randn(numsamples,1)),

% Set up carrier spacing depending on number of carriers and the
total % span they occupy
if numcarriers > 1,
   spacing = [500e6 400e6 400e6 500e6],%span /(numcarriers - 1),
end                     %Spacing between successive carriers in
System


% Puts the bit pattern into bitslots for modulation
moding_sig = 0,
```

```
modıng_sıg = Bıt_Allocator(bıtsequence, fm1, numcarrıers, Fs, 0,
TFınal),

% Sets up a low pass fılter and fılters the data pattern
[b,a] = cheby2(5,70, 028),
for x = 1 1 numcarrıers,
fıltered_modıng_sıg(x, ) = fıltfılt(b, a, modıng_sıg(x, )), %
Fıltratıon of Receıved Current sıgnal
end

%%%%%%%%%%%%%%%%%%%%%%%%%%%%%%%%%%%%%%%%%%%%%%%%%%%%%%%%%%%%%%%%%%%%%%%%%%%%
%%
%% USES THE FUNCTION Data_ODE45 TO CALCULATE THE VALUE OF PHOTON
%% DENSITY, CARRIER DENSITY AND PHASE FOR DIFFERENT TIME SAMPLES FOR
%% MODULATING CURRENT
%%%%%%%%%%%%%%%%%%%%%%%%%%%%%%%%%%%%%%%%%%%%%%%%%%%%%%%%%%%%%%%%%%%%%%%%%%%%
%%
tspan = [0 Ts TFınal],      % tıme span wıth samplıng freq

y0 = [Phı0,S0,N0],% ınıtıal CONDITIONS (steady state values from
above)
[t,p] = ode45('Data_ODE45',tspan,y0),
%%%%%%%%%%%%%%%%%%%%%%%%
fc1= fc1-(spacıng(1)-400e6)
fc(1)=fc1,
ınput_sıgnal = 0,
for x = 2 1 numcarrıers,
fc(x) = fc(x-1) + spacıng(x-1),    %sets the carrıer frequencıes
% Thıs lıne upconverts the data sıgnal to the carrıer frequency
end,
for x=1 1 numcarrıers,
 moded_sıg( ,x) = ((fıltered_modıng_sıg(x, )')  * (A(x) *
cos(2*pı*fc(x)*t))),
% Thıs models the electrıcal power coulper for each carrıer
ınput_sıgnal = ınput_sıgnal + moded_sıg( ,x),
end

% Bıas tee
I = I_bıas + ınput_sıgnal,

%Take values of Phase, Photon Densıty and Carrıer Densıty back from
ODE45
Phı = p( ,1),
S = p( ,2),
N = p( ,3),

% Convert Photon Densıty, to Optıcal Power ın Watts
Pout = S *c/(2*OCF*n)*h*f_laser*Ar*(1-R),

%%%%%%%%
% Next 3 lınes model the varıable attenuator used ın the BER
measurements
%%%%%%%%
atten = 15,
ratıo = 10^(atten/10),
Pout = Pout/ratıo,%
Power = 10*log10(mean(Pout))  % Average Power

%%%%%%%% CALCULATE ELECTRICAL SPECTRUM %%%%%%%%%%%%%%%

%%%%%%%%
```

```
% No of points For Fourier Transform
%%%%%%%%
L = 32768*16,
g = L/2,
freq = Fs*(0 g)/L,  % Important half of 'F' axis

FPin = fft(I,L),              % Getting fast fourier transform of
Input signal
Fin = FPin * conj(FPin) / L,  % Remove complex components
Fin(1) = Fin(2),              % Removes the DC value
LFin = 20*log10(Fin),         % Puts into log scale

FPout = fft(Pout,L),          % Fourier transform of output signal
Fout = FPout * conj(FPout) / L,
Fout(1) = Fout(2),
LFout = 20*log10(Fout),

%%%%%%%% Display output %%%%%%%%%%%%%%%%%%%%%%%%%%%%
% Plot the input to and output from the laser in the time and
frequency domains
%%%%%%%%%%%%%%%%%%%%%%%%%%%%%%%%%%%%%%%%%%%%%%%%%%%%%%%
figure,
subplot(2,1,1),
plot(t,I),
ylabel('Input Pulse'),
grid,
subplot(2,1,2),
plot(t,Pout),
ylabel('Output Power'), xlabel('Time'),
grid,

figure,
%subplot(2,1,1),
plot(freq *1e-9,LFin(1 g+1)),
ylabel('Power (dBm)'),
grid,
figure
%subplot(2,1,2),
plot(freq *1e-9,LFout(1 g+1)),
ylabel('Power (dBm)'), xlabel('Frequency (GHz)'),
grid,

%%%%%%%%%%%%%%%%%%%%%%%%%%%%%%%%%%%%%%%%%%%%%%%%%%%%%%%%%%%%%%%%%%%%%%%
%This line models the detector
%*************************************************************
I_received =(Pout  * responsivity),
%*************************************************************

for x = 3                    %ONLY THE CENTRAL CHANNEL
   downconvert = demod(I_received, fc(x), Fs, 'am'), % Downconvert
back to baseband


%Set up the low pass filter, and filter with the addition of noise
[b,a] = cheby2(8,80, 028),
Rx_Data_signal = filtfilt(b, a, downconvert)+thermal_noise,
     for i=1 1 10*214
     Rx_Data_signal(i)=Rx_Data_signal(i+10*214+1),
      end,
%%%%%%%%%%%%%%%%%%%%%%%%%%%%%%%%%%%%%%%%%%%%%%%%%%%%%%%%%%%%%%%%%%%%%%%
%   This plots the initial data signal and the recovered data signal
```

```
%%%%%%%%%%%%%%%%%%%%%%%%%%%%%%%%%%%%%%%%%%%%%%%%%%%%%%%%%%%%%%%%%%%%%%%
mod_interest = filtered_moding_sig(x, ), %The initial data signal
figure,
subplot (2,1,1),
plot(t, mod_interest),
ylabel('I/P Data Signal'),
grid,
subplot (2,1,2),
plot(t, Rx_Data_signal),
ylabel('O/P Data Signal  [mA]'),
xlabel('time (ns) '),
grid,

%%%%%%%%%%%%%%%%%%%%%%%%%%%%%%%%%%%%%%%%%%%%%%%%%%%%%%%%%%%%%%%%%%%%%%%
% The final section plots the eye diagram and calculates the BER
%%%%%%%%%%%%%%%%%%%%%%%%%%%%%%%%%%%%%%%%%%%%%%%%%%%%%%%%%%%%%%%%%%%%%%%
interval = bitperiod * Fs, %number of samples per bit interval
figure,
title ('Eye Diagram'),
ylabel('Current [Amps]'),
xlabel('Bit Period'),
hold on,
x_values = -0 5 1/interval 1 5, %2000 samples from -0 5 to 1 5
HI_values = 0, %Initialise Variables
LO_values = 0,

% Sets the sample range for each bit ie (1 2001), (2001 4001) etc
for z = 1 numbits,
   y_lower = (z-1) * interval + 1,
   y_higher = y_lower + interval,

%Next lines set up 4000 samples (2 bit periods) to plot
%It starts halfway through 1st then the full 2nd then half 3rd to
give %eye diagram
%(-999 3001) doesnt plot, (999 5001) plots etc
   start = y_lower - (interval/2),
   finish = y_higher + (interval/2),
   if (start > 0) & (finish < (numbits * interval))
        plot (x_values, Rx_Data_signal(start finish)), %Uses the X
   end                                              % values - 5 up to 1 5


Mean_Rx_Signal = mean(Rx_Data_signal), %Gets the average to work out
                                       % the threshold for the BER
% If the average bit value is greater than the threshold then take it
% as a 1 otherwise take it as 0
if (mean(Rx_Data_signal(y_lower y_higher)) > Mean_Rx_Signal), %bit
    HI_values = [HI_values,Rx_Data_signal(y_lower +       %value is
HI
            floor(interval/4) y_higher - floor(interval/4))],
   else                                                  %bit value is
LO
         LO_values = [LO_values,Rx_Data_signal(y_lower +
            floor(interval/4) y_higher - floor(interval/4))],
   end
end
%Takes mean values and standard deviations to work out threshold
value
%according to the equation
mean_HI = mean(HI_values),
mean_LO = mean(LO_values),
```

```
sigma_HI = std(HI_values),
sigma_LO = std(LO_values),

Thresh_Lev = ((sigma_LO*mean_HI) + (sigma_HI*mean_LO))/(sigma_LO +
sigma_HI),

%Uses the equation for BER to work it out for each channel
BER(x) = 0 25 * (erfc((mean_HI - Thresh_Lev)/(sqrt(2)*sigma_HI)) +

      erfc((Thresh_Lev - mean_LO)/(sqrt(2)*sigma_LO))),
end
BER % Prints out the Bit Error Rates
```

Random Bit Allocator

```
%%%%%%%%%%%%%%%%%%%%%%%%%%%%%%%%%%%%%%%%%%%%%%%%%%%%%%%%%%%%%%%%%%%%%%%%
% This function is called when the user wants a random rather than
% a fixed bit pattern  It accepts the modulation rate, the number
% of bits An the number of channels and uses the rand function to
% assign a value of 1 or 0 to each  The last bit of each pattern is
% set to 0 this was done to avoid some spurious values
%%%%%%%%%%%%%%%%%%%%%%%%%%%%%%%%%%%%%%%%%%%%%%%%%%%%%%%%%%%%%%%%%%%%%%%%

function [x,n] = Random_Bit_Allocator(mod_rate, num_bits,
num_channels)

bitperiod = (1/mod_rate),

x = rand(num_bits, num_channels),

for j = 1 1 num_channels,
   for i = 1 1 num_bits-1,
      if x(i, j) >= 0 5,
         x(i, j) = 1,
      else
         x(i, j) = 0,
      end
   end
   x(num_bits, j) = 0,
end

x = x',  % This transposes the matrix to get it in a form suitable
for
         % use in the program
```

Bit Allocator

```
%%%%%%%%%%%%%%%%%%%%%%%%%%%%%%%%%%%%%%%%%%%%%%%%%%%%%%%%%%%%%%%%%%%%%%%%
% This function is called to convert from a sequence of 1s and 0s to
% a set of samples depending in the time and the modulation rate etc
% It basically sets the samples taken up be each bit period to the
% relevant value 1 or 0
%%%%%%%%%%%%%%%%%%%%%%%%%%%%%%%%%%%%%%%%%%%%%%%%%%%%%%%%%%%%%%%%%%%%%%%%

function [x,n] = Bit_Allocator(bitseq, mod_rate, num_channels,
F_sample,
   t_init, t_final)

bitperiod = (1/mod_rate),

numbits = size(bitseq,2),

nmin = t_init*F_sample,
nmax = t_final*F_sample,

%n = nmin 1/step nmax,
x = zeros(num_channels, nmax+1),

n_lower = 0,
n_higher = 0,
bit_interval = floor(bitperiod*F_sample),

for i = 1 1 num_channels,
   for j = 1 1 numbits,
      bitvalue = bitseq(i, j),
      n_lower = nmin + (j-1)*bit_interval,
      n_higher = n_lower + bit_interval,
      x(i, n_lower+1 n_higher+1) = bitvalue,
   end
end
```

Data_Ode45 m

```
%%%%%%%%%%%%%%%%%%%%%%%%%%%%%%%%%%%%%%%%%%%%%%%%%%%%%%%%%%%%%%%%%%%%%
%%%%%%%%%%%%
% The call to ODE-45 in Data m calls this function and integrates
% the odes described in this M-file over the time period t-initial to
% t-final   %
%%%%%%%%%%%%%%%%%%%%%%%%%%%%%%%%%%%%%%%%%%%%%%%%%%%%%%%%%%%%%%%%%%%%%
%%%%%%%%%%%%
function dp = Data_ODE45(t,p)
global  Ar  Nom  OCF  tp  B  q  V  numcarriers  spacing  moding_sig
input_signal      sample_number span fc1 Ac I_bias tn g0 x fm1 TFinal
Fs numbits f Tex bitsequence
Ts filtered_moding_sig bitvalue deltaw alpha Si Kc f,
%%%%%%%%%%%%%%%%%%%%%%%%%%%%%%%%%%%%%%%%%%%%%%%%%%%%%%%%%%%%%%%%%%%%%
%
%%%%%%%% Setup the Electrical input signal %%%%%%%%%%%%%%%
input_signal = 0,
sample_number = floor(t/Ts),
bitvalue = filtered_moding_sig( ,sample_number+1),
for x = 1 1 numcarriers,
    fc(x) = fc1 + ((x-1) * spacing),
    carrier_value( ,x)      =      ((bitvalue(x, ))      *      (Ac      *
cos(2*pi*fc(x)*t))),
    input_signal = input_signal + carrier_value( ,x),
end
%**************************        Composite        Input        Signal
******************
I = I_bias + input_signal, %Pass this value to the equations to get
               %corresponding  values  of  Photon&Carrier  Density  &
Phase
%*********************************************************************
*
% Rate Equations
Phi = p(1),
S = p(2),
N = p(3),
dp    =    [(alpha/2)*(OCF*g0*(N-Nom)    -    1/tp)    -    (deltaw)    -
(Kc*sqrt(Si/S)*sin(Phi)),
((OCF*g0*(N-Nom)      -      (1/tp))*S)      +      ((OCF*B*N)/tn)      +
((2*Kc)*sqrt(Si*S)*cos(Phi)),
I/(q*V)) - (g0*(N-Nom)*S) - (N/tn)],
```

Appendix D

Refereed Journals

1 L P Barry, P Anandarajah and A Kaszubowska "Optical Pulse Generation at Frequencies up to 20 GHz using External – Injection Seeding of a Gain-Switched Commercial Fabry-Perot Laser", *IEEE Photon Technol Lett*, vol 13, pp 1014-1016, Sept 2001

2 A Kaszubowska, P Barry and P Anandarajah "Improved Performance of a Hybrid Radio/Fiber System Using a Directly Modulated Laser Transmitter with External Injection", *IEEE Photon Technol Lett*, vol 14, pp 233-235, Feb 2002

3 A Kaszubowska, P Barry and P Anandarajah "Multiple RF Carrier Distribution in a Hybrid Radio/Fiber System Employing a Self Pulsating Laser Diode Transmitter", *IEEE Photon Technol Lett*, vol 14, pp 233-235, Nov 2002

4 A Kaszubowska, P Barry and P Anandarajah "Effects of Intermodulation Distortion the Performance of a Hybrid Radio/Fiber System Employing a Self Pulsating Laser Diode Transmitter", *IEEE Photon Technol Lett* vol 14, pp 233-235, June 2003

4 A Kaszubowska, P Barry and P Anandarajah "Multifunctional Operation of a Fiber Bragg Grating in WDM/SCM Radio over Fiber Distribution System", *IEEE Photon Technol Lett*, vol 16, pp 233-235, Feb 2004

5 F Smyth, A Kaszubowska, L P Barry "Overcoming Laser Diode Nonlinearity Issues in Multi-Channel Radio-over-Fiber Systems", *Optics Comms* 231, pp 217-2125, 2004

Reviewed Conferences

1 A Kaszubowska, P Anandarajah and L P Barry "Optically Fed Microwave System using Laser Diodes with Enhanced Modulation Bandwidth", *IEEE Postgraduate Colloquium*, Dublin 2000

2 P Anandarajah, A Kaszubowska and L P Barry "High Frequency Pulse Generation using a Gain-Switched Commercial Semiconductor Laser with Strong External Injection", *IEEE Postgraduate Colloquium*, Dublin 2000

3 A Kaszubowska, P Anandarajah and L P Barry "Generation of Optical Microwave Signals using Laser Diodes with Enhanced Modulation Response for Hybrid Radio-Fibre Systems", *IEEE ICTON 2001*, Cracow

4 A Kaszubowska, P Anandarajah and L P Barry "Hybrid Radio/Fiber System Based on a Directly Modulated Laser Transmitter with External Injection", *IEEE Postgraduate Colloquium*, Cardiff 2001

5 A Kaszubowska, L P Barry and P Anandarajah "Optical Generation of Millimeter-wave Frequencies for Hybrid Radio/Fiber Systems", *IEI/IEE Telecomm Symposium 2001*, Dublin

6 A Kaszubowska, L P Barry, P Anandarajah "Enhanced Performance of an Optically Fed Microwave Communication System Using a Directly Modulated Laser Transmitter with External Injection", *IEEE LEOS 2001*, San Diego

7 A Kaszubowska, P Anandarajah and L Barry "Multiple RF Carrier Distribution Using a Hybrid Radio/Fiber System Based on a Directly Modulated Laser Transmitter", *URSI 2002*, Poznan

8 A Kaszubowska, L P Barry and P Anandarajah "Hybrid Radio/Fiber System Employing SCM for the Distribution of Multiple RF Carriers with a Directly Modulated Laser Transmitter", *SPIE Opto-Ireland 2002*, Galway

9 A Kaszubowska, L P Barry and P Anandarajah "Self-pulsating Laser Diode for the Generation of Multiple RF Data Channels in Hybrid Radio/Fiber Systems", *IEEE LEOS 2002*, Glasgow

10 A Kaszubowska, L P Barry and P Anandarajah "Development of Highly Flexible Broadband Networks Incorporating Wavelength Division Multiplexing

and Sub-Carrier Division Multiplexing in a Hybrid Radio/Fiber Distribution System", *ICTON 2003*, Warsaw

11 A Kaszubowska, L P Barry and P Anandarajah " Development of Highly Flexible Broadband Networks Incorporating WDM and SCM in a Hybrid Radio/Fiber Distribution System", *IT&T Conference 2003*, Letterkenny

12 A Kaszubowska, L P Barry and P Anandarajah "Multifunctional Operation of a Fiber Bragg Grating in a WDM/SCM Radio over Fiber Distribution System", *LEOS 2003*, Tucson